AN INVESTIGATION INTO THE EFFECTS OF ASPALATHIN ON MYOCARDIAL GLUCOSE TRANSPORT USING CARDIOMYOCYTES FROM CONTROL AND OBESITY-INDUCED INSULIN RESISTANT RATS, AND TERMINALLY DIFFERENTIATED H9C2 CELLS

by

SYBRAND ENGELBRECHT SMIT

Thesis presented in fulfilment of the requirements for the degree
Master of Science in Medical Sciences
in the Faculty of Medicine and Health Sciences
at Stellenbosch University

Supervisor: Prof. Barbara Huisamen
Co-supervisor: Dr. Rabia Johnson

March 2016

DECLARATION

By submitting this thesis electronically, I declare that the entirety of the work contained therein is my own, original work, that I am the sole author thereof (save to the extent explicitly otherwise stated), that reproduction and publication thereof by Stellenbosch University will not infringe any third party rights and that I have not previously in its entirety or in part submitted it for obtaining any qualification.

ABSTRACT

Introduction:

Rooibos is an indigenous South African plant ingested as herbal tea and well-known for its strong anti-oxidant effects. Rooibos has shown to have cardioprotective properties *in vitro* and *in vivo*, but the role of individual Rooibos flavonoids in cardioprotection still remains unclear. This *in vitro* study investigated Aspalathin, a dihydrochalcone unique to rooibos, for (i) cardioprotective effects in the context of age- and obesity-induced insulin resistance, known to attenuate myocardial glucose uptake and utilization and (ii) the applicable signaling pathways involved.

Methods:

Male Wistar rats were allocated into three groups: 16-30 weeks feeding with either standard rat chow (C) or a high-fat, high-caloric diet (HFD), or 6-7 weeks feeding with C. Cardiomyocytes were isolated by collagenase perfusion digestion, using a Langendorff apparatus and glucose uptake determined by 2-[^{3}H]-deoxyglucose (2DG) accumulation using liquid scinitillation analysis. In addition, H9C2 cells were differentiated into cardiomyocyte analogs and also used. Viability was tested by either Trypan-blue exclusion, JC-1-staining or PI-staining and FACS analysis, and metabolic activity determined with an ATP assay. Intracellular signaling was evaluated using Western blot analysis and commercially available antibodies to PKB and AMPK.

Results:

HFD caused significant increases in body weight gain, visceral adiposity, fasting and non-fasting blood glucose, serum insulin levels and an elevated HOMA-IR index. HFD cardiomyocytes were glucose uptake resistant to increasing concentration of insulin (1-100nM). Aspalathin (10uM) and insulin (10nM) co-incubation for 45mins induced 2DG uptake in younger control cardiomyocytes, while incubation for longer than 90 mins with aspalathin (10uM) induced 2DG uptake independent of insulin in younger control cardiomyocytes and differentiated H9C2 cells. Aspalathin improved metabolic activity and membrane integrity in cultured, differentiated H9C2 cells. Aspalathin also enhanced insulin-mediated 2DG uptake in older control cells, but failed to induce 2DG uptake in HFD cells. Acute treatment with aspalathin (15min) in conjunction with insulin *in vitro* significantly increased PKB activation and AMPK expression. Extended treatment with aspalathin (90mins) in young cells resulted in significantly increased AMPK activation/expression ratio, whereas aspalathin co-treatment with insulin resulted in increased PKB activation. Aged rats had significantly higher AMPK expression and activation compared to young rats.

Conclusions:

A high-fat, high-sucrose diet of at least 16 weeks is an effective model to induce insulin-resistant, obese rats. Aspalathin and insulin co-treatment for 45 mins in cardiomyocytes isolated from young rats, and co-treatment for 90 mins in aged, control rats, induced glucose uptake. Aspalathin of at least 90 mins induced glucose uptake in cardiomyocytes from young Wistar rats, and differentiated H9C2 cells. In addition, it resensitized the insulin-signaling pathway in cardiomyocytes, possibly through activation of PKB and AMPK, resulting in an additive response. These beneficial effects of aspalathin may ultimately be due to its antioxidant capacity, receptor-mediated actions or role in GLUT4 translocation, but this remains to be established.

ABSTRAK

Inleiding:

Rooibos is ‘n inheemse plant, eie aan Suid-Afrika, wat as tee gedrink word en bekend is vir sy sterk anti-oksidant eienskappe. Rooibos speel ‘n belowende rol in die beskerming van die hart, maar die rol van sy individuele flavanoïdes moet steeds ondersoek word in die konteks van die hart. In hierdie *in vitro* studie is die rol van aspalatien, ‘n ‘dihidrochalcone’ uniek aan rooibos, ondersoek vir sy: (i) vermoë om die hart te beskerm in die konteks van ouderdom- en vetsug-geïnduseerde insulienweerstandigheid (albei risiko faktore wat glukose opname deur die hartspiere verswak), en (ii) die moontlike seintransduksiepaaie betrokke tydens hierdie proses.

Metodiek:

Manlike Wistar rotte is ingedeel in drie groepe: ‘n 16-30 weke dieet met standaard rotkos (C), ‘n hoë vet, hoë koolhidraat dieet vir 16-30 weke (HFD), of ‘n 6-7 weke standaard rotkos groep. Kardiomiosiete is deur kollagenase perfusievertering geïsoleer deur gebruik te maak van ‘n Langendorff sisteem, en daarna is die glukose opname bepaal deur 2-[^{3}H]-deoksiglukose (2DG) akkumulasie te meet. Verder is H9C2 selle gedifferensieer om hartsel analoë te vorm en ook bestudeer. Sellewensvatbaarheid is bepaal deur Trypan-blou eksklusie, JC-1-kleuring of propidium jodied-kleuring en vloeisitometrie en die metaboliese aktiwiteit is bepaal deur ATP vlakke te meet. Intrasellulêre seinstransduksie is ondersoek deur Western klad analise en die kommersiëel-beskikbare teenliggaampies teen PKB and AMPK.

Resultate:

HFD het beduidende verhogings in liggaamsgewig, intraperitoneale vet, vastende- en nie-fastende bloed glukose, serum insulienvlakke en die HOMA-IR indeks tot volg gehad. Verder was die glukose opname van HFD hartselle onderdruk in reaksie op stapsgewyse verhogings in insulin konsentrasies (1-100nM). In jong rothartselle kon ‘n kombinasie van aspalatien (10uM) en insulin (10nM) vir 45min 2DG opname verhoog, terwyl ten minste 90min van aspalatien behandeling nodig was om 2DG opname in jong rot hartselle en gedifferensieerde H9C2 selle te verhoog. Verder het 1uM aspalatien ook die metaboliese aktiwiteit en membraanintegriteit van gedifferensieerde H9C2 selle in kultuur verhoog. Aspalatien kon insulien-afhanklike 2DG opname in hartselle van C diere verhoog, slegs na 90 minute in kombinasie met insulien. Aspalatien het geen effek gehad as behandeling op HFD selle nie. Akute behandeling met 10nM insulien in kombinasie met 10uM aspalatien (15mins) *in vitro* het ‘n verhoogde PKB aktivering en AMPK uitdrukking tot volg gehad. Verlengde behandeling met aspalatien (90mins) het gelei tot ‘n beduidende verhoging in die

AMPK aktiverings-/uitdrukking verhouding, terwyl kombinasie met insulien PKB beduidend geaktiveer het. Ouer rotte het beduidend hoër vlakke en aktivering van AMPK as jonger rotte gehad.

Gevolgtrekking:

‘n Hoë-vet, hoë-sukrose dieet van ten minste 16 weke is voldoende om insulienweerstandigheid en vetsug te induseer in ‘n Wistar rot model. Aspalatien kan insulien-afhanklike glukose opname verhoog na 45 minute behandeling in jong rothart selle, terwyl ten minste 90 minute benodig word om dieselfde effek in ouer kontrole rotte te verkry. Aspalatien het glukose opname in die hartselle van jong Wistar rotte, asook gedifferensieerde H9C2 selle ontlok na ten minste 90 minute van behandeling. Verder het aspalatien die insulien-seinstransduksie pad in hartselle gesensitiseer, heel moontlik deur aktivering van PKB and AMPK wat lei tot ‘n verhoogde glukose opname in kombinasie met insulien. Hierdie voordelige effekte van aspalatien kan heel moontlik aan sy antioksidant kapasiteit toegeskryf word, asook die spesifieke reseptor-gemedieerde effekte, en/of sy rol in GLUT4 translokering, maar dit moet nog bevestig word.

ACKNOWLEDGEMENTS

I would like to express my deep and sincere gratitude towards:

- my promoter: Prof. Barbara Huisamen, a true commandant! The one with the answer! Was a true honour to learn from you and be inspired to pursue science even deeper. Without your aid, the story of this thesis would've been very bland. I thank thee for every bit of advice and constructive feedback.
- my ko-promoter: Dr. Rabia Johnson, vir al haar bereidwilligheid deur hierdie hele proses! Daar was swaar gekou op tye, maar tog het ons die vrugte gepluk van ons moeite! Baie dankie vir al die ondersteuning met die MRC se logistieke en aanstelling van Phiwa om my wys te maak in die dinge van die wetenskap. Ek waardeer!

I am also grateful for:

- Phiwa Dludla (Diabetes Discovery Platfrom, Medical Research Council Cape Town) for training in cell culturing and many more! Thank you, Phiwa
- Yolandi Espach (Cardiovascular Research Group, Division of Medical Physiology, Stellenbosch University) for training and assistance in Langendorff isolations
- Mignon van Vuuren (Cardiovascular Research Group, Division of Medical Physiology, Stellenbosch University) for assistance with Langendorff isolation experiments
- Dr. John Lopes (Cardiovascular Research Group, Division of Medical Physiology, Stellenbosch University) for fluorescent training and assistance with JC-1 Staining technique.
- Dr. Sven Friedrich (TASK Applied Science Research Group, Division of Medical Physiology, Stellenbosch University) for assistance with PI Staining technique.
- Mr. Noel Markgraaff and all staff of the Animal unit for assistance in feeding, handling and transport of the animals
- All staff and fellow students in the Department for all forms of assistance. The social environment has made it a pleasure to come to do my work.

I would like to thank the Division of Medical Physiology (Stellenbosch University) and the National Research Foundation for financial support.

My special gratitude is due to my family, friends, brothers and sisters, for prayers and encouragement. My wife-to-be, Allie, for support and patience during the preparation of this thesis.

All Glory be to the Lord Jesus Christ, my GOD, for inspiration, strength and knowledge. Each step of my journey was under His control and without Him I could do nothing.

PUBLICATIONS DURING THE STUDY

PRESENTATIONS AT SCIENTIFIC MEETING

1. **Smit, S.E.**, & Huisamen, B. An Investigation into the effects of aspalathin on myocardial glucose transport and GLUT 4 translocation, using cardiomyocytes from control and insulin-resistant rats. Oral presentation, Diabetic Discovery Platform Symposium, Research Symposium, Cape Town, **2014**.
2. **Smit, S.E.**, & Huisamen, B. An Investigation into the effects of aspalathin on myocardial glucose transport and GLUT 4 translocation, using cardiomyocytes from control and insulin-resistant rats, and terminally differentiated H9C2 cells. Oral presentation, Biomedical Research and Innovation Platform, Research Symposium, Cape Town, **2015**.
3. **Smit, S.E.,** Huisamen, B., Johnson, R., & Dludla, P. An Investigation into the effects of aspalathin on myocardial glucose transport and GLUT 4 translocation, using cardiomyocytes from control and insulin-resistant rats, and terminally differentiated H9C2 cells. Oral presentation, Physiological Society of South Africa, Parys, South Africa, **2015**.
4. **Smit, S.E.,** Huisamen, B., Johnson, R., & Dludla, P. An Investigation into the effects of aspalathin on myocardial glucose transport and GLUT 4 translocation, using cardiomyocytes from control and insulin-resistant rats, and terminally differentiated H9C2 cells. Oral presentation, Academic Year Day, Tygerberg Medical Campus, Stellenbosch University, South Africa, **2015**.

TABLE OF CONTENT

DECLARATION ..... **ii**

ABSTRACT ..... **iii**

ABSTRAK ..... **v**

ACKNOWLEDGEMENTS ..... **vii**

PUBLICATIONS DURING THE STUDY ..... **ix**

PRESENTATIONS AT SCIENTIFIC MEETING ..... **ix**

TABLE OF CONTENT ..... **x**

LIST OF ILLUSTRATIONS ..... **xvi**

FIGURES ..... **xvi**

TABLES ..... **xix**

LIST OF ABBREVIATIONS ..... **xx**

I. UNITS OF MEASUREMENT ..... **xx**

II. CHEMICAL COMPONENTS ..... **xxi**

III. PROTEIN ABBREVIATIONS ..... **xxii**

IV. OTHER ABBREVIATIONS ..... **xxiv**

MOTIVATION FOR RESEARCH ..... **xxv**

GENERAL AIM ..... **xxvi**

CHAPTER 1 - LAYMAN'S OVERVIEW OF THE THESIS **1**

CHAPTER 2 - LITERATURE REVIEW **4**

1. OBESITY AND INSULIN RESISTANCE FROM THE HEART'S PERSPECTIVE **4**

1.1 INTRODUCTION **4**

1.2 OBESITY **4**

1.2.1 Overview of Obesity 4

1.2.2 Assessment 5

1.2.3 Epidemiology 6

1.2.3.1 Children and Adolescence 6

1.2.3.2 Socio-economic Status 7

1.2.4 Obesity-related Conditions 7

1.2.4.1 Coronary Heart Disease and Strokes 7

1.2.4.2 Metabolic Syndrome 7

1.2.4.3 Diabetes 8

- **Diabetes Overview** 8
- **Treatment** 9

1.2.4.4 Other Conditions 10

1.3 THE HEART 10
1.3.1 Overview of the Heart 10
1.3.2 Energy Metabolism 11
1.3.2.1 ATP 11
1.3.2.2 Glucose Metabolism 12
- **Glycolysis** 13
- **Glucose Oxidation** 14
- **Glycogen Synthesis** 15

1.3.2.3 Fatty Acid Metabolism 16
- **Source of Fatty Acids** 17

1.3.2.4 Interspecie differences 17
1.3.2.5 Alterations in Obesity and Diabetes 18

1.4 INSULIN RESISTANCE 19
1.4.1 Overview of Insulin Resistance 19
1.4.2 Assessment 20
1.4.2.1 Hemoglobin A1c 20
1.4.2.2 Fasting Plasma Glucose Test 20
1.4.2.3 Oral Glucose Tolerance Test 21
1.4.3 Insulin 21
1.4.4 Insulin Secretion 22
1.4.5 Insulin Function 23
1.4.6 Insulin Signaling 24
1.4.6.1 PI3K/PKB pathway 25
- **IR** 25
- **IRS 1** 26
- **PI3K** 26
- **PTEN** 27
- **PKB** 27
- **GSK-3** 30
- **GLUT4** 30

1.4.6.2 Ras/MAPK pathways 31
1.4.6.3 CAP/Cbl pathway 31
1.4.6.4 Insulin-Independent Mechanisms 31
- **AMPK** 31

1.4.7 Cause of Insulin Resistance 33
1.4.8 Summary of Insulin Resistance 33

2. ASPALATHIN: A POLYPHENOL WITH PURPOSE 34

2.1 INTRODUCTION 34

2.2 ROOIBOS 34
2.2.1 Overview of Rooibos 34
2.2.2 Processing 35

2.3 ASPALATHIN 36
2.3.1 Overview of Aspalathin 36
2.3.2 Structure 37
2.3.2.1 Rooibos tea colouration 37
2.3.3 Aspalathin Synthesis 37

2.3.4 Bioavailability 38
2.3.4.1 Mechanism of Metabolism 39
2.3.4.2 Metabolites 39
2.3.4.3 Clinical Studies 39
2.3.4.4 Animal Toxicity 40
2.3.4.5 Human Toxicity 40
2.3.5 Aspalathin Function 40
2.3.5.1 Antioxidant Potential 40
- **In vitro** 41
- **In vivo** 42
- **Synergy between related compounds in rooibos** 42
- **Anti-ageing Effects** 42
2.3.5.2 Cardioprotection 43
2.3.5.3 Glucose Uptake 43
- **PKB-dependent mechanism** 43
- **AMPK-dependent mechanism** 43
2.3.5.4 Restore Glucose Homeostasis 44
- **Synergy between related compounds in rooibos** 44
2.3.5.5 Lipid Profile 44
2.3.5.6 Hyperuricemia 44
2.3.5.7 Anti-apoptotic 45
2.3.5.8 Antimutagenicity 45
2.3.5.9 Steroid metabolism 45

CHAPTER 3 - MATERIALS AND METHODS 46

1. MATERIALS 46

2. EQUIPMENT 47

3. METHODS 49

Aim 1 : Establish a Wistar Rat Model of Insulin Resistance and Obesity 49
1.1. Study design: grouping, feeding and treatment 49
1.2. Animal Care 50
1.3. Oral Glucose Tolerance Test 50
1.4. Intraperitoneal Fat 50
1.5. Insulin assay 50

Aim 2: Determine the possible efficacy and toxicity of using aspalathin to induce glucose uptake, in cardiomyocytes from: 53
2.1. Isolation of Cardiomyocytes 53
2.2. Cell Viability Assays 55
2.2.1. Trypan Blue Exclusion Assay 55
2.2.2. Propidium Iodide Staining 55
2.3. Glucose Uptake Assay 57
2.4. Lowry Protein determination 59

Aim 3: Determine the possible efficacy and toxicity of extended aspalathin treatment on differentiated cardiomyocytes derived from H9C2 cells: 60
3.1. Cell Culturing 60
3.1.1. Splitting of Cells 60
3.1.2. Trypan Blue Exclusion Assay 60
3.1.3. Mycoplasm Detection Assay 61
3.2. Differentiation of H9C2 Cells 61
3.3. JC-1 Staining 62
3.4. Metabolic Activity 63
3.5. Glucose Uptake Assay 64
3.6. Bradford Protein Determination 65

Aim 4: Understand the mechanism of action of aspalathin, by using: 66
4.1. General Preparation of Extracts for Western Blotting 66
4.2. Bradford Protein Determination 67
4.3. GLUT4 Translocation in Isolated Cardiomyocytes 68
4.4. Western Blot Analysis 71
4.4.1. Loading and separation of proteins 71
4.4.2. Protein transfer and visualization 71
4.5. Statistical analysis 72

CHAPTER 4 - RESULTS: MODEL OF DIET-INDUCED OBESITY AND INSULIN RESISTANCE 73

1. Characteristics of Young, Control and High-Fat, High-Caloric Diet Rats 73
1.1 Body Weight of Young, Control and HFD Rats 73
1.2 Visceral Adipose Tissue of Control and HFD Rats 74
1.3 Fasting Blood Glucose of Control and HFD Rats 75
1.4 Non-Fasting Blood Glucose of Young, Control and HFD Rats 76
1.5 Serum Insulin Levels of Control and HFD Rats 77

CHAPTER 5 - RESULTS: ASPALATHIN AND ISOLATED VENTRICULAR CARDIOMYOCYTES FROM YOUNG, CONTROL AND HFD RATS 78

1. Cell Viability Assays 78
1.1 Cell Viability of Isolated Adult Ventricular Cardiomyocytes from Young Rats after Isolation 78
1.2 Cell Viability of Isolated Cardiomyocytes from Young Rats after Treatments 79

2. Glucose Uptake Assays of Isolated Cardiomyocytes 82
2.1 Acute Aspalathin Dose Response of Cardiomyocytes from Young Rats 82
2.2 Acute Aspalathin and Insulin Dose Response in Cardiomyocytes from Y-Rats 83
2.3 Acute Insulin Dose Response of Cardiomyocytes from Young, Control and High-Fat, High-Sucrose Diet Rats 84
2.4 Acute Aspalathin and Insulin Response in Cardiomyocytes from Young, Control and High-Fat, High-Sucrose Diet Rats 85
2.4.1 Normalized to Basal 85
2.4.2 Absolute Amounts of Glucose Uptake 86
2.5 Extended Aspalathin AND Insulin Response in Cardiomyocytes from Young, Control and High-Fat, High-Sucrose Diet Rats 87
2.5.1 Normalized to Basal 87

2.5.2 Absolute Amounts of Glucose Uptake 88

CHAPTER 6 - RESULTS: ASPALATHIN AND DIFFERENTIATED H9C2 CELLS 90

1. Cell Viability Assays 90
1.1 Metabolic Activity of Differentiated H9C2 Cells After Treatment 90
1.2 Membrane Integrity of Differentiated H9C2 Cells After Treatment 91

2. Glucose Uptake Assay in Differentiated H9C2 Cells 93
2.1 Delayed Aspalathin and Insulin Response in Differentiated H9C2 Cells 93

CHAPTER 7 - RESULTS: THE MECHANISM OF ACTION OF ASPALATHIN 94

1. Insulin-Dependent Glucose Uptake Inhibition 94
1.1 Acute Aspalathin with Wortmannin In Isolated Cardiomyocytes from Young Rats . 94
1.2 Extended Aspalathin with Wortmannin In Isolated Cardiomyocytes from Control and HFD Rats 95

2. Protein Expression After Acute Aspalathin Treatment in Young Rats 96
2.1 Myocardial PKB Content and activation 96
2.2 Myocardial AMPK Content and activity 98

3. Protein Expression after extended Aspalathin Treatment in Young, control and HFD Rats 99
3.1 Myocardial PKB Content and Activity 99
3.2 Myocardial AMPK Content and Activation 102
3.3 Myocardial GLUT4 Content and Activity 104

CHAPTER 8 - DISCUSSION 109

1. Introduction 109

2. Characteristics of a high-fat, high-caloric diet 110

3. Acute (45 minutes) treatment with aspalathin 111
3.1 Cell Viability of Cardiomyocytes following the Isolation Protocol 111
3.2 Effects of acute aspalathin treatment on glucose uptake in cardiomyocytes isolated from young rats 111
3.3 Effects of acute aspalathin co-treated with insulin on glucose uptake in cardiomyocytes isolated from young and aged obese-insulin resistant rats 112

4. Extended (1h - 6h) treatment with aspalathin 113
4.1 Effects of chronic aspalathin co-treated with insulin in differentiated H9C2 cells . 113
4.2 Effects of extended aspalathin/insulin co-treatment on glucose uptake in young, control and HFD rats 114

5. Aspalathin's mechanism of action 114
5.1 PI3K-dependence 115
5.1.1 PKB-mediated effects 115
5.2 PI3K-independence 116
5.2.1 AMPK-mediated effects 116
5.2.2 AMPK and Ageing 117
5.3 Glut4-mediated effects 117
5.4 Antioxidant-mediated effects 118

6. Summary of findings 119

7. Study Limitations 121

CHAPTER 9 - CONCLUSION AND FUTURE RESEARCH 123

1. Conclusion 123

2. Perspectives for the Future 123

CHAPTER 10 - APPENDIX A 125

1. Secondary Factors contributing to Obesity 125
1.1 Inactivity 125
1.2 Unhealthy Diet 125
1.3 Pregnancy 125
1.4 Lack of Sleep 125
1.5 Medication 126
1.6 Medical Problems 126

2. Heart Disorders 127
2.1 Causes 127
2.2 Epidemiology 127
2.3 Treatments for Cardiovascular Diseases 127
2.3.1 Lifestyle Changes 128
2.3.2 Interventions 128
2.3.3 Medication 128

3. Investigating Heart Function 129
3.1 In vivo model (Whole Body Organism) 129
3.2 Ex vivo model (Isolated Hearts) 129
3.2.1 Rat and Mice Heart Models 129
3.3 In vitro model (Heart Cells) 130
3.3.1 Cardiac Cell Lines 130
3.3.2 Neonatal Cardiomyocytes 130
3.3.3 Adult Cardiomyocytes 131
- **Anaesthesia** 131
- **Animal Handling** 131
- **Excision of the Heart** 132
- **Cannulation of the Heart** 132
- **Perfusion Solutions** 133
- **Temperature of Perfusion** 133
- **Oxygen during Perfusion** 133
- **Calcium Paradox** 133
- **Enzymatic Digestion** 134

4. Alternative Pathways of Insulin-dependent Glucose Uptake 135
4.1. ERK Pathway 135
4.2. p38 Pathway 135
4.3. JNK Pathway 135

CHAPTER 11 - REFERENCES 137

LIST OF ILLUSTRATIONS

FIGURES

CHAPTER TWO

Figure 2.1 Body mass index classification according to metric height and weight 5
Figure 2.2 Anti-diabetic therapies and their method of action 9
Figure 2.3 AMP signals up- or downregulated by adenylate kinase in response to various processes. 12
Figure 2.4 Simplified Glucose Metabolism Overview 13
Figure 2.5 Glycolysis Pathway 14
Figure 2.6 Glucose Oxidation Pathway 15
Figure 2.7 Glycogen Synthesis Pathway. 16
Figure 2.8 Simplified Schematic of Insulin Resistance 19
Figure 2.9 Blood glucose tests used as indicator of insulin resistance in humans 21
Figure 2.10 Insulin Synthesis 22
Figure 2.11 Insulin Dependent and –Independent Pathways of Glucose Uptake 25
Figure 2.12 Insulin Receptor 26
Figure 2.13 Schematic of Protein Kinase B 27
Figure 2.14 Model of PKB activation and inhibition through PH-domain dependent mechanisms 28
Figure 2.15 Cellular Functions of PKB's Substrates 29
Figure 2.16 Molecular Structure of the AMPK complex 32
Figure 2.17 Major compounds present in rooibos tea 35
Figure 2.18 Structure of aspalathin and the root chemical structure, dihydrochalcone 37
Figure 2.19 Comparison of the aspalathin's free radical scavenging ability compared to other rooibos flavonoids 41

CHAPTER THREE

Figure 3.1 Study layout of animal groups and objectives 52
Figure 3.2 Standard Langendorff Isolation 53
Figure 3.3 Fluorescence-activated cell sorter 56
Figure 3.4 Standard protocol for glucose uptake after acute treatments 57
Figure 3.5 Extended protocol for glucose uptake after acute treatments 58
Figure 3.6 Glucose molecule compared to a 2DG molecule 59
Figure 3.7 Retinoic acid induces differentiation of H9C2 cells 62
Figure 3.8 JC-1 Staining Protocol 63

Figure 3.9 ATP Assay Protocol 64
Figure 3.10 Glucose uptake protocol in H9C2 cells 65
Figure 3.11 Standard experimental protocol to prepare lysates from cardiomyocytes 66
Figure 3.12 Simplified protocol to prepare lysates of cytosol and membrane fractions 68
Figure 3.13 Cell fractionation by differential centrifugation 70

CHAPTER FOUR

Figure 4.1 Body weight of rat models 73
Figure 4.2 Visceral fat of diet rat models 74
Figure 4.3 OGTT of rats on a 16 week control or high fat, high-sucrose diet 75
Figure 4.4 Non-fasting blood glucose prior to sacrificing of rats 76
Figure 4.5 Fasting serum insulin levels of control and HFD rats 77

CHAPTER FIVE

Figure 5.1 Cell viability of isolated cardiomyocytes from young rats 78
Figure 5.2 Effect of treatments on cell viability of isolated cardiomyocytes. 79
Figure 5.3 Dot plot representing total events acquired and final gated population of untreated isolated cardiomyocytes 80
Figure 5.4 Dot plot representing total events acquired and final gated population of treated isolated cardiomyocytes 81
Figure 5.5 2DG after 45 mins of aspalathin dose response in cardiomyocytes 82
Figure 5.6 2DG after 45 mins aspalathin and insulin dose response in cardiomyocytes 83
Figure 5.7 2DG uptake after 45 mins insulin dose response in cardiomyocytes from rat models 84
Figure 5.8 %2DG uptake after 45 mins aspalathin and insulin treatment in cardiomyocytes from rat models. 85
Figure 5.9 Absolute 2DG uptake after 45 mins aspalathin and insulin treatment in cardiomyocytes from rat models 86
Figure 5.10 %2DG uptake after 1-3h of treatment in cardiomyocytes from rat models 87
Figure 5.11 Absolute 2DG uptake after 1-3h of treatment in cardiomyocytes from rat models 88

CHAPTER SIX

Figure 6.1 Metabolic Activity (ATP Assay) after 3h of treatment 90
Figure 6.2 JC-1 Staining assay after 3h of treatment 91
Figure 6.3 JC-1 Staining assay of Differentiated H9C2 cells after 3h of treatment 92
Figure 6.4 2DG uptake in differentiated H9C2 cells after 3h and 6h of treatment 93

CHAPTER SEVEN

Figure 7.1 2DG uptake after inhibition of PI3K with wortmannin and stimulation with aspalathin and insulin in cardiomyocytes 94
Figure 7.2 2DG uptake after inhibition of PI3K with wortmannin and stimulation with aspalathin and insulin in cardiomyocytes. 95
Figure 7.3 PKB expression and activation in isolated cardiomyocytes from young rats after 15 minutes in vitro stimulation. 96
Figure 7.4 AMPK expression and activation in isolated cardiomyocytes from young rats after 15 minutes in vitro stimulation. 98
Figure 7.5 Treating cardiomyocytes with 10nM insulin for 1 h 30 mins, leads to overexpression and activation of PKB compared to baseline 99
Figure 7.6 PKB expression and activation in isolated cardiomyocytes from young, control and HFD rats after 1h 30 mins in vitro stimulation with aspalathin. 100
Figure 7.7 PKB expression and activation in isolated cardiomyocytes from young, control and HFD rats after 1h 30 mins in vitro stimulation with aspalathin plus insulin. 101
Figure 7.8 Representative blot of AMPK expression and activation in young, control and HFD rats. 102
Figure 7.9 AMPK expression and activation in isolated cardiomyocytes from young, control and HFD rats after 1h 30 mins in vitro stimulation 103
Figure 7.10 GLUT4 expression in cytosolic and membrane fractions obtained from young, rat cardiomyocytes. 104
Figure 7.11 GLUT4 expression in cytosolic and membrane fractions obtained from young, age-matched control and HFD rat cardiomyocytes. 105
Figure 7.12 GLUT4 expression in membrane fractions obtained from young, age-matched control and HFD rat cardiomyocytes. 107
Figure 7.13 GLUT4 expression in cytosolic fractions obtained from young, age-matched control and HFD rat cardiomyocytes. 108

CHAPTER EIGHT

Figure 8.1 Aspalathin's proposed mechanism of action to induce glucose uptake in cardiomyocytes 118

CHAPTER TEN

Figure 10.1 Cannulation of the rat heart 132
Figure 10.2 Langendorff apparatus 134

TABLES

CHAPTER TWO

Table 2.1 Aspalathin and nothofagin content of unfermented (green) and fermented (traditional) rooibos tea (Joubert & Schulz, 2006)..... 36

CHAPTER THREE

Table 3.1 Diet composition of Control and High-Fat, High-Sucrose Diet..... 49
Table 3.2 Buffer Compositions used in Isolation Protocol..... 54
Table 3.3 Buffer and Gel Compositions used in Western Blotting Protocol..... 67
Table 3.4 Optimized protocol for each primary and secondary antibody..... 72

CHAPTER FOUR

Table 4.1 Characteristics of Animal Models 77

CHAPTER FIVE

Table 5.1 Cell viability after 1 or 3 hours of treatment..... 79

LIST OF ABBREVIATIONS

I. UNITS OF MEASUREMENT

% : percentage

°C : degree celcius

bpm : beats per minute

cm : centimeter

CPM : counts per minute

DPM : disintegrations per minute

g: gram

Hg : mercury

IU : International unit

kg : kilogram

kJ : kilojoules

L : litre

M : molar

mA : milliampere

mg : milligram

min : minute

mm : millimeter

mM : millimolar

mmol : millimol

p : pico

rpm : revolutions per minute

sec : second

V : volt

v : volume

α : alpha

β : beta

ζ : zeta

λ : lambda

μ : micro

μL : microlitre

μm : micrometer

II. CHEMICAL COMPONENTS

2,3-BDM : 2,3-butanedione monoxime

2DG : 2-deoxy-D-3[H] glucose

Acrylamide : N,N'-Methylenebisacrylamide

ALP : Alkaline phosphatase

ALT : Alanine transaminase

Ca^{2+} : Calcium

$CaCl_2$: Calcium chloride

CO_2 : Carbon dioxide

$CuSO_4$: Copper sulfate

dH_2O : Distilled water

DMSO : Dimethyl sulfoxide

$DPPH^{\bullet}$: 2,2-diphenyl-1-picrylhydrazyl free radical

EDTA : Ethylenediaminetetraacetic acid

EGTA : Ethyleneglycoltetraacetic acid

H_2O : Water

HCl : Hydrochloric acid

HEPES : 4-(2-hydroxyethyl)-1-piperazineethanesulfonic acid

JC-1 : 5,5',6,6'-tetrachloro-1,1',3,3'-tetraethylbenzimidazole-carbocyanide iodine

KCl : Potassium chloride

KH : Krebs-Henseleit buffer

KH_2PO_4 : Potassium dihydrogen phosphate

$MgSO_4$: Magnesium sulphate

Na^+ : Sodium

Na^+K^+-tartrate : Sodium potassium tartrate

Na_2CO_3 : Disodium carbonate

Na_2HPO_4 : Disodium hydrogen phosphate

Na_2SO_4 : Sodium sulphate

Na_3VO_4 : Sodium orthovanadate

NaCl : Sodium chloride

NaH_2PO_4 : Sodium dihydrogen phosphate

$NaHCO_3$: Sodium bicarbonate

NaOH : Sodium hydroxide

NO : Nitric oxide

O_2 : Oxygen

$O_2^{\bullet}$: Superoxide radical

PI : Propidium iodide

PMSF : Phenylmethyl sulfonyl fluoride

SDS : Sodium dodecyl sulfate

STZ : Streptozotocin

TBS : Tris-buffered saline

TEMED : N,N,N',N',-tetramethylethylendiamin

TTC : Triphenyltetrazolium chloride

III. PROTEIN ABBREVIATIONS

ADP : Adenosine diphosphate
ADP : Adenosine diphosphate
AGE : Advanced glycation end products
AICAR : 5-aminoimidazole-4-carboxamide-1-beta-D-ribofuranoside
AID : Autoinhibitory domain
AMP : Adenosine monophosphate
AMPK : AMP-activated protein kinase
AS160 : Akt substrate of 160 kDa
ATP : Adenosine triphosphate
ATP : Adenosine triphosphate
BAD : Bcl-2-associated death promoter
BSA: Bovine serum albumin
CAMKKβ : Calcium-calmodulin-activated protein kinase β
cAMP : Cyclic adenosine monophosphate
CD : Conjugated dienes
CK2 : Casein kinase 2
CPT-1 : Carnitine palmitoyl transferase-1
DNP : 2,4-dinitrophenol
ER : endoplasmic reticulum
ERK : Extracellular signal regulated kinase
FADH : Flavin adenine dinucleotide
FBS : Fetal bovine serum
FFA : Free fatty acids
FITC : Fluorescein isothiocyanate
FOXO3 : Forkhead box O3
G-1-P : Glucose-1-phosphate
G-6-P : Glucose-6-phosphate
GAP : GTPase-activating protein
GIP : glucose-dependent insulinotropic polypeptide
GLP-1 : Glucagon-like peptide 1
GLUT1/4 : Glucose transporter 1/4
GS : Glycogen synthase
GSH : Glutathione
GSK-3 : Glycogen synthase kinase-3
GSSG : Glutathione disulfide
GTP : Guanosine triphosphate
HDL : High-density lipoproteins
HDL-C : High-density lipoproteins cholesterol
HRP : Horseradish Peroxidase
IgG : Immunoglobulin G
IL-6 : Interleuken-6
IR : Insulin receptor
IRS : Insulin receptor substrate
JNK : c-Jun N-terminal kinase
KD : Kinase domain
LDL-C : Low-density lipoproteins cholesterol
LKB1 : Liver kinase B1
MAPK : Mitogen activated protein kinase
mPTP : Mitochondrial permeability transition pore
mTOR : Mammalian target of rapamycin
NAC : N-acetyl-cysteine
NADH Nicotinamide adenine dinucleotide
NOS : Nitric oxide synthase
PARP : Poly ADP-ribose polymerase
PC : Prohormone convertases
PDH : Pyruvate dehydrogenase
PDK-1 : Phosphoinositide-dependant kinase 1
PFK-1 : Phosphofructokinase-1
PH : Pleckstrin homology
PI : Propidium iodide
PI3K : Phosphatidylinositol 3 kinase
PIP2 : (Ptdlns(4,5)P2) Phosphatidylinositol (4,5) bisphosphate
PIP3 : (Ptdlns(3,4,5)P3) Phosphatidylinositol (3,4,5) triphosphate

PKA : Protein kinase A (cyclic AMP-dependent protein kinase)
PKB : Protein kinase B
PKC : Protein kinase C
PPAR-γ : Peroxisome proliferator-activated receptor γ
PPase : Protein phosphatases
P-PKB : Phospho-Protein kinase B
PS : Penicillin-Streptomycin
PTEN : Phosphatase and tensin homolog deleted on chromosome 10
RER : Rough endoplasmic reticulum
Ser : Serine
SH-2 : Src homology 2
SHIP : Src homology 2 domain containing inositol 5' phosphatase 2
SR : Sarcoplasmic reticulum
TAG : Triacylglycerols
TBARS : Thiobarbituric acid reactive substances
Thr : Threonine
TNF-α : Tumor necrosis factor-α
UDP-glucose : Uridine-5'-diphosphate glucose
VLDL : Very low-density lipoproteins
XOD : Xanthine oxidase

IV. OTHER ABBREVIATIONS

ARC : Agricultural Research Council
ARF : Aspalathin-enriched fractions
BAT : Brown adipose tissue
BC : Before Christ
BMI : Body Mass Index
CDC : Center for Disease Control and Prevention
CT : Computerized Tomography
CVD : Cardiovascular disease
DCM : Diabetic cardiomyopathy
DDP : Diabetes Discovery Platform
DEXA : Dual Energy X-ray Absorptiometry
DIO : Diet-induced-obesity
DMEM : Dulbecco's modified Eagle's medium
ECACC: European Collection of Cell Cultures
ECL : Enhanced chemiluminescence
FA : Fatty acids
FACS : Fluorescence-activated cell sorting
FFA : Free fatty acids
FRE : Fermented rooibos extract
GRE : Green rooibos extract
HIC : High income countries
HMIC : Higher middle income countries
HOMA-IR : Homeostasis model assessment of insulin resistance
HPLC-DAD : High Performance Liquid Chromatography – Diode Array Detector
HR : Heart rate
IFG : Impaired fasting glucose
IFS : Infarct size
IGT : Impaired glucose tolerance
IHD : Ischemic heart disease
IPGTT : Intraperitoneal glucose tolerance test
IR : Insulin resistance
LIC : Low income countries
LMIC : Lower middle income countries
MRC : Medical Research Council
MRI : Magnetic Resonance Imaging
NCDs : Non-communicable Diseases
NIH : National Institutes of Health
PVDF : Polyvinylidene fluoride
QC : Quality Control
ROS : Reactive oxygen species
RSA : Republic of South Africa
SAT : Subcutaneous adipose tissue
SDS-PAGE : Sodium dodecyl sulphate-polyacrylamide gel electrophoresis
SEM : Standard error of the mean
T2D : Type 2 Diabetes
UK : United Kingdom
USA : United States of America
VAT : Visceral adipose tissue
WHO : World Health Organization

MOTIVATION FOR RESEARCH

- **Obesity and Insulin Resistance Concerning Risk Factors for Cardiovascular Disease**

Obesity is currently classified as a pandemic and recognized as one of the leading causes in the development of the metabolic syndrome, a cluster of pathophysiological conditions giving rise to cardiovascular disease (Grundy, 2004). Conditions related to the metabolic syndrome also include insulin resistance or glucose intolerance (pre-diabetes), hypertension, atherogenic dyslipidaemia and proinflammatory states. These indicators lead to non-communicable diseases (NCDs) and chronic diseases such as heart disease, stroke, cancer, respiratory disease and diabetes. As the leading cause of death globally, NCDs were responsible for 38 million (68%) of the world's 56 million deaths in 2012. More than 40% of them (16 million) were premature deaths under the age of 70 years. Almost three quarters of all NCD deaths (28 million), and the majority of premature deaths (82%), occur in low- and middle-income countries (Global Status Report on Noncommunicable Diseases, World Health Organization, 2014). In South Africa, cardiovascular disease is currently the 4th leading cause of death (4.7%) (Statistics South Africa, 2011). Recently, there has been a shift towards research into natural products, including plant extracts (concentration of active compounds in plants), phytochemicals (isolation of active compounds in plants) and microbial metabolites (isolation of microbes present in plants) (Lahlou, 2013). These products are increasingly getting recognized for their potential in treating and preventing the metabolic syndrome, and subsequent type 2 diabetes (T2D) and cardiovascular diseases.

- **Rooibos Beneficial for Cardiovascular Health**

Rooibos (*Aspalathus Linearis*) is an indigenous herbal tea of South Africa. Traditionally, rooibos has been used as a treatment or ointment for alleviating stress-related ailments such as insomnia and anxiety. Rooibos has been shown to exhibit antioxidant potential, antimutagenicity and improve cardiovascular health in humans (Van der Merwe et al., 2006; Marnewick et al., 2011). Furthermore, it has been demonstrated that rooibos resensitized insulin signalling in C2C12 skeletal muscle cells, via specific biochemical pathways, including Protein Kinase B (PKB) and through activation of the insulin-independent Adenosine Monophosphate Protein Kinase (AMPK) pathway, which culminated in increased levels of glucose uptake via the Glucose Transporter 4 (GLUT4) (Mazibuko et al., 2013).

- **Rooibos' Aspalathin Promising**

Aspalathin is a unique, primary polyphenol present only in rooibos. It has been implicated as one of the main contributors of rooibos' antioxidant potential (Joubert et al., 2009; Dludla et al., 2014) and could also prove essential in eliciting rooibos' other therapeutic effects. Kawano et al. (2009) recently reported that aspalathin improved glucose uptake in muscle cells and insulin secretion from pancreatic β-cells. These findings were confirmed by Son et al. (2013) who also reported that aspalathin increased glucose uptake in L6 myotubes by increasing AMPK phosphorylation and GLUT4 translocation to the membrane. Further, in *ob/ob* mice, aspalathin reduced fasting blood glucose levels, and reduced hypertriglyceridaemia by reducing enzymes related to gluconeogenesis, glycogenolysis and lipogenesis. No research has been performed to date to determine the cardiovascular consequences of aspalathin treatment.

- **We have plenty of Aspalathin :)**

A recent patent, claiming aspalathin for the prevention and treatment of T2D has been awarded to our members of Diabetes Discovery Platform (DDP) of the South African Medical Research Council (SA MRC) and the Agricultural Research Council at Stellenbosch (ARC) in collaboration with the University of Free State (UFS). This method is currently the only protocol whereby aspalathin can be synthesised in the required 5 steps or less, providing a unique opportunity for research using synthetically produced pharmaceutical grade aspalathin. This product has the potential to be developed into an effective therapy in preventing and managing the metabolic consequences associated with obesity and T2D, and thereby contribute to the health of South Africans.

GENERAL AIM

We propose to use aspalathin to induce glucose uptake in heart cells isolated from various rat models, including young rats, a 16 – 30 week diet induced obesity and insulin resistant group, and their age-matched controls. The secondary aim is to understand the mechanism of actions of aspalathin and to ensure its effectiveness and safety using cell culture and rat models.

CHAPTER 1

LAYMAN'S OVERVIEW OF THE THESIS

We are all aware that too much of anything, is a bad thing. In the case of type 2 diabetes, too much glucose in the blood, can give rise to various problems, including insulin insensitivity, damaged nerves and arteries, and all of these increase your risk for heart attacks and strokes. It is estimated that people with type 2 diabetes are 4 times more likely to die of heart disease or stroke, and at least 65 percent of people with type 2 diabetes die from these complications. In 2012 alone, 1.5 million deaths globally were attributed to diabetes. All of this being said, type 2 diabetes remain one of the major controllable risk factors for cardiovascular disease. So, how do we control diabetes? Quite simply, as always: Through diet; and exercise. However, if healthy living fails, it becomes the hope of medicine together with ongoing research to prevent further deterioration of health in diabetic patients. Various medications are already prescribed to treat type 2 diabetes, each with it's own set of pros and cons. Each of these medications have a different mode of action, including: enhancing insulin action in peripheral tissues, enhancing the amount of insulin secreted by the body, suppressing glucose production, and also by delaying the absorption of carbohydrates after meals. The biggest problem with these medications are that they are only treatments, but not in themself a cure. There is also high costs involved with being dependent on these medications, and prolonged use can carry the risk of weakening the heart and causing liver toxicity.

The diabetic journey brings us to our humble country, where rooibos might bring new hope. Rooibos or *aspalathin linearis* is indigenous to the Western Cape region of South Africa. The plant is most commonly consumed as a herbal infusion, by which hot water is added to the "fermented" rooibos tea to extract the inherent polyphenols. It has been shown, however, that through the process of fermentation the polyphenolic content of the plant is severely diminished, consequently reducing the plants' antioxidant capacity. Lately, there has been a shift towards consuming the green or unfermented rooibos and it's also the grade of choice when isolating aspalathin. Of the various compounds within rooibos, aspalathin is the most prominent polyphenol and the biggest contributor to rooibos' beneficial effects. Aspalathin was first isolated and characterised in 1965 by Koepen and colleagues and since then has amounted about 60 mentions in research, alot of which were studies done with fermented and unfermented rooibos. Of these articles, about 33 are of direct relevance to this research. The major effects attributed to aspalathin is its strong antioxidant capacity, and also its ability to stimulate glucose uptake in skeletal muscle cells.

In the present study, we investigated whether asplathin can induce glucose uptake in cardiomyocytes from both healthy and compromised heart cells. And if so, through which cellular mechanism does this occur? I made use of three groups of animals:

(i) Young controls of at least 220g and 6-7 weeks of age

(ii) One group with 16 – 30 week diet-induced obesity and insulin resistance; and

(iii) Age-matched control group. Groups (ii) and (iii) were 22-36 weeks of age.

The first part of all the experiments is to isolate the cardiomyocytes. We do this by using a Langendorff perfusion system, by which we use solutions with enzymes, such as collagenase to perfuse and digest the dissected heart. The cardiomyocytes can then be stabilized and used in subsequent experiments. To determine glucose uptake, cells were treated with radioactive 2-deoxyglucose and analyzed using liquid scintillation counting.

First, we tried to establish an aspalathin dose response in cardiomyocytes of young control rats. We could not find a direct stimulation of glucose uptake by aspalathin, and to the contrary it appeared to inhibit the glucose uptake. To test for the cytotoxic effects of DMSO, used as solvent for synthetic aspalathin, we performed a cell viability assay using propidium iodide. There was no significant difference in cell viability between the treatment groups and the observed suppression in glucose uptake was not due to DMSO, but possibly through some other responsive mechanism. Next, we tried to see whether asplathin might have an indirect effect on glucose uptake through stimulation of insulin. 10μM aspalathin was able to increase glucose uptake in conjunction with 10nM Insulin.

Then we moved on to the animal models, and first had to determine that the high-fat, high -sucrose diet did in fact cause hyperglycemia, obesity and insulin resistance. An oral glucose tolerance test, fasting blood glucose and non-fasting blood glucose all showed elevated blood glucose levels in diet rats compared to controls. The diet rats also had significantly higher total body weight and intraperitoneal fat compared to controls. The young rats had the most sensitive response to insulin, followed by our age-matched control groups that also had a healthy response. The high-fat, high-carbohydrate diet had a weak response to increasing concentrations of insulin, and was deemed insulin resistant. A preliminary study done on cardiomyocytes from the diet rats, showed no significant differences when treated with aspalathin.

We made use of embryonic rat-heart derived H9C2 cells to verify whether aspalathin can induce glucose uptake independent of insulin as this was previously published. Initially, these cells are immortal cells, but once differentiated by reducing the amount of serum in the culture medium and adding Retinoic Acid, the cell's nuclei start to "clump together" and they have a closer resemblance

to the isolated cardiomyocytes. Glucose uptake in differentiated H9C2 cells was assayed for 3 and 6 hours, and for both instances, aspalathin induced a significant increase in glucose uptake, with 6 hours being more pronounced.

Returning to the rat models, we extended our experiments to 3 hours in the isolated cardiomyoctes. Surprisingly, incubating the aspalathin for a mere 30 mins longer than the previous experiments, had a significant increase in glucose uptake in young controls, while the effect in conjunction with insulin was even more pronounced. This was also evident in older controls with aspalathin inducing a significant increase in insulin-mediated glucose uptake. The high fat diet group showed no significant increases when treated with aspalathin. Also, no effect was visible after 1 and a half hours of treatment.

The mechanism by which aspalathin induced this slight increase in myocardial glucose uptake by western blot analysis was investigated. In particular, the markers of interest were: Protein Kinase B (PKB), an insulin-dependent, pro-'life', growth marker; and Adenosine Monophosphate Protein Kinase (AMPK) – the body's key metabolic regulator, which is an insulin-independent marker of glucose uptake quite central to all cell signaling. PKB activation was significantly increased in young rats treated for 15 minutes with both insulin and aspalathin. This effect was also observed when comparing the ratio of activated PKB to the total amount of PKB expressed. After 1 and a half hour of treatment, PKB activation was also significantly increased with aspalathin together with insulin in young rats. No significant differences were found for the older diet rats. Aspalathin significantly increased AMPK activation WITH insulin, as well as increased the expression of AMPK in young rats after 15 minutes of stimulation. Aspalathin increased the phospho-to-total ratio of AMPK in young rats, possibly explaining the mechanism by which aspalathin induced glucose uptake at the hour and a half time point. Also, both expression and activation of AMPK was elevated in aged-diet controls compared to young controls. This might point towards AMPK becoming a more prominent metabolic regulator as ageing progresses.

In summary, the high-fat, high-sugar diet was an effective model to induce insulin resistance in rats. Aspalathin induces myocardial glucose uptake directly in young rats and indirectly through mediating insulin's action in aged control rats. The possible mechanism for this is through activation of PKB and increasing the expression and activation to expression ratio of AMPK. Aspalathin had no significant effect when used as treatment in heart cells from high-fat, high-caloric diet rats.

CHAPTER 2
LITERATURE REVIEW

1. OBESITY AND INSULIN RESISTANCE FROM THE HEART'S PERSPECTIVE

1.1 INTRODUCTION

Cardiovascular diseases (CVD) are the leading cause of death worldwide, constituting 31% of all annual global deaths (17.5 million people) (Cardiovascular Diseases, WHO, 2015). This shocking figure is in part aggravated by the presence of individual risk factors such as obesity (excessive energy storage) and insulin resistance (declining ability to utilize blood glucose in the presence of a given level of insulin). Under normal physiological conditions, the heart's contractile function enables circulation of nutrient rich blood through the arteries and veins of the entire body. The heart also relies on these nutrients, including glucose and free fatty acids, as energy substrates for its contracting cardiomyocytes. The rate at which nutrients are transported into all cells and used as substrates is heavily dependent on the action of the hormone, insulin. Insulin induces anabolic processes through activating energy consumption, while simultaneously counterbalancing blood glucose levels. However, in diseased conditions, such as type 2 diabetes (T2D), various complications start to arise hindering the heart's performance. Ineffective clearing of blood glucose, primes the pancreas to increase insulin production in order to compensate for elevated blood glucose levels, and when this state progresses, insulin receptors become so desensitized that the pancreas cannot maintain sufficient insulin levels (Shanik et al., 2008). The effect of a decreased insulin potential detrimentally affects peripheral insulin sensitive organs, namely the muscle, fat and liver . According to Kannel & McGee (1979), a prolonged insulin desensitized state leads to a 4-fold increase for the risk of developing coronary heart disease and strokes. Furthermore, as a direct consequence of obesity, meaning having excess fat mass, higher levels of circulating free fatty acids and cholesterol are also present in the blood. These can cause a plaque build-up inside arteries, narrowing or completely blocking blood flow (Kwan et al., 2014). Arguably, the slightest reduction in blood flow to the heart is severely detrimental to the heart's function.

1.2 OBESITY

1.2.1 OVERVIEW OF OBESITY

Obesity and overweight are defined as abnormal or excessive fat accumulation that presents a risk to health (Obesity, WHO, 2015). These two related conditions can severely alter metabolism and contribute to a cluster of pathophysiological conditions, collectively called the metabolic syndrome (Grundy, 2004). Furthermore, the risk of cancer, coronary heart disease, ischemic stroke and T2D also increase as the severity of obesity increases (Chamie et al., 2013; Eckel, 1997; Saboor Aftab et al., 2014). Essentially, a body fat percentage of at least 3-5% in men and 12-15% in women is

required for healthy functioning. The fats are stored in all major tissue types and are especially essential in maintaining hormonal balance and pregnancy in women (Kotecki, 2011). Additional fat is retained in adipose tissue (fat cells) which protects internal organs against impact trauma, insulate the body to prevent temperature fluctuations and serve as reserve energy stores. Specifically, brown adipose tissue (BAT) dissipates chemical energy in response to cold and overfeeding and can modulate energy balance (Stanford et al., 2012). Under normal physiological conditions, it is estimated that adipose tissue account for <5% of glucose clearance (Thiebaud et al., 1982). Furthermore, adipose tissue is also a metabolically active endocrine organ and produces biologically active substances, including pro-inflammatory cytokines, angiotensin II, leptin, resistin and adiponectin (Kershaw & Flier, 2004). Continually having an excess intake of calories (energy) compared to what the body is able to utilize by regular daily metabolic demands, results in the storage of these excess calories in the adipocytes, contributing to body weight gain and eventual obesity. The secondary contributing factors are physical inactivity, an unhealthy diet, pregnancy, lack of sleep, as well as certain medical conditions and medications (**Appendix A – Secondary Causes of Obesity**).

1.2.2 Assessment

A crude method of determining obesity is given by the body mass index (BMI), in which a person's weight (in kg) is divided by the square of their height (in meters) (Center for Disease Control and Diabetes, 2009). A BMI between 25 and 30 kg/m^2 is considered overweight, whereas a BMI of above 30 kg/m^2 is classified as obese (**Figure 2.1**).

BMI (kg/m^2)	Weight Status
Below 18.5	Underweight
18.5-24.9	Normal
25.0-29.9	Overweight
30.0-34.9	Obese (Class I)
35.0-39.9	Obese (Class II)
40.0 and higher	Morbidly Obese (Class III)

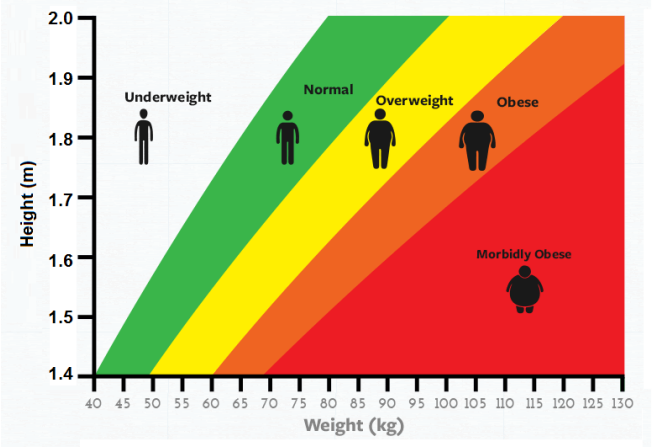

Figure 2.1 Body mass index classification according to metric height and weight (Obtained from Global Diabetes Community, 2015).

However, total body mass constitutes fat mass and lean body mass (muscle, bone, organ tissue, blood). Therefore, BMI alone can not indicate total amount of body fat since it does not distinguish between fat and lean body mass. This makes the test unreliable in classifying young people,

pregnant women and muscular patients, such as professional athletes. Health experts use BMI in conjunction with a measure of percentage body fat and body proportions to assess health risk. These assessments include:

- waist circumference (circumference of natural waist)
- waist-to-hip ratio (waist circumference divided by hip circumference) (Noble, 2001)
- skinfold thickness (measure subcutaneous fat using calipers) (Gray, 1990)
- underwater weighing (body density measurement) (Kotecki, 2011)
- bio-electrical impedance (electrical current passed through body to determine electrical impedance, which serves as a measure of total body fat) (Gray, 1990).

Additional tests, used only in research settings and to confirm the accuracy of above mentioned techniques, include Dual Energy X-ray Absorptiometry (DEXA) (X-ray beams used to distinguish between fat-free mass, fat mass and bone mineral density), Computerized Tomography (CT) (X-ray images used to generate cross-sectional and three-dimensional images of internal organs and structures) and Magnetic Resonance Imaging (MRI) (protons/hydrogen atoms in water molecules of different tissues detected and used to construct three-dimensional image of entire body composition) (Hu, 2008). To date, the most accurate assessment of body composition is given by CT and MRI scans.

1.2.3 Epidemiology

Annually, 2.8 million people die as a consequence of being overweight or obese (Obesity, WHO, 2015). In 2008, 35% of adults worldwide over the age of 20 were overweight, and an estimated 205 million (3%) men and 297 million (4%) women over the age of 20 were obese.

1.2.3.1 Children and Adolescence

Obesity is a growing concern amongst children and adolescence. Globally, the prevalence of overweight and obese infants and young children (0 to 5 years of age) increased from 32 million in 1990 to 42 million in 2013 (Obesity, WHO, 2015). In Africa, the number of overweight or obese young children more than doubled, from 4 million to 9 million children. In developed countries, such as the United States, childhood obesity (6 – 11 years of age) increased from 7% in 1980 to 18% in 2012, while adolescent obesity (12 – 19 years of age) also increased from 5% to 21% in this period. These figures estimate that over one third of all children and adolescents in the United States are overweight or obese (Ogden et al., 2014). No current data exists for the developing world, but regardless, without therapeutic intervention, obesity will likely proceed into childhood, adolescence and adulthood.

1.2.3.2 Socio-economic Status

Additionally, a country's socio-economic status also influences the prevalence of obesity as was determined by Pampel et al. (2012). They sampled 67 different countries around the world and classified them as either low-income and low middle-income countries (LIC and LMIC) or high middle- and high-income countries (HMIC and HIC) – South Africa is classified as a HMIC. They found that the higher the country's income level, the higher the prevalence of raised BMI's. HMIC and HIC had an overweight prevalence of more than double that of LIC and LMIC. For obesity, the prevalence more than triples from 7% obesity in LMIC to 24% in HMIC. In LIC and LMIC, obesity was twice as prevalent in women as in men, whereas it was similar in high-income countries.

The increasing trend of overweight individuals also hinders the overall health of a population. Overweight individuals present with an array of chronic conditions and can suffer premature mortality. This trend is prevalent in developed countries, and is becoming an increasing concern in developing countries as well (Popkin, 2009). Even though socio-economic development advances our management of health, it also creates new problems. For instance, in higher income countries, the dilemma of malnutrition is systematically replaced by overconsumption (Pampel et al. 2012). Arguably, the group to be most severely impacted by this growing trend of obesity, will be those least financially advantaged.

1.2.4 Obesity-related Conditions

1.2.4.1 Coronary Heart Disease and Strokes

Obesity is not just a superficial term for excess weight, but has long-standing health implications. As your severity of obesity increase, so too does your risk for coronary heart disease (CHD) – the leading cause of CVD (Cardiovascular Disease, WHO, 2015). CHD is the consequence of a sustained plaque build-up in the coronary arteries which supplies the heart with oxygen-rich blood (National Institutes of Health, 2015). As the arteries narrow, blood supply to the heart is reduced causing chest discomfort and could possibly trigger a heart attack when coronary arteries are completely blocked. Similarly, an overworked heart can fail completely, preventing adequate blood supply to meet the body's needs. Another implication of obesity-induced plaque buildup is the potential rupture of a plaque region, forming blood clots. These clots can cause a stroke by blocking off oxygenated blood flow to the brain, causing irreversible neuronal damage or premature deaths.

1.2.4.2 Metabolic Syndrome

Metabolic syndrome (or insulin resistance syndrome) refers to a collection of conditions prevalent in overweight and obese individuals that have been known to increase the risk for CVD and T2D. The characteristics include:

- large waist size (≥102cm for men, ≥89cm for women)

- elevated blood triglycerides (≥150mg/dL)
- abnormal blood cholesterol (HDL cholesterol of ≥40mg/dL for men or ≥50mg/dL for women)
- high blood pressure (≥130/85)
- high blood glucose levels (fasting blood glucose level ≥100mg/dL or ≥5.6mmol/L)

Metabolic syndrome is the prevalence of at least 3 of these characteristics and besides CVD and T2D, have also been linked to non-alcoholic fatty acid liver disease, chronic kidney disease and polycystic ovary syndrome (a condition which detrimentally affect women's hormone levels and ovulation cycle) (Alberti et al. 2009).

1.2.4.3 DIABETES

- **DIABETES OVERVIEW**

Diabetes mellitus has become one of the most common metabolic diseases worldwide (Wild et al., 2004). The disease can be sub-divided into Type 1, Type 2 or gestational diabetes. Type 1 diabetes (T1D) is an autoimmune disease that selectively targets the destruction of pancreatic β-cells, leading to an inability to produce sufficient insulin to meet the body's energy demands. Type 2 diabetes (T2D) on the other hand, is the result of a decline in insulin sensitivity of peripheral insulin sensitive tissues, such as the liver, adipose tissue and muscle (DeFronzo, 1999). This results in an overexpression of insulin, exacerbated β-cell function and an eventual inability to effectively clear blood glucose. Initially it was proposed that diabetic patients present solely with insulin resistance, rather than insulin deficiency (Himsworth, 1936). However, it is now understood that both insulin resistance together with impaired β-cell function is essential in the disease progression of T2D. The third most common type of diabetes, gestational diabetes, is defined as having a degree of glucose intolerance during pregnancy (Metzger & Coustan, 1998). Gestational diabetes is prevalent in approximately 7% of all pregnancies, especially during the third trimester (24 – 28 weeks of gestation) and increases the risk of developing T2D post-pregnancy (American Diabetes Association, 2003). T2D has a much higher incidence (about 95% of all cases of diabetes) and is usually connected to obesity. Typically, T1D is predominantly diagnosed in younger people, while older individuals are diagnosed with T2D, but recent years have indicated a growing trend in younger people developing T2D as well (Huang et al., 2009). Futhermore, the genetic make-up of a person also contributes to the development of diabetes – T1D and T2D is dependent on the control of multiple genes together with the epigenetic changes caused by a person's environment. Some forms of diabetes, for example maturity-onset diabetes (Fajans et al., 2001) and neonatal diabetes (Støy et al, 2010), are the direct effect of a single gene mutation that alters pancreatic β-cells. These single-gene disorders account for less than 2% of cases. In general, the multiplicity of genes responsible for T2D makes risk assessment and therapeutic interventions based on genetic make-up problematic.

- **TREATMENT**

Maintaining blood glucose levels is the primary concern when treating diabetes and preventing further complications (Polonsky, 2012). T1D can also be managed with dietary changes and exercise (Eiselein et al., 2004), but the most prominent treatment for T1D still remains injectable insulin, which remains the only treatment proven safe and effective after clinically significant pancreatic β-cell destruction. Additionally, T2D treatments also include non-insulin oral antidiabetic medications, comprising of sulfonylureas, biguanides, α-glucosidase inhibitors, and thiazolidinediones. Each class of medication has a unique mechanism of action (**Figure 2.2**):

- sulfonylureas increase insulin production by the pancreatic β-cells (Raptis & Dimitriadis, 2001);
- metformin (biguanide) increases the liver's insulin sensitivity and restores its glucose metabolism (Viollet et al., 2012);
- α-glucosidase inhibitors delay the absorption of carbohydrates from the gastro-intestinal tract (Willms et al., 1991);
- thiazolidinediones increase insulin sensitivity in peripheral tissues, such as the muscles and fat cells (Kahn et al., 2000).

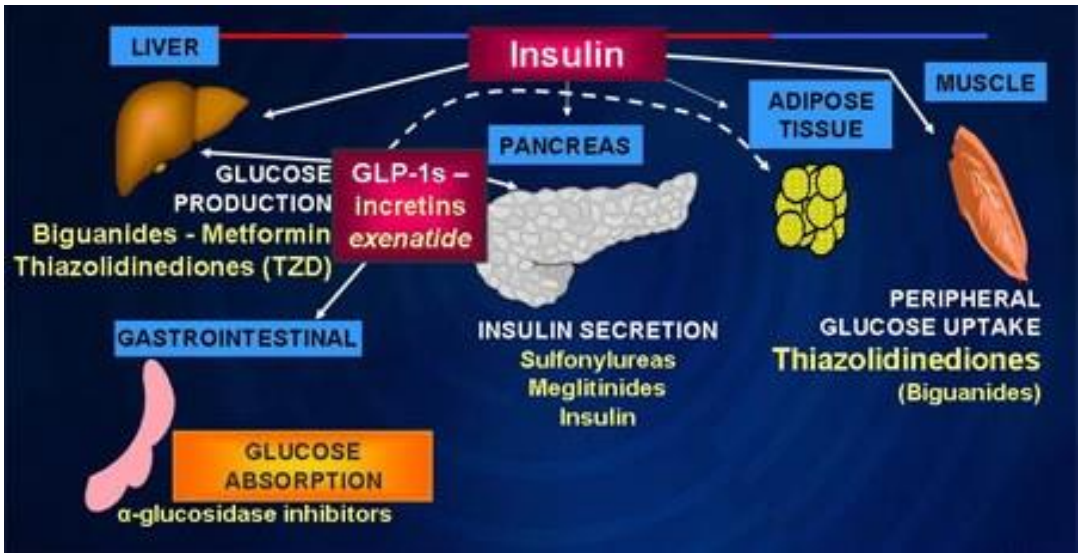

Figure 2.2 Anti-diabetic therapies and their method of action (Obtained from Beaser et al., 2015).

The different oral agent classes have different effects on basal insulin and postprandial glucose – effects which only become apparent as T2D progresses. The latest drugs available for treating T2D are incretins, such as glucagon-like peptide-1 (GLP-1) – a gastrointestinal hormone that increase insulin production in β-cells (Kjems et al., 2003). Similarly, dipeptidyl peptidase-4 (DDP-4) inhibitors can be used to delay the breakdown of GLP-1 (Dicker, 2011). All of the above have, however, been linked to a variety of serious adverse health effects, prompting a search for safer natural hypoglycemic agents to be used (Patel et al., 2012).

1.2.4.4 OTHER CONDITIONS

Obesity is related to an increased risk for cancer, specifically colon, breast, endometrial and gallbladder cancers (Vucenik & Stains, 2012). As mentioned as part of the metabolic syndrome, obesity is also associated with increased risk for high levels of triglycerides and cholesterol in the blood. Accumulation of cholesterol, specifically, can lead to hard, stone-like pieces within the gallbladder, called gallstones, inducing stomach or back pain (Erlinger, 2000). Obesity, together with injury and aging, can also cause osteoarthritis – a condition whereby the protective cartilage at bone junctions start to degrade leading to joint pain and decreased joint function. This effect is due to the added mechanical stress put on joints by extra body weight (Cooper et al., 1998). Furthermore, obesity can lead to sleep apnea, a common disorder in which individuals have episodes of ceased breathing while sleeping. Excessive fat accumulation over the chest, abdomen and around the neck in obese individuals can potentially narrow the airway and thus make breathing more troublesome (Vgontzas, 2000). Another respiratory condition associated with obesity is obesity hypoventilation syndrome (OHS), whereby shallow breathing leads to oxygen scarcity and excessive carbon dioxide in the blood (BaHamman & Al Dabal, 2009). Fertility is also negatively correlated with obesity (Pasquali et al., 2007). In women, early development of obesity can cause menses irregularities, chronic oligo-anovulation and could lead to eventual infertility in adults. Obesity also increases the risk for miscarriages. In men, as the severity of obesity increases, the production of testosterone and sperm decrease, and frequency of erectile dysfunction increases, contributing towards infertility (Pasquali et al., 2007).

1.3 THE HEART

1.3.1 OVERVIEW OF THE HEART

“The heart is the conductor of all human beings.” It sets the rhythm and tempo of a person’s entire metabolic state. The heart beats an average 100 000 times per day, pumping 7 500 liters of blood through the body (Watson, 2009). On average a male human heart weighs only 280g, whereas a female heart weighs in at 230g – constituting on average a mere 0.5% of our entire body weight (The Normal Size of the Heart Muscle Weight, 1951). At the size of a human fist, the heart circulates blood through 95 000 km of veins and arteries, feeding organs and tissues along the way. Furthermore, by increasing the heart rate through exercise the cardiac output (the amount of blood the heart circulates per minute through the body) can be increased as much as 6-fold (Baggish & Wood, 2011). Heart rate can also vary from as little as 40 beats per minute (bpm) at rest to more than 200 bpm (Uusitalo et al., 1998). It has been determined that a person’s maximum heart rate is an innate genetic feature that decreases with age (Jose & Collision, 1970). Furthermore, it is estimated that a mere 1% of all heart cells are renewed per year from age 20, and declines to 0.3% by 75 – equating to less than 50% turnover of heart cells during an entire lifespan (Bergmann et al., 2009). Even though regular exercise is strongly associated with good

health it does not exclude cardiovascular complications, as is evident from pro-athletic patients with cardiovascular diseases, stemming from various structural and functional heart abnormalities (Baggish & Wood, 2011). Understandably, any damage inflicted to this organ, albeit via damage to the heart's chambers, veins or valves, or in the circulatory system via occlusions, constrictions, or loss of blood, forces the system to overcompensate in order to maintain the body's functional demand for nutrient rich blood.

1.3.2 Energy Metabolism

The heart consists of specialized muscle cells and has the unique feature of uninterrupted contraction and relaxation (An & Rodrigues, 2006). This also makes the heart the most metabolically active organ in the body (Neubauer, 2007), needing a high supply of energy equating, to 6kg of adenosine triphosphate (ATP) per day to circulate nearly 10 tons of blood daily (Raff, 2003) to meet the demands of cellular maintenance and sustaining contractile function (Shah & Shannon, 2003). The heart has very little stored ATP content (5 μmol/g of wet heart) and a high turnover of ATP (~30 μmol/g of wet heart per minute at rest), meaning the entire pool of ATP can be turned over every 10 seconds (Bing et al., 1954; Opie et al., 1968; Opie et al., 1969). The heart can utilize various substrates for energy generation (An & Rodrigues, 2006), but the most prominent are fatty acids, which account for 50-70% of ATP production (Lopaschuk et al., 1994). The remaining energy is derived from glucose, amino acids, lactate and ketones. The heart switches between these substrates to facilitate optimal energy production during different physiological (post-prandial and fasted) or pathological conditions. These conditions can influence the demand for energy, the amount of oxygen supplied to the heart, the amount of fatty acid supplied to the heart and the prevalence of the competing substrates, as well as change the mechanisms of substrate uptake and utilization within the cell (Lopaschuk et al., 2010).

1.3.2.1 ATP

ATP is the primary form of energy used on molecular level to support contractile proteins, facilitate ion transport and enable enzymes to be functional. It is generated when phosphate ions are linked to adenosine diphosphate (ADP) through complex cellular processes (Lodish et al., 2000). Under normal physiological conditions, energy production and utilization are in balance. However, when ATP usage exceeds the supply, intracellular ADP increases. This leads to ADP molecules combining and reconverting into ATP and adenosine monophosphate (AMP) by action of the adenylate kinase enzyme. Though this process renews ATP, the excess AMP serves as an internal cell signaling molecule that indicates the presence of metabolic stress, amongst other things (**Figure 2.3**). AMP is extremely sensitive to a compromised energy status (Hardy et al., 2006) and directly regulates AMP-activated protein kinase (AMPK) - its main effector. Furthermore, it regulates enzymes involved in metabolism, such as glycogen phosphorylase and

phosphofructokinase-1 (PFK-1), which respectively releases glucose from glycogen stores and regulates glucose entry into glycolysis (Dzeja & Terzic, 2009).

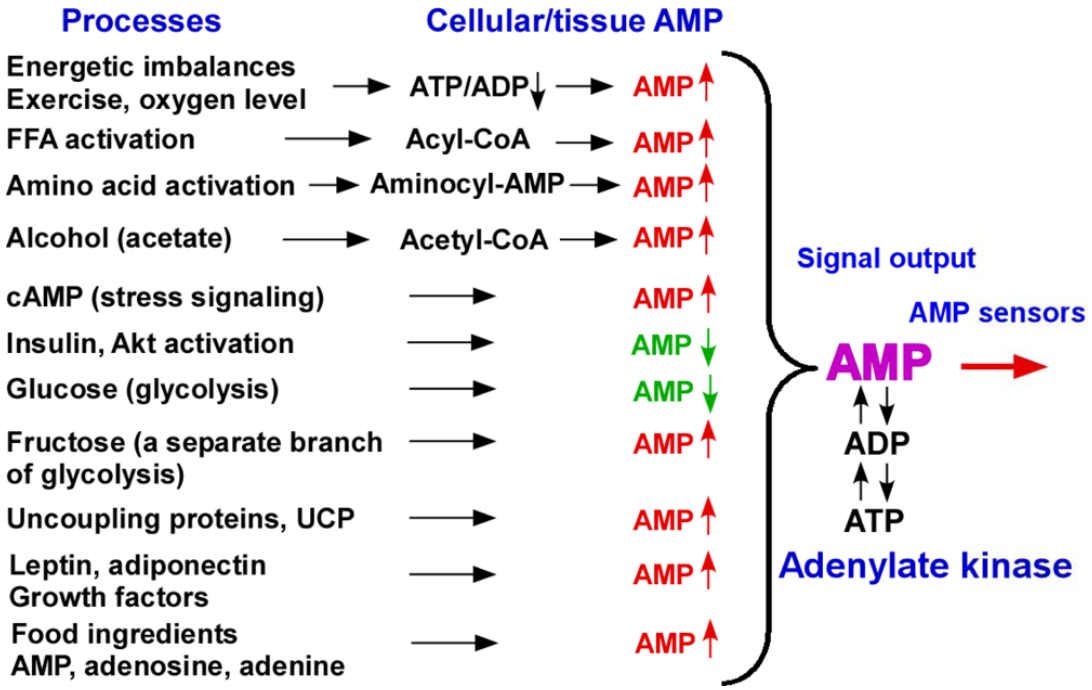

Figure 2.3 AMP signals up- or downregulated by adenylate kinase in response to various processes.

1.3.2.2 GLUCOSE METABOLISM

Glucose, a monosaccharide carbohydrate, is one of the major fuels utilized by the heart under normal physiological conditions. Glucose can either be derived from carbohydrates, such as sugars and starches after being processed by the digestive tract, or endogenously made by the body through breakdown of muscle and liver glycogen, or by de novo synthesis from lactate, glycerol, alanine and glutamine (Newsholme, 2003). Its entry into cells is facilitated by glucose transporters, denoted GLUT's, of which there are 14 isoforms with varying tissue distribution and subcellular localization described to date (Augustin, 2010). Upon contractile stimulation during movement or insulin secretion after a meal, GLUT4 translocates to the plasma membrane to facilitate glucose uptake (**Figure 2.4**). Glucose utilization is always limited by the rate of uptake, rather than the rate of phosphorylation of glucose-dependent processes - as a result, the concentration of free glucose inside the cardiomyocytes are always lower than within the blood, creating a glucose gradient favouring glucose entry (Manchester et al., 1994). After entering cardiomyocytes or skeletal muscle cells, glucose can either be converted to energy through the processes of glycolysis (in the cytosol) and glucose oxidation (in the mitochondria), or stored as glycogen.

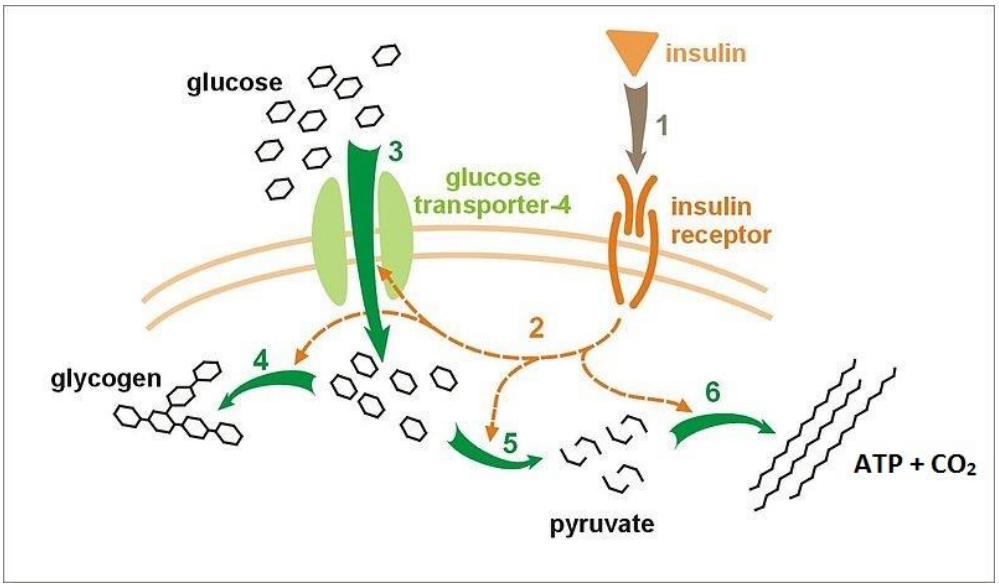

Figure 2.4 Simplified Glucose Metabolism Overview. 1) Insulin binds the insulin receptor, **2)** activating kinase cascades and **3)** recruiting GLUT4 to the plasma membrane, facilitating glucose uptake. Glucose is then either stored as **4)** glycogen, used in **5)** glycolysis or **6)** glucose oxidation. (Adapted from en.wikipedia.org/wiki/Insulin)

- **GLYCOLYSIS**

The initial stage of glucose metabolism, known as glycolysis, occurs in the absence of oxygen in the cytosol of cells. The whole process only amounts to 2 ATP and 2 three-carbon pyruvate compounds per glucose molecule (**Figure 2.5**). The first step in glycolysis is the phosphorylation of glucose to glucose-6-phosphate (G-6-P) by hexokinase. In the heart, hexokinase is prevalent in 2 different isozymes: hexokinase I, predominantly in fetal and newborn hearts; and hexokinase II, predominantly in the adult heart (Printz et al., 1995). Hexokinase is situated in both the cytosolic fraction of the cells, as well as being bound to the outer mitochondrial membrane (Arora & Pedersen, 1988). Under physiological conditions, an estimated two-thirds of G-6-P is converted to glycogen (DeFronzo & Tripathy, 2009), whereas the rest enters glycolytic pathways to generate ATP. The first regulator that commits glucose to glycolysis is 6-phosphofructo-1-kinase (PFK-1), catalyzing the phosphorylation of fructose-6-phosphate (F-6-P) to fructose-1,6-bisphosphate (F-1,6-BP). It is considered to be the rate-limiting step of glycolysis given the complexity of allosteric control - ATP, citrate and protons are all negative allosteric effectors, while AMP and fructose-2,6-diphosphate are positive allosteric effectors (Uyeda, 1979). Glyceraldehyde-3-phosphate dehydrogenase (GAPDH) catalyzes the oxidation and phosphorylation of glyceraldehyde 3-phosphate (G-3-P) into 1,3-diphosphoglycerate (1,3-DG). The activity of GAPDH, similar to other dehydrogenases, is decreased in the presence of high concentration of NADH and protons (Mochizuki & Neely, 1979). Pyruvate kinase (PK) irreversibly catalyzes phosphoenol pyruvate into pyruvate, and can increase glycolytic flux in response to stimulation by F-1,6-BP, the product of

PFK-1. PFK-1 is thus capable of accelerating glycolytic flux, without causing a buildup of various glycolytic intermediates (Kiffmeyer & Farrar, 1991).

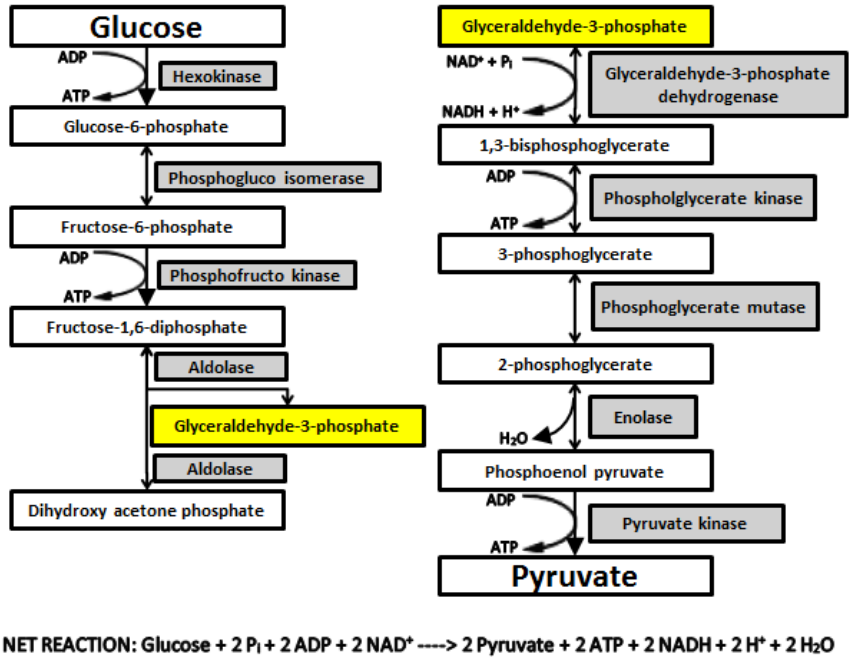

Figure 2.5 Glycolysis Pathway. Two molecules of ATP generated by conversion of one glucose molecule to 2 pyruvate molecules.

- **GLUCOSE OXIDATION**

In aerobic cells, pyruvate, produced from either glycolysis or exogenous lactate, enters the mitochondria where it is further oxidized in the presence of O_2 to CO_2. After full oxidation of a glucose molecule a further 34 molecules ATP are generated (**Figure 2.6**). Pyruvate enters the mitochondria via a monocarboxylate carrier (Poole & Halestrap, 1993). It is then further oxidized to acetyl coenzyme A (acetyl-CoA) by the pyruvate dehydrogenase complex (PDC) and convened into the tricarboxylic acid (TCA) or citric acid cycle. Pyruvate can also be transformed into TCA cycle intermediates such as oxaloacetate by action of pyruvate carboxylase or malic enzyme (Peukhurinen et al., 1982). PDC can either be inhibited by pyruvate dehydrogenase kinase (PDK) following stimulation by acetyl-CoA and NADH (produced from fatty acid oxidation), or activated when PDK is inhibited by pyruvate (Roche & Hiromasa, 2007). PDC in working hearts are activated in response to increased workloads or during perfusion with epinephrine, resulting in increased mitochondrial Ca^{2+} entry (McCormack & Denton, 1990). In the end, the majority (80 – 90%) of glucose undergoing glycolysis is converted to ATP, carbon dioxide and water, while the remainder is converted to lactate (DeFronzo & Tripathy, 2009).

During prolonged contraction of skeletal muscles, oxygen supply grows limited, inhibiting complete oxidation of glucose. In this scenario, glucose is fermented to two molecules of ATP and lactic acid, rather than pyruvate (Lodish et al, 2000). Lactic acid accumulates in skeletal muscle

(arguebly, leading to muscle and joint aches) till it is cleared by secretion into the blood. Once in circulation, it is either taken up by the heart or liver, where it can be reprocessed to pyruvate and further metabolized to ATP and CO_2 or converted back to glucose (Lodish et al., 2000).

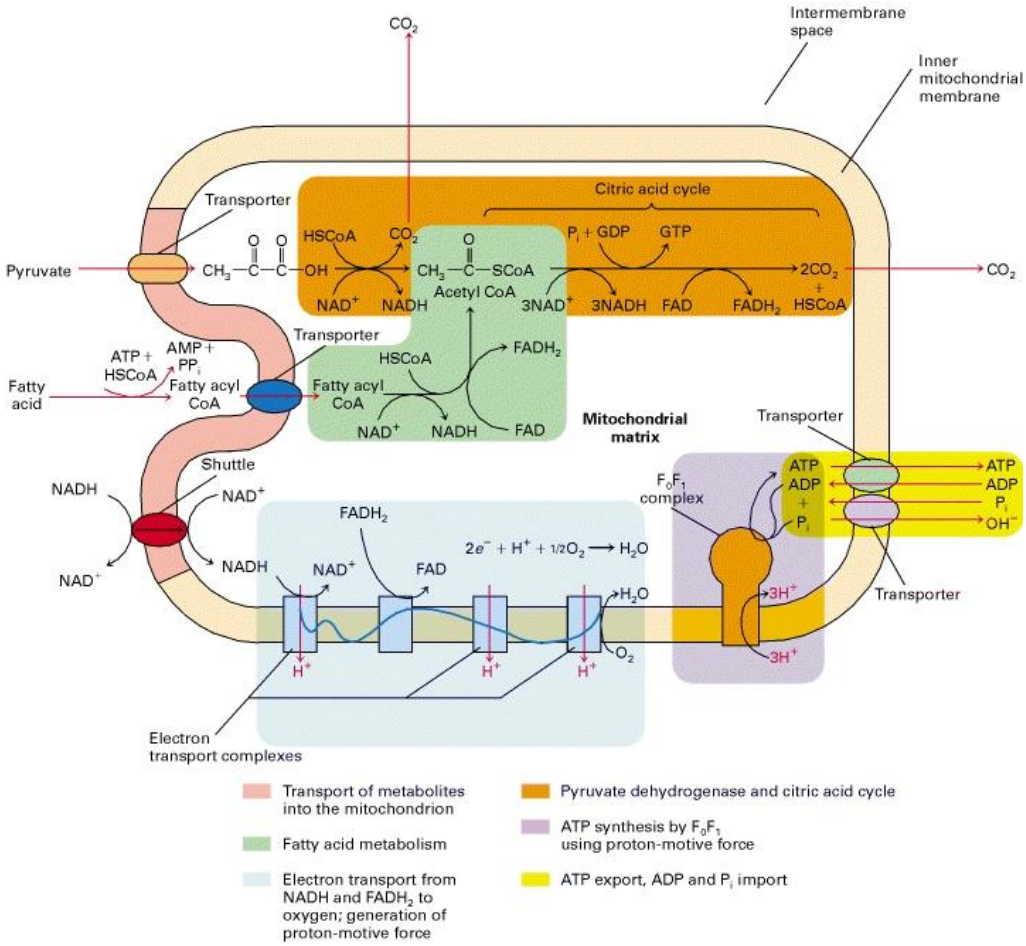

NET REACTION: 2 Pyruvate + 6 O_2 + 34 P_I + 34 ADP + 34 H^+ → 6 CO_2 + 34 ATP + 40 H_2O

Figure 2.6 Glucose Oxidation Pathway. 34 molecules of ATP generated by conversion of 2 pyruvate molecules (1 glucose molecule). (Obtained from Lodish et al., 2000)

- **GLYCOGEN SYNTHESIS**

Cardiac glycogen concentration can vary based on training status, exercise and diet (Depré et al., 1998). Glycogen comprises about 2% of the adult heart cell volume, and 30% of fetal and newborn cardiomyocytes (Shelley, 1961). In contrast to liver and skeletal muscle cells, cardiomyocytes produce glycogen during fasting (Schneider et al., 1991). In times of fasting, fatty acids become the predominant fuel for the heart, whilst glycolysis (to a greater extent) and glucose uptake is decreased. This leads to a repurposing of glucose for glycogen synthesis. Glycogen stores can be further expanded as a result of insulin, which simultaneously stimulates glucose transport and glycogen synthase activity (Moule & Denton, 1997). Glycogen synthesis is also upregulated when lactate is used as the primary fuel for the heart (Laughlin et al., 1994). The rate of glycogen

synthesis is limited by the enzyme, glycogen synthase (GS) (**Figure 2.7**), which transfers glucose from UDP-glucose to an amylose chain. The enzyme has 2 distinct conformations, namely a G-6-P-dependent or inactive D-form, and a G-6-P-independent or active I-form. Control of these conformations are dependent on phosphorylation-dephosphorylation reactions.

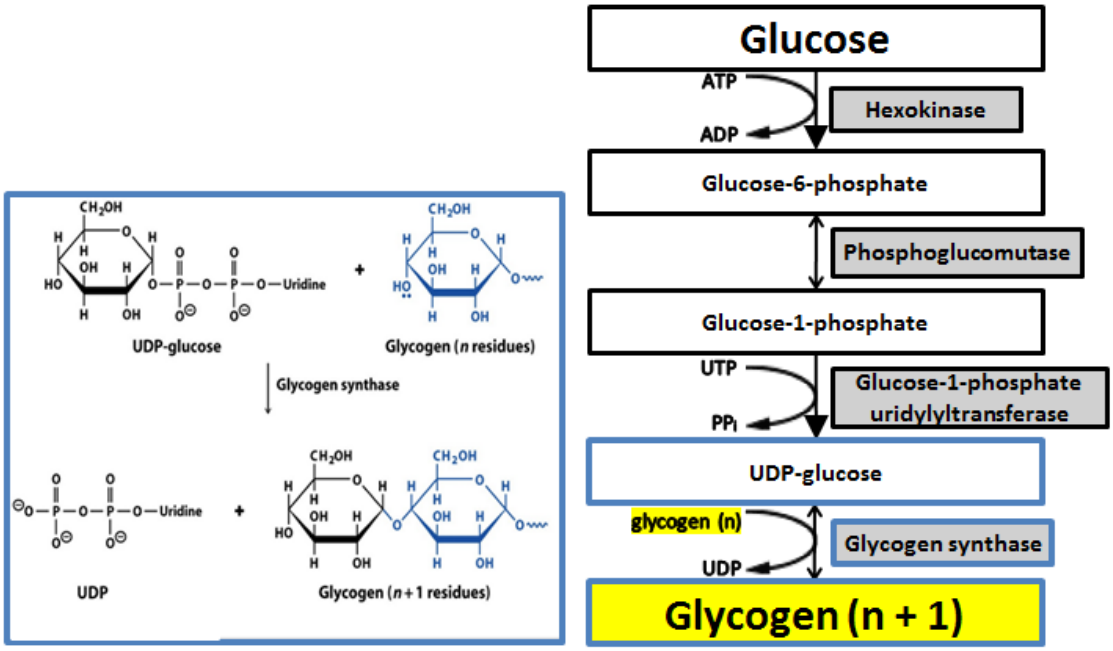

Figure 2.7 Glycogen Synthesis Pathway.

Furthermore, heart glycogen can also be broken down in response to adrenaline or oxygen deprivation to produce glucose (Morgan & Parmeggiani, 1964). Glycogenolysis is controlled by glycogen phosphorylase, which is activated in direct response to increased Ca^{2+} concentrations and indirectly through cyclic AMP-dependent protein kinase (PKA). Both these activators can be upregulated in response to catecholamines (Depré et al., 1998).

In a failing heart, metabolism switches to glucose as the preferred substrate due to the efficiency of glucose oxidation in the generation of high-energy phosphates (Shah & Shannon, 2003). Increasing the amount of energy derived from glucose requires the upregulation of glucose transport and glucose oxidation. However, in the case of insulin resistance, glucose uptake and oxidation are both impaired, leading to less ATP generated from glucose.

1.3.2.3 Fatty Acid Metabolism

Mammalian adipose tissue responds to two distinct classes of peptide hormones, namely 'adipokinetic' hypophyseal peptides (stimulate lipolysis resulting in free fatty acids), and insulin (stimulate the conversion of glucose into CO_2, triglycerides and glycogen) (Girolamo et al., 1965). In the heart, utilizing fatty acids (FAs) for energy metabolism is very dynamic and can account for

nearly 100% of total energy requirements or feature only in a minor capacity (Bing et al., 1954; Opie et al., 1968; Opie et al., 1969).

The degree of FA utilization is subject to:

- the energy demand
- the presence of competing energy substrates
- FA concentration, type available and supply to the heart
- the amount of oxygen available
- allosteric control of FA uptake into cells and transport to mitochondria
- esterification of FA to Coenzyme A (FA must be esterified to CoA before they can undergo lipid oxidation)
- functioning of the mitochondria which includes β-oxidation, TCA cycle and electron transport chain (ETC) activity
- the presence of lipoprotein lipase (LPL) which derives FFA from chylomicrons, effectively lowering VLDL concentration
- transcription of new enzymes involved in FA metabolism (Lopaschuk et al., 2010).

- **SOURCE OF FATTY ACIDS**

FAs reach the heart in one of two forms: free FAs (FFAs) bound to albumin or FAs released from triacylglycerol (TAG) found in chylomicrons or very-low-density lipoproteins (VLDL) (Van der Vusse et al., 2000). Both are equally important in metabolism by heart cells. Under normal physiological conditions, FFAs circulate at concentrations between 0.2 and 0.6 mM, but under diseased conditions such as myocardial ischemia and diabetes, concentrations can rise to above 2 mM (Kurien & Oliver, 1971). Excess body fat can be broken down and released as FFAs to meet energy requirements. It is estimated that one kilogram of bodily fat contains 7740 calories of potential energy (Jennings & Lesser, 2012), which is double the amount of energy stored in equal amounts of glycogen (Kotecki, 2011). However, persisting levels of high circulating FFAs in obesity and diabetes is a strong determinant of high rates of FA uptake and β-oxidation in these diseased states.

1.3.2.4 INTERSPECIE DIFFERENCES

Curiously, in mouse hearts perfused with high fatty acid levels, sensitivity to insulin persists and still leads to dramatic increases in glucose oxidation rates, whereas in rats, insulin sensitivity was inhibited by the presence of fatty acids (Abdel-aleem & Lowe, 2012; Chandrasekera & Pippin, 2014). Also, insulin did not reduce myocardial fatty acid β-oxidation rates in rats in the presence of high levels of FA (Saddik & Lopaschuk, 1991), but did reduce the rates in mice (Folmes et al., 2006). Interspecie differences in regulating fatty acid and insulin sensitivity are an important

concept researchers need to be aware of when aiming to duplicate high-fat diet, obesity and diabetic studies.

In humans, the primary insulin-sensitive tissue is the skeletal muscle which account for 50-90% of glucose clearance, and stores up to 10 times more glycogen than the liver (DeFronzo & Tripathy, 2009). In contrast, in rodents the primary site for glucose clearance is the liver, which stores 5-10 times more glycogen than the skeletal muscle (Kuo et al., 1999). Furthermore, in human skeletal muscle, glucose uptake is primarily regulated by a high affinity GLUT4, which also serves as the rate-limiting step, whereas in rodent livers, glucose uptake is facilitated by a low affinity of GLUT2 and the rate-limiting step is given by glucose phosphorylation rather than glucose uptake (Petersen & Shulman, 2002). Thus, comparatively, physical exercise capable of mimicking the actions of insulin, target skeletal muscles in humans more significantly than in rodents by increasing glucose uptake and glycogen synthesis, whereas the exercise-mediated glucose transport in the liver is less significant (Jensen & Richter, 2012). Furthermore in humans, insulin resistance present with a significantly reduced GLUT4 content, and subsequently impaired glucose transport into skeletal muscles, impaired glycogen synthesis and high blood glucose (DeFronzo & Tripathy, 2009). However, GLUT4-knockout mice and rodents lacking GLUT4 do not present with high blood glucose (Fam et al., 2012). Furthermore, in humans, impaired glucose uptake result from decreased GLUT4 expression levels, whereas in rodents, it is a result of impaired GLUT4 translocation to the cell membrane (Hansen et al., 1998).

1.3.2.5 Alterations in Obesity and Diabetes

Under normal physiological conditions, excess supply of energy not utilized for immediate energy needs, are stored in the form of triacylglycerols (TAG) in adipocytes. The release of FFA is also acutely regulated to meet the energy requirements. When this balance is disturbed through mechanisms such as persistent overconsumption of food, adipose tissue greatly expands, leading to greater release of FFA into circulation and in turn elevated levels of circulatory FFA and TAG (Boden, 2008). Elevated FFA in circulation leads to increased VLDL-TAG synthesis in the liver, further exacerbating hyperlipidemia. In both experimental animals and humans, elevated circulating fatty acids and TAG levels are important contributors to cardiac substrate selection in obesity (Koutsari & Jensen, 2006; Lopaschuk et al., 2010). Thus, there is an increase in fatty acid oxidation with increased obesity and insulin resistance (Lopaschuk et al., 1991; Turcotte et al., 2001). In the heart, myocardial triglyceride content has been found to proportionally increase with BMI (Szczepaniak et al., 2003) and is a strong indicator of cardiac dysfunction and heart failure (Sharma et al., 2004). In diabetic patients without heart disease, an increase in fatty acid circulation has also been correlated with a decrease in heart metabolism and diastolic functioning (stiff heart muscles leading to slower filling of the ventricles after a contractile cycle) (Lopaschuk et al. 2010; Leichman et al., 2006). Increasing FA supply to the heart can lead to increased FA

uptake and in turn increased β-oxidation in obesity and diabetes. This can lead to accelerated FA oxidation and has been shown to contribute to the development of diabetic cardiomyopathies by decreasing glucose oxidation and lowering cardiac mechanical efficiency (How et al., 2006). Fortunately, contractile function can be improved in diabetic patients by pharmacologically inhibiting fatty acid metabolism and activating glucose metabolism (Stanley, 1997).

1.4 INSULIN RESISTANCE

1.4.1 OVERVIEW OF INSULIN RESISTANCE

Insulin resistance is the condition whereby the insulin sensitive tissues in the body become gradually less sensitive to insulin, giving way to ineffective glucose utilization (Beale, 2013). This leads to glucose accumulation in the blood instead of being cleared through entering muscle, fat and liver cells. In order to compensate for the decrease in insulin sensitivity, higher levels of insulin are needed to facilitate glucose uptake by the cells. Initially, the β-cells within the pancreas increases insulin production to meet the demand (Leibiger et al., 2008). This response is responsible for maintaining normal blood glucose levels in healthy individuals. However, insulin resistance left untreated, overburden the β-cells, leading to a lack of insulin to effectively clear blood glucose (**Figure 2.8**). Insulin insensitivity together with a decline in insulin secretion, over time, lead to T2D mellitus, and contributes to the metabolic syndrome, increasing the risk for cardiovascular disease.

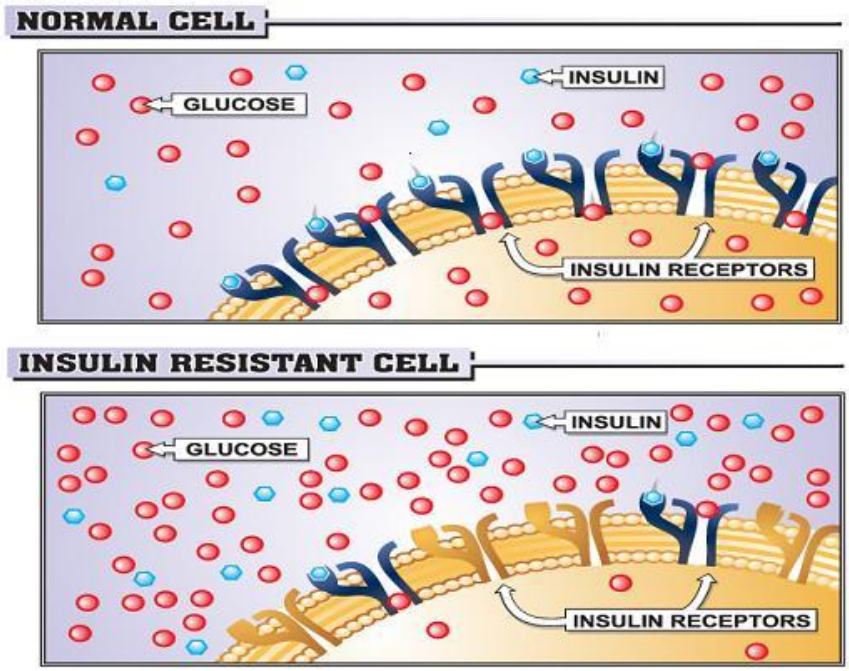

Figure 2.8 Simplified Schematic of Insulin Resistance. (Obtained from Steiner-Victorin et al., 2014)

1.4.2 ASSESSMENT

Insulin resistance can be assessed by measuring the insulin levels in the blood or by measuring the glucose levels in response to insulin (Bray & Hamman, 2014). The first test, known as a hyperglycemic clamp, requires keeping blood glucose levels constantly elevated through hyperinfusion of glucose and measuring the response of pancreatic β-cells to produce insulin. The second test, known as an euglycemic clamp, intravenously infuses high levels of insulin into a patient's blood, while simultaneously measuring the fluctuating blood glucose levels. The euglycemic clamp is considered to be the gold standard in human trials and pharmacodynamic studies of drug interactions in diabetes patients (Bray & Hamman, 2014). However, the test is too costly and impractical to be used for clinical assessment of diabetes pathology. Rather, blood tests are performed to determine the likely presence of insulin resistance, a strong indicator for prediabetes. All blood tests involve drawing blood by a health care provider, followed by further laboratory analysis. In humans, instant glucose measuring devices serve purely as indicator of blood glucose levels, but further analysis is needed to make a diagnosis of prediabetes/diabetes.

1.4.2.1 HEMOGLOBIN A1C

Hemoglobin A1c (HbA1c), or glycohemoglobin, is used as an indicator of average blood glucose over the past 3 months (Insulin Resistance and Prediabetes, National Institutes of Health (NIH), 2015). The test is based on binding of glucose to hemoglobin, the oxygen-carrier protein present in red blood cells, which typically have a lifespan of 3 months. The percentage of bound HbA1c can be used to determine a person's diabetic status. A percentage between 5.7 and 6.4 is considered prediabetic (**Figure 2.9**). It is considered to be the most reliable test, but not always the most sensitive to recent developments in prediabetes. However, the HbA1c test can be unreliable for diagnosing prediabetes in people of African, Mediterranean or Southeast Asian descent, as well as people having a known familial history of sickle cell anemia, due to possesing a hemoglobin variant that interferes with the results of the HbA1c test.

1.4.2.2 FASTING PLASMA GLUCOSE TEST

Measuring fasting blood glucose in people who have not eaten for at least 8 hours, can serve as a strong indicator of prediabetes (Insulin Resistance and Prediabetes, NIH, 2015). A fasting glucose level between 100 to 125mg/dL (5.6–6.9 mmol/L) (**Figure 2.9**) is indicative of prediabetes and known as impaired fasting glucose (IFG). The test is most reliable when performed in the morning hours following sleeping and fasting.

1.4.2.3 ORAL GLUCOSE TOLERANCE TEST

Similar to the fasting plasma glucose test, the oral glucose tolerance test (OGTT) also entails 8 hours of fasting, but additionally, at the start of the test, a person receives a sweet (glucose-prevalent) liquid to consume, succeeded by follow-up blood glucose tests to determine how quickly the blood glucose is cleared (Insulin Resistance and Prediabetes, NIH, 2015). A blood glucose level between 7.8–11.0 mmol/L (140 and 199mg/dL) (**Figure 2.9**) is indicative of prediabetes and known as impaired glucose tolerance (IGT).

Blood Test Levels for Diagnosis of Diabetes and Prediabetes

	A1C (percent)	Fasting Plasma Glucose (mg/dL)	Oral Glucose Tolerance Test (mg/dL)
Diabetes	6.5 or above	126 or above	200 or above
Prediabetes	5.7 to 6.4	100 to 125	140 to 199
Normal	About 5	99 or below	139 or below

Figure 2.9 Blood glucose tests used as indicator of insulin resistance in humans (Obtained from Standards of Medical Care in Diabetes, 2012)

1.4.3 INSULIN

Insulin is a peptide hormone that plays a crucial role in energy metobolism. In response to an increase in blood glucose or amino acids, insulin is produced by the β-cells present in pancreatic islets. The produced insulin is then secreted into the blood circulation where it facilitates the absorption and utilization of glucose as energy substrate by organs in the body. Insulin's action is essential for tissue development, growth and maintaining energy homeostasis (Sesti, 2006). Insulin also influences lipid metabolism by regulating lipid synthesis in liver cells and adipocytes, restricting fatty acid breakdown of fat tissue (Sesti, 2006), regulating food intake, stimulating sympathetic activity, inducing energy uptake in peripheral tissues, as well as being involved in learning and memory (Zhao & Alkon, 2001). Insulin was first discovered in 1921 (Banting et al., 1956), in search of an effective therapy for diabetes. Today, it is still used as one of the major treatments for T1D.

1.4.4 INSULIN SECRETION

Insulin is synthesized from a polypeptide, called preproinsulin, in pancreatic β-cells (**Figure 2.10**). As the preproinsulin is translocated into the lumen of the rough endoplasmic reticulum (RER), the polypeptide is cleaved forming proinsulin (Chhabra, 2015). Further maturation of proinsulin into insulin occurs at the trans-Golgi apparatus via action of cellular endopeptidases, such as prohormone convertases (PC1 and PC2) and exoprotease carboxypeptidase E. PC1 and PC2 cleave proinsulin at the B-chain-C-peptide junction and C-peptide-A-chain junction respectively (Smeekens et al., 1992), releasing a C-peptide fragment and 2 peptide chains, referred to as the B- and A-chains which are linked by 2 disulfide bonds. These bonded chains are collectively called insulin and stored in mature secretory granules within the pancreatic β-cells, where it is exocytosed from the cell into the systemic circulation after stimulation by most notably glucose. Insulin secretion is also induced by amino acids (such as leucine and arginine) and lipids (non-esterified fatty acids) (Fu et al., 2013), incretins (gastrointestinal tract stimulated hormones, including glucose-dependent insulinotropic polypeptide (GIP) and GLP-1) (Baggio & Drucker, 2007), vagal nerve stimulation (Ahrén & Taborsky, 1986) and various other hormones (growth hormone, glucagon, secretin, cholecystokinin, gastrin, VIP, gastrin-releasing peptide) (Wilcox, 2005).

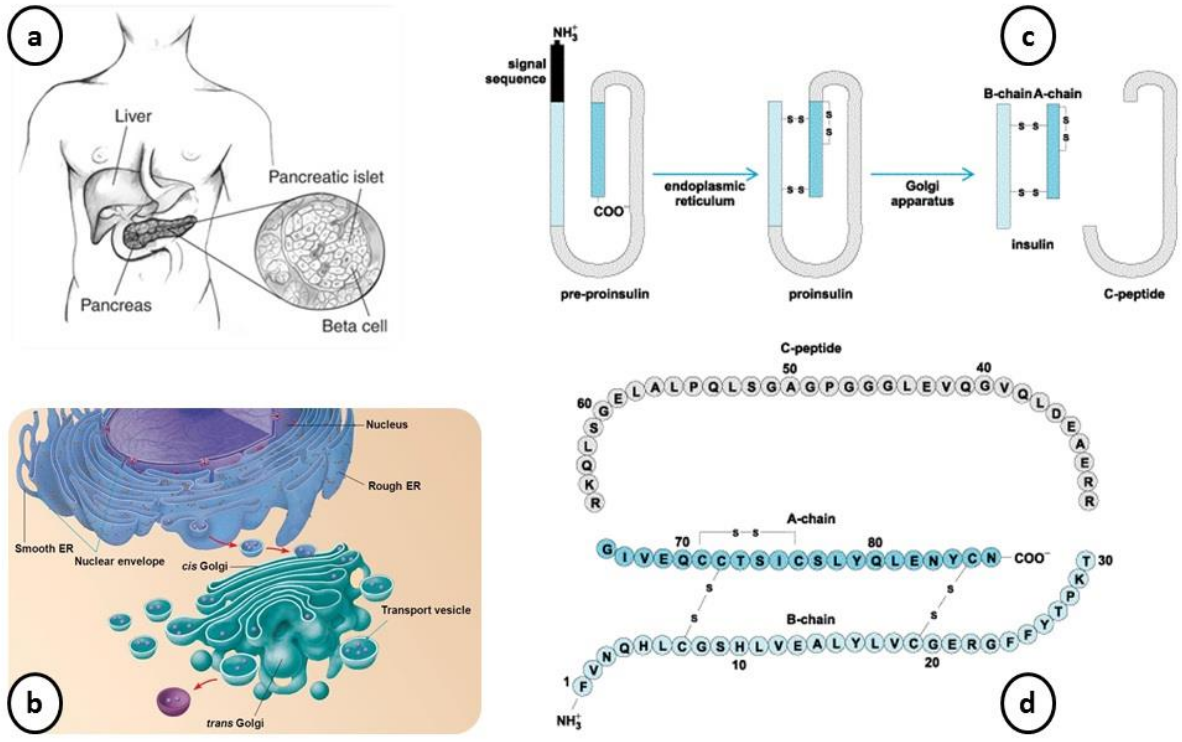

Figure 2.10 Insulin Synthesis. a) The pancreas contain clusters of cells (islets) which contain β-cells. **b)** Within the β-cells, insulin is synthesized between the endoplasmic reticulum and the trans Golgi apparatus. **c)** Pre-prosinsulin, a pro-hormone, is cleaved several times to produce mature insulin. **d)** The structure of the final insulin product which is released into the blood in response to high blood glucose. (Adapted from Chhabra, 2015)

After consuming a meal, blood glucose rises and insulin is subsequently released into the blood via the pancreas. Insulin plays a multifunctional role within the body. Firstly, it aids in the absorbtion of blood glucose by muscle, fat and liver cells, which in turn lowers blood glucose. It also facilitates in converting excess blood glucose levels into glycogen in the liver, muscle and heart tissues. Lastly, insulin inhibits the production of glucose by the liver, effectively lowering blood glucose levels. Interplay between glucose and insulin in healthy individuals help maintain normal blood glucose levels.

1.4.5 Insulin Function

Insulin has been shown to play an intermediate role in a variety of body tissues, eliciting a specific response for each organ or tissue target (Benito, 2011). In the heart, skeletal muscle and fat cells, insulin stimulates the uptake of glucose by promoting translocation of GLUT4 from an intracellular reservoir compartment to the cell border or plasma membrane. Insulin is mainly responsible for substrate utilization in the heart, but also augments cardiomyocyte contraction, affects myocardial relaxation, promotes angiogenesis and cell survival, downregulates apoptosis, enhances myocardial microcirculation and reduces coronary artery resistance, which improves blood perfusion of the myocardium (Iliadis et al., 2011). Under normal physiological conditions, skeletal muscle is the primary organ responsible for glucose uptake and clears an estimated 80% of total blood glucose (Thiebaud et al., 1982). Of this glucose, up to 80% of insulin-stimulated muscle glucose is converted to glycogen, while the rest is oxidized to CO_2 and H_2O (Abdul-Ghani & DeFronzo, 2010). Insulin plays a dual role in pancreatic β-cells - historically, insulin is suggested to negatively impact β-cells through autocrine feedback, but it has also been found to play a positive role in transcription, translation, ion flux, insulin secretion, proliferation, and β-cell survival (Liebiger et al., 2008). Insulin is also crucial for proper kidney function (Hale & Coward, 2013). Poor insulin signalling, as in the case of insulin resistance, can lead to renal complications such as hypertension and albuminuric glomerular disease (Re, 2015). A strong link between endothelial dysfunction and insulin resistance has also been observed, further aggravating metabolic and cardiovascular diseases (Muniyappa & Quon, 2007). In the brain, insulin was shown to serve as a key neuromodulator in behavioural, cellular, biochemical and molecular studies (Derakhshan & Toth, 2013).

1.4.6 INSULIN SIGNALING

The insulin hormone is circulated throughout the body via the blood, until it reaches its target tissue where it binds to the insulin receptor (IR). From this point, three distinct pathways can follow: the phosphatidyl-inositol 3-kinase (PI3K)/Akt pathway; Ras-mitogen-activated protein kinase (Ras-MAPK) or the CAP/CbI/TC10 pathway. Once activated these pathways elicit the effects of insulin which pertain to (Wilcox, 2005):

Carbohydrate Metabolism

- translocation of GLUT4 to the membrane – increases glucose uptake into cells
- inhibits glycogen synthase kinase-3 (GSK-3) – increases glycogen synthesis
- inhibits glycogen phosphorylase kinase – decreases glycogen breakdown
- activates pyruvate kinase - increases glycolysis (**Figure 2.5**)
- inhibits 2,6-bisphosphate kinase – decreases gluconeogenesis
- enhances irreversible pyruvate to acetyl Co-A conversion (**Figure 2.6)**

Lipid Metabolism

- activates acetyl CoA carboxylase – increases fatty acid synthesis and storage
- inhibits carnitine acyltransferase – decreases fat oxidation
- stimulates esterification of glycerol phosphate – increases triglyceride synthesis
- inhibits hormone sensitive lipase – decreases triglyceride breakdown
- activates HMG-CoA reductase – increases cholesterol synthesis
- inhibits cholesterol esterase – decreases cholesterol breakdown

Protein Synthesis

- enhances mRNA transcription of glucokinase, pyruvate kinase, fatty acid synthase, albumin in liver
- enhances mRNA transcription of pyruvate carboxylase in adipose tissue
- enhances mRNA transcription of casein in mammary gland
- enhances mRNA transcription of amylase in pancreas.
- Protein translation heavily influenced by the presence of insulin-like growth factor-1

1.4.6.1 PI3K/PKB PATHWAY

The PI3K/PKB pathway is the primary signaling cascade mediating metabolic effects induced by insulin. Briefly (**Figure 2.11**), activation of the IR initiates tyrosine phosphorylation of insulin receptor substrates (IRS) 1-4, leading to association with the p85 regulatory subunit of PI3K. PI3K phosphorylates phosphatidylinositol phosphates (PIPs) in the membrane e.g. phosphatidylinositol 4,5-bisphosphate (PIP2) to create phosphatidylinositol 3,4,5-triphosphate (PIP3). Following this activation, phosphoinositide-dependent kinase-1 (PDK1) and related down stream effector molecules are recruited and activate PKB/Akt, which elicits the metabolic effects of insulin.

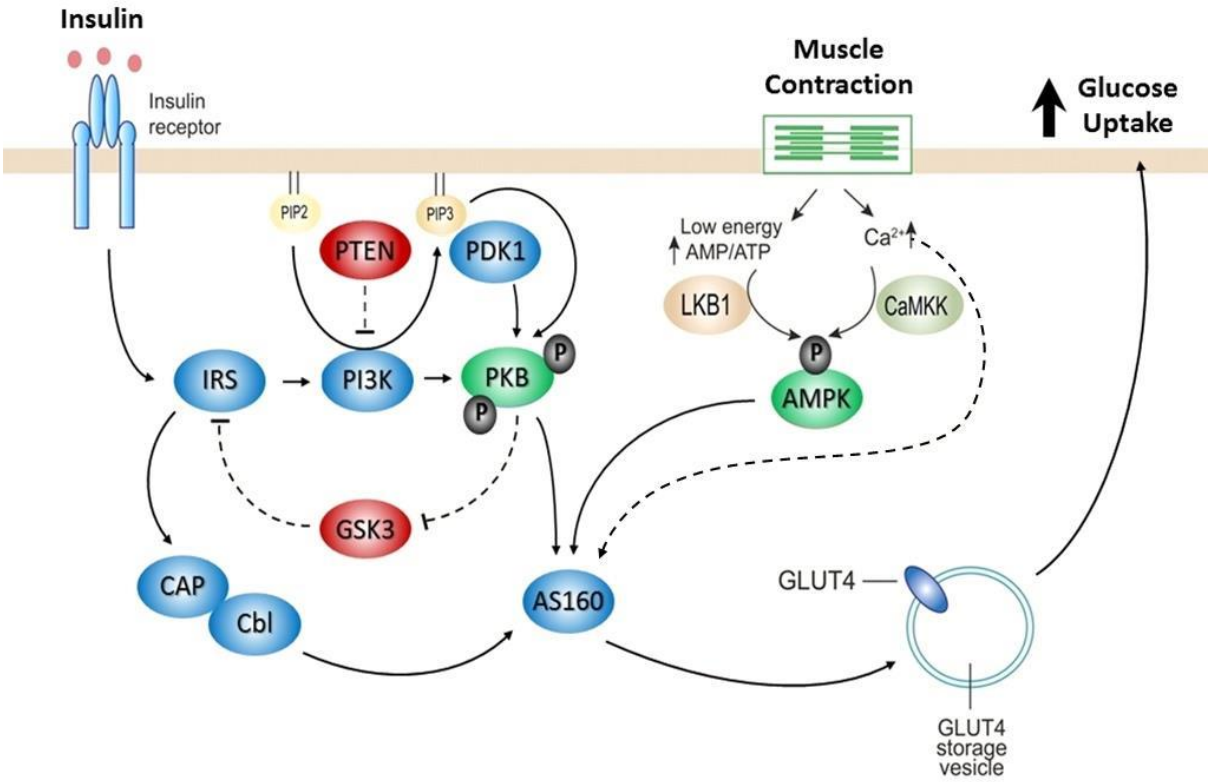

Figure 2.11 Insulin Dependent and –Independent Pathways of Glucose Uptake

- **IR**

IR (**Figure 2.12**) is a tetrameric enzyme consisting of two extracellular α-subunits and two transmembrane β-subunits linked together by disulfide bonds (Ottensmeyer et al., 2000). Upon insulin binding to the α-subunits of the receptor (**Figure 2.11**), the intrinsic tyrosine kinase activity of the β-subunits are activated. This causes an autophosphorylation of various tyrosine residues present in the β-subunits. This creates phosphotyrosine binding domains that can be recognized by proteins containing Src Homology 2 (SH-2) domains in their structure. Once activated, IR binds its downstream effectors, insulin receptor substrate (IRS) family and Shc. This induces the activation of two primary pathways, namely the PI3K and the MAPK pathways, respectively (Bertrand et al., 2008).

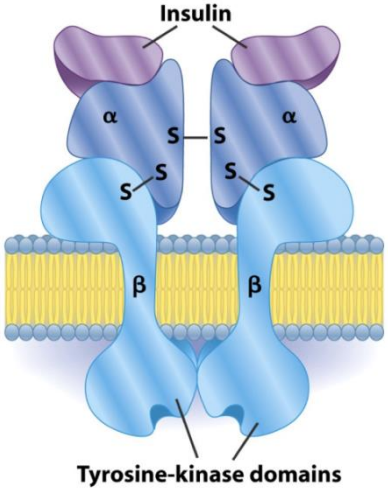

Figure 2.12 Insulin Receptor (Obtained from Nelson et al., 2008)

- **IRS 1**

IRS proteins are primary insulin signaling regulators central to cell growth, survival and metabolism (Liberman & Eldar-Finkelman, 2005). They serve as a link between the IR and downstream signaling molecules with SH2 domains (**Figure 2.11**). The IRS family consists of four different isoforms, IRS-1, IRS-2, IRS-3 and IRS-4, each expressed to different degrees in specific tissue types and subcellular localization. IRS-1's function pertains primarily to glucose uptake in cardiac, skeletal muscle and adipose tissue, whereas IRS-2 regulates glucose production in the liver and insulin production in pancreatic β-cells (Sesti et al., 2001). In insulin-resistant states, such as obesity and type 2 diabetes, only defective IRS-1 and IRS-2 expression has been implicated, whereas the rest of the IRS family plays an insignificant role.

- **PI3K**

Phosphatidylinositol-4,5-bisphosphate 3-kinase (PI3K) is a heterodimeric protein consisting of a p110 catalytic and a p85 regulatory subunit (Mora et al., 2005). Once activated in response to insulin, PI3K recruits to the plasma membrane. The regulatory subunit, consisting of SH2 domains, binds to phosphorylated tyrosine residues on IR and IRS adaptor proteins. PI3K primarily phosphorylates phosphatidylinositol-3,4-bisphosphate (PIP_2) lipids into phosphatidylinositol-3,4,5-triphosphate (PIP_3) on the plasma membrane creating rafts where proteins containing a pleckstrin homology (PH) domain can associate. This induces further recruitment of phosphoinositide-dependent kinase 1 (PDK1) and PKB. In the heart (**Figure 2.12**), it has been shown in PDK1 knockout mice that PDK1 is necessary for the activation of cardiac PKB (Mora, 2003). Thus, in response to insulin stimulation, co-localization of both PDK1 and PKB is important for metabolism. Synergy between PDK1 and PKB is also essential in regulating glucose uptake in the heart (Dummler & Hemmings, 2007).

- **PTEN**

PTEN (Phosphatase and tensin homolog) is a phosphatase involved in cell cycle regulation, controlling cell growth and division (Besson et al., 1999). It plays a role in the hydrolyses of phospho-inositide substrates, such as converting the product of PI3K, PIP_3 into phosphatidylinositol-4,5-bisphosphate, thereby inhibiting the PKB signaling pathway (Sasaoka et al., 2006). Inhibition of PKB signaling also regulates cell cycling by preventing cells from growing and dividing too rapidly (Chu & Tarnawski, 2004). Inhibiting further cell division is an important mechanism in apoptosis of cancer cells and suppressing tumor growth, and therefore, PTEN plays a central role as a tumor suppressor as well (Gupta & Dey, 2012). Mutation of the *PTEN* gene has been linked to various forms of cancer. Inhibition of PTEN in skeletal muscle and adipose tissue can serve as a protective mechanism in insulin resistance and diabetes (Wijesekara, 2005).

- **PKB**

Protein Kinase B (PKB) or Akt is a serine/threonine kinase which plays a diverse cellular signaling role in especially insulin metabolism. The PKB family has 3 major isoforms, PKB1, PKB2 and PKB3, which are all activated in response to PI3K recruitment. Furthermore, the PKB pathway is also activated in response to receptor tyrosine kinases, integrins, B and T cell receptors, cytokine receptors, G-protein coupled receptors (GPCRs) and especially, stimulation of PKB's upstream activators PIP_3 and PDK1 (Hemmings & Restuccia, 2012). PKB consists of a N-terminal PH domain, followed by a catalytic domain and a short C-terminal tail (Alessi, 1996) (**Figure 2.13**). PKB activation results from phosphorylation of PKB's two main regulatory subunits: Thr^{309}, located within the T loop of the catalytic domain; and Ser^{474}, located in the C-terminal, non-catalytic region of the enzyme referred to as the hydrophobic motif.

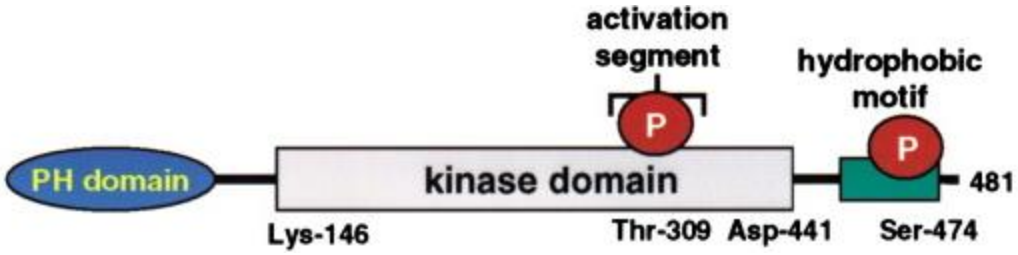

Figure 2.13 Schematic of Protein Kinase B (Obtained from Yang, 2002)

Our current understanding of PKB activation, inactivation and inhibition is indicated in **Figure 2.14**. Once PKB is recruited to the plasma membrane by binding of its PH domain to PIP_3, the Thr^{309} subunit is activated by PDK-1 (Alessi, 1996), whereas the Ser^{474} subunit is proposed to be activated in response to PDK-2, however this mechanism remains elusive since various other mediators have also been implicated including MAPKAP kinase-2, protein kinase C (PKC) isoforms, integrin-linked kinases, DNA-dependent protein kinase, ataxia telangiectasia mutated

(ATM) and PDK-1 itself (Farese, 2002; Bayascas & Alessi, 2005). It has also been proposed that the Ser^{474} subunit of PKB might be activated through autophosphosphorylation after Thr^{309} phosphorylation (Bayascas & Alessi, 2005). Post activation, PIP_3 decreases and PKB activity is surpressed through inactivation by serine/theonine phosphatases (Nicholson & Anderson, 2002). Inhibition of PKB occurs when inhibitors induce a conformational change near the PH domain. This results in a 'closed-off' conformation of PKB, obstructing the binding site for PDK-1 (Barnett et al., 2005). PKB activation by insulin and other growth factors is blocked when cells are pre-incubated with PI3K inhibitors, such as wortmannin (Burgering & Coffer, 1995).

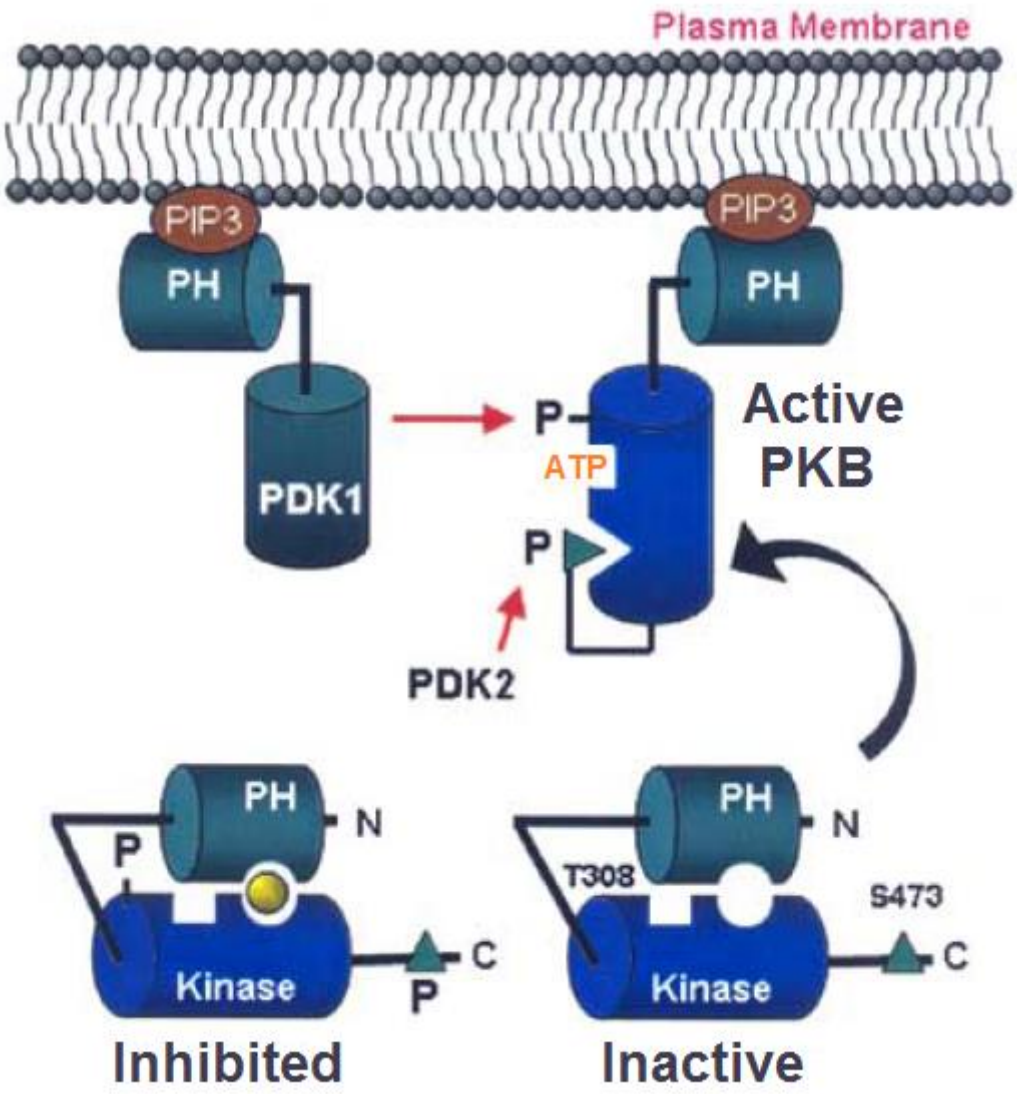

Figure 2.14 Model of PKB activation and inhibition through PH-domain dependent mechanisms (Obtained from Barnett et al., 2005)

PKB plays an important role in insulin signaling and glucose metabolism, and mutation in the *PKB* gene has been identified in promoting cancerous conditions and impair glucose metabolism (Carnero et al., 2008). PKB regulates cell cycling and proliferation by direct action on the cyclin-

dependent kinase inhibitors, p21 and p27, preventing it's localization to the nucleus where it inhibits cell-cycle effects (Viglietto et al., 2002) (**Figure 2.15**). PKB can also regulate cell cycling indirectly by acting on the transcription factor, p53 (Hlobilkova et al., 2007). PKB can promote cell survival by inhibition of pro-apoptotic signals, such as Bcl-2-associated death promoter (BAD) and forkhead box O3 (FOXO3) (Manning & Cantley, 2007).

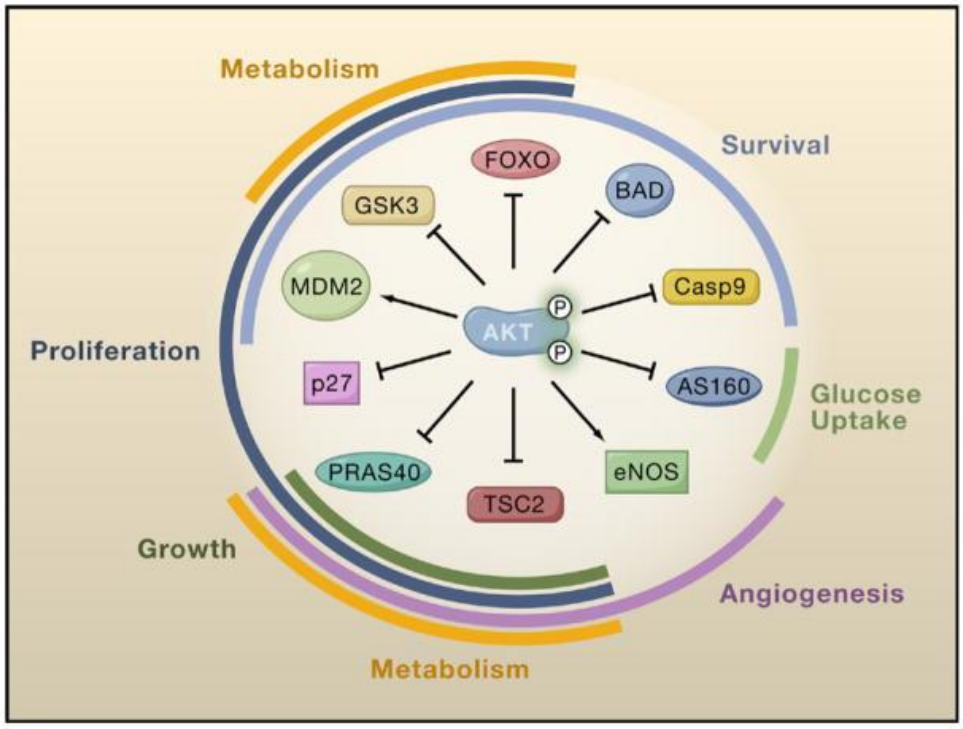

Figure 2.15 Cellular Functions of PKB's Substrates (Obtained from Manning & Cantley, 2007)

In the heart, PKB activation is regulated by insulin and nutritional status (Shiojima, 2002), exercise training (Konhilas et al., 2005), pressure overload (Naga et al., 2000) and advanced heart disease (Taniyama, 2005). PKB signaling can regulate myocyte size through the activation of the TSC1/2 complex and mTOR-dependent pathways (Shioi, 2002), suppression of GSK3β (Haq, 2000) and FOXO3a (Skurk, 2005) (**Figure 2.15**). Activation of the PKB pathway in response to insulin and diet-induced changes in body size has been found to induce cardiac growth (Shiojima, 2002). Shiojima et al. also found that overexpression of PKB1 in cultured rat heart cells can lead to non-pathological hypertrophy. PKB1 also plays a protective role in the myocardium of both acute and chronic cardiac ischemic injuries (Fujio et al., 2000). PKB1 is the most characterised isoform, while very little is still known about the roles of PKB2 and PKB3 in the heart (Walsh, 2006). PKB2 is highly expressed in the heart and other tissues involved in metabolism, including skeletal muscle and the liver (Altomare et al., 1995). PKB3 is expressed at low levels in the non-stressed heart and upregulated in the diseased heart, whereas PKB1 and PKB2 expression remains constant (Taniyama, 2005). The diversity of PKB's influence has made it a prominent therapeutic target for treating cancer, diabetes, strokes and neurodegenerative diseases.

- **GSK-3**

GSK-3 (glycogen synthase kinase-3) is a protein kinase responsible for glycogen synthase regulation and plays a prominent role in glucose homeostasis (Ali et al., 2001). Within the heart it contains two isoforms, GSK-3α and GSK-3β, with molecular weights of 51 kDa and 37 kDa respectively (Woodgett, 1990). GSK-3 plays a multifunctional role in cell signaling involved in proliferation, migration, inflammatory responses, glucose transport, glycogen synthesis, apoptosis and muscle contractility (Huisamen & Flepisi, 2014; Huisamen & Lochner, 2010). As discussed previously, upon entry into the cell, glucose is either metabolised to pyruvate through the glycolytic pathways or converted into glycogen by the enzyme glycogen synthase (GS) (**Section 1.3.2.2 – Glucose metabolism**). In response to insulin stimulation, PI3K and PKB is activated, which inactivates GSK-3 by phosphorylation of the Ser21 site in GSK-3α and Ser9 site in GSK-3β, leading to GS activation (Cohen et al., 1997). In contrast, GSK-3 can be activated by CK2 (casein kinase 2) which in turn inhibits glycogen synthesis (Rayasam et al., 2009). Also, once active, GSK-3 phosphorylates IRS-1 and IRS-2 at their Ser307 and Ser332 sites accordingly, inhibiting IRS-1 signaling and decreasing subsequent PI3K activation (Eldar-Finkelman & Krebs, 1997). This has implicated GSK-3 as a potential negative effector of glucose uptake contributing to insulin resistance (Flepisi et al., 2013; Aguirre et al., 2000).

- **GLUT4**

Glucose transport type 4 (GLUT4) is an insulin-regulated transporter of glucose into cells, present in fat, muscle and heart tissues (Olson & Pessin, 1996). Within the heart cells, five isoforms; GLUT1 and GLUT4 (which are most highly expressed), and also GLUT8, GLUT11 and GLUT12 are responsible for glucose uptake (Abel, 2007). GLUT1 is constitutively present in the sarcolemma and facilitates basal myocardial glucose uptake, especially in dormant heart cells, whereas GLUT4 is found in intracellular vesicular compartments at basal conditions (Joost & Thorens, 2001). GLUT4 is primarily dependent on insulin, and its functioning is impaired when insulin signaling is defective (Garvey et al., 1998). Insulin signaling leads to the activation of PKB, which in turn phosphorylates PKB substrate of 160kDa (AS160) on 5 suggested sites, of which the Ser588 and Thr642 are the most prominent (Manning & Cantley, 2007), resulting in stimulation of GLUT4 translocation to the cell membrane. Mutations at these two sites significantly inhibits insulin-induced GLUT4 translocation (Sano et al., 2003). Currently, the mechanism proposed for PKB-AS160 mediation of GLUT4 translocation, states that PKB activation on the various binding sites on AS160 inhibits GTPase-activating protein (GAP) activity, recruiting a Rab-family GTPase to become GTP loaded. Upon stimulation, GLUT4 vesicles translocates to the plasma membrane and facilitate the uptake of glucose from the blood stream (Mîinea, 2005) (**Figure 2.11**). Alternatively, AMPK has also been found to phosphorylate AS160 independent of insulin (Treebak et al., 2006).

Skeletal muscle is responsible for 75-80% of glucose disposal from the blood circulation (Abdul-Ghani & DeFronzo, 2010) and also the most affected tissue type at the onset of insulin resistance (Shimokawa et al., 2000). However, GLUT4 levels still remain normal in insulin resistant states within the muscle, which implicates defective translocation of GLUT4 as a major contributor to insulin resistance (Garvey et al., 1998). Likewise in T2D patients, GLUT4 translocation in skeletal muscle is downregulated, while the GLUT4 contents remain the same (Volchuk, 1998). The defective translocation is thus either due to impaired insulin signaling or a problem specific to the GLUT4 transport system. Various studies have shown that physical exercise can effectively resensitize the insulin signaling pathway and increase glucose uptake in skeletal muscles via upregulated GLUT4 translocation (Kennedy, 1999).

1.4.6.2 RAS/MAPK PATHWAYS

The Ras-MAPK-dependent pathway cooperates with the PI3-K/PKB pathway to control cell proliferation. MAP kinases (MAPK's) consists of 3 groups of serine threonine kinases: extracellular signal-regulated kinases (ERK1/2/3), c-Jun amino-terminal kinase/stress-activated protein kinases (JNK), and p38 MAPK's (discussed in more depth in **Appendix A – Alternative Pathways of Insulin-dependent Glucose Uptake**). Depending on the extracellular stimuli, these kinases can initiate a network of cell signaling cascades with various responses. The different isoforms of ERK, JNK, and the p38 MAPK's are expressed in nearly all types of tissues and cells (Deng et al., 2012).

1.4.6.3 CAP/CBL PATHWAY

The CAP/Cbl pathway is the third proposed mechanism of glucose uptake (Saltiel & Kahn, 2001). According to this pathway, after activation of IRS, the Cbl associated protein (CAP) recruits the proto-oncogen Cbl resulting in a cascade that also recruit GLUT4 translocation (**Figure 2.11**). The insulin signaling pathways, PI3K-Akt pathway and Cap/Cbl pathway, work together to coordinate the regulation of GLUT4 vesicle trafficking, protein synthesis, enzyme activation and inactivation, and gene expression which facilitates the actions of insulin such as regulation of glucose, lipid and protein metabolism (Sesti, 2006)

1.4.6.4 INSULIN-INDEPENDENT MECHANISMS

- **AMPK**

AMPK (AMP-activated protein kinase) is one of the main metabolic energy sensors within cells and plays an imperative role in maintaining energy homeostasis (Hardie et al., 2006). AMPK is a heterotrimeric protein that contains a catalytic subunit (α) and two regulatory subunits (β and γ) (**Figure 2.16**). AMPKα2 is most commonly expressed in liver, skeletal muscle and heart tissues

(Hardie & Carling, 1997). AMPK remains in an unphosphorylated inactive state through interplay between the kinase domain (KD), autoinhibitory domain (AID) and N-terminus of the regulatory β subunit. AMPK is activated in response to an increase in intracellular AMP/ATP ratio,which effects the α hook domain (H) bringing about a conformational change in the heterotrimeric complex by relieving AID. Conditions of stress, such as exercise and hypoxia (Mungai, 2011), initiate the binding of AMP to AMPK, exposing the regulatory Thr^{172} site in the catalytic α-subunit, which promotes phosphorylation and enhance AMPK activity (Frederich & Balschi, 2002). This also protects AMPK from protein phosphatases (PPase) that remove the phosphate groups from the Thr^{172} site, which would lead to the deactivation of AMPK. The β-subunit also contains a glycogen binding domain (GBD) which further modulates kinase activation (Zaha & Young, 2012). Once activated, AMPK promotes energy generating pathways and inhibits energy consuming processes. Additionally, AMPK can be phosphorylated by upstream AMPK kinases, such as liver kinase B1 (LKB1) and calcium-calmodulin-activated protein kinase β (CAMKKβ) (Woods, 2003) under the influence of hormones such as adiponectin (Shibata et al., 2005) and insulin (Beauloye, 2001), which also modulates AMPK activity. Adiponectin is a hormone derived from fat cells, and plays a protective role when blood supply to the heart is restricted, by activating AMPK to generate energy using countermeasures. In contrast, insulin inhibits AMPK activation in response to an excess of nutrients. Insulin promotes glycogen, triglyceride and protein synthesis, while AMPK inhibits these energy consuming processes (Towler & Hardie, 2007). AMP-activated protein kinase has been shown to directly stimulate glucose uptake in skeletal muscle, thereby improving insulin insensitivity (Fisher et al., 2002) (**Figure 2.11**).

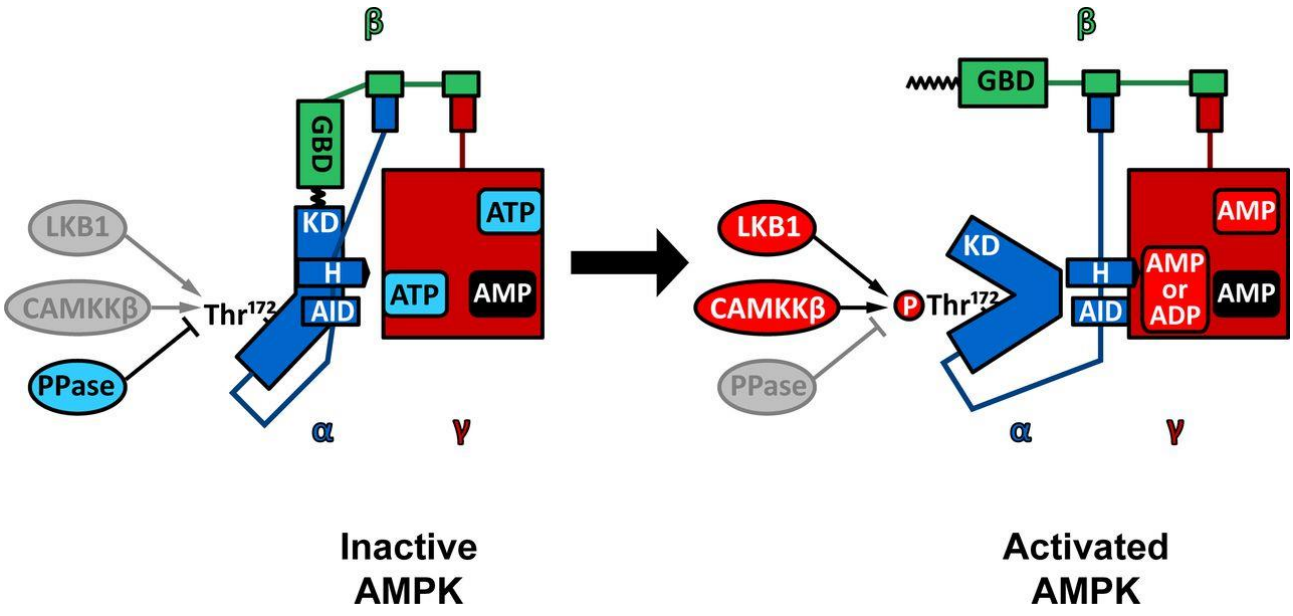

Figure 2.16 Molecular Structure of the AMPK complex. (Obtained from Zaha & Young, 2012)

1.4.7 Cause of Insulin Resistance

The mechanism underlying insulin resistance is still not completely understood. Maintaining a positive or surplus energy balance leads to expanded adipose tissue (obesity) and obesity-related disorders, which are commonly associated with insulin resistance. Furthermore, the relationship between lipid displacement, insulin resistance and the subsequent development of serious disorders including type 2 diabetes, hypertension, dyslipidemia and disorders of coagulation and fibrinolysis are well established and can lead to cardiovascular diseases (Boden, 2011). Also, adipose tissue not only stores additional calories, but as an endocrine organ also secrete pro-inflammatory cytokines (Wieser et al., 2013), angiotensin II (Ogihara et al., 2002), leptin, resistin, adiponectin, PAI-1. These compounds, when expressed in great quantities, can produce insulin resistance. Insulin resistant obese individuals often present with low levels of systemic inflammation, as well as adipose tissue inflammation (Wieser et al., 2013). The pro-inflammatory cytokines tumour necrosis factor (TNF-α), interleukin (IL)-1 and IL-6 expressed in adipose tissue are all upregulated in an insulin state. Angiotensin II has been implicated in the development of both hypertension and insulin resistance (Ogihara et al., 2002). It is speculated that elevated angiotensin II levels give rise to increased oxidative stress, which impairs downstream activation of PI3K – thus, inhibiting the insulin signaling pathway. However, to confirm a significant link between obestiy and insulin resistance, these factors need to be elevated to such extent that it induces insulin resistance, and conversely, lowering the factors need to reduce insulin resistance (Boden, 2011).

Impaired glycogen synthesis, especially in muscle, is one of the earliest detectable defects in insulin resistance (Bonadonna, 1993). In skeletal muscle and adipose tissue, glucose uptake is initiated through insulin action. Given that nearly 80% of glucose entering the skeletal muscles is converted to glycogen, impairment in the synthesis of glycogen, and thus the subsequent lack of clearance of glucose from the blood, is one of the major indicators of insulin resistance (DeFronzo & Tripathy, 2009). Pancreatic β-cells respond to insulin resistance, regardless of the cause of the condition, by increasing the secretion of insulin. However, this leads to abnormally high circulating insulin levels in blood plasma that further deteriorates insulin sensitivity in especially skeletal muscles (DeFronzo & Tripathy, 2009). Thus, hyperinsulinemia is not only a response to insulin resistance, but also exarcerbates the condition (Cavaghan et al., 2000).

1.4.8 Summary of Insulin Resistance

The increased prevalence of obesity in insulin resistant patients is evident. However, insulin resistance is only viewed as an adaptive mechanism (to protect cells against acute lipid overload and inflammation) which becomes ineffective and leads to multiple metabolic abnormalities in the chronic state (Tsatsoulis et al., 2013). Althought many of these abnormalities can also occur in non-insulin resistant subjects (McLaughlin et al., 2004), they are closely related to obesity (Cornier et al., 2008) and are strongly associated with increased risk for cardiac diseases (Reaven,1988).

2. ASPALATHIN: A POLYPHENOL WITH PURPOSE

2.1 INTRODUCTION

In South Africa, 80% of the population appeal to indigenous or traditional medicines for primary health care (Street & Prinsloo, 2013). Moreover, the Chinese have been using tea medicinally since 2700 BC (Heiss & Heiss, 2011). The Western culture was the last to discover the value of tea and made it popular in the 17th century, albeit mostly as a social beverage. In recent years, teas and herbal teas have yet again been receiving more and more attention as a dietary supplement due to their health-promoting effects. Besides water, teas are the most popular drink of choice in the world (MacFarlane & MacFarlane, 2004). Generally speaking, teas are aromatic beverages prepared by adding hot water to cured leaves of *Camellia sinensis* or green tea. In comparison, herbal teas are infusions made from fruits or herbs, without using the green tea plant (Zhang, 2002). Consuming tea has also been reported to lower the risk of cardiovascular disease (Bøhn et al., 2012) and certain teas have especially potent antioxidant and hypoglycemic properties, which aid in preventing oxidative damage to cell structure and function. One of these prominent teas, which has gained international acclaim for it's beneficial properties, is Rooibos - a caffeine-free herbal tea with a low-tannin status.

2.2 ROOIBOS

2.2.1 OVERVIEW OF ROOIBOS

Rooibos is produced by an infusion of the foliage, stems and leaves of *Aspalathus Linearis* (from the Latin *aspalathus* or Greek *aspalathos* – a scented and spiny bush) (Quattrocchi, 2012). In the industry, hot water extracts of rooibos are used as a food ingredient in food products, such as yogurt and jam, and in beverages, such as instant tea drinks (Joubert & De Beer, 2011). The popularity of rooibos has grown significantly since it became a commodity in 1904. In 2010, nearly a quarter of teas sold in South Africa was Rooibos, constituting approximately 5 000 tons of produce, while 5 000 tons were exported for consumption in Germany, the Netherlands, the United Kingdom, Japan and the United States of America (Street & Prinsloo, 2013).

Traditionally, rooibos has been used as a treatment or ointment for alleviating stress-related ailments such as insomnia and anxiety. Rooibos polyphenols (**Figure 2.17**) also exhibit similar properties to the polyphenols of honeybush (*Cyclopia intermedia*), black and green (*Camellia sinensis*) teas when comparing antioxidant potential and antimutagenicity (Van der Merwe et al., 2006). Furthermore, increased antioxidant levels in unfermented rooibos compared to fermented rooibos (FRE), led to the development of green rooibos (GRE). This has become a prominent product for nutraceutical industries isolating rooibos compounds for its anti-oxidant properties. Rooibos is gaining more popularity as a dietary antioxidant supplement and drinking merely 2 cups of either fermented or unfermented rooibos has the potential to raise plasma anti-oxidant levels in

healthy adults (Villaño et al., 2011). Furthermore, in adults susceptible to cardiovascular disease, consuming 6 cups of fermented rooibos infusions per day for 6 weeks has been shown to improve lipid profiles and redox status (Marnewich et al., 2011).

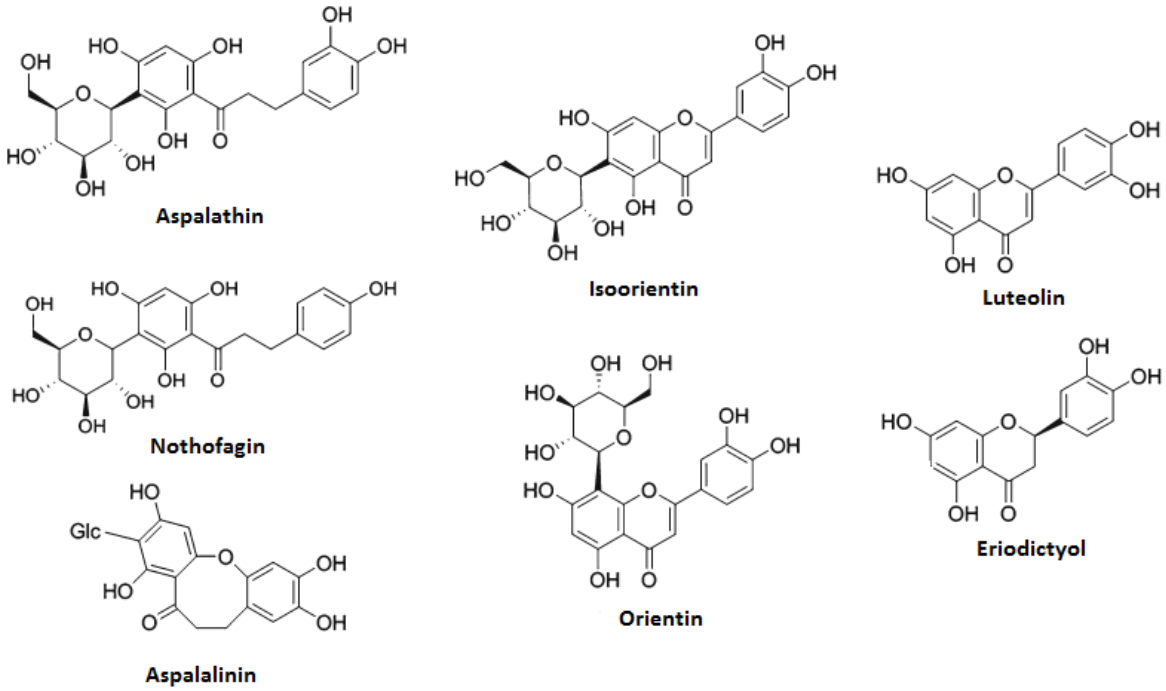

Figure 2.17 Major compounds present in rooibos tea

2.2.2 PROCESSING

Commercially, rooibos shoots are shredded and bruised, and left to enzymatically and chemically oxidize. This is followed by fermentation and sun drying (Joubert & Schultz, 2006). Finally, the tea is steam pasteurized to ensure that the final product is microbiologically safe. However, steam pasteurization significantly reduces the soluble solids, total polyphenols, total colour and most importantly, aspalathin contents of rooibos infusions (Koch et al., 2013). The polyphenol content (specific chemical structures with strong anti-oxidant capacity occuring naturally in plants) in rooibos extracts, especially the aspalathin and nothofagin (another prominent polyphenol in rooibos) content, are dependent on the concentration present in the plant (Schulz et al., 2003) and the extent to which the plant material is fermented (Joubert, 1996) (**Table 2.1)**.

Table 2.1 Aspalathin and nothofagin content of unfermented (green) and fermented (traditional) rooibos tea (Joubert & Schulz, 2006)

Tea	Parameter	Aspalathin (g/100g)	Nothofagin (g/100g)
Unfermented	Range	3.84 – 9.66	0.2 – 1.24
	Average (n = 97)	6.62	0.67
Fermented	Range	0.02 – 1.16	0 – 0.40
	Average (n = 89)	0.26	0.12
***n = number of different strains tested**			

Rooibos processed using hot-water extracts for commercial purposes has similar total polyphenol and dihydrochalcone content, but lower flavone content compared to a fresh cup of tea (Joubert & De Beer, 2012). Citric acid, a natural preservative found in citrus fruits, and ascorbic acid (vitamin C) is usually added to aspalathin-related products to stabilize aspalathin content during heat treatment and long term storage (De Beer et al., 2011, Joubert et al., 2010). However, commercial beverages such as iced teas contain low to no detectable aspalathin or the related oxidation products, orientin and isoorientin (Joubert et al., 2009).

2.3 ASPALATHIN

2.3.1 Overview of Aspalathin

Aspalathin is the primary polyphenol and flavonoid present in the leaves of Rooibos or *Aspalathus Linearis* (Koeppen & Roux, 1966). Flavonoids are plant-derived polyphenols which are naturally present in fruits, vegetables, teas and herbs, however aspalathin occurs exclusively in rooibos. Aspalathin can either be isolated from rooibos extracts or synthetically produced. It is gaining increasing popularity in research as a potent anti-oxidant (Dludla et al., 2014; Joubert et al., 2009), stimulant of glucose clearance in muscle cells (Muller et al., 2012) and regulator of energy metabolism (Son et al., 2013). Very few studies have been done in humans, and aspalathin have been found to have a very low detectable bioavailability, ranging between 0.1 and 0.9% of total aspalathin consumed (Kreuz et al., 2008). Aspalathin, is absorbed, metabolized and its glucuronidated and sulfonated conjugated metabolites excreted in the urine (Courts & Williamson, 2009). It is however possible that aspalathin can aggregate over time and elicit its various physiological responses.

2.3.2 STRUCTURE

Aspalathin (2',3,4,4',6'-pentahydroxy-3-C-β-D-glucopyranosyldihydrochalcone) is considered to be a C-glycosyl dihydrochalcone (**Figure 2.18**). Aspalathin is soluble in water and other polar solvents, but insoluble in non-polar media. It is also not stable during heat treatment, and oxidizes rapidly in the presence of light. Aspalathin is biogenetically related to other flavonoids isolated from rooibos tea (Koeppen & Roux, 1966). It is one of the few naturally occuring dihydrochalcones, together with nothofagin and pterosupin, also discovered in plants (Yoshida et al., 1993) and a rare class of flavonoid compound (Williams, 1964). To date, aspalathin is found to be exclusively present in *Aspalathus Linearis.*

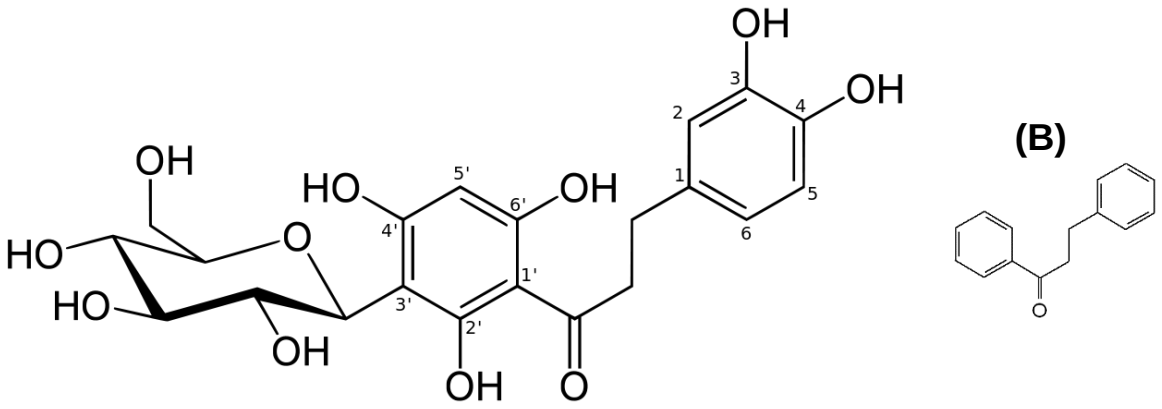

Figure 2.18 Structure of aspalathin (A) **and the root chemical structure, dihydrochalcone** (B)

2.3.2.1 ROOIBOS TEA COLOURATION

Koeppen & Roux (1966) found that, in the presence of oxygen and sunlight, aspalathin produced the flavanones 2,3-dihydro-iso-orientin and 2,3-dihydro-orientin, which converted to unknown brown products. This was thought to be the mechanism by which the red-brown colour development of rooibos tea occurred till Joubert (1994) was able to show the colouration in the absence of sunlight under controlled conditions, implicating aspalathin as the sole colouration agent (Joubert, 1994).

2.3.3 ASPALATHIN SYNTHESIS

Fermentation of rooibos is very detrimental to aspalathin content with losses as high as 98% reported (Schulz et al., 2003). Aspalathin is degraded through various nonenzymatic mechanisms during fermentation. The first mechanism to be elucidated is through oxidation in the presence of heat and light - aspalathin is converted into the flavanones (S)- and (R)-eriodictyol-6-C-β-D-glucopyranoside, which further converts to the flavones, iso-orientin and orientin (Marais et al., 2000). The second mechanism, also by means of oxidation, results in aspalathin dimers formation, when O-quinones are nucleophilically linked to aspalathin compounds (Krafczyk & Glomb, 2008). A

third mechanism, and key to the colour formation of rooibos during fermentation, was discovered by Heinrich et al. (2012), by which aspalathin is oxidized to coloured structures with dibenzofuran skeletons, called (S)- and (R)-3-(7,9-dihydroxy-2,3-dioxo-6-β-D-glucopyranosyl-3,4-dihydrodibenzo[b,d]furan-4a(2H)-yl) propionic acid. Yepremyan et al. (2010) was also able to synthetically isolate aspalathin in 8 steps, using tribenzyl glucal, tribenzylphloroglucinol, and either 4-(benzyloxy) phenylacetylene or 3,4-bis(benzyloxy)phenylacetylene with 20% overall yield.

2.3.4 BIOAVAILABILITY

Bioavailability is assessed by quantifying the metabolites of a compound in order to determine the extent of flavonoid metabolism, and in this case metabolites of rooibos compounds *in vivo* (Walle, 2004). It has been repeatedly shown that *in vitro* activity does not necessarily mimic *in vivo* activity. This is especially true for polyphenols which are known to be first metabolized by phase I and II liver enzymes, as well as the kidneys, resulting in conjugates forming in the blood plasma and urine (McGurk et al., 1998). Unfortunately, the biological properties of the majority of these products still remain unknown (Scalbert et al., 2002). Through conjugation, the biological effects of the parent compound can be either reduced or completely inhibited (Day et al., 2000). Flavonoids bind to proteins, such as albumin, effectively lowering the detectable free flavonoid levels in the plasma (Manach et al., 1997), while the majority of flavonoids can be directly transported to the large intestine.

Huang et al. (2008) tested the transport of aspalathin across human skin and Caco-2 intestinal epithelial cells. They found that only 0.01% of the initial dose administered was able to cross the skin-barrier, while nearly 80% of the aspalathin was transported across the Caco-2 cell monolayer. Breiter et al. (2011) found low bioavailability of flavonoids in plasma (only 0.26% of the total flavonoids ingested), which correlated with no significant increase in antioxidant capacity of the blood. After ingestion of aspalathin, the glycoronyl and sulphate conjugates are present in rat liver extracts (Van der Merwe et al., 2010) and O-linked methyl-, sulphate-, glucoronide-, and O-methyl-O-glucoronide derivates in human urine and plasma (Stalmach et al., 2009). Unmetabolized aspalathin is also detectable in human plasma (Laue et al., 2009). Aspalathin has a very low estimated absorption rate between 0.1% and 0.9% in pigs and humans (Kreuz et al., 2008, Courts & Williamson, 2009, Stalmach et al., 2009). The unconjugated polyphenols as well as the remaining conjugates, could possibly aggregate in the body and elicit pharmacological activities (Zhang et al., 2007), which is to say, even though aspalathin has a low bioavailability in humans, it could still accumulate and produce effects in tissue and body fluids.

2.3.4.1 MECHANISM OF METABOLISM

The metabolism of aspalathin is dependent on how aspalathin is distributed between the aqueous (cytosolic) and lipid (membrane) compartments in the cell. At a physiological pH of 7.4, the majority of polyphenols associate with the polar head groups of the membrane phospholipids, exposing its OH-group for glucoronidation (Verstraeten et al., 2003). Polar metabolites accumulate in the cytosol of cells and undergo methylation and sulfation. For instance, the major urinary metabolite of aspalathin, O-methyl glucoronide (Stalmach et al., 2009), seems to be the result of methylation in the cytosol, followed by glucoronidation in the endoplasmic reticulum. Also, conjugation increases hydrophilicity compared to the parent compounds, altering their site of action, and should they retain their anti-oxidant properties, cause altered interaction with cellular antioxidants. Glucoronidation of aspalathin dissipates its antioxidant potential, but it can still elicit other biological properties, as compared with the conjugation of another rooibos compound, quercetin (O'Leary et al., 2003; Day et al., 2000). The rate of conjugation reactions can also be impeded due to high demand for the same substrates. The factors influencing the rate include the concentration or dose of polyphenol administered and the hydrophobic/hydrophilic nature of the subcellular environment (Koster et al., 1981). The higher the dose, the more likely sulfation conjugation will occur, rather than glucoronidation. Even though polyphenolic conjugation is well recognized, most biological studies still incorporate unmetabolized, natural, plant polyphenols.

2.3.4.2 METABOLITES

Breiter et al. (2011) identified 5 different metabolites derived from aspalathin in urine. Of these, 4 are conjugated forms, namely sulphated, glucoronidated, methylated and both glucoronidated and methylated aspalathin and the 5th is referred to as the aglycone (glucoronidated-2,3,4,4',6-pentahydroxy-dihydrochalcone) of aspalathin. Also, unchanged aspalathin was identified in the urine of volunteers consuming rooibos tea and isolated aspalathin-enriched rooibos fractions (ARF). Methylated aspalathin was detected in a higher concentration, compared to free aspalathin, indicating methylation as a significant conjugation pathway (Breiter et al., 2011). Metabolites are still excreted 5 hours after consumption of aspalathin-containing drinks, indicating the small intestine as the primary point of absorption (Stalmach et al., 2009).

2.3.4.3 CLINICAL STUDIES

Fermented rooibos consumed as part of a dietary regime was shown to elevate total blood plasma polyphenol levels and improve the lipid profile and redox status (Marnewick et al., 2011). Villano et al. (2010) was also able to verify an increase in blood plasma antioxidant potential 1 hour after healthy adults consumed 2 cups of fermented rooibos, similar to other strong antioxidants, such as black tea (Widlansky et al., 2005), green tea (Coimbra et al., 2006) and cranberry juice (Duthie, 2005).

2.3.4.4 Animal Toxicity

Marnewick et al. (2003) treated ten Fisher 344 rats with 2 g/100 ml GRE and FRE for 10 weeks and found no adverse effects on body weight, liver, kidney or serum parameters (including aspartate transaminase, alanine transaminase (ALT), alkaline phosphatase (ALP), creatinine, bilirubin, total protein, cholesterol and iron status).

2.3.4.5 Human Toxicity

Poorly processed rooibos contains high amounts of Salmonella, a gram-negative bacteria which can cause severe diarrhea, fever and abdominal cramps in infected patients (Gouws et al., 2014). However, proper processing of rooibos usually insures that the rooibos is microbially safe (Joubert & Schultz, 2006). In 2010, Sinisalo et al. reported a case study describing a 42-year-old woman who had been experiencing possible hepatotoxicity from consuming 1L of rooibos tea (Forsman Rooibos tea; Vantaa, Finland) per day for 2 weeks. She exhibited elevated plasma levels of ALT, ALP and gamma-glutamyl transferase. Given that this was an isolated incident regarding rooibos' toxicity, it is speculated that the hepatotoxicity could be due to a genetic predisposition to one of the bioactive compounds in rooibos causing an adverse reaction, or that the specific brand of rooibos she consumed might have been laced with hepatotoxic compounds (Sinisalo et al., 2010). In contrast, Marnewick and colleagues (2011) gave 40 volunteers six cups of fermented rooibos per day for six weeks (equating to ~1.5L per day) and found some individuals to present with minor elevations in hepatic enzymes, but not enough to be of clinical significance. Overall, rooibos has been confirmed as safe for human consumption by at least 3 studies (Hesseling et al., 1979; Breet et al., 2005; Marnewick et al., 2011).

2.3.5 Aspalathin Function

2.3.5.1 Antioxidant Potential

Under baseline conditions, cells have a natural scavenging capacity to balance reactive oxygen species (ROS) production through anti-oxidants such as glutathione (GSH). During diseased condition such as diabetes, however, there is an increased vulnerability for cellular damage and apoptosis due to an imbalance in the antioxidant to oxidative stress ratio. It has repeatedly been shown that diets consisting of primarily plant-based foods and beverages can lower the risk of developing chronic diseases (Hu, 2003). Consuming flavonoids reduces the incidence of cardiovascular diseases and cancer (Arts & Hollman, 2005; Knekt et al., 2002). Also, dietary interventions consisting of polyphenol-rich foods, have shown to improve plasma antioxidant capacity and total phenolic content (Lotito & Frei, 2006). Conversely, as shown by Prior et al. (2007), consuming nutrients without anti-oxidants, results in a loss of anti-oxidant potential in the blood. Moreover, strong anti-oxidant polyphenols have been researched in treating diabetic-associated complications (Zang et al., 2006). Aspalathin is implicated as one of the main contributors of rooibos' antioxidant potential (Joubert et al., 2009) (**Figure 2.19**), which is partly due

to the relatively high content of aspalathin in rooibos, compared to the other compounds, and also its radical scavenging activities.

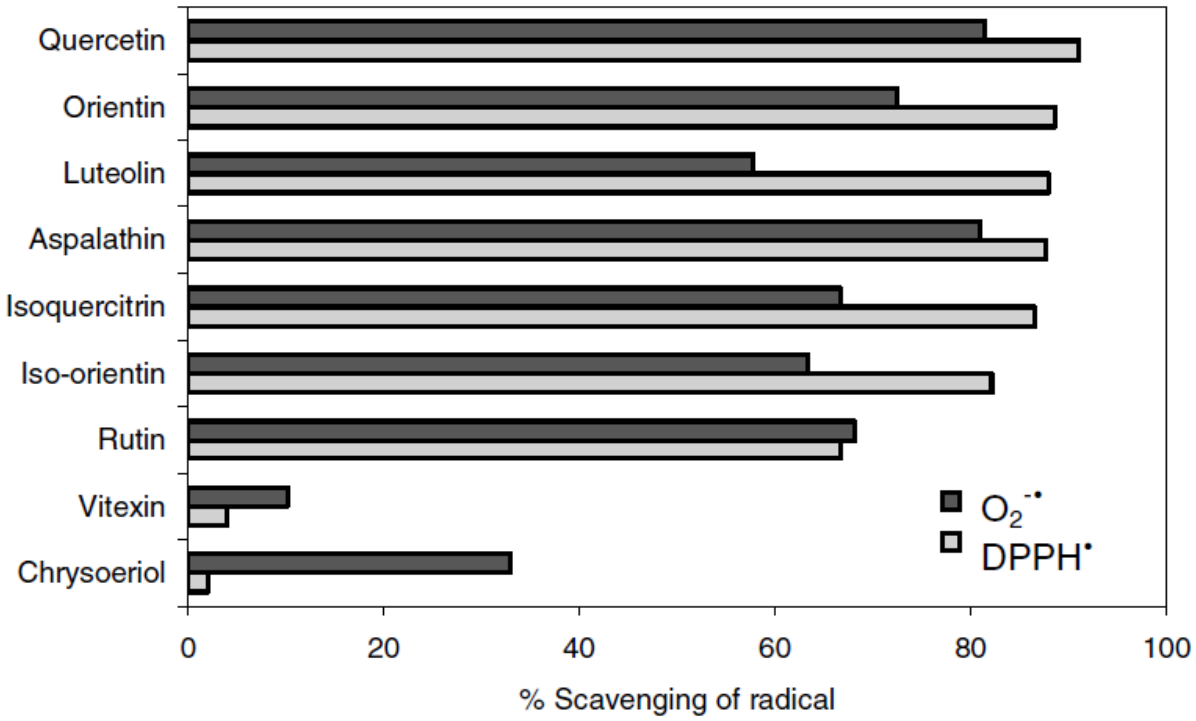

Figure 2.19 Comparison of the aspalathin's free radical scavenging ability compared to other rooibos flavonoids. DPPH$^\bullet$: 2,2-diphenyl-1-picrylhydrazyl free radical, $O_2^\bullet$: superoxide radical (Joubert et al., 2006)

- **IN VITRO**

Dludla et al. (2014) showed that pretreating cardiomyocytes with FRE improved the anti-oxidant status of the cells by reducing intracellular ROS and cell death in response to pro-oxidants (exogenous H_2O_2). This was tested within a solution mimicking an ischemic environment (Dludla et al., 2014). Furthermore, FRE preserved GSH and ATP content in cardiomyocytes. They also showed that fermented rooibos extract is more effective at protecting cardiomyocytes against cell damage than the antioxidant vitamin E (a strong anti-oxidant used in radiotherapy treatment) (Prasad et al., 2002). Aspalathin was found to have even greater antioxidant potential than the commercial standard EGCG (epigallocatechin gallate), which is the most abundant catechin in green tea (Snijman et al., 2007). However, high dosages of polyphenols are known to exhibit pro-oxidant, rather than anti-oxidant effects (Mennen et al., 2005). This was verified by Dludla et al. (2014) as high doses of FRE reduced its protective effect against exogenous H_2O_2. Aspalathin also proved a potent scavenger of ROS induced advanced glycation end products (AGE) in RIN-5F cells (Son et al., 2013). In addition, GRE and aspalathin was able to protect against juglone toxicity (used in high dosages to generate intracellular superoxides, $O_2^\bullet$ and H_2O_2) by scavenging the superoxide anion radicals. Rooibos protects against acute oxidative damage by upregulating hsp-16, a protein involved in the insulin/IGF-1 signaling pathway. Also, rooibos upregulated sod-3, an

enzyme that eliminates ROS, leading to an increase in stress resistance. Similarly, rats treated with rooibos tea, had upregulated serum SOD (superoxide dismutatase) levels (Baba et al., 2009).

Chen et al. (2013) investigated the protective properties of aspalathin, GRE and FRE in *C.elegans* - an invertebrate organism used for investigating hyperglycemic conditions, ageing and longevity through simulation of a high glucose environment (Schlotterer et al., 2009). They found that both rooibos and aspalathin ameliorate the amount of hydrodren peroxide anions and related ROS generating compounds, such as juglone. Furthermore, ARF and purified aspalathin inhibited the activity of xanthine oxidase (XOD), an enzyme responsible for generating reactive oxidant species. Aspalathin was found to be a competitive inhibitor of XOD with an inhibition constant (Ki) of 3.1 μM, comparative to other flavonoids like phloretin, which has a K_i of 0.66 μM (Nagao et al., 1999).

- **IN VIVO**

Rats treated with both GRE and FRE displayed increased myocardial total GSH content and reduced oxidative stress, which was also associated with improved aortic output recovery after ischemia/reperfusion (Pantsi et al., 2011). In a study done by Marnewick et al. (2011), 40 human adults at risk for cardiovascular disease consumed 6 cups of fermented rooibos for 6 weeks, and were shown to have an improved redox status and elevated plasma GSH levels. Likewise, Villaño et al. (2010) found elevated plasma antioxidant capacity for 1 hour in healthy adults following the consumption of 2 cups of both fermented and unfermented rooibos tea.

- **SYNERGY BETWEEN RELATED COMPOUNDS IN ROOIBOS**

Simpson et al. (2013) showed that the antioxidant activity of green and fermented rooibos infusions are controlled by the presence of the two active dihydrochalcones, aspalathin and nothofagin. They also found that, by preparing artificial infusions, using the most abundant polyphenols in similar concentrations present in natural rooibos infusions, created a synergistic effect between the polyphenols allowing a greater antioxidant activity than that of natural infusions.

- **ANTI-AGEING EFFECTS**

Glucose shortens the life span of *C.elegans* through inhibition of the FOXO transcription factor daf-16, present in the insulin-signaling pathway (Lee et al., 2009), however Chen et al. showed that aspalathin is able to reverse these aging effects by upregulating daf-16. The balance between internal and external ROS production in response to stress, is at the core of the ageing process and many age-related diseases. Aspalathin, as a strong anti-oxidant, is able to intervene in the ageing mechanism (Finkel & Holbrook, 2000).

2.3.5.2 CARDIOPROTECTION

Pretreatment of cardiomyocytes with fermented rooibos prevented damage induced by ischemia, as indicated by a reduced amount of high fatty acid binding protein leakage (Dludla et al., 2014). The effect of pure aspalathin on the heart, heart cells or heart cell analogs have not been investigated to date.

2.3.5.3 GLUCOSE UPTAKE

Aspalathin has been found to dose-dependently increase glucose uptake in rat L6 skeletal myotubes at concentrations between 1 and 100 μM (Kawano et al., 2009; Son et al., 2013).

- **PKB-DEPENDENT MECHANISM**

In rats supplemented for 7 weeks with GRE and FRE, Pantsi et al. (2011) found low to no effect by rooibos flavonoids on total PKB levels in the hearts. Mazibuko et al. (2013) also found no influence on total PKB, but found that rooibos did in fact increase phospho-PKB (P-PKB) levels in the heart. Arguably, the specific composition of polyphenols present in the rooibos extracts used in their respective studies could have contributed to this effect. In another study done by Son et al. (2013), rooibos also did not activate PKB in normal L6 myocytes, whereas Mazibuko et al. was able to show activation of PKB in insulin resistant C2C12 myocytes when treated with rooibos. Mazibuko et al. observed that chronic exposure to saturated free fatty acids, such as palmitate, reduces downstream activation of IRS-1 resulting in decreased PKB activation and GLUT4 translocation, effectively producing more insulin resistant cells (Bhattacharya et al., 2007). However, when treated with rooibos, the P-PKB levels of the palmitate treated cells resembled that of normal PKB levels when stimulated by insulin, suggesting that rooibos can resensitise downstream insulin signaling.

- **AMPK-DEPENDENT MECHANISM**

Mazibuko et al. (2013) found that insulin resistant mouse C2C12 skeletal muscle cells treated with rooibos, resulted in the activation of the insulin-independent AMPK pathway which culminated in increased levels of GLUT4. Similarly, Son et al. (2013) found that aspalathin activated AMPK signaling and promoted endogenous GLUT4 translocation to the plasma membrane in L6 myocytes and in skeletal muscle of *ob/ob* mice fed a diet substituted with 0.1% aspalathin for 5 weeks (effective aspalathin dose 100mg/kg/day/mouse), but did not affect PKB activation. In C2C12 mouse skeletal muscle cells, Muller et al. (2012) also showed aspalathin is able to improve glucose uptake, while this same effect could not be mimicked in Chang liver cells, which does not contain GLUT4. This strongly implicates GLUT4 and AMPK as essential role players in eliciting aspalathin's response.

2.3.5.4 RESTORE GLUCOSE HOMEOSTASIS

Mazibuko et al. (2013) found that treating palmitate-induced insulin-resistant C2C12 skeletal muscle cells with either FRE or GRE enhanced glucose uptake, mitochondrial activity and ATP production. GRE also completely reversed the effects of palmitate by restoring basal glucose uptake. Aspalathin suppressed elevated fasting blood glucose and improved impaired glucose tolerance in *ob/ob* mice (Son et al., 2013) and *db/db* mice (Kawano et al., 2009). Aspalathin also suppress gene expression of enzymes related to gluconeogenesis and glycogenolysis, while upregulating glycogenesis in the liver of *ob/ob* mice, resulting in a reduced blood glucose levels (Son et al., 2013). In RIN-5F pancreatic β-cells aspalathin upregulates insulin secretion at concentrations of 100 μM, a further mechanism leading to improved glucose homeostasis (Kawano et al., 2009).

- **SYNERGY BETWEEN RELATED COMPOUNDS IN ROOIBOS**

Muller et al. (2012) showed that Streptozotocin (STZ)-induced T1D Wistar rats (STZ used to ablate insulin producing pancreatic β-cells) pretreated for 1 hour with ARF, suppressed blood glucose level increases. Purified aspalathin was unable to elicit the same response, but when aspalathin was combined with rutin (another prominent flavanoid present in rooibos), blood glucose was effectively suppressed for upto 6 hours (Muller et al., 2012).

2.3.5.5 LIPID PROFILE

A person's lipid profile is determined by screening the blood for abnormalities in lipids, including cholesterol and triglycerides. In adults at risk for cardiovascular disease, it was found that 6 cups of fermented rooibos per day for 6 weeks improved the lipid profile by lowering the LDL-cholesterol and TAG levels, and increasing the HDL-cholesterol (Marnewick et al., 2011). In addition, fermented rooibos reduced lipid peroxidation, by decreasing conjugated dienes (CDs) and thiobarbituric acid reactive substances (TBARS). Furthermore, 0.1% aspalathin administered for 5 weeks (effective aspalathin dose 100mg/kg/day/mouse) reduced hypertriglyceridemia, serum TBARS and adiponectin levels in *ob/ob* mice (Son et al., 2013). Aspalathin also suppressed gene expression of enzymes related to lipogenesis leading to reduced serum triglyceride levels (Son et al., 2013)

2.3.5.6 HYPERURICEMIA

Hyperuricemia is considered to be one of the risk factors in developing metabolic syndrome and cardiovascular disease (Dawson et al., 2007; Soltani et al., 2013). Increases in uric acid levels can be attributed to a high intake of purine-rich foods, fructose, alcohol and obesity (Emmerson, 1997; Nakagawa, 2005). During the metabolism of purines, xanthine and hypoxanthine are converted to uric acid by the enzyme xanthine oxidase in the liver and intestine (Borges et al., 2002). Kondo et

al. found that ARF and purified aspalathin both significantly suppressed plasma uric acid levels in hyperuricemic mice (Kondo et al, 2013).

2.3.5.7 ANTI-APOPTOTIC

Pantsi et al., (2011) showed that both GRE and FRE fed to rats for 7 weeks, were able to significantly decrease poly ADP ribose polymerase (PARP) cleavage (a pro-apoptotic protein), while only FRE was able to decrease caspase-3 (also a pro-apoptotic protein) activity, inhibiting apoptosis and thereby having a cardioprotective effect.

2.3.5.8 ANTIMUTAGENICITY

GRE has been shown to reduce oesophageal papilloma (cancer) development in rats (Sissing et al., 2011). This strongly implicates rooibos polyphenols as having key anti-cancer potential. In an earlier study done by Van der Merwe et al. (2006), FRE was found to be more effective than GRE, but highly mutagen specific. Snijman et al. (2007) tested the antimutagenic activity of the major flavonoids in rooibos. They found that aspalathin and nothofagin only exhibited moderate antimutagenic properties, compared to luteolin and chrysoeriol, and concluded that the antimutagenic properties of rooibos is probably not due to aspalathin, but more likely a synergistic mechanism between the rooibos compounds.

2.3.5.9 STEROID METABOLISM

In a study done in non-steroidogenic COS-1 cells by Schloms & Swart (2014), five of the major flavonoid compounds present in rooibos (the dihydrochalcones, aspalathin and nothofagin; the flavones, orientin and vitexin; and a flavonol, rutin) caused inhibition of adrenal steroidogenic enzymes, P450 17α-hydroxylase/17,20-lyase (CYP17A1) and 3BHSD2 (3β-hydroxysteroid dehydrogenase). These enzymes guide steroid metabolites in the glucocorticoid, mineralocorticoid and andrenal androgen pathways (Schloms & Swart, 2014), and thus serve as upstream regulators of the adrenal steroidal pathways. Physiologically, inhibition of steroidogenesis can be beneficial in individuals presenting with chronic elevated levels of hormones, such as cortisol which have been implicated in metabolic disorders, including obesity, insulin resistance, hypertension, CVDs and T2Ds (Chrousos, 2009).

CHAPTER 3

MATERIALS AND METHODS

1. MATERIALS

AMERSHAM BIOSCIENCES CORP. (GE HEALTHCARE LTD.), UNITED STATES

Enhanced chemiluminescence (ECL™) western blotting detection reagents

BAYER HEALTHCARE ANIMAL HEALTH, SOUTH AFRICA

Eutha-naze (sodium pentobarbital)

BDH CHEMICAL LTD., UNITED KINGDOM

Glycerol

BIOMEDICAL RESEARCH AND INNOVATION PLATFORM, MEDCIAL RESEARCH COUNCIL, SOUTH AFRICA

Aspalathin

BIO-RAD LABORATORIES, INC., UNITED STATES

Bovine Serum Albumin, Clarity™ Western ECL Substrate, Millipore Immobilon-p Polyvinyledene Fluoride (PVDF) microporous membrane, Quick Start™ Bradford, Mini-PROTEAN® Precast Gels, TGX Stain-Free™ FastCast™ Acrylamide Kit, 10%, Trans-Blot® Turbo™ Transfer Buffer, Trans-Blot® Turbo™ RTA Transfer Kit, Mini-PROTEAN® TGX Stain-Free™ Precast Gels

CELL SIGNALING TECHNOLOGY®, UNITED STATES

Anti-rabbit and anti-mouse IgG HRP-linked secondary antibody, Total-(AMPKα, GLUT4 (1F8) mouse mAb, PKB) primary antibodies, Phospho-(AMPKα (Thr^{172}), PKB (Ser^{473})) primary antibodies

CLOVER S.A. (PTY) LTD., SOUTH AFRICA

Elite fat-free milk powder

GLUCOPLUS INC., CANADA

Blood glucose meter strips

HANNA INSTRUMENTS (PTY) LTD., SOUTH AFRICA

HI 70300L pH Electrode Storage Solution, HI 7004 and HI 7007 pH Buffer Solution

LASEC SA (PTY) LTD, SOUTH AFRICA

Parafilm

LONZA GROUP LTD., SWITZERLAND

DMEM (with high glucose and L-Glutamine), ViaLight™ Plus kit, phosphate buffer saline (PBS), MycoAlert™ PLUS Mycoplasma Detection Kit

MERCK (PTY) LTD., SOUTH AFRICA

HCl, KCl, KH_2PO_4, $MgSO_4$, Na_2HPO_4, Na_2SO_4, NaCl, NaH_2PO_4, $NaHCO_3$, Na^+K^+-Tartrate, NaOH, tetra-Na^+-pyrophosphate, tris (hydroxymethyl) aminomethane, dimethyl sulfoxide (DMSO), butanol,

Folin-Ciocalteu's phenol reagent, Millipore Rat/Mouse Insulin ELISA, Luminata Forte Western HRP substrate, Calbiochem® SignalBoost™ Immunoreaction Enhancer Kit

NEXT ADVANCE, INC., UNITED STATES

0.15 mm diameter zirconium oxide beads

PERKIN-ELMER INC., UNITED STATES

2-Deoxy-[H^3]-glucose, Emulsifier Scintillator Plus™

ROCHE PRODUCTS (PTY) LTD. - DIAGNOSTICS, SOUTH AFRICA

BSA fraction V - fatty acid free, BSA fraction V

SEMPERMED TECHNICAL PRODUCTS, AUSTRIA

SemperCare® Examination Gloves

SIGMA-ALDRICH LIFE SCIENCE, UNITED STATES

2,3-BDM, 2-deoxy-D-glucose, 2-mercaptoethanol (solution), acrylamide, aprotonin, $CaCl_2$, D-(+)-glucose, DMEM (without glucose, L-glutamine, phenol red, sodium pyruvate and sodium bicarbonate), EDTA, EGTA, HEPES hemisodium salt, insulin, leupeptin, $MgCl_2$, Na^+-pyruvate, SDS, TEMED, trypan blue stain (0.4%), trypsin-EDTA solution, Tween-20, wortmannin, β-glycerophosphate, β-mercaptoethanol, ammonium persulfate (APS), Triton® X-100, 2-mercaptoethanol, phenylmethylsulfonyl fluoride (PMSF), Coomassie Brilliant Blue G, sodium orthovanadate, propidium iodide, JC-1 solid, retinoic acid, phloretin

THERMO FISHER SCIENTIFIC INC., SOUTH AFRICA

Countess® Cell Counting Chamber Slides, Fetal Bovine Serum, PageRuler™ Prestained Protein Ladder (Fermentas Life Sciences), Penicillin-Streptomycin, 15/50ml Falcon™ Conical Centrifuge Tubes, Horse Serum

WORTHINGTON BIOCHEMICAL CORP., UNITED STATES

Collagenase type 2

2. EQUIPMENT

AMERSHAM BIOSCIENCES CORP. (GE HEALTHCARE LTD.), UNITED STATES

Electrophoresis Power Supply (EPS) 301

BANTE INSTRUMENTS LTD., CHINA

PHS-3BW Digital pH Meter

BECTON DICKINSON BIOSCIENCES INC., UNITED STATES

BD FACSCalibur™

BECKMAN-COULTER INC., UNITED STATES

L7 Ultracentrifuge, LS6500 Liquid Scintillation Counter

BENCHMARK SCIENTIFIC INC., UNITED STATES

Incu-Shaker Mini

BIO-RAD LABORATORIES, INC., UNITED STATES

ChemiDoc™ MP System, Image Lab Version 5.0, Mini 2-D Cell, Mini-PROTEAN® Tetra System, PowerPac™ Basic, Trans-Blot® Turbo™ Transfer System

BIOTEK INSTRUMENTS INC., UNITED STATES

ELx800 Absorbance Reader

GLUCOPLUS INC., CANADA

Blood glucose meter

GRANT INSTRUMENTS LTD., UNITED KINGDOM

Water Bath

GRAPHPAD SOFTWARE INC., UNITED STATES

GraphPad Prism 5

HAUSSER SCIENTIFIC COMPANY, UNITED STATES

Haemocytometer

INTERNATIONAL EQUIPMENT COMPANY, UNITED STATES

Model CM Centrifuge

LASEC SA (PTY) LTD., SOUTH AFRICA

Sigma 1-14K Refrigerated Microfuge

NEXT ADVANCE, INC., UNITED STATES

Bullet Blender®

NEW BRUNSWICK SCIENTIFIC INC., UNITED STATES

Galaxy R CO_2 Incubator

OLYMPUS LIFE SCIENCE INC., JAPAN

Olympus CKX41 Inverted Microscope

ORTO ALRESA, SPAIN

Digicen 20 Centrifuge

OXFORD UNIVERSITY, UNITED KINGDOM

HOMA2 Calculator 2.2.3

PERKIN-ELMER INC., UNITED STATES

Tri-Carb® 2810 TR Liquid Scintillation Analyzer

SENSOR SCIENTIFIC INC., UNITED STATES

Temperature probe

SIGMA-ALDRICH LIFE SCIENCE, UNITED STATES

Eppendorff® Minispin®plus

THE LAB WORLD GROUP, UNITED STATES

Nikon TMS-F Microscope, Nikon Eclipse Ti

THERMO FISHER SCIENTIFIC INC., SOUTH AFRICA

Invitrogen™ Countess™ Automated Cell Counter, Spectronic® 20 Genesys™ Spectrophotometer, HiMark™ Pre-Stained Protein Standard

3. METHODS

AIM 1 : ESTABLISH A WISTAR RAT MODEL OF INSULIN RESISTANCE AND OBESITY

a. Determine the biometric parameters of rats fed a high-fat, high-sucrose diet for 16-30 weeks compared to age-matched control groups.
b. Determine the metabolic parameters of rats fed a high-fat, high-sucrose diet for 16-30 weeks compared to age-matched control groups

1.1. STUDY DESIGN: GROUPING, FEEDING AND TREATMENT

Male Wistar rats at 6 weeks of age and weighing 190±10 g were randomly selected and grouped into control and high-fat, high-sucrose diet (HFD) groups. Control rats received a standard commercial rat chow containing 1,272 kJ/100 g and unlimited drinking water, whereas the HFD groups received a diet consisting of normal chow, supplemented with sucrose, condensed milk and holsum fat containing a fairly similar 1,354 kJ/100 g (**Table 3.1**)**.** Additionally, young control rats on a standard commercial rat chow diet weighing between 180-300 g was used throughout the study as positive controls to verify the validity of experimental protocols. The present investigation was divided into 3 sub-studies according to their specific aim (**Figure 3.1**). H9C2 cell line was also used to test for the efficacy of using the compound.

Table 3.1 Diet composition of Control and High-Fat, High-Sucrose Diet

Diet	Control	HFD
Protein (%)	17.1	8.3
Carbohydrates (%)	34.6	42
Sugar(g/100 g)	6.6	24.4
Fat (g/100 g)	4.8	11.6
Saturated Fat (g/100 g)	0.9	7.6
Mono-unsatured Fat (g/100 g)	1.5	2.9
Poly-unsaturated Fat (g/100 g)	2.4	1.1
ω-3 Polyunsaturated Fat (g/100 g)	0.2	0.1
ω-6 Polyunsaturated Fat (g/100 g)	2.2	1.0
Cholesterol (mg/100 g)	3	13
Energy (kJ/100 g)	1272	1354
Average Energy Intake Daily (kJ)	~380	-

*HFD: High-Fat, High-Sucrose Diet

1.2. Animal Care

Age and weight matched male Wistar rats were used in the present study. At 4 weeks after birth, rats were weaned and allowed free access to standard rat chow and water. Rats were housed in cages (maximum 5 per cage) in a stable environment of 22 °C, 40% humidity and a 12 hour artificial day/night cycle (light from 06:00 to 18:00) at the Central Research Facility, Stellenbosch University. The experimental procedure was revised and approved by the Committee for Ethical Animal Research for the Faculty of Health Sciences, University of Stellenbosch (**Ethical Clearance: SU-ACUM14-00013**). The revised South African National Standard for the care and use of laboratory animals for scientific purpose was followed (**SABS, SANS 10386, 2008**).

1.3. Oral Glucose Tolerance Test

The Oral Glucose Tolerance Test (OGTT) was used to determine the efficacy of rats to clear blood glucose following oral ingestion of glucose. Animals were fasted overnight (with access to drinking water), before being anaesthetized by intraperitoneal injection with a very low dose of sodium pentobarbital (15 mg/kg) (Euthanaze, Bayer HealthCare, RSA). The body weights of the animals were determined and the initial, fasting blood glucose levels established from a tail prick using a standard glucometer (GlucoPlus Inc., Canada). In addition, 1 ml of fasting blood was collected directly from the carotid artery. Thereafter, a solution of 50% sucrose at a dose of 1 mg/g body weight, was administered by oral gavage and blood glucose levels monitored by a drop of blood from the tail prick and subsequent glucometer readings at various time points (3, 5, 10, 15, 20, 25, 30, 45, 60, 90 and 120 mins). After the OGTT, animals were allowed to recover for one week from this metabolic insult before being sacrificed in other experiments.

1.4. Intraperitoneal Fat

The intra-peritoneal fat of the control and HFD animals were dissected out and weighed at an opportune time after sacrifice and isolation of heart.

1.5. Insulin assay

The serum from the fasting blood was used to determine insulin levels of the animals. For the determination of serum insulin levels we made use of a commercially available Millipore Rat/Mouse Insulin Enzyme-linked immunosorbent assay (ELISA) (Merck (Pty) Ltd., RSA). This non-radioactive quantification assay contained an anti-rat insulin coated 96-well microplate and all relevant reagents were supplied by the assay kit. Before the assay, all reagents were pre-warmed to room temperature (25ºC). The required number of wells for all the blank, standard, quality control (QC) and serum samples were washed 3 times with 300 µl 10X diluted Wash buffer and aspirated. 10 µl Assay buffer (0.05 M phosphosaline, pH 7.4, containing 0.025 M EDTA, 0.08% sodium (Na)-azide and 1% BSA) was added to each blank and sample well and 10 µl Matrix solution (charcoal stripped pooled mouse serum) was added to the blank, standard and QC wells. Following this, the

standards (10 µl/ml, 5 µl/ml, 2 µl/ml, 1 µl/ml, 0.5 µl/ml, 0.2 µl/ml, 0 µl/ml) were prepared in duplicate. 10 µl of each standard was pipetted into the respective wells, 10 µl of the two QC samples were added to their appropriate wells, and 10 µl serum of both the control and HFD animals were added sequentially in duplicate to the remaining wells. 80 µl rat pre-titered biotinylated anti-insulin detection antibody was added to all the standards (including the blank and QC samples) and the serum samples followed by an incubation period of 2 hours at room temperature at moderate rotation speeds (400-500 rpms) (Incu-Shaker Mini, Benchmark Scientific Inc., USA). Afterwards, all the fluid was aspirated and the wells were washed thoroughly with 300 µl 10X Wash Buffer. 100 µl pre-titered Streptavidin-Horse Radish Peroxidase (HRP)-conjugate in buffer was pipetted to each well and incubated for 30 mins at room temperature to visualize the target molecule, insulin. After washing the wells again 3 times with 300 µl 10X Wash Buffer, 100 µl 3,3',5,5'-Tetramethylbenzidine (TMB) One-Step Substrate Reagent was added to each well and incubated for 15 mins at room temperature. Finally, 100 µl 0.3 M Stop Solution was pipetted into each well. This sulphuric acid solution changed the blue colour to a yellow colour. The intensity of the colour was immediately measured within 5 mins on the microplate reader at 450 nm and 590 nm respectively. A 4-parameter logistic equation dose-response curve was set up by plotting the absorbance unit of 450 nm less that of 590 nm, on the Y-axis against the rat insulin standard concentrations on the X-axis. The increase in absorbance is directly proportional to the amount of insulin measured in the unknown serum samples; therefore the curve was set up with known standard insulin concentrations used as a reference for the determination of the samples of interest. The homeostasis model assessment for insulin resistance (HOMA-IR) index was calculated using the HOMA2 Calculator 2.2.3 software (Oxford University, UK), which calculates the product of fasting glucose concentration (mmol/L) multiplied by the fasting insulin concentration (µIU/mL) divided by 22.5 (HOMA-IR = [fasting glucose concentration X fasting insulin concentration]/22.5), as well as the product of 20 times insulin concentration divided by 3.5 units less than the fasting glucose concentration (HOMA-%B = [20 × fasting insulin concentration]/[fasting glucose concentration − 3.5]), which corrects for beta cell function (Levy et al., 1998).

Similar to Western Blotting, the principle of ELISAs rely on immunodetection. Briefly, insulin detection using the Sandwich ELISA occurs through capture of the insulin molecules in a sample by binding to the monoclonal mouse anti-rat insulin antibody pre-treated microtiter plate wells, followed by binding of biotinylated polyclonal antibodies to the captured insulin. After washing off the free enzyme conjugates, the enzyme HRP is added and binds to the biotinylated antibodies. This is followed by addition of the substrate, TMB, inducing a colorigenic reaction - decreasing absorbency at 590 nm and increasing absorbency at 450 nm due to TMB's ability to act as a hydrogen donor in response to HRP's reduction of hydrogen peroxide to water. The increase in absorbency, or the increase in yellow colour development, is directly proportional to the amount of

bound insulin, and thus the insulin concentration of the samples and can be determined by comparing the absorbency with a standard curve of known insulin concentrations.

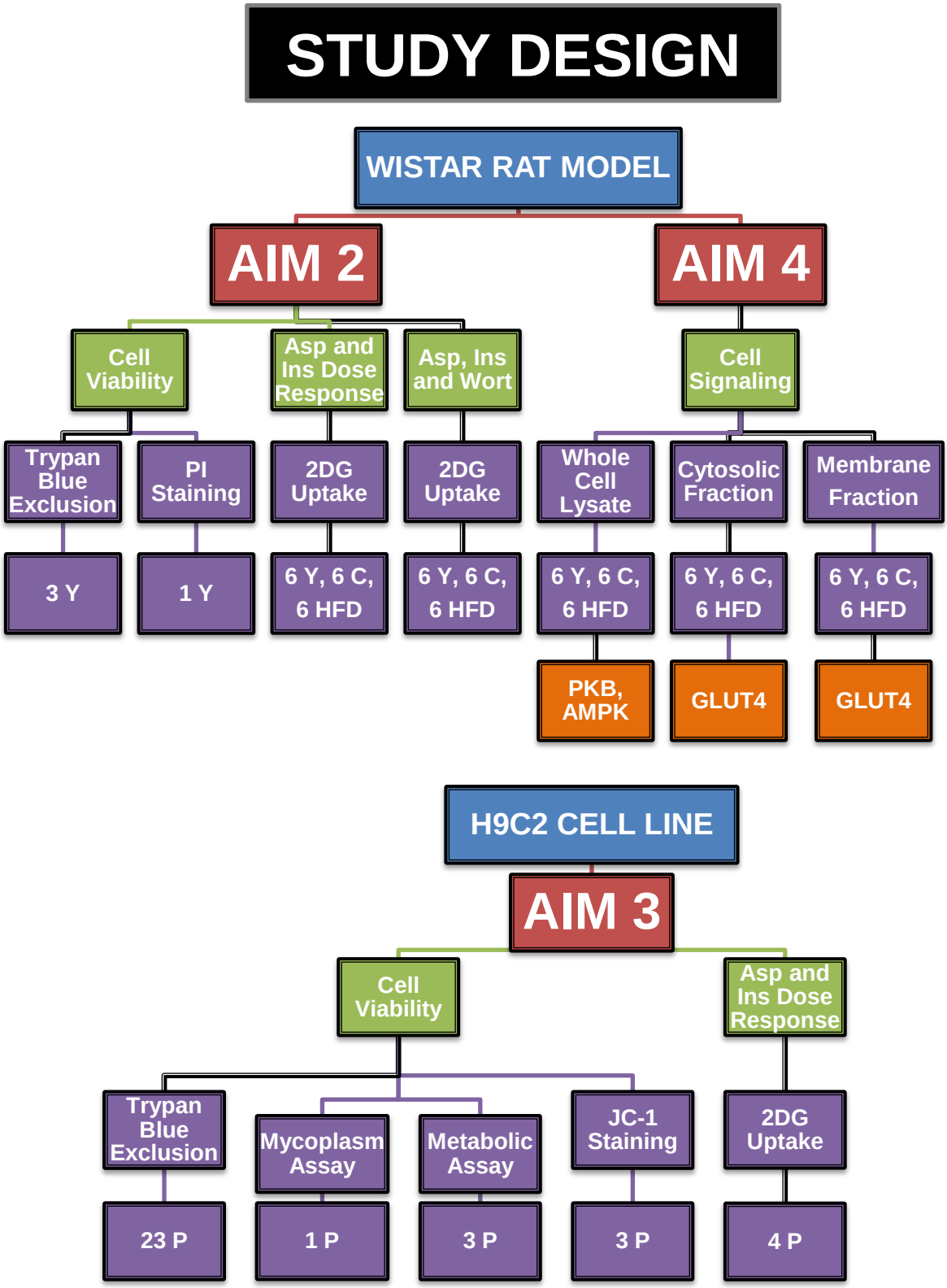

Figure 3.1 Study layout of animal groups and objectives. Y, Young; C, control; HFD, high-fat, high-sucrose diet; P, Plates; 2DG, 2-deoxyglucose; PKB, protein kinase B; AMPK, AMP-activated kinase; GLUT4, glucose transporter 4.

AIM 2: DETERMINE THE POSSIBLE EFFICACY AND TOXICITY OF USING ASPALATHIN TO INDUCE GLUCOSE UPTAKE, IN CARDIOMYOCYTES FROM:

c. young control rats to determine the effect of aspalathin on cell viability
d. young, control and HFD rats to generate a glucose uptake response curve with 1-100μM aspalathin and 1-100 nM insulin as positive control
e. control and HFD rats to determine the effects of the inhibitor wortmannin (inhibits PI3K) on aspalathin-induced glucose uptake

2.1. ISOLATION OF CARDIOMYOCYTES

Rats were collected from the animal house a week prior to being used in experiments to reduce the stress of handling on the day of experimentation. Rats were anaesthetized with sodium pentobarbital (160 mg/kg) (Euthanaze, Bayer HealthCare, RSA). The rats were weighed and the non-fasting blood glucose (or random blood glucose test) value of the animals were determined from a tail prick using a standard glucometer (GlucoPlus Inc., Canada). After determining deep anaesthesia via an unresponsive foot pinch (pedal reflex), hearts were quickly excised (<1 minute after first incision) and arrested in ice cold Krebs-Henseleit (KH) buffer (**Table 3.2**). Cardiomyocytes in an unstimulated state were isolated essentially as initially described by Fischer et al. (1991). The hearts were mounted via the aorta onto a Langendorff perfusion system (<2 mins after removal) (**See Excision of the Heart in Appendix A for supplementary detail**). The hearts were retrogradely perfused with a calcium-free HEPES-based medium containing 5.5 mM D-glucose and 2 mM pyruvic acid (**Solution A, Table 3.2**), at 37 ^{o}C in the presence of 100% O_2 for 5 mins to rinse out residual blood in the heart. The perfusion medium was then switched to a second recirculating medium containing 0.1% type 2 collagenase (Worthington Biochemical Corp., USA) and 15 mM 2,3-BDM (Sigma-Aldrich Life Science, USA) (**Solution B, Table 3.2**). After 20 and 25 mins respectively, $CaCl_2$ concentration was gradually increased, in order to prevent the calcium paradox (**See Calcium Paradox in Appendix A for supplementary detail**), to reach a total concentration of 200 μM $CaCl_2$. Perfusion was continued till the perfusate streamed continuously from the heart or for a total time of approximately 40 mins (**Figure 3.2**).

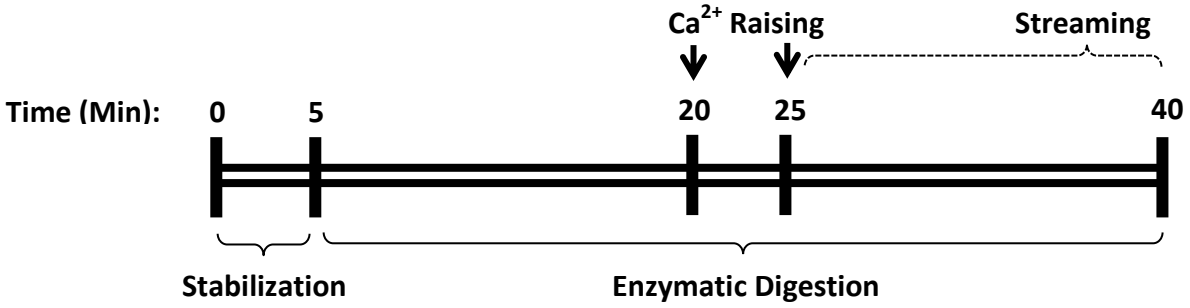

Figure 3.2 Standard Langendorff Isolation Protocol

After digestion, hearts were removed from the system, the ventricles carefully isolated from the atrial and vascular remnants, minced with tweezers, and suspended in the same perfusion medium mentioned above, but containing 200 μM $CaCl_2$ and half the concentration of collagenase and 2,3-BDM (**Solution C, Table 3.2**). The suspension was placed in a flat-bottomed flask in a shaking incubator (Incu-Shaker Mini, Benchmark Scientific Inc., USA) at 110 rpms and 37 °C and further digested for 20 mins in the presence of 100% O_2. The $CaCl_2$ concentration was gradually raised to 1.25 mM over the last 5 min period. The isolated cells were filtered through a nylon mesh (200X200 μm) and gently spun down at 100 rpms for 3 mins (Model CM Centrifuge, International Equipment Company, USA). The pellet obtained was resuspended in the first perfusion buffer, containing 1.25 mM $CaCl_2$ and 2% fatty acid free BSA (**Solution D, Table 3.2**) and the viable cells allowed to settle through the BSA solution for 5 mins. The supernatant was carefully aspirated, and the loose pellet resuspended in the same buffer and allowed to recover from the trauma of isolation while slowly rotating (30 rpms) at 37 °C for at least 1 hour. The cells were then washed three times in a substrate-free medium (**Solution E, Table 3.2**), each time aspirating the supernatant and spinning down at 300 rpms for 3 mins. Finally, the cells were resuspended in the desired volume of Solution E.

Table 3.2 Buffer Compositions used in Isolation Protocol

Solution	Composition
KH Buffer (pH = 7.4)	119 mM NaCl, 25 mM $NaHCO_3$, 4.75 mM KCl, 1.2 mM KH_2PO_4, 0.6 mM $MgSO_4$, 0.6 mM Na_2SO_4, 1.25 mM $CaCl_2$ and 10 mM glucose
HEPES Buffer (pH = 7.4)	128 mM NaCl, 6 mM KCl, 1 mM Na_2HPO_4, 0.2 mM NaH_2PO_4, 1.4 mM $MgSO_4$, 10 mM HEPES
Solution A	128 mM NaCl, 6 mM KCl, 1 mM Na_2HPO_4, 0.2 mM NaH_2PO_4, 1.4 mM $MgSO_4$, 10 mM HEPES, 5.5 mM D-glucose, 2 mM pyruvic acid
Solution B	128 mM NaCl, 6 mM KCl, 1 mM Na_2HPO_4, 0.2 mM NaH_2PO_4, 1.4 mM $MgSO_4$, 10 mM HEPES, 5.5 mM D-glucose, 2 mM pyruvic acid, 0.7% BSA fatty acid free (faf) 22 500 U type 2 collagenase, 15 mM 2,3-BDM
Solution C	128 mM NaCl, 6 mM KCl, 1 mM Na_2HPO_4, 0.2 mM NaH_2PO_4, 1.4 mM $MgSO_4$, 10 mM HEPES, 5.5 mM D-glucose, 2 mM pyruvic acid, 11 250 U type 2 collagenase, 7.5 mM 2,3-BDM, 1% BSA, 1% BSA (faf), 200 uM $CaCl_2$
Solution D	128 mM NaCl, 6 mM KCl, 1 mM Na_2HPO_4, 0.2 mM NaH_2PO_4, 1.4 mM $MgSO_4$, 10 mM HEPES, 5.5 mM D-glucose, 2 mM pyruvic acid, 2% BSA (faf), 1.25 mM $CaCl_2$
Solution E	128 mM NaCl, 6 mM KCl, 1 mM Na_2HPO_4, 0.2 mM NaH_2PO_4, 1.4 mM $MgSO_4$, 10 mM HEPES, 2% BSA (faf), 1.25 mM $CaCl_2$

2.2. Cell Viability Assays

2.2.1. Trypan Blue Exclusion Assay

Cell viability was determined using a trypan blue exclusion assay. Live cells contain intact cell membranes which do not allow the trypan blue dye to cross inside the cytosol, whereas, the loss of membrane integrity in dead cells allow the dye to be taken up. This allows for visual assessment of the cell suspension – in viable cells we observe a clear cytoplasm; in non-viable cells the cytoplasm appears blue. For manual counting, 10 µl of the cell suspension obtained at the end of the isolation protocol was vortexed with 10 µl 0.4% trypan blue solution, loaded onto a haemocytometer and visualized using a standard light microscope (Olympus CKX41 Inverted Microscope). The amount of viable cells was obtained for each quadrant, totaled together and divided by 4 to obtain the average amount of viable cells. This number of cells were then multiplied by 10^5 to obtain the amount of viable cells present in 10 ml of the cell suspension. Each heart typically yielded approximately 5 million cardiomyocytes.

2.2.2. Propidium Iodide Staining

To investigate the effect of treatments on myocardial cell viability, isolated cardiomyocytes were pre-treated for both 1 or 3 hours with either DMSO, 10 µM aspalathin or 10 nM insulin, and stained using propidium iodide (PI). Treatments were done in duplicate with one series receiving 5 µM of PI, and the other series remaining unstained (negative). This was followed by resuspending the cells in Lucham tubes and a 15 mins period of incubation at room temperature in the dark. The samples were then analysed at simultaneous 617 nm/535 nm wavelengths using fluorescence-activated cell sorting (FACS) analysis. The PI-negative samples were used to establish the background fluorescence of the experimental samples and necessary to set up the photomultiplier tube voltages of the instrument using BD CellQuest Pro 5.2.1 software (BD FACSCalibur™, Becton Dickinson Biosciences Inc., USA) (**Figure 3.3**). The captured files generated by the PC were analysed with the same software used for acquisition. First, viable cardiomyocytes were identified and separated from dead cells and debris using a defined region on an appropriate Forward/Sidescatter plot. Then the gated cells were analysed for their signal in fluorescence channel 2 using a FL-2 histogram. The percentages of PI positive and negative cells were determined for each sample and intervention by using a fixed border defined by a file from an unstained sample and applied to all files from stained samples (treated and untreated). PI staining occurs when there is a loss in cell membrane integrity, allowing the the PI-probe to enter the cell and then intercalate between double stranded DNA base pairs within the nucleus. PI has a fluorescence excitation maximum of 535 nm and an emission maximum of 617 nm. This staining serves as a marker of the non-viable or nectrotic cell population.

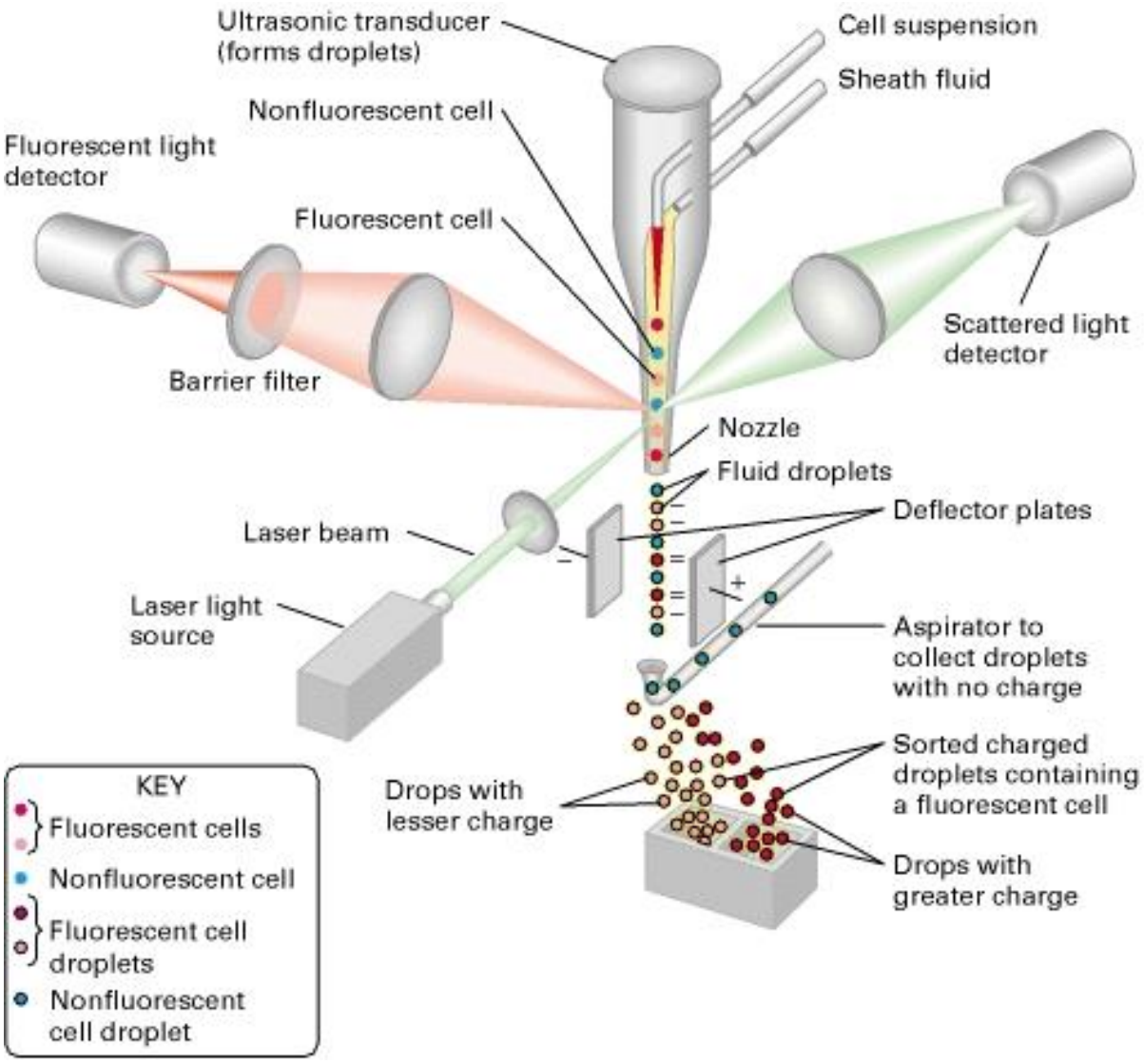

Figure 3.3 Fluorescence-activated cell sorter. PI is added to a concentrated cell suspension and then binds to double stranded DNA. The fluorescence of each cell is measured as it narrowly passes through a light beam. The angle, as well as the intensity of light can be measured, and used to determine cell size and shape. As the cells pass through the nozzle of the FACS machine, it receives an electric charge relative to its fluorescent count, which is an indication of the amount of bound dye. Using an electric field, the cells can be sorted according to charge, and the overall membrane integrity of the cell population determined. (Obtained from Craig, 2007)

2.3. GLUCOSE UPTAKE ASSAY

Glucose uptake by adult ventricular myocytes was essentially determined according to the method published by Fisher et al. (1991). This method renders cells that are calcium tolerant but are in a quiescent and unstimulated state with GLUT4 situated in the internal compartments of the cell. This allows for measurement of stimulation of GLUT4 mediated glucose uptake. For the glucose uptake assay, the isolated cardiomyocytes were glucose starved in an oxygenated medium (**Solution E, Table 3.2**), while preincubating in a shaking water bath (Grant Instruments Ltd., UK) for 1-2 hours at 37°C. Each experimental series was incubated with or without 400 μM phloretin (for measurement of non-carrier or baseline mediated glucose uptake), 1-100 nM insulin, 1-100 μM aspalathin, 0.1% DMSO (used as solvent for synthetic aspalathin) and 100nM wortmannin as indicated. For the administration of aspalathin (**Biomedical Research and Innovation Platform, MRC, South Africa**) to isolated cardiomyocytes, the compound was first dissolved in dimethyl sulfoxide (DMSO) as stock solution for storage as aliquots at -80^{o}C as this protects the compound against oxidation. The stock solution was then diluted in medium buffer (**Solution E, Table 3.2**) to render final concentrations of 1 μM, 10 μM or 100 μM. Insulin (Sigma-Aldrich Life Science, USA) stock solution was similarly made up as a 10μM solution in Solution E and stored as aliquots at -80 ^{o}C. This was then diluted to final concentrations of 1 nM, 10 nM and 100 nM in medium buffer (**Solution E, Table 3.2**). Phloretin (Sigma-Aldrich Life Science, USA) and wortmannin (Sigma-Aldrich Life Science, USA) were dissolved in DMSO as stock solutions of 64 mM and 2 mM respectively and stored as aliquots at −20 °C or -80 °C. Both were diluted with medium buffer (**Solution E, Table 3.2**) and used at final concentrations of 400 μM Phloretin and 100 nM wortmannin. Each experiment was performed with two replicates per concentration per plate and the experiments repeated at least 3 times (n=3). At 35 mins, (**Figure 3.4**) after stimulation of the cells, glucose uptake was initiated by addition of 1.8 μM (specific activity, 1.5 μCi/ml) 2-deoxy-D-[^{3}H]glucose (2DG). The experiment was allowed to proceed for 30 mins, after which the glucose uptake reaction was stopped by adding a final concentration of 400 μM phloretin.

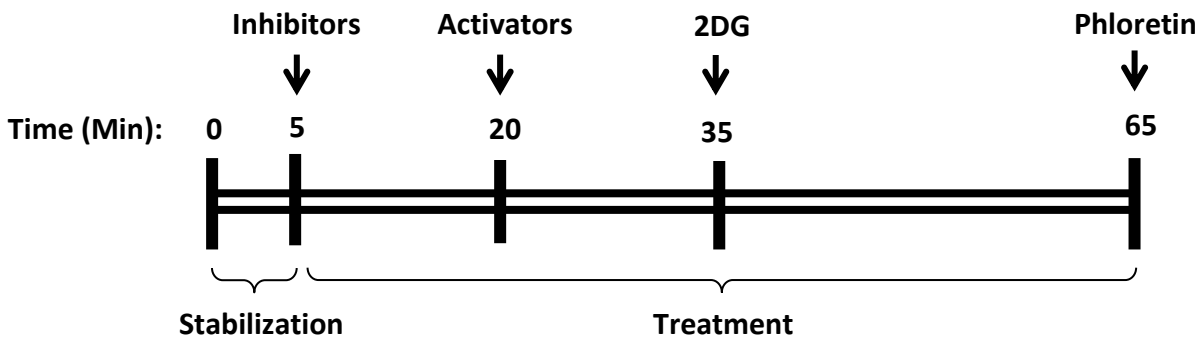

Figure 3.4 Standard protocol for glucose uptake after acute treatments

The standard protocol was modified in subsequent experiments by allowing incubation of activators and inhibitors to proceed for either 60, 90, 120 or 150 mins before addition of 2DG for the last 30 mins of the protocol (**Figure 3.5**). Cells were aspirated and resuspended in 1.5ml Eppendorf tubes and centrifuged at 14,500 rpm for 90 seconds at room temperature using an Eppendorff® Minispin® plus (Sigma-Aldrich Life Science, USA). The resultant supernatant was carefully aspirated and the cells washed with HEPES buffer (**Table 3.2**) to remove all traces of radiolabelled 2DG in the supernatant. Aspiration and rewashing with HEPES buffer was repeated 2 more times, after which 500 µl 1N NaOH was added and samples heated in a water bath at 60 °C to dissolve the pellets. 500 µl dH_2O was then added to dilute the samples to a final concentration of 0.5N NaOH and samples were then vortexed thoroughly. An aliquot of 50 µl per sample was used to assay its protein content in duplicate by the method of Lowry et al. (1951) (**described below in section 2.4**), while 100 µl per sample was aliquoted into radioscintillation vials containing 3 ml scintillation fluid (Emulsifier Scintillator Plus™, Perkin-Elmer Inc., USA), and counted for radioactivity in duplicate using a LS6500 Liquid Scintillation Counter (Beckman-Coulter Inc., USA). One vial, used as a blank, only contained scintillation fluid, and another vial had 1.8 µM (25 µl) 2DG to measure the total radioactive count to enable calculation of the specific activity.

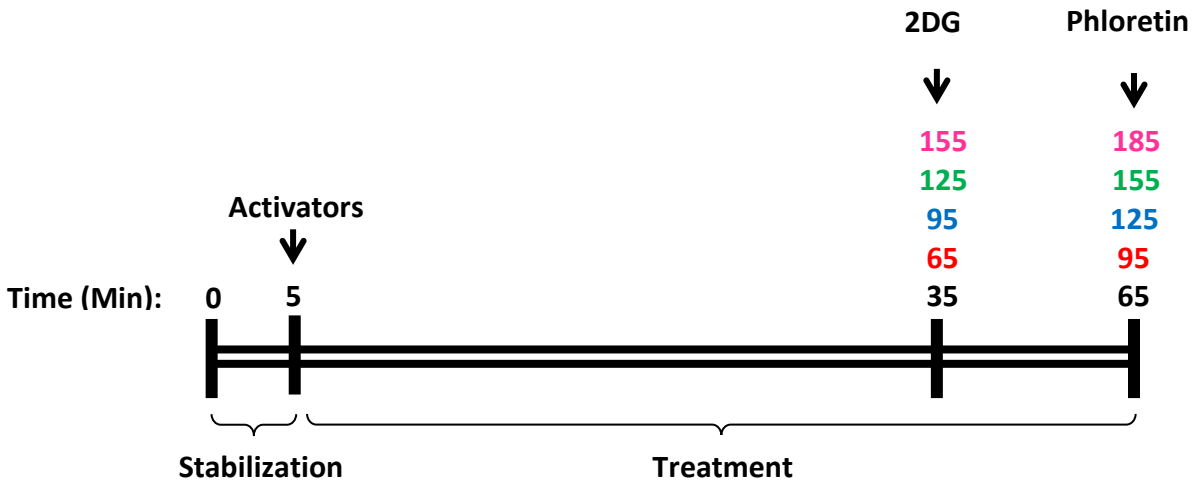

Figure 3.5 Extended protocol for glucose uptake after acute treatments

The principle of 2DG uptake is explained as follows: Hexokinase phosphorylates glucose into G-6-P as part of the first regulatory step committing glucose to further metabolism (**refer to Chapter 2: Literature Review, Figure 2.5**). However, hexokinase is also able to phosphorylate 2DG, a molecule with similiar structure to glucose (**Figure 3.6**), into 2-deoxyglucose-6-phosphate which is

unable to undergo further metabolism. The K_m or half-maximal binding concentration of hexokinase for 2DG is effectively 10 times higher than that for glucose (Russell et al., 1992). Through this process, 2DG competitively inhibits glucose phosphorylation and reduces glycolysis which will eventually slow or inhibit glucose uptake. To be able to state that 2DG glucose uptake by cells is equivalent to glucose uptake, the concentration of 2DG should be in the low micromolar range. In addition, it has been shown by Fischer et al. (1991), that 2DG uptake, using this low concentration of 2DG, is linear up to 60 mins.

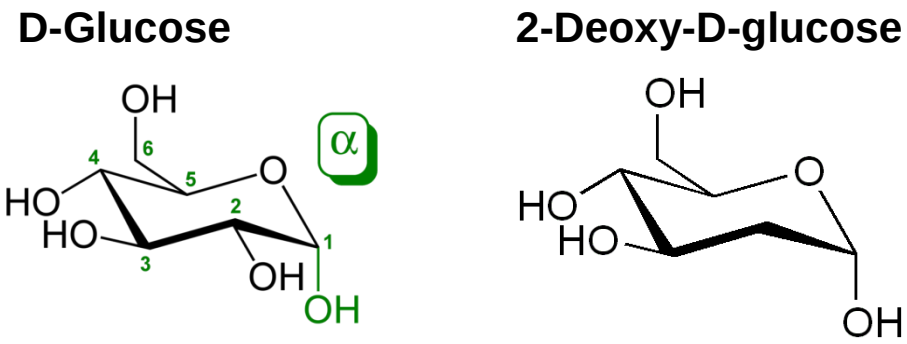

Figure 3.6 Glucose molecule compared to a 2DG molecule. The 2-hydroxyl group of glucose is replaced with a hydrogen atom. 2DG: 2-deoxy-D-[^{3}H]glucose

2.4. LOWRY PROTEIN DETERMINATION

To determine the protein concentration of each sample, 50 µl protein sample, 3 BSA concentrations (0.161, 0.322 and 0.644 mg/ml 0.5 N NaOH), used as standards and 0.5 N NaOH (used as blank) was pipetted into Lucham tubes in triplicates. 1ml reaction buffer, containing 2% Na_2CO_3, 1% $CuSO_4 \bullet 5H_20$ and 2% Na^+K^+-Tartrate, was added to each tube, vortexed and incubated at room temperature for 10 mins. Hereafter, 0.1 ml of a 1:3 dH_20 diluted Folin Ciocalteus reagent was added to each tube, vortexed and incubated for 30 mins after which OD values were determined using a spectrophotometer (Spectronic® 20 Genesys™ Spectrophotometer, Thermo Fisher Scientific Inc., RSA) at 750 nm. A standard curve was generated and the protein content of the samples determined.

Under alkaline conditions, cupric ions (Cu^{2+}) chelate with the peptide bonds of a protein resulting in a reduction of cupric ions (Cu^{2+}) to cuprous ions (Cu^+). Addition of reagents such as Folin Ciocalteu (phosphomolybdic-phosphotungstic acid) with the Cu^+ creates chromogens that give a colour reaction resulting in an increased absorbance between 550 nm and 750 nm. Absorbance at the peak wavelength of 750 nm quantitate protein concentrations between 1-100 mg/ml, whereas 550 nm is more suitable for quantifying higher protein concentrations (Sengupta & Chattopadhyay, 1993). The amount of colour produced can be readily detected and is proportional to the amount of peptide bonds, and thus an indication of the amount of protein.

AIM 3: DETERMINE THE POSSIBLE EFFICACY AND TOXICITY OF EXTENDED ASPALATHIN TREATMENT ON DIFFERENTIATED CARDIOMYOCYTES DERIVED FROM H9C2 CELLS:

3.1. CELL CULTURING

Experiments were performed using an embryonic rat-heart derived H9C2 cardiomyoblast cell line (ECACC No. 8809294; Gifted by Prof F. Essop, Department of Physiological Sciences, Stellenbosch University, South Africa). During routine maintenance, cells were exponentially grown as monolayers in Dulbecco's modified Eagle's Medium (DMEM) with 5.5 mM glucose (supplemented with 10% foetal bovine serum (FBS) and 1% Penicillin-Streptomycin) at 37 °C in a humidified atmosphere of 95% air with 5% CO_2 (Galaxy R CO_2 Incubator). Cells were first allowed to proliferate in T75 culture dishes until they reached 70-80% confluency before being split into appropriate treatment plates or dishes. Sub-confluent cell populations were used for all experiments. Plating densities were previously determined (Dludla et al., 2014) for each cell subculture so that equivalent (sub-confluent) cell populations were always present at the time of treatment.

3.1.1. SPLITTING OF CELLS

Splitting was accomplished by washing the cell monolayer with 5ml sterile warm phosphate buffered saline (PBS) followed by incubation with 4 ml 0.25% Trypsin- Ethylenediaminetetraacetic acid (EDTA) solution at 37 °C for 4 mins, with occasional agitation to completely loosen the cells. Thereafter, double the volume of growth medium was added (8 ml per T75 flask) and the cells resuspended in a 15 ml Falcon tube. The tube was centrifuged at 1500 rpms for 3 mins using a Digicen 20 Centrifuge (Orto Alresa, Spain), the supernatant decanted and the cell pellet resuspended in an appropriate volume of medium. Cells were counted using the trypan blue assay (**described in 3.1.2 below**) and diluted with warm, growth medium to the appropriate concentration (seeding density of ~500,000 cells per T75 flask, 50,000 cells per well in 24-well plate, or 40,000 cells per well in 96-well plate) and volume, before aliquoted into flasks or plates.

3.1.2. TRYPAN BLUE EXCLUSION ASSAY

The viability of cells was determined prior to splitting and plating by using a trypan blue exclusion assay. The assay was performed either manually or automatically. Manual counting was performed as discussed in **2.2.1**. above using a Nikon TMS-F Microscope (The Lab World Group, USA). 10 μl of the cell suspension was mixed with 10 μl 0.4% trypan blue solution. For automatic counting, 10 ul of the homogenized solution was loaded onto a Countess® Cell Counting Chamber Slide (Thermo Fisher Scientific Inc., South Africa) and counted using the Invitrogen™ Countess™ Automated Cell Counter (Thermo Fisher Scientic Inc., South Africa). Briefly, automatic counting occurs in the central location of the counting chamber. The entire volume of cells counted is 0.4 μL, the same as counting four (1mm x 1mm) squares in a standard haemocytomer. The

desired concentration of viable cells and the amount of cells needed for splitting into appropriate amount of wells or flasks were then calculated using the Invitrogen™ software.

3.1.3. Mycoplasm Detection Assay

To test for contamination of H9C2 cell stocks, a mycoplasm detection kit was used (MycoAlert™ PLUS, Lonza Group Ltd., Switzerland). Mycoplasma are the smallest and simplest prokaryotes and are well recognized as a common contaminant in cell culture. The mycoplasma competes with cells for nutrients and as a result decreases cellular proliferation and influence cell functioning. These fluctuations can be detected using the MycoAlert™ Kit with a similiar mechanism to the Metabolic Assay described in **3.4 below**. The experimental procedure was as follows: Just prior to plating of cells, 2 ml of cell suspension was centrifuged at 200xg for 5 mins to pellet the cells. Cells were resupsended in fresh media. 100 μL of the cell suspension was placed in a luminometer and 100 μL MycoAlert™ PLUS Reagent added to each sample, followed by a 5 min waiting step at room temperature (optimum temperatures for kit enzymes). The absorbance was read using an ELx800 Absorbance Reader (BioTek Instruments Inc., USA). After reading, 100 μL MycoAlert™ PLUS Substrate was added to each sample followed by a 10 min waiting step at room temperature. The absorbance was read once again and the ratio of second reading to first reading calculated. Briefly, viable mycoplasm are lysed and react in response to MycoAlert™ PLUS Substrate, which catalyzes the conversion of ADP to ATP. By measuring the level of ATP before and after the addition of the substrate, a ratio can be obtained which either implicates the presence or absence of mycoplasm. Should mycoplasm be present, the second reading will have a higher absorbance, indicating a reaction with the MycoAlert™ PLUS Substrate.

3.2. Differentiation of H9C2 Cells

H9C2 cells were initially plated onto either 96-well, 24-well or 6 well plates with a seeding density of respectively 40,000, 50,000 or 100,000 cells/well and differentiated for 6-8 days, by reducing the serum content from 10% FBS to 1% horse serum and by adding 10nM retinoic acid (RA). The morphology of cells were monitored daily to determine when differentiation into adult cardiomyocytes occurred. Initially, H9C2 cells are immortal cells, but once differentiated, the cell nuclei start to migrate together, having a closer morphological resemblance to the isolated cardiomyocytes (**Figure 3.7**).

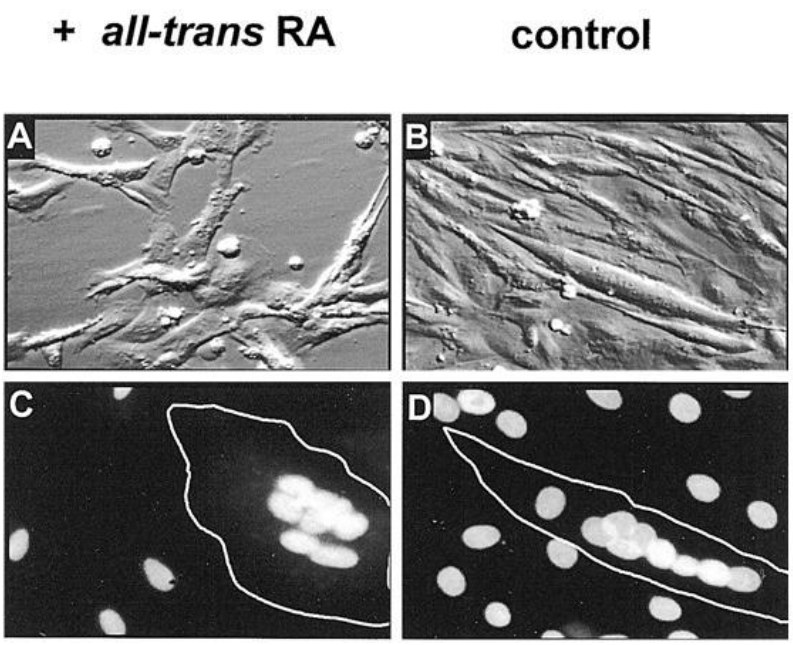

Figure 3.7 Retinoic acid induces differentiation of H9C2 cells. A) Phase-contrast image of typical cells treated with 10nM all-trans-RA for 7 days, compared to control cells in **B)**. **C)** Nuclear staining of differentiated H9C2 cells, compared to controls in **D)**. (Adapted from Ménard et al, 1999)

3.3. JC-1 STAINING

The change in mitochondrial membrane potential ($\Delta\Psi m$) of the H9C2 cells was assessed using the fluorescent probe, 5,5',6,6'-tetrachloro-1,1',3,3'-tetraethylbenzimidazole-carbocyanide iodine (JC-1). Once fully differentiated into adult cardiomyocytes in dark 96-well plates, the cells were incubated at 37 °C in the presence of 95% O_2 and 5% CO_2 for 3h with DMEM with 5.5 mM glucose, containing or without 1 uM Aspalathin (**Figure 3.8**). 15 mins before the end of the experiment 1 nM Insulin was added to half the treated and untreated groups. At 3 hours, the cells were washed once with PBS and then stained with 2 mg/ml JC-1, made up in PBS buffer, and incubated for a further 15 mins at 37°C. The plates were then scanned with a fluorescence microscope (Nikon Eclipse Ti, The Lab World Group, USA), using a Texas red-FITC (fluorescein isothiocyanate) filter cube. Qualitative analysis of cell morphology, and comparison of red:green fluorescence was performed.

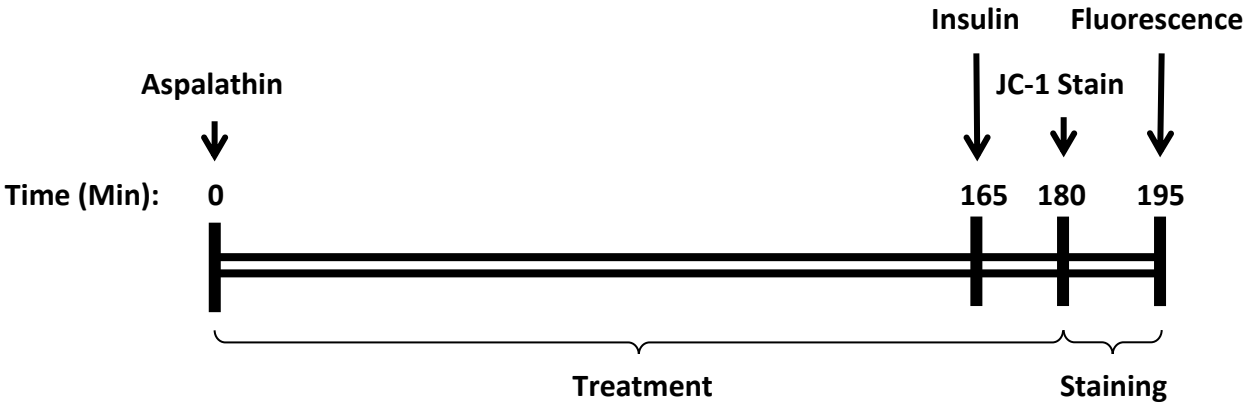

Figure 3.8 JC-1 Staining Protocol

In healthy cells, an intact mitochondrial membrane potential allows for mitochondrial uptake of the positively charged JC-1. As JC-1 accumulates, it forms J-aggregates, that fluoresce bright red (λ_{ex} 596 nm) under a microscope (Cossarizza et al., 1993). In contrast, in apoptotic and necrotic cells, the membrane potential collapses, thereby preventing JC-1 from entering the mitochondria. The result is an accumulation of JC-1 in the cytosol, which fluoresce green (λ_{ex} 520 nm).

3.4. Metabolic Activity

Metabolic activity was determined with an adenosine triphosphate (ATP) assay using a ViaLight™ Plus kit (Lonza Group Ltd., Switzerland). Since all cells are metabolically dependent on ATP to remain viable and perform specialized functions, detecting fluctuations or decreases in cytoplasmic ATP levels can be used to assess cell injury. The technique incorporates the enzyme luciferase, which catalyzes the formation of light from ATP and luciferin according to the following equation:

$$\text{ATP + Luciferin + } O_2 \xrightarrow[Mg^{2+}]{\text{Luciferase}} \text{Oxyluciferin + AMP + } PP_i + CO_2 + \text{LIGHT}$$

The intensity of light emitted by this reaction is proportional to the ATP concentration and can be measured with a luminometer or β-counter.

Once fully differentiated into adult cardiomyocytes in white 96-well plates, the cells were incubated at 37 °C in the presence of 95% O_2 and 5% CO_2 for 3 h with DMEM and 5.5 mM glucose, with or without 1uM Aspalathin (**Figure 3.9**). 15 mins before the end of the experiment 1 nM insulin was added to half the treated and untreated groups. At 3 hours, the cells were removed and left at room temperature to acclimatise. The assay was conducted at room temperature (22 °C), which is the

optimal temperature for luciferase enzymes. Half the contents of each well was aspirated and replaced with Cell Lysis Reagent of the ViaLight™ Plus kit (Lonza Group Ltd., Switzerland) and left for 10 mins. Following this, ATP monitoring reagent plus (AMR plus), containing the luciferase, was added to generate a luminescent signal for 2 mins. The plate was then read using a luminometer (ELx800 Absorbance Reader, BioTek Instruments Inc.,USA). The direct luminometer output was used to calculate cellular response and cytotoxicity of the different treatments.

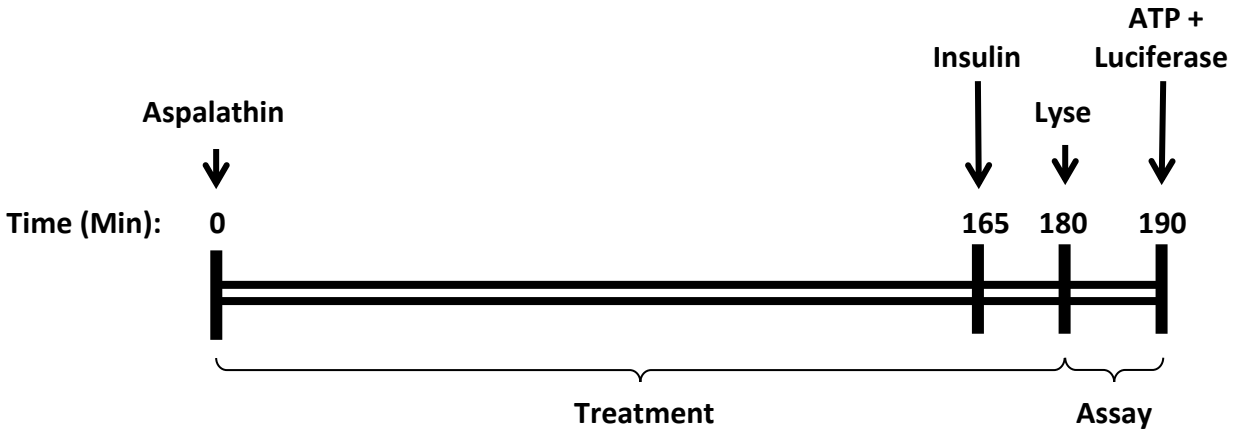

Figure 3.9 ATP Assay Protocol

3.5. GLUCOSE UPTAKE ASSAY

Cells were plated into a 24-well plate with a seeding density of 50,000 cells per well and differentiated for 6 days. Once fully differentiated, the cells were assayed in the presence of 5.5 mM glucose and treated with or without 1μM Aspalathin for 3 or 6 hours, while incubating at 37 °C in the presence of 95% O_2 and 5% CO_2 (**Figure 3.10**). 15 mins prior to the 3 hour or 6 hour time point respective, 1 nM Insulin was added to half the treated and untreated groups and glucose uptake was initiated by addition of 2-deoxy-D-[^{3}H]glucose (1.5 μCi/ml; final concentration 1.8 μM) (Perkin-Elmer Inc., USA). The experiment was allowed to proceed for 15 mins, after which the glucose uptake reaction was stopped by removing the supernatant and washing twice with ice cold PBS (**For a more detailed description of the technique, see section 2.3. in the Methods section**).

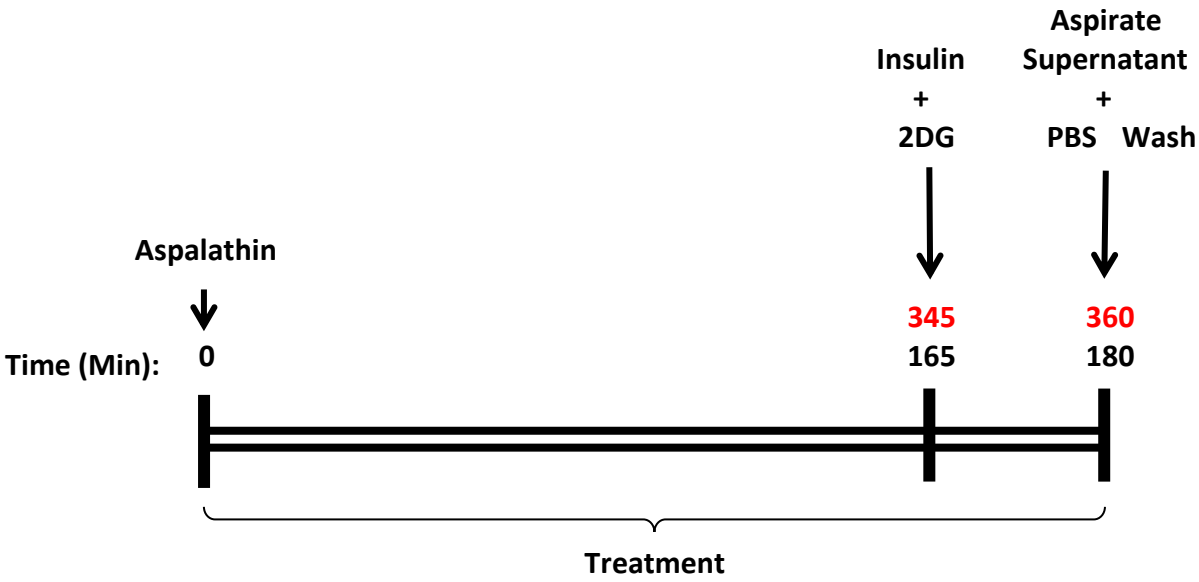

Figure 3.10 Glucose uptake protocol in H9C2 cells. Time points in black for 3 h protocol and red for 6 h protocol.

500 µl 1N NaOH was added to each well and samples heated in a shaking incubator at 60 °C (Incu-Shaker Mini, Benchmark Scientific Inc., USA) to dissolve the cells. 500 µl distilled H_2O (dH_2O) was then added to dilute the samples to a final concentration of 0.5 N NaOH and vortexed thoroughly. An aliquot of 50 µl of this solution was used to assay protein content by the Bradford method (**refer to section 3.6 below**), while 100 µl per sample was counted for radioactivity using a Tri-Carb® 2810 TR Liquid Scintillation Analyzer (Perkin-Elmer Inc., USA) in duplicate. One vial, used as a blank, only received scintillation fluid, and another vial had 1.8 µM (25 µl) 2-deoxy-D-[^{3}H]glucose (2DG) to measure the total radioactive count. Average disintegrations per minute (DPM) was recorded for each sample and the blank subtracted. The specific activity, given as the activity of a radioisotope per unit mass, was determined by using the DPM of the total radioactive count divided by the exact amount of 2DG (1100 pmol in 25 ul of 1.8 µM 2DG). This value could then be used to calculate the average DPM values for each sample, and together with the protein determination, determine the average pmol 2DG uptake per mg cell protein.

3.6. Bradford Protein Determination

The Bradford protein determination method was used to determine the protein content of each well in the treatment plates (Bradford, 1976). A bovine serum albumin (BSA) stock solution with a concentration of 2mg/ml in dH_2O. Just prior to protein determination, the stock was serially diluted into duplicate microtitre plate wells to generate concentrations between 0.125 and 2.0 mg/ml in a volume of 150 µl, creating a standard curve. 150 µl supernatant of the samples generated in the above experiments, were also aliquoted in duplicate microtitre plate wells. All standards and samples then received 150 µl of Quick Start™ Bradford reagent (Bio-Rad Laboratories Inc., USA),

and were incubated for 30 mins at room temperature. The absorbance values were measured using a microtitre plate spectrophotometer (ELx800 Absorbance Reader, BioTek Instruments Inc., USA) at 595 nm and the protein content of the samples determined from the standard curve plotted.

AIM 4: UNDERSTAND THE MECHANISM OF ACTION OF ASPALATHIN, BY USING:

e. Young, control and HFD rats with the same experimental treatments as in Aim 2 (d and e) above to determine expression and activation of the biochemical intermediates (total- and phospho-subunits of PKB and AMPK antibody) using standard Western blotting techniques
f. young, control and HFD rats to determine Glut4 translocation induced by aspalathin

4.1. GENERAL PREPARATION OF EXTRACTS FOR WESTERN BLOTTING

To prepare lysates for immunoblotting, cardiomyocytes were isolated using the same procedure described in **section 2.1**. The cells were then glucose starved in an oxygenated medium (**Solution E, Table 3.2**), and left to preincubate in a shaking water bath (Grant Instruments Ltd., UK) for 5 ms at 37 °C. Each experimental series was incubated with or without 10 nM insulin, 10 µM aspalathin, 0.1% DMSO (used as solvent for synthetic aspalathin) and 100 nM wortmannin (Sigma-Aldrich Life Science, USA) for a period of 15 to 90 mins, depending on the aim. Figure 3.11 contains an overview of the standard experimental protocol followed to prepare lysates for acute treatment. Each experiment was performed with two replicates per treatment per plate and the experiments repeated at least 3 times (n=3) in order to yield enough lysates to investigate all the mechanisms of interest. At the end of the incubation period, the cells were quickly centrifuged and washed with ice-cold HEPES buffer without albumin.

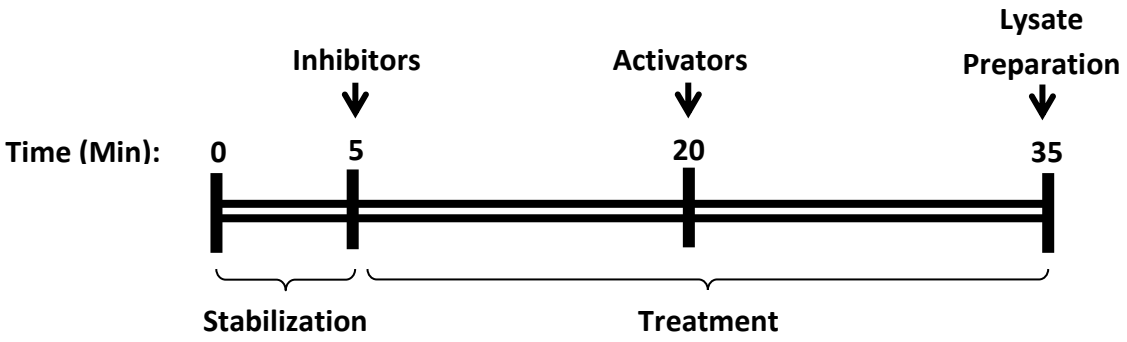

Figure 3.11 Standard experimental protocol prior to preparation of lysates from cardiomyocytes

The cells were homogenized and lysed in Lysis buffer (**Table 3.3**), using a Bullet Blender® (Next Advance Inc., USA) at 4 °C for 5 ms, with a scoop of 0.15 mm diameter zirconium oxide beads equivalent to the volume of cells. The lysates were then microfuged at 1000 rpms for 10 mins at 4 °C (Sigma 1-14K Refrigerated Microfuge, Lasec SA (Pty) Ltd., RSA) and 5 μL supernatant was

used in Bradford protein determination (**described below in section 3.2.**). Hereafter, the protein concentration for each sample was calculated, and supernatant pipetted into Eppendorf tubes. Lysis buffer was added in order to dilute all samples to equal protein concentrations (50 μg/12 μl final solution). Finally, a mix of 850 μl 1:2 Laemmli sample buffer (**Table 3.3**) with 150 μl mercaptoethanol was made and added to the samples in a volume equal to half of the lysis buffer and sample buffer. The samples were boiled for 5 mins and stored at -80 °C for future analysis by Western blotting.

Table 3.3 Buffer and Gel Compositions used in Western Blotting Protocol

Solution	Composition
Lysis Buffer	20 mM Tris-HCl, 1 mM EGTA, 1 mM EDTA, 150 mM NaCl, 1 mM β-glycerophosphate, 2.5 mM tetra-Na^+-pirophosphate, 1 mM Na_3VO_4, 1% Triton X-100, 10 μg/ml Leupeptin, 10 μg/ml Aprotinin, 50 μg/ml PMSF
Fractionated Lysis Buffer	20 mM Tris-HCl, 1 mM EGTA, 1 mM EDTA, 150 mM NaCl, 1 mM Na_3VO_4, 50 μg/ml PMSF, 1% Triton X-100 (Membrane Fractions only)
Laemmli Sample Buffer	62.5 mM Tris-HCl (pH 6.8), 4% SDS, 10% glycerol, 0.03% bromophenol blue, 5% β-mercaptoethanol
Bradford Reagent	100 mg Coomassie Brilliant Blue G-250, 50 ml 95% Ethanol, 100 ml 85% (w/v) Phosphoric Acid, 850 ml dH_2O
10% Polyacrylamide Resolving Gel	4.9 ml dH_2O, 2.5 ml 1.5 M Tris-HCl (pH 8.8), 100 uL 10% SDS, 2.5 ml 40% acrylamide, 50 uL 10% APS, 20 uL 99% TEMED
4% Polyacrylamide Stacking Gel	3.05 ml dH_2O, 1.25 ml 0.5M Tris-HCl (pH 6.84), 50 uL 10% SDS, 0.5 ml 40% Acrylamide, 50 uL 10% APS, 10 uL 99% TEMED
10% Fast-Cast Kit Resolving Gel	3 ml TGX Stain-Free™ FastCast™ Resolver A, 3 ml TGX Stain-Free™ FastCast™ Resolver B, 30 uL 10% APS, 3 uL TEMED
10% Fast-Cast Kit Stacking Gel	1ml TGX Stain-Free™ FastCast™ Stacker A, 1ml TGX Stain-Free™ FastCast™ Stacker B, 10 uL 10% APS, 2 uL TEMED
Running Buffer	25 mM Tris-HCl,192mM Glycine, 0.1% SDS (made up with dH_2O)
Trans-Blot Turbo Buffer	600 mL dH_2O, 200 mL 99.8% Ethanol, 200 mL Trans-Blot® Turbo™ Buffer
TBS-Tween Buffer (pH 7.6)	20 mM Tris-HCl, 137 mM NaCl, 0.1% Tween-20 (diluted with dH_2O)

4.2. Bradford Protein Determination

The Bradford protein determination method was used to determine the protein content of tissue lysates (Bradford, 1976). A BSA stock solution (Bio-Rad Laboratories Inc., USA) with a

concentration of 5 mg/ml in dH_2O was used. Just prior to protein determination, the stock solution was diluted 1:5 times with dH_2O and then serially diluted into duplicate test tubes to generate concentrations between 1 and 30 µg in a volume of 100 µl. 5 µl supernatant of the samples generated in the above experiments, was diluted 1:10 with dH_2O to dilute all detergents that may interfere with the assay. The diluted samples were then further diluted 1:20 in test tubes to reach a volume of 100 ul. All standards and samples received 900 µl of double filtered Bradford reagent (diluted 1:5 with H_2O) (**Table 3.3**), vortexed and incubated for 30 mins at room temperature. The absorbance values were measured using a spectrophotometer (Spectronic® 20 Genesys™ Spectrophotometer, Thermo Fisher Scientific Inc., RSA) at 595 nm and the protein content of the samples determined from the standard curve plotted.

4.3. GLUT4 Translocation in Isolated Cardiomyocytes

Distribution of GLUT4 was observed by fractionating the cells into cytosolic and membrane compartments by differential centrifugation followed by Western blots of the separated proteins probed with a specific GLUT4 antibody. Cardiomyocytes were isolated using the same procedure described in section 2.1. Two hearts were combined per experiment to render enough cells to accommodate the membrane fractionation involved in this protocol (Webster et al. 2010). The cells were glucose starved in an oxygenated medium (**Solution E, Table 3.2**), while incubating at 37 °C (Incu-Shaker Mini, Benchmark Scientific Inc., USA) and shaking at 30 rpm in the presence of 100% O_2. Each experimental series was incubated with or without 10 nM insulin and 10 µM aspalathin. At the end of the incubation period, the cells were quickly centrifuged and washed with ice-cold HEPES buffer without albumin. **Figure 3.12** contains an overview of the simplified experimental protocol followed. Each experiment was repeated 3 times for each of the Young, Control and HFD groups.

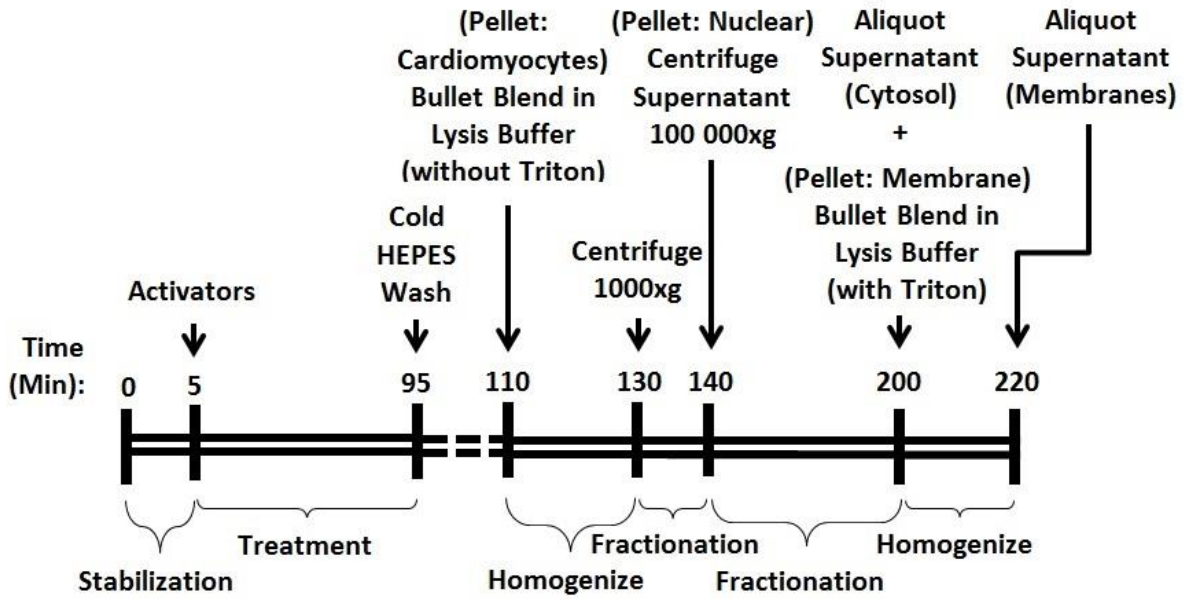

Figure 3.12 Simplified protocol to prepare lysates of cytosol and membrane fractions

The cells were homogenized and lysed in 200 μL Fractionated Lysis buffer without Triton X-100 (**Table 3.3**), using a Bullet Blender® (Next Advance Inc., USA) at 4 °C for 5 mins, with a scoop of 0.15 mm diameter zirconium oxide beads equivalent to the cell pellet size. The homogenates were then kept on ice for a further 15 mins after which they were microfuged at 1,000*g* for 10 mins at 4 °C (Sigma 1-14K Refrigerated Microfuge, Lasec SA (Pty) Ltd., RSA). The supernatant, containing the cytosol and membrane fractions (**Figure 3.13**), was carefully aspirated, without touching the beads and nuclear proteins (the pellet), and placed in 0.5 ml eppindorf tubes. The tubes were subsequently ultracentrifuged in a Beckman Ti50 rotor using adaptors for 0.5 ml eppindorf tubes, at 40,000 rpms (100,000*g)* for 60 mins at 4 °C in a L7 Ultracentrifuge (Beckman-Coulter Inc., USA). The supernatant was collected and considered to contain the cytosolic fraction. 100 uL Fractionated Lysis buffer with 1% Triton X-100 (**Table 3.3)** was added to the pellet, containing the membrane fractions, and homogenized using a Bullet Blender® (Next Advance Inc., USA) at 4 °C for 5 mins, with a scoop of 0.15 mm diameter zirconium oxide beads equivalent to the size of the pellet . The homogenate was then quickly spun down to sediment the beads at 14,500 rpms with an Eppendorff® Minispin®plus (Sigma-Aldrich Life Sciences Inc., USA) and the supernatant collected considered as the membrane fraction. 5 *μ*L of the supernatant was used to determine the protein concentration using the method of Bradford (**described above in section 3.6.**). Hereafter, the concentration for each sample was calculated, and a volume of supernatant containing equal amounts of protein, pipetted into Eppendorf tubes. Fractionated Lysis buffer (without 1% Triton X-100 for cytosol fractions and with 1% Triton X-100 for membrane fractions) was added in order to dilute all samples to equal protein concentrations (50 μg/12 μl final solution). Finally, a mix of 850 μl 1:2 Laemmli sample buffer (**Table 3.3**) with 150 μl mercaptoethanol was made and added to the samples in amounts equal to half of the lysis buffer and sample buffer. The samples were boiled for 5 mins and stored at -80 °C for future analysis by Western blotting.

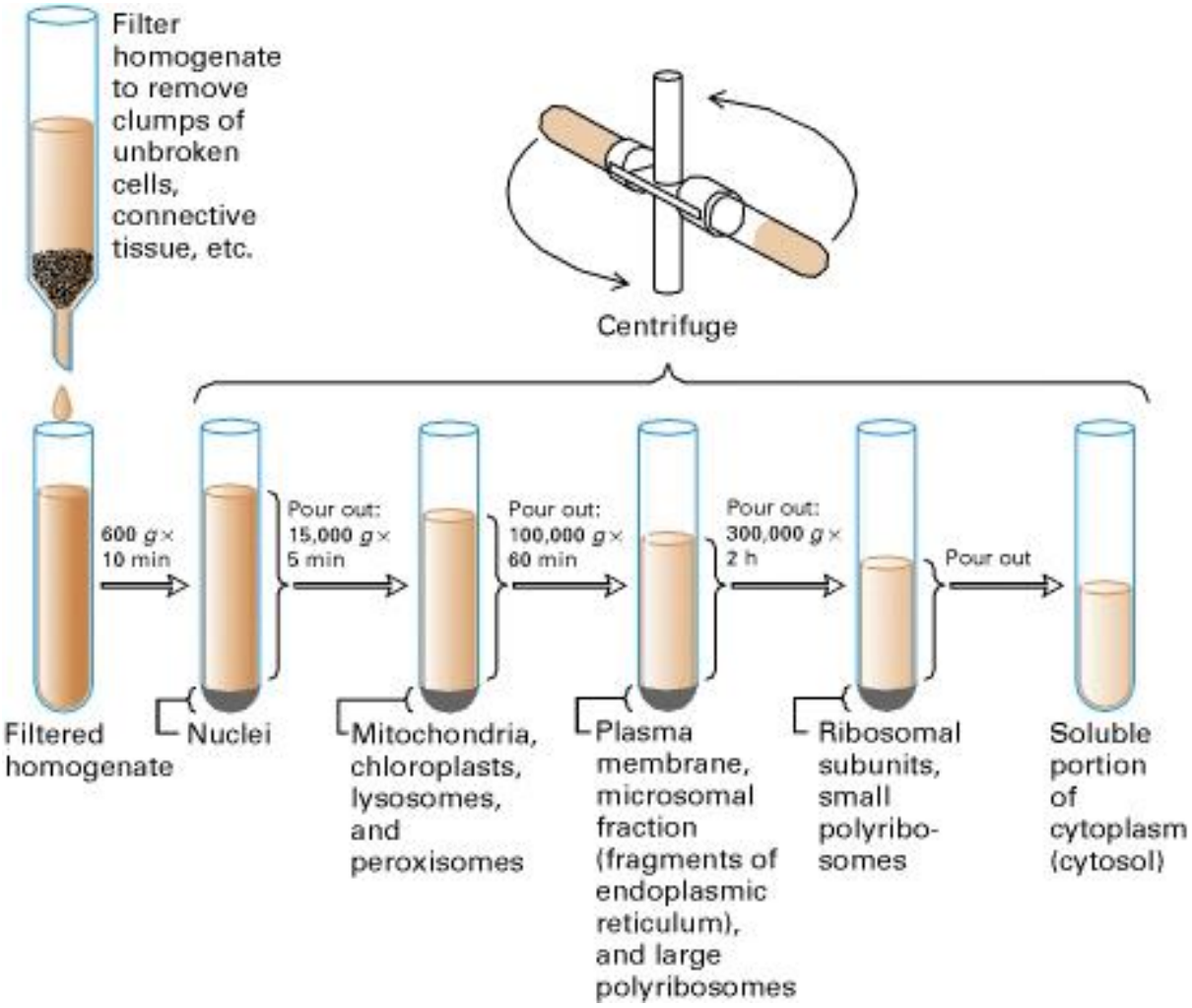

Figure 3.13 Cell fractionation by differential centrifugation. A cell suspension can be centrifuged at increasing speeds for increasing durations to selectively pellet specific cell structures. First, a centrifugal force of 600*g* (600 times the force of gravity) for 10 mins is necessary to sediment nuclei. The supernatant can then be further fractionated by cenrifugation at 15,000*g* for 5 mins to obtain the mitochondrial fraction.. A subsequent centrifugation of the supernatant in an ultracentrifuge (100,000*g* × 60 mins) results in deposition of the plasma membrane. At 100,000*g* (50,000 rpm in an ultracentrifuge), the centrifuge rotor chamber is vacuum sealed and refrigerated to reduce friction-induced heating between the hyperspinning rotor and air molecules. The supernatant contains the cytosol and small ribosomal proteins en enzymes (Obtained from Lodish, 2000)

4.4. Western Blot Analysis

4.4.1. Loading and separation of proteins

Gels were either prepared by (i) polymerizing the 10% polyacrylamide resolving gel (**Table 3.3**) for 30 mins, followed by addition and polymerization of 4% polyacrylamide stacking gel for 15 mins, (ii) by adding 10% Fast-Cast Kit resolver gel (**Table 3.3**), followed by immediately adding the 10% Fast-Cast Kit stacking gel and polymerizing for 40 mins (TGX Stain-Free™ FastCast™ Acrylamide Kit), or (iii) Mini-PROTEAN® TGX Stain-Free™ Precast gradient (4-15%) Gels were used (Bio-Rad Laboratories Inc., USA). After polymerization, the gels were placed in a Mini-PROTEAN® Tetra System (Bio-Rad Laboratories Inc., USA) and filled with Running Buffer (**Table 3.3**). After boiling the lysates, 50 ug of each sample was loaded onto the 4% stacking polyacrylamide gels. The first lane position on each gel was loaded with 5ul PageRuler™ Prestained Protein Ladder (Fermentas Life Sciences, RSA) for proteins of interest smaller than 100 kDa, whereas either 7.5 ul HiMark™ Pre-Stained Protein Standard (Thermo Fisher Scientific Inc., RSA) for proteins of interest larger than 100 kDa, to aid with determination of molecular weights of specific bands. The second lane was loaded with untreated controls, and subsequent lanes contained treated groups. Proteins were then separated using the principle of sodiumdodecyl sulphate polyacrylamide gel electrophoresis (SDS-PAGE). Gels were run for 10 mins at 100 V and 200 mA, followed by 50 mins at 140 V and 140 mA, in Running Buffer (**Table 3.3**).

4.4.2. Protein transfer and visualization

Following SDS-PAGE, proteins of interest <100 kDa were electrotransfered to polyvinylidene fluoride (PVDF) membranes, using a semi-dry Trans-Blot® Turbo™ Transfer System (Bio-Rad Laboratories Inc., USA) for 30 mins at 25 V and 1.0 A. The membranes were then visualized with the ChemiDoc™ MP System (Bio-Rad Laboratories Inc., USA), and images stored for later use in normalization of samples. After washing of the membranes with TBS-Tween Buffer (**Table 3.3**), the membranes were blocked in TBS-Tween Buffer with 5% (w/v) fat-free dry milk, while gently agitating for 2 hours at room temprature. The membranes were then 3 times washed with TBS-Tween Buffer for 5 mins, followed by incubation overnight at 4°C with 1:1000 dilution of different antibodies in TBS-Tween Buffer, including the Total- or Phospho(Ser473)-PKB, Total- or Phospho(Thr172)AMPK, and Total-GLUT4. The membranes were then washed 3 times with TBS-Tween Buffer for 5 mins, followed by agitation for 1 hour with 1:4,000 dilution in TBS-Tween Buffer of either anti-mouse or anti rabbit immunoglobulin G (IgG) horseradish peroxidase (HRP) linked whole antibody (Amersham Biosciences, UK, and Dako Cytomation, Denmark) at room temperature. Following secondary antibody incubation, membranes were washed again with TBS-Tween Buffer and then visualized using either Clarity Western ECL Substrate for 5 mins or Luminata Forte Western HRP substrate for 2 mins and exposed with the Bio-Rad Chemidoc MP Imager for a specific time depending on the antibody used (**Table 2.3**). The optical density

readings of each band was expressed relative to the two untreated controls present in the second lane. All visualizations and quantification of protein bands on membranes were analyzed using Image Lab 5.0 (Bio-Rad Laboratories).

Table 3.4 Optimized protocol for each primary and secondary antibody

Proteins	MW (kDa)	Gel%	Protein Loaded (ug)	1st Antibody Preparation		2nd Antibody Preparation		Time Exposed
				Dilution Factor	% Milk	Dilution Factor	% Milk	
PKB	60	10	50	1:1000	0%	1:4000	0%	10s – 10mins
AMPKα	62	10	50	1:1000	0%	1:4000	5%	10s – 20mins
GLUT4	45	10	50	1:1000	5%	1:4000	5%	10s – 30mins

4.5. STATISTICAL ANALYSIS

Unless stated otherwise, all results are presented as the means ± standard error of the mean (SEM). For comparative studies, statistical analysis was done with a Student's t-test (unpaired) or one-way analysis of variance (ANOVA) followed by Bonferroni multiple comparisons test (for $p<0.05$) using GraphPad Prism 5 (Graphpad Software Inc., USA). $P<0.05$ was considered as significant.

CHAPTER 4

RESULTS: MODEL OF DIET-INDUCED OBESITY AND INSULIN RESISTANCE

1. CHARACTERISTICS OF YOUNG, CONTROL AND HIGH-FAT, HIGH-CALORIC DIET RATS

1.1 BODY WEIGHT OF YOUNG, CONTROL AND HFD RATS

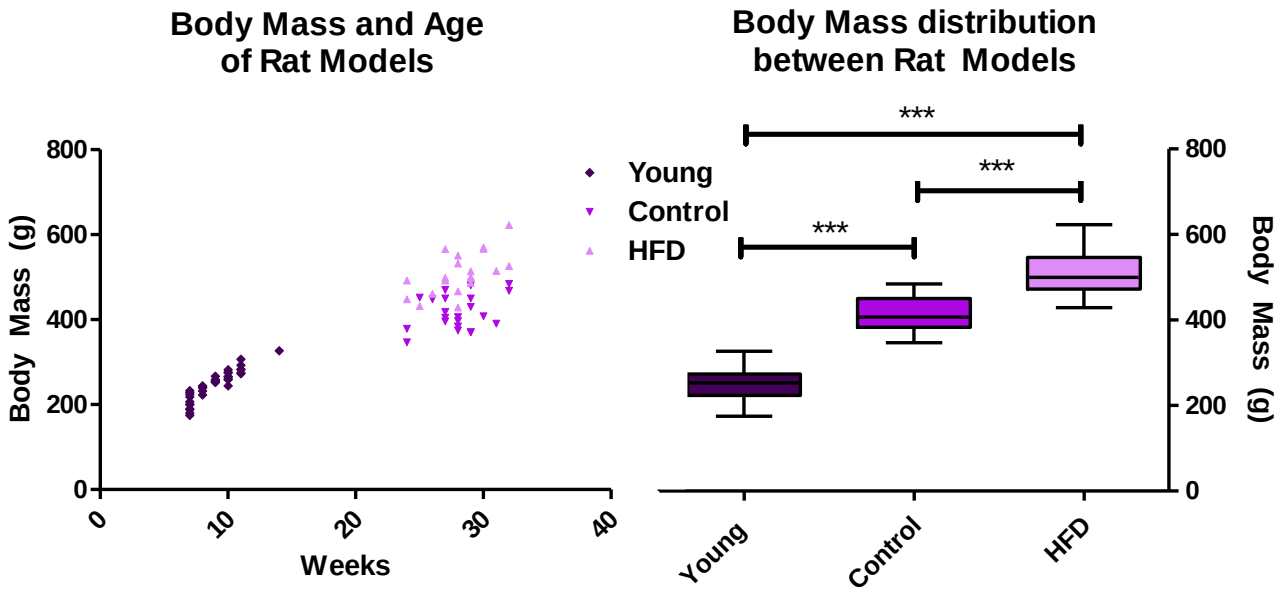

Figure 4.1 Body weight of rat models – young (7 – 14 weeks; n=38), control (n=22) and HFD (24 – 32 weeks; n=20); HFD: high-fat, high-sucrose diet; ***p<0.001 (Young vs Control and HFD, Control vs HFD)

Table 4.1 summarizes the characteristics of the 3 animal models. At 7–14 weeks of age, the body weight of young rats averaged 246.8±6 g (n=38). At 24-32 weeks of age, the body weight of control rats averaged 417.3±9 g (n=22) and that of HFD rats averaged 508.5±11 g (n=20). The high-fat, high-sucrose diet had an average higher body weight of 91.2 g or 21.9% (p< 0.001) (**Figure 4.1**).

1.2 VISCERAL ADIPOSE TISSUE OF CONTROL AND HFD RATS

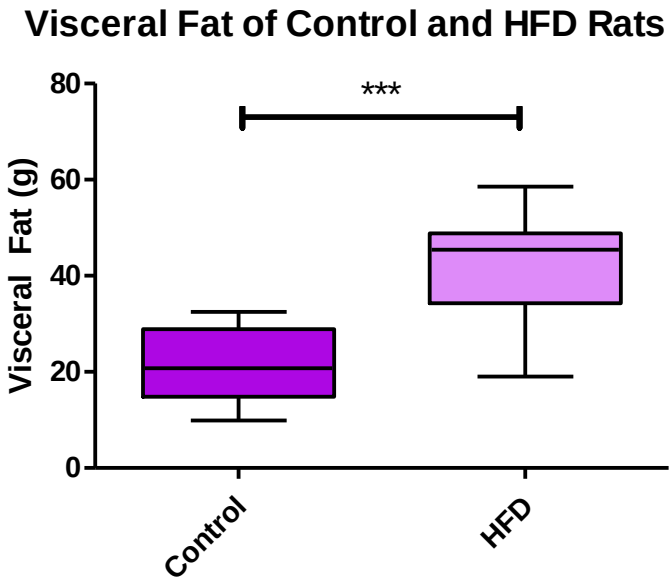

Figure 4.2 Visceral fat of diet rat models; HFD: high-fat, high-sucrose diet; ***p<0.001 (Control vs HFD)

After 24 - 32 weeks of feeding, the visceral fat of control rats averaged 21.75±1.5g (n=22) and that of the HFD rats averaged 42.30±2.3g (n=20). The HFD rats had an average 94.5% higher visceral fat than the control rats (p< 0.001) (**Figure 4.2**).

1.3 Fasting Blood Glucose of Control and HFD Rats

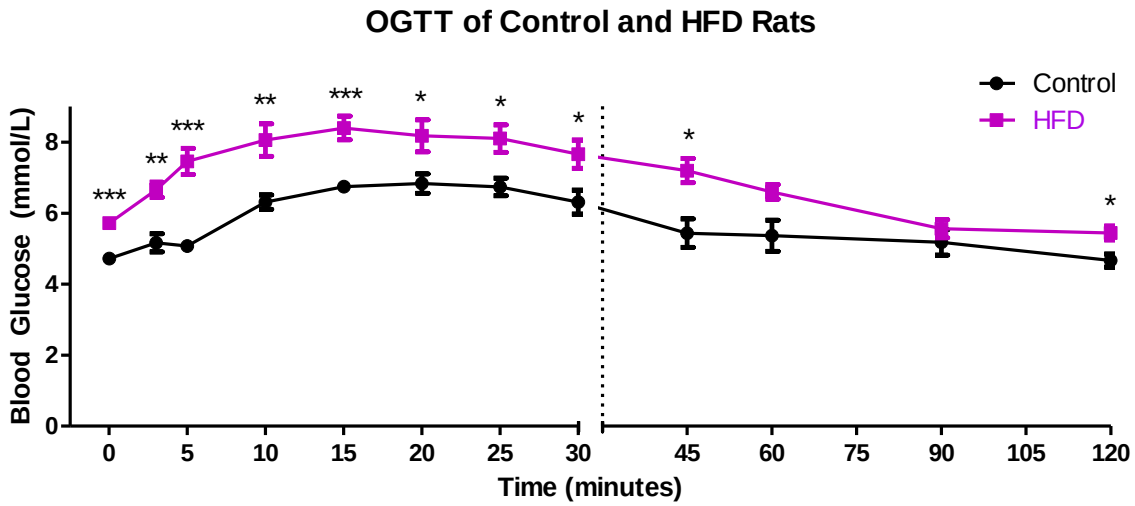

Figure 4.3 OGTT of rats on a 16 week control or high fat, high-sucrose diet; OGTT: Oral glucose tolerance test, HFD: high-fat, high-sucrose diet; *p<0.05 (Control vs HFD at 20, 25, 30, 45 and 120 mins after glucose administration post fasting), **p<0.01 (Control vs HFD at 3 and 10 mins after glucose administration post fasting), ***p<0.001 (Control vs HFD at 0, 5 and 15 mins after glucose administration post fasting)

To test for whole-body insulin resistance following a 16 week HFD, an OGTT was performed (**Figure 4.3**). Following overnight fasting, rats fed a high-fat, high-sucrose diet had elevated basal blood glucose levels compared to the controls (5.7±0.2 (n=5) vs 4.7±0.1 (n=9) mmol/L; p<0.001). After an oral glucose injection, the blood glucose levels of HFD rats continuted to remain significantly elevated for up to 45 minutes (7.2±0.3 (n=5) vs 5.4±0.4 (n=8) mmol/L; p<0.05). 90 minutes after the test, the HFD and control group had the closest resembling blood glucose levels (5.6±0.3 (n=5) vs 5.2±0.4 (n=8) mmol/L; p=0.4571). However, at the end of the test (at 120 minutes), the HFD rats once again had an elevated blood glucose level compared to the control rats (5.4±0.2 (n=5) vs 4.7±0.2 (n=9) mmol/L; p<0.05).

1.4 Non-Fasting Blood Glucose of Young, Control and HFD Rats

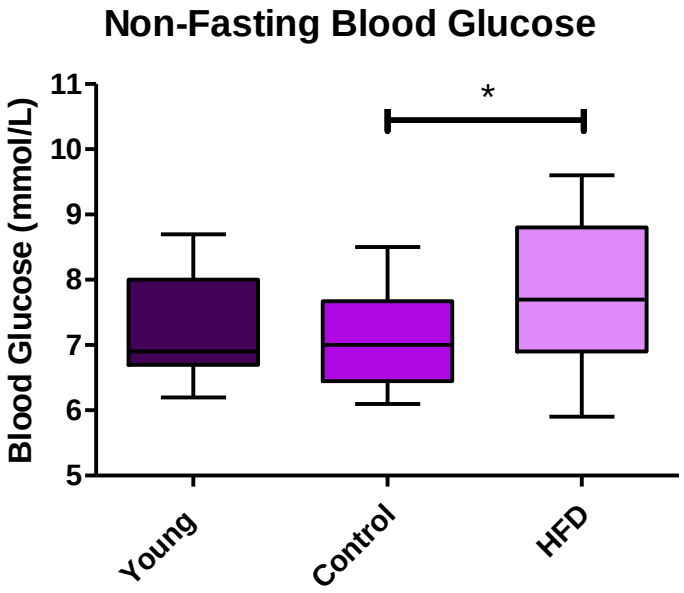

Figure 4.4 Non-fasting blood glucose prior to sacrificing of rats; HFD: high-fat, high-sucrose diet; *p<0.05 (Control vs HFD)

Non-fasting blood glucose levels were obtained just prior to sacrificing rats. Young rats had an average blood glucose level of 7.3±0.3 mmol/L (n=9), control rats 7.1±0.2 mmol/L (n=20) and HFD rats 7.8±0.2 mmol/L (n=19). Non-fasting blood glucose levels were 9.9% higher in HFD rats compared to control rats (p<0.05) (**Figure 4.4**).

1.5 Serum Insulin Levels of Control and HFD Rats

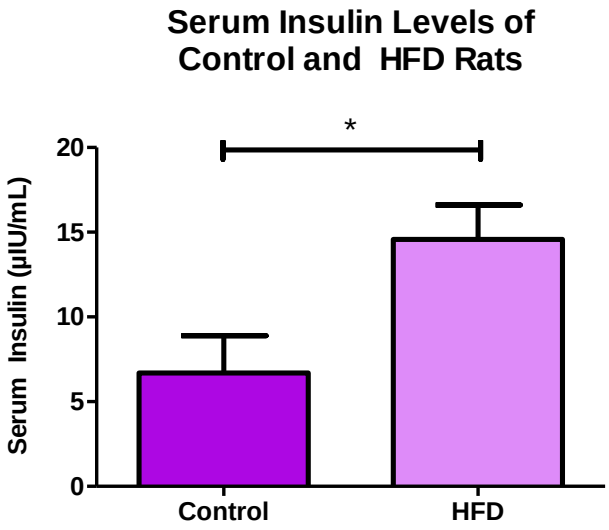

Figure 4.5 Fasting serum insulin levels of control and HFD rats; HFD: high-fat, high-sucrose diet; *p<0.05 (Control vs HFD)

Fasting insulin levels were obtained from blood collected directly from the carotid artery. HFD rats had a signifcantly higher fasting serum insulin levels compared to controls rats (14.58±2.04 µIU/mL; n=5 vs 6.68±2.21 µIU/mL; n=6; p<0.05), constituting an increase in serum insulin levels of 118% (**Figure 4.5**).

Table 4.1 Characteristics of Animal Models

Parameters	Young	n	Control	n	HFD	n
Body weight (g)	246.8±6	38	417.3±9	22	508.5±11 (***)	20
Intraperitoneal Fat (g)	-	-	21.75±1.5	22	42.30±2.3 (***)	20
Fasting blood glucose (mmol/L)	-	-	4.7±0.1	9	5.7±0.2 (***)	5
Non-fasting blood glucose (mmol/L)	7.3±0.3	9	7.1±0.2	20	7.8±0.2 (*)	19
Fasting serum insulin (µIU/mL)	-	-	6.68±2.21	6	14.58±2.04 (*)	5
HOMA-IR index	-	-	0.86±0.28	6	1.93±0.28 (***)	5

HFD: High-fat, high-sucrose diet; HOMA-IR: Homeostasis Model Assessment of Insulin Resistance; *p<0.05, **p<0.01, ***p<0.001 (Control vs HFD).

CHAPTER 5

RESULTS: ASPALATHIN AND ISOLATED VENTRICULAR CARDIOMYOCYTES FROM YOUNG, CONTROL AND HFD RATS

1. CELL VIABILITY ASSAYS

1.1 CELL VIABILITY OF ISOLATED ADULT VENTRICULAR CARDIOMYOCYTES FROM YOUNG RATS AFTER ISOLATION

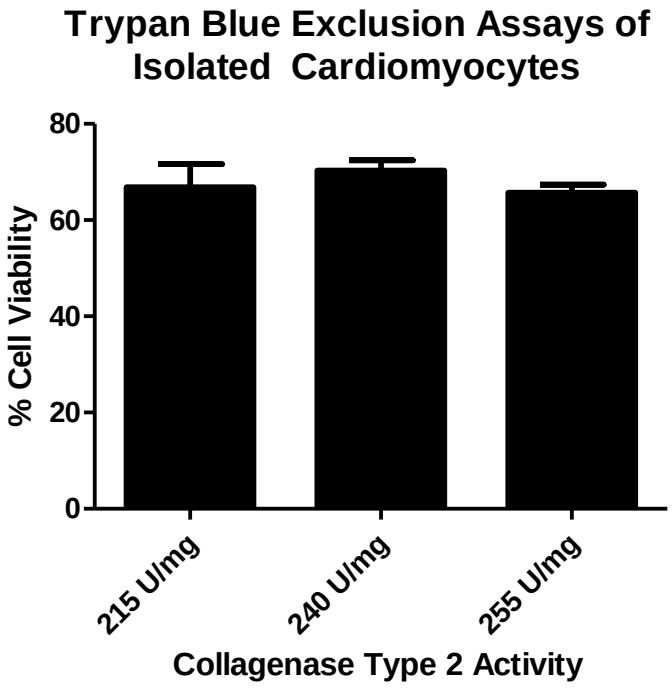

Figure 5.1 Cell viability of isolated cardiomyocytes from young rats (using different collagenase type 2 batches)

Proper enzyme selection is critical for successful isolation of cardiomyocytes (Johnson et al., 2014). Therefore, each new batch of collegenase was tested to prevent batch variation affecting digestion and cell viability (Johnson et al., 2014). Trypan blue exclusion assays of isolated cardiomyocytes were performed using 3 different collagenase type 2 batches to assess the cell viability of the isolation protocol (**Figure 5.1**). There were no significant differences in cell viability between either 215U/mg (66.8±4.8% viable; n=1), 240U/mg (70.3±2.1% viable; n=1) or 255U/mg (65.7±1.7% viable; n=1) activity.

1.2 Cell Viability of Isolated Cardiomyocytes from Young Rats after Treatments

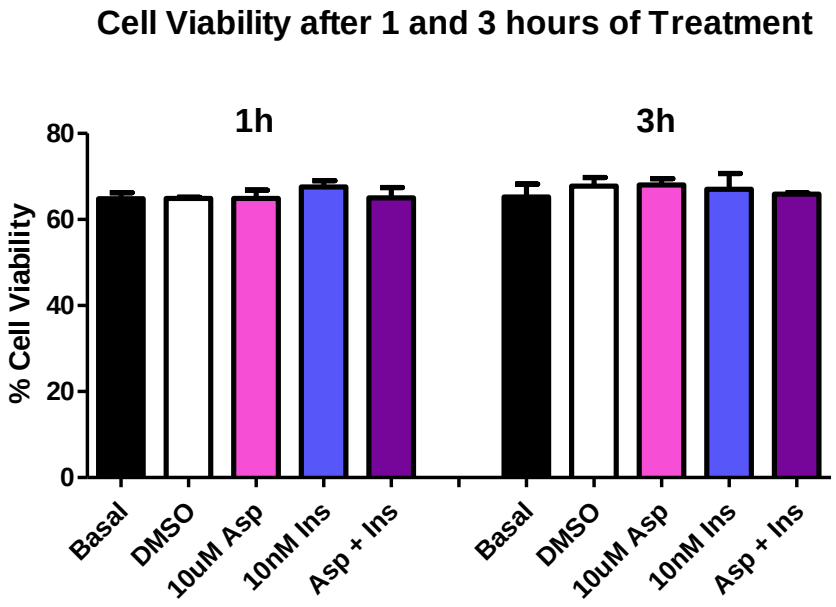

Figure 5.2 Effect of treatments on cell viability of isolated cardiomyocytes. DMSO: Dimethyl sulfoxide, Asp: Aspalathin, Ins: Insulin; n = 1 individual young rat .

To assess the cell viability of isolated cardiomyocytes from young rats (n=1) after 1 or 3 hours of treatment with DMSO, aspalathin or insulin, a PI-staining assay was performed as previously described (**Figure 5.2**). There was no significant diffences between treatment groups for either 1 or 3 hours of treatment. After 1 hour of treatment, basal cell viability was 64.8±1.4%, DMSO treated groups 64.9±0.2%, 10μM aspalathin treated groups 64.9±1.9%, 10 nM insulin treated group 67.6±1.4% and 10 μM aspalathin with 10 nM insulin 65.1±2.3%. After 3 hours of treatment, basal cell viability was 65.3±3.0%, DMSO treated groups 67.8±2.0%, 10 μM aspalathin treated groups 68.1±1.4%, 10 nM insulin treated group 67.1±3.7% and 10 μM aspalathin with 10 nM insulin 65.9±0.3% (**Table 5.1**).

Table 5.1 Cell viability after 1 or 3 hours of treatment

Treatment Time	Cell Viability (%)					
	Basal	**DMSO**	**10 μM Asp**	**10 nM Ins**	**10 μM Asp + 10 nM Ins**	**n**
1 h	64.8±1.4	64.9±0.2	64.9±1.9	67.6±1.4	65.1±2.3	1
3 h	65.3±3.0	67.8±2.0	68.1±1.4	67.1±3.7	65.9±0.3	1

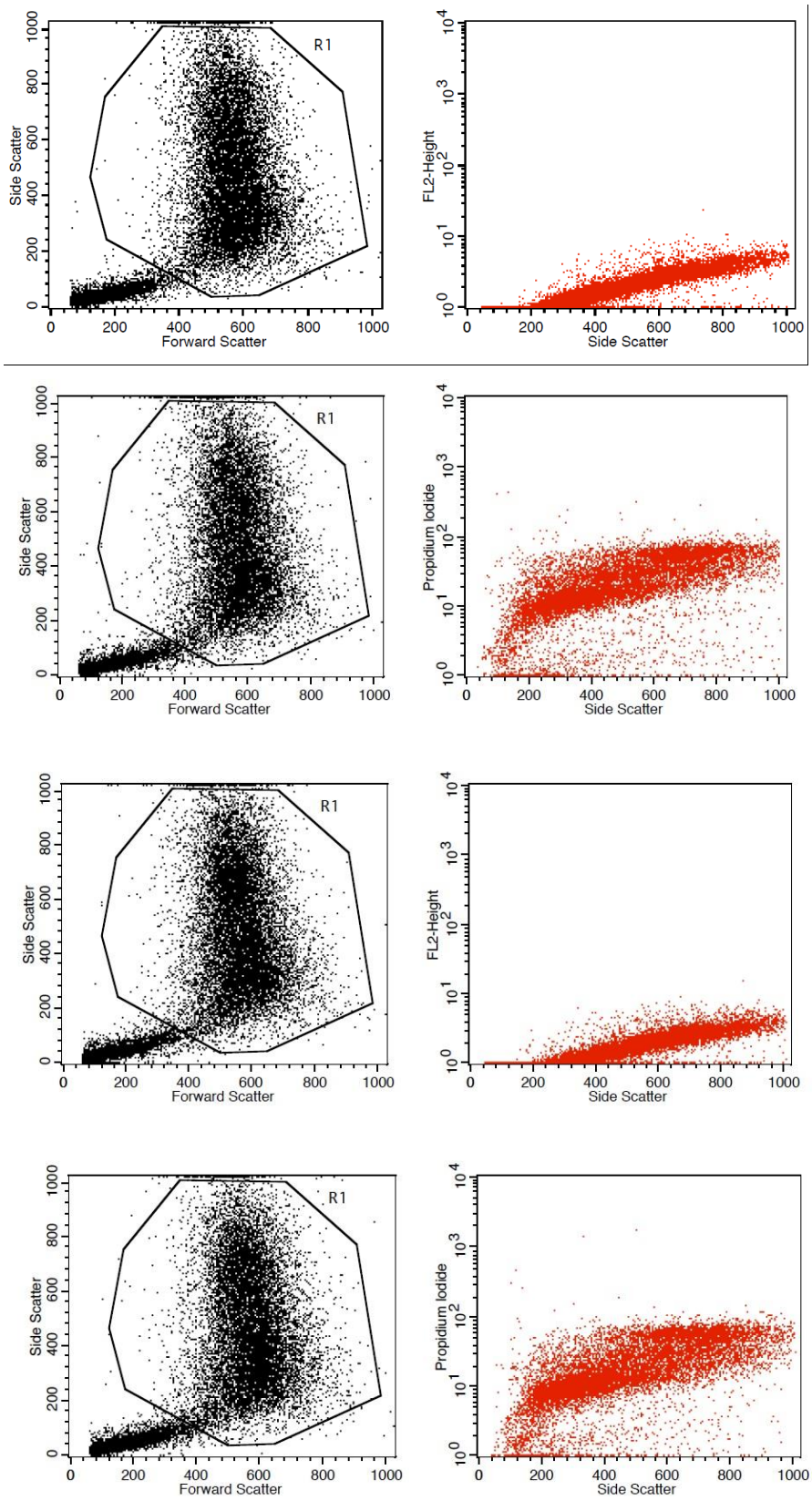

Figure 5.3 Dot plot representing total events acquired and final gated population of untreated isolated cardiomyocytes. A forward-scatter against side-scatter plot was used to distinguish the cells (gated/encircled) from the debris. There was no significant difference in cell viability between 1 or 3 hours of incubation.

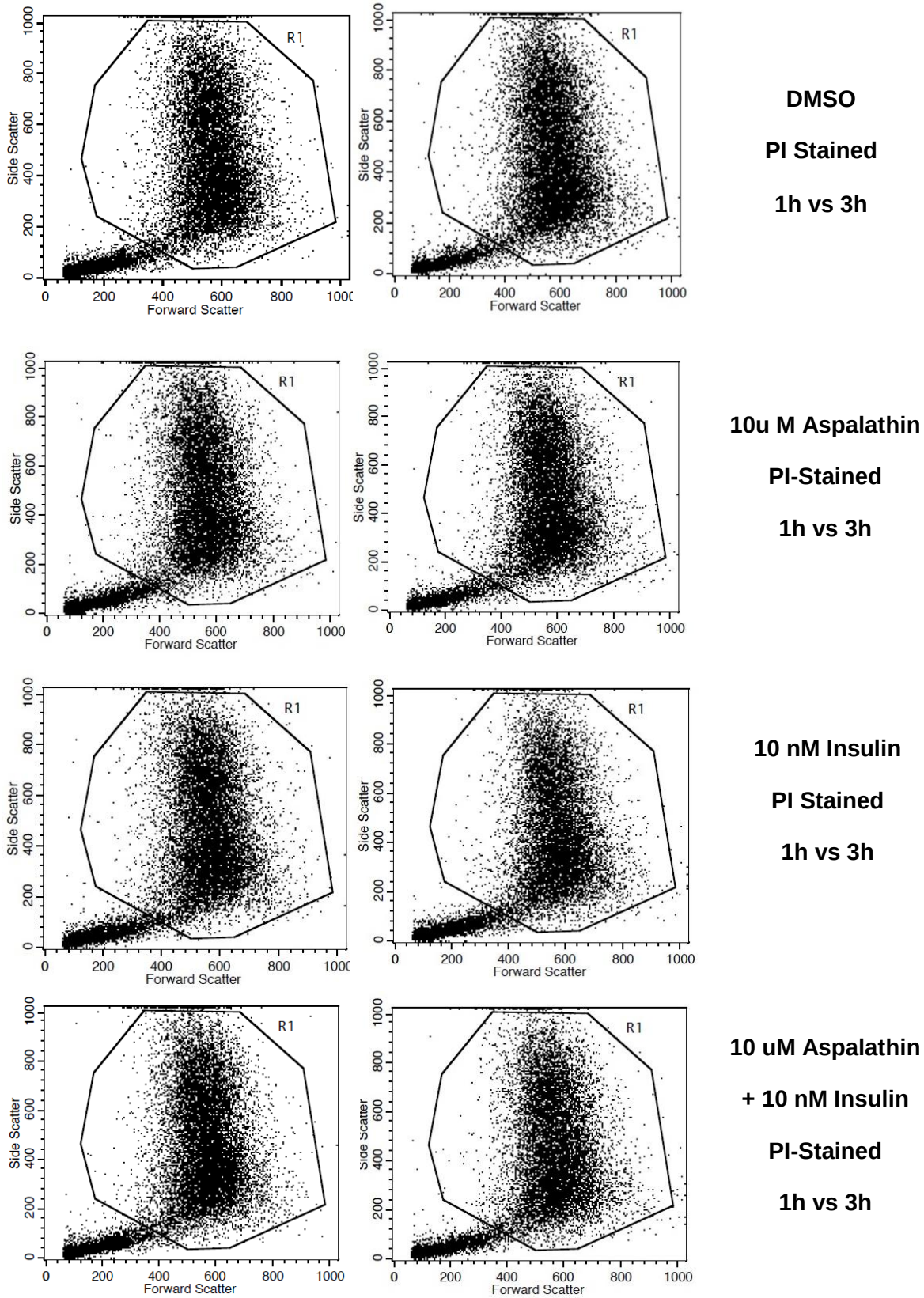

Figure 5.4 Dot plot representing total events acquired and final gated population of treated isolated cardiomyocytes. A forward-scatter against side-scatter plot was used to distinguish the cells (gated/encircled) from the debris. There was no significant difference in cell viability between 1 or 3 hours of treatment.

2. GLUCOSE UPTAKE ASSAYS OF ISOLATED CARDIOMYOCYTES

2.1 ACUTE ASPALATHIN DOSE RESPONSE OF CARDIOMYOCYTES FROM YOUNG RATS

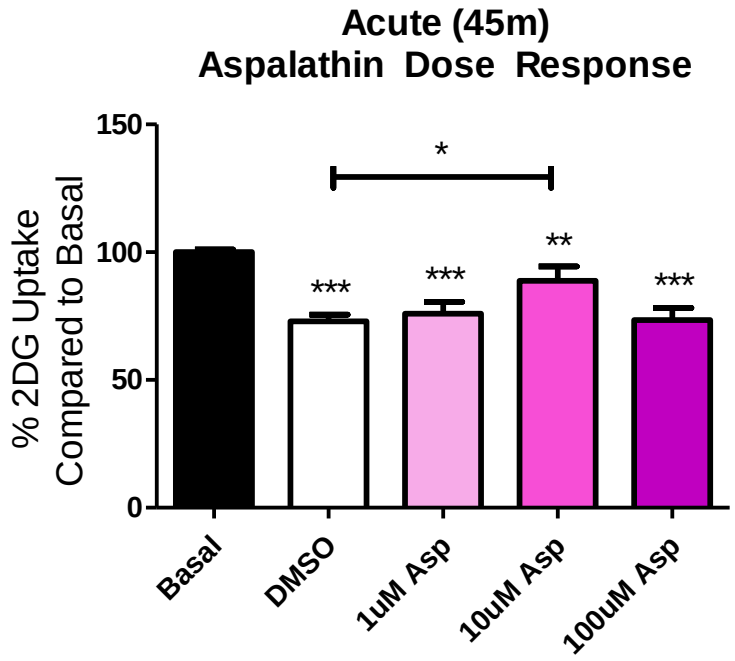

Figure 5.5 2DG after 45 mins of aspalathin dose response in cardiomyocytes (from young control rats). 2DG: 2-deoxy-D-[H^3]-glucose, DMSO: Dimethyl sulfoxide, Asp: Aspalathin; n = 2 - 9 individual preparations; *<p0.05 (DMSO vs. 10 μM Asp), **p<0.01 (Basal vs. 10 μM Asp), ***p<0.001 (Basal vs. DMSO, 1 μM Asp and 100 μM Asp)

We initially tried to establish an asapalthin dose response in isolated cardiomyocytes from young rats (**Figure 5.5**). Acute aspalathin treatment showed a significant decrease in glucose uptake for all three aspalathin dosages of 1 uM aspalathin (76.0±4.6% n=2; p<0.001), 10 uM aspalathin (88.9±5.6%; n=3; p<0.01) and 100 uM aspalathin (73.5±4.7%; n=3; p<0.001) compared to basal (100.0±1.0%; n=9). 0.1% DMSO, the effective concentration used for 100 uM synthetic aspalathin, also presented with a significant decrease in glucose uptake (75.4±3.5%; n=9; p<0.001) compared to basal. However, a dose of 10 uM aspalathin in 0.01% DMSO had an increase in glucose uptake of 14.5% compared to a 10% stronger concentration of DMSO.

2.2 Acute Aspalathin and Insulin Dose Response in Cardiomyocytes from Young Rats

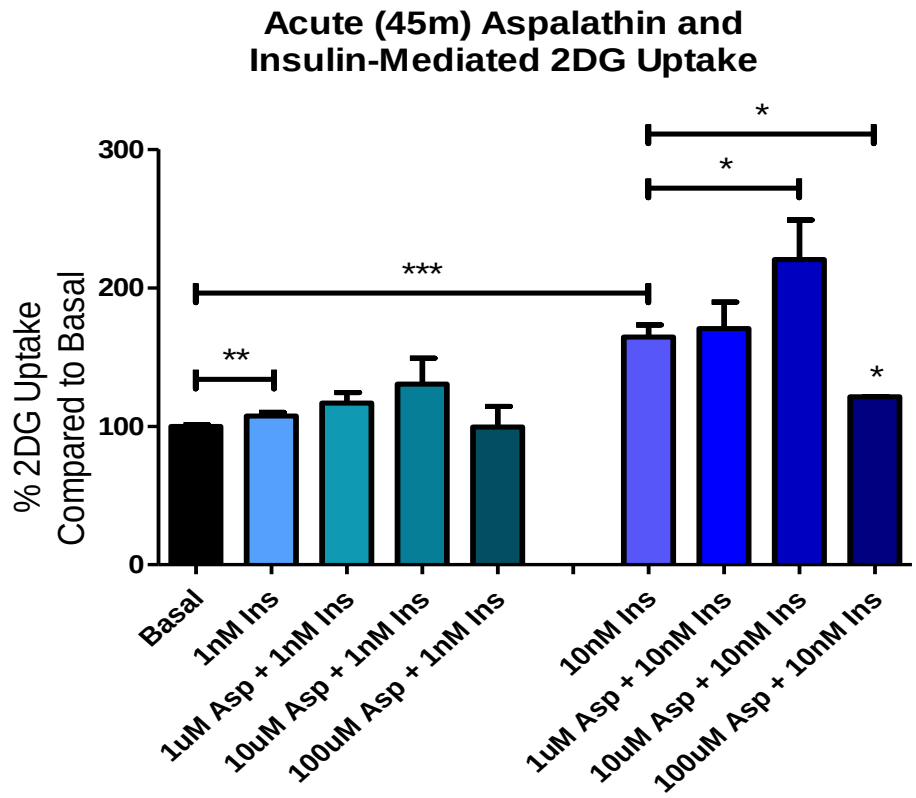

Figure 5.6 2DG after 45 mins aspalathin and insulin dose response in cardiomyocytes (from young control rats). 2DG: 2-deoxy-D-[H^3]-glucose, Ins: Insulin, Asp: Aspalathin; n = 3 individual preparations; *p<0.05 (10 nM Ins vs. 10 μM Asp + 10 nM Ins; 10 nM Ins vs 100 uM Asp + 10 nM Ins), **p<0.01 (Basal vs.1 nM Ins), ***p<0.001 (Basal vs. 10 nM Ins)

We investigated whether asapalathin can acutely induce glucose uptake through enhancing insulin's action in isolated cardiomyocytes from young rats (**Figure 5.6)**. Acute insulin was able to significantly induce glucose uptake of both 1 nM insulin (107.4±2.6%; p<0.01) and 10 nM insulin (158.3±9.4%; p<0.001) compared to basal (100.0±1.0%). Co-treating 1 nM insulin with increasing aspalathin concentrations showed a strong trend towards dose-dependent increases in glucose uptake for 1 uM aspalathin (116.9±7.5%) and 10 uM aspalathin (130.4±18.7%), while the effect was dissipated when co-treating with 100 uM aspalathin (99.6±14.9%). Likewise, co-treating 10 nM insulin with aspalathin also showed a strong increase in glucose uptake for concentrations of 10 uM aspalathin (220.5±28.4%), while the effect was dissipated when co-treating with 100 uM aspalathin (121.3±0.2%). Co-treating 10 nM insulin with 10 uM aspalathin had a significant increase in glucose uptake (220.5±28.4%; p<0.05) compared to 10 nM insulin (158.3±9.4%). This equated to an effective increase in glucose uptake of 62.2%.

2.3 Acute Insulin Dose Response of Cardiomyocytes from Young, Control and High-Fat, High-Sucrose Diet Rats

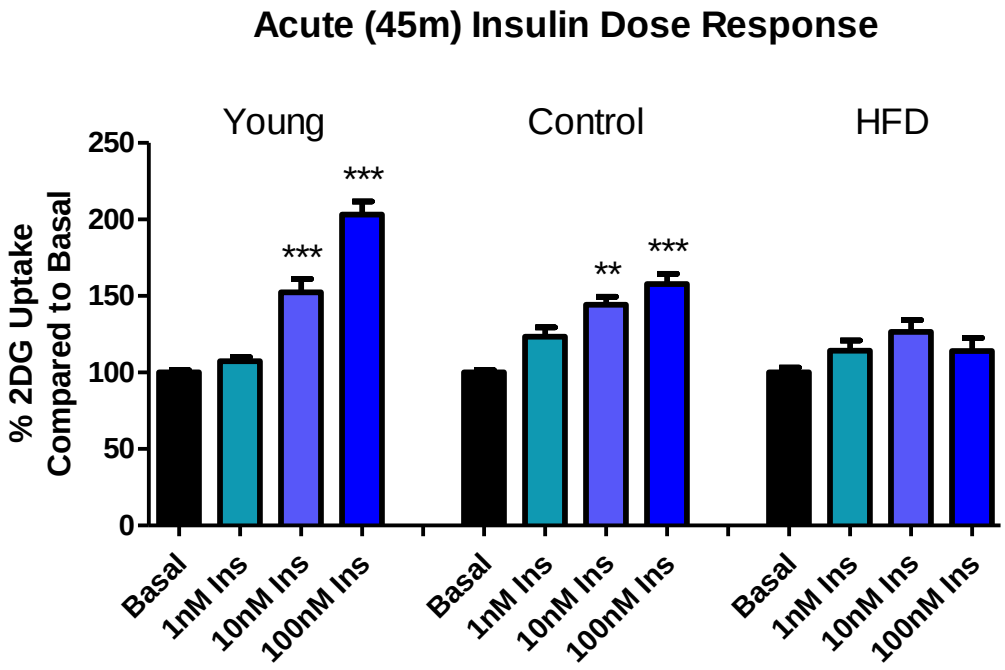

Figure 5.7 2DG uptake after 45 mins insulin dose response in cardiomyocytes from rat models (young control, diet control and high-fat diet rats**).** 2DG: 2-deoxy-D-[H^3]-glucose, HFD: high-fat, high-sucrose diet, Asp: Aspalathin, Ins: Insulin; n = 3-7 individual preparations; **p<0.01 (Control Basal vs. 10 nM Ins), ***p<0.001 (Young Basal vs. 10 nM Ins and 100 nM Ins; Control Basal vs. 100 nM Ins).

A 45 minute insulin dose response (**as described in Materials and Methods, Figure 3.4**) was performed on cardiomyocytes isolated from young, control and HFD rats (**Figure 5.7**). The young group had the strongest glucose uptake response to increasing concentrations of insulin, with 10 nM insulin having a significant increase of 45.4±8.4% (n=7; p<0.001) and 100nM insulin 97.1±14.3% (n=3; p<0.001) compared to basal (100.0±1.8; n=7). The control group also presented with an increase in glucose uptake response to increasing concentrations of insulin, with 10 nM inducing a significant increase in glucose uptake of 46.2±5.1% (n=5; p<0.01) and 100 nM insulin 56.0±6.2% (n=5; p<0.001) compared to basal 101.4±2.0% (n=5). The HFD group had no significant glucose uptake response to increasing concentrations of insulin.

2.4 Acute Aspalathin and Insulin Response in Cardiomyocytes from Young, Control and High-Fat, High-Sucrose Diet Rats

2.4.1 Normalized to Basal

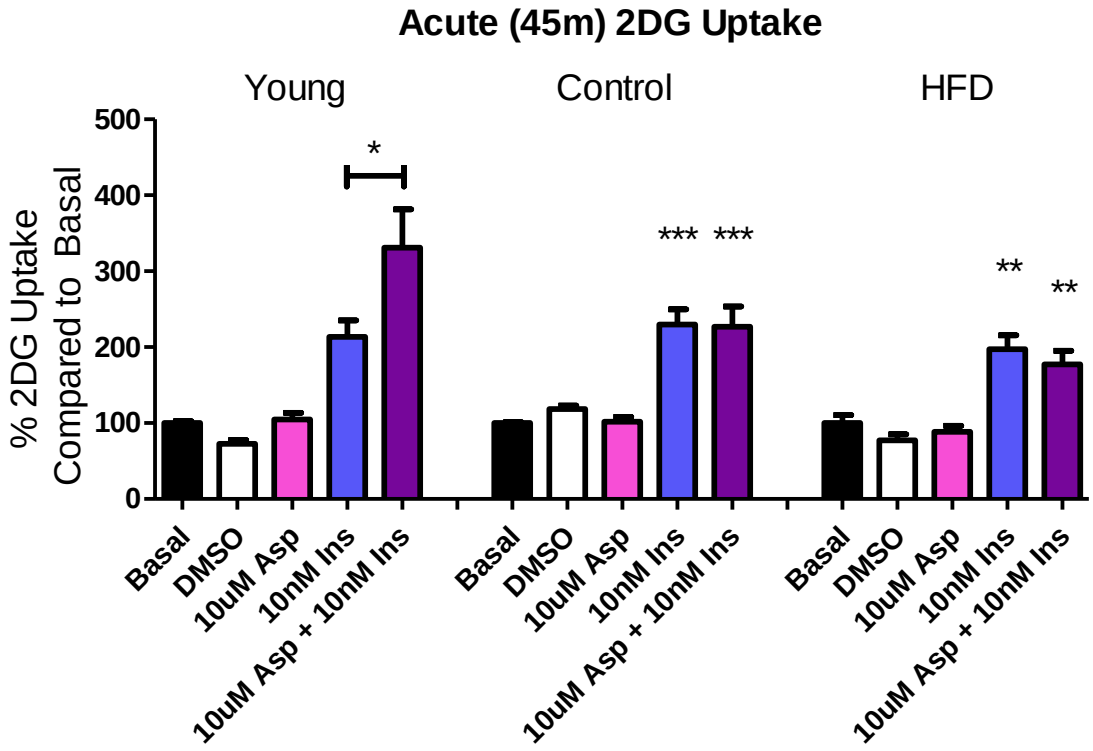

Figure 5.8 %2DG uptake after 45 mins aspalathin and insulin treatment in cardiomyocytes from rat models (young control, diet control and high-fat diet rats)**.** 2DG: 2-deoxy-D-[H^3]-glucose, HFD: high-fat, high-sucrose diet, Asp: Aspalathin, Ins: Insulin; n = 3 - 5 individual preparations; *p<0.05 (Young 10 nM Ins vs. 10 uM Asp + 10 nM Ins), **p<0.01 (HFD Basal vs. 10 nM Ins and 10 uM Asp + 10 nM Ins), ***p<0.001 (Control Basal vs. 10 nM Ins and 10 uM Asp + 10 nM Ins).

We performed a preliminary study on cardiomyocytes isolated from diet rats to investigate whether asapalthin can acutely induce glucose uptake in the presence or absence of insulin (**Figure 5.8)**. The addition of aspalathin to insulin was able to significantly increase glucose uptake in the young group (331.1±50.2%; n=5; p<0.05) compared to insulin alone (213.7±21.5%; n=5) (**Figure 5.6**), resulting in a 117% glucose uptake induction. Insulin significantly induced glucose uptake in both age-matched control groups (229.8±19.9%; n=3; p<0.001) and HFD groups (197.1±18.65%; n=3; p<0.01) compared to their respective basal levels (100.0±1.3; n=3 and 100.0±10.7; n=3). Co-treatment of insulin samples with aspalathin did not induce a further significant uptake in glucose for either of the aged or diet rats compared to insulin samples (226.9±26.5%; n=3; p<0.001 compared to control basal) (177.1±17.9%; n=3; p<0.01).

2.4.2 Absolute Amounts of Glucose Uptake

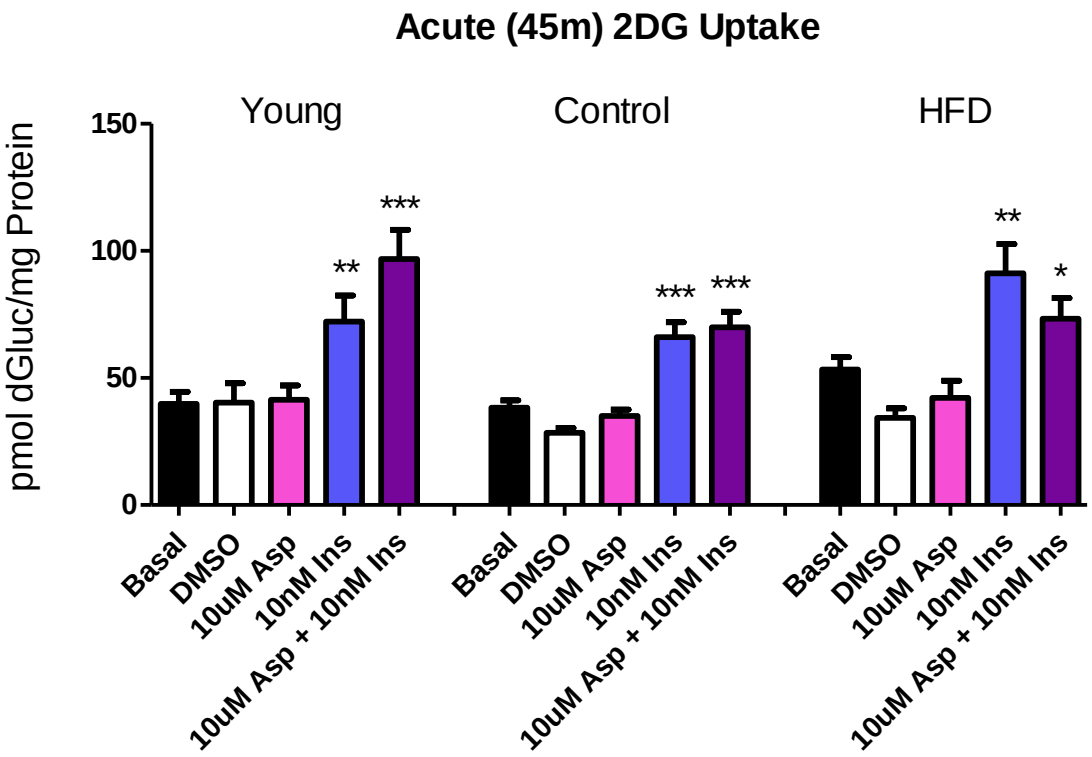

Figure 5.9 Absolute 2DG uptake after 45 mins aspalathin and insulin treatment in cardiomyocytes from rat models (young control, diet control and high-fat diet rats)**.** 2DG: 2-deoxy-D-[H^3]-glucose, HFD: high-fat, high-sucrose diet, Asp: Aspalathin, Ins: Insulin; n = 3 - 5 individual preparations; *p<0.05 (HFD Basal vs. 10 uM Asp + 10 nM Ins), **p<0.01 (Young Basal vs. 10 nM Ins; HFD Basal vs. 10 nM Ins), ***p<0.001 (Young Basal vs. 10 uM Asp + 10 nM Ins; Control Basal vs. 10 nM Ins and 10 uM Asp + 10 nM Ins).

The results from the previous experiment (**Figure 5.8**) was recalculated to the absolute concentrations of 2DG uptake, normalized to the amount of protein of each sample (**Figure 5.9**). At 45 mins treatment, 10 nM insulin independently, as well as in combination with 10 uM aspalathin significantly increased glucose uptake in cardiomycoytes isolated from all 3 rat models compared to basal (in pmol 2DG/mg protein): young rats (72.17±10.26; n=10; p<0.01 and 96.84±11.51; n=5; p<0.001 vs 39.75±4.81; n=11), control rats (66.08±5.80; n=6; p<0.001 and 69.96±6.10; n=6; p<0.001 vs 38.29±2.92; n=6) and HFD rats (91.19±11.53; n=6; p<0.01 and 73.27±8.15; n=4; p<0.05 vs 53.37±4.81; n=6). There was no significant difference in glucose uptake between the 3 different animal models in response to any treatment.

2.5 Extended Aspalathin AND Insulin Response in Cardiomyocytes from Young, Control and High-Fat, High-Sucrose Diet Rats

2.5.1 Normalized to Basal

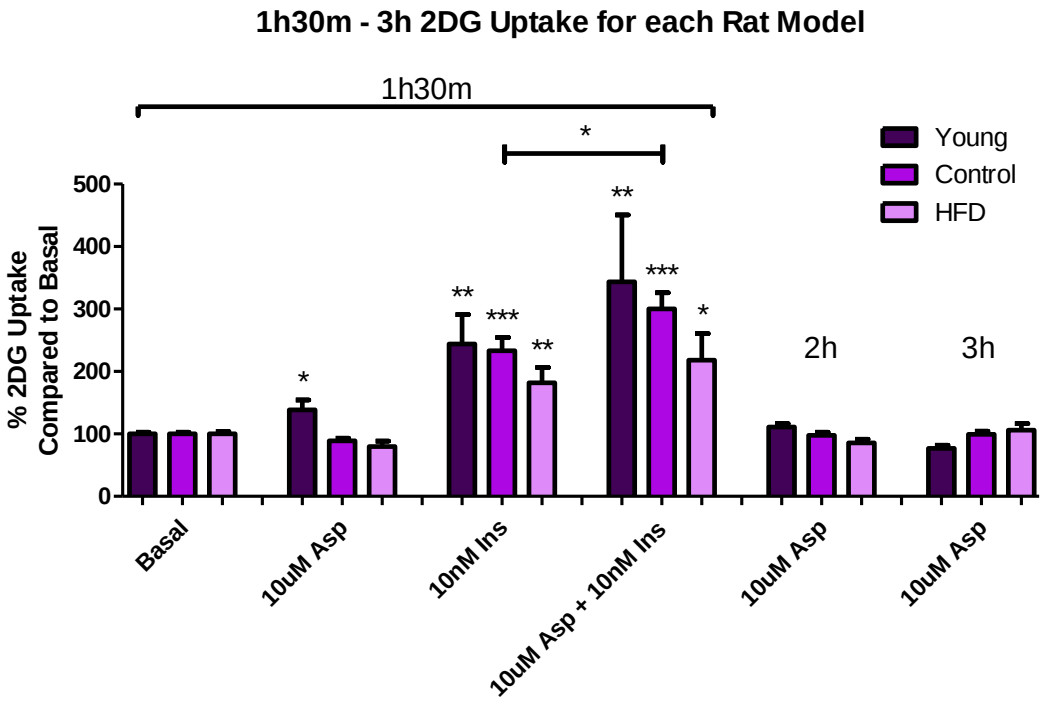

Figure 5.10 %2DG uptake after 1-3h of treatment in cardiomyocytes from rat models (young control, diet control and high-fat diet rats); 2DG: 2-deoxy-D-[H^3]-glucose, HFD: high-fat, high-sucrose diet, Asp: Aspalathin, Ins: Insulin; n = 3 - 5 individual preparations; *p<0.05 (Young Basal vs. 10 uM Asp at 1h30m; Control 10 nM Ins vs. 10 uM Asp + 10 nM Ins at 1h30m; HFD Basal vs 10 uM Asp + 10 nM Ins at 1h30m), **p<0.01 (Young Basal vs. 10 nM Ins and 10 uM Asp + 10 nM Ins at 1h30m; HFD Basal vs. 10 nM Ins at 1h30m), ***p<0.001 (Control Basal vs. 10 nM Ins and 10 uM Asp + 10 nM Ins at 1h30m)

Extending the activation time up to 3 hours, we repeated the aspalathin and insulin stimulation in cardiomyocytes isolated from young, control and HFD rats (**Figure 5.10, Figure 5.11**). **Figures 5.8** and **5.9** illustrate that 45 minutes of aspalathin treatment was not sufficient to induce glucose uptake in isolated cardiomyocytes. However, at 1 and a half hours of treatment, 10 μM aspalathin, independent of insulin, significantly increased glucose uptake in cardiomycoytes isolated from young rats (138.3±15.9%; n=4; p<0.05) compared to basal (100.0±2.7%; n=4), resulting in a 38% increase in glucose uptake. No further increase in glucose uptake by sole action of aspalathin was observed for either of the rat models, even when the experiment was allowed to run for 3 hours. Aspalathin also induced glucose uptake in conjunction with insulin in the aged control group (300.2±25.7%; n=5; p<0.05) compared to insulin (226.1±21.8%; n=5). There was no signifcant difference in glucose uptake when co-treating insulin with aspalathin in young rats (343.4±107.2%;

n=3; p=0.3388) compared to insulin (244.0±46.9%; n=4), as well as in HFD rats (218.2±42.50%; n=4; p=0.4719) compared to insulin (181.8±24.75%; n=4). Consistently, younger rats had a more robust response to insulin, followed by the aged-matched control group, and lastly the high-fat, high-sucrose diet group.

2.5.2 Absolute Amounts of Glucose Uptake

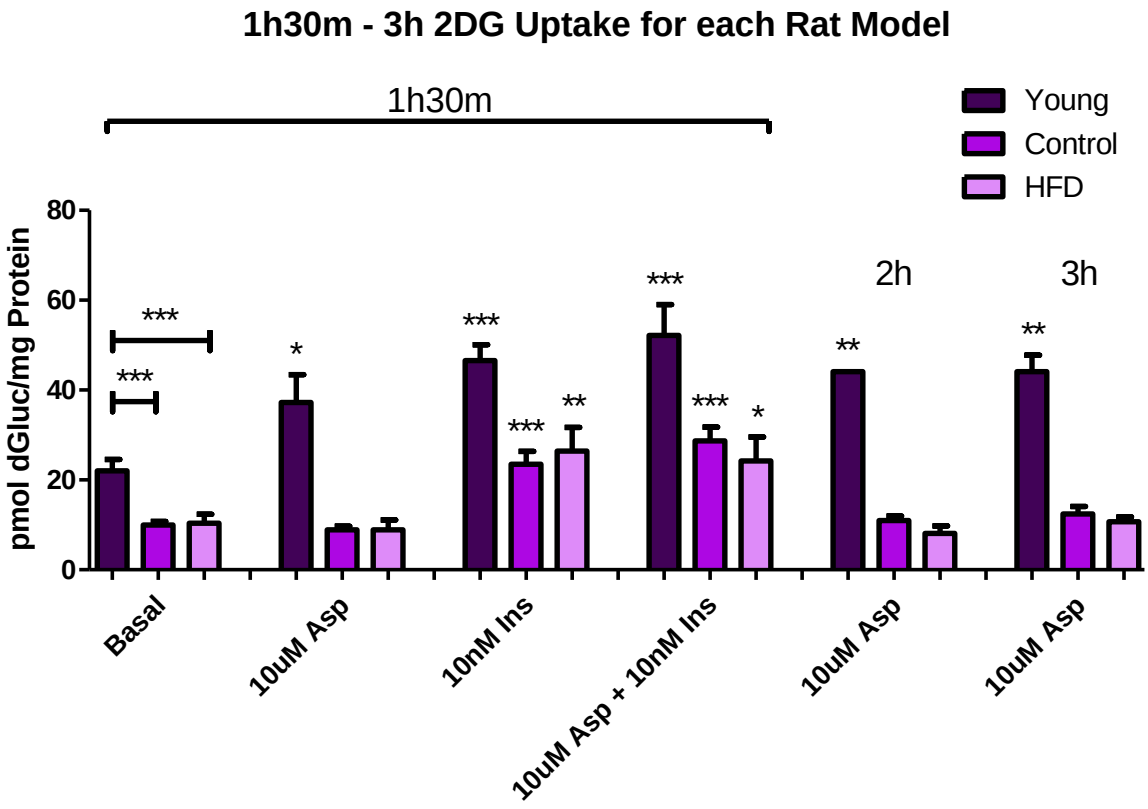

Figure 5.11 Absolute 2DG uptake after 1-3h of treatment in cardiomyocytes from rat models (young control, diet control and high-fat diet rats); 2DG: 2-deoxy-D-[H^3]-glucose, HFD: high-fat, high-sucrose diet, Asp: Aspalathin, Ins: Insulin; n = 3 - 6 individual preparations; *p<0.05 (Young Basal vs 10 uM Asp at 1h30m; Control Basal vs 10 uM Asp + 10 nM Ins; HFD Basal vs 10 uM Asp + 10 nM Ins), **p<0.01 (Young Basal vs 10 uM Asp at 2h and 3h; HFD Basal vs 10 nM Ins), ***p<0.001 (Young Basal vs Control Basal and HFD Basal, 10 nM Ins and 10 uM Asp + 10 nM Ins; Control Basal vs 10 nM Ins and 10 uM Asp + 10 nM Ins)

The results from the previous experiment (**Figure 5.10**) were recalculated to the absolute concentrations of 2DG uptake, normalized to the amount of protein of each sample (**Figure 5.11**). The young rats had a significantly higher basal glucose uptake at 1 and a half hours compared to the control and HFD rats (22.0±2.5 pmol dGluc/mg protein; n=4 vs. 10.0±0.8 pmol dGluc/mg protein; n=6 and 10.3±2.0 pmol dGluc/mg protein; n=4; p<0.001). At 1 and a half hours of treatment, 10 μM aspalathin, 10 nM insulin and a combination of both all significantly increased

glucose uptake in cardiomycoytes isolated from young rats (37.2±3.6 pmol dGluc/mg protein; n=3; p<0.05, 46.6±3.6 pmol dGluc/mg protein; n=3; p<0.001, and 52.2±6.8 pmol dGluc/mg protein; n=3; p<0.001 vs basal: 22.0±2.5 pmol dGluc/mg protein; n=4). Furthermore, 10 uM aspalathin treatment in young rats significantly increased glucose uptake for both 2 hours and 3 hours (44.1±0.01 pmol dGluc/mg protein; n=2; p<0.01 and 44.1±3.7 pmol dGluc/mg protein; n=2; p<0.01) compared to basal. In aged control rat cardiomyocytes, treatment with 10 nM insulin and a combination of 10 uM aspalathin and 10 nM insulin for 1 and half hours both significantly increased glucose uptake compared to basal (23.5±2.9 pmol dGluc/mg protein; n=6; p<0.001 and 28.7±3.0 pmol dGluc/mg protein; n=5; p<0.001 vs 10.0±0.8 pmol dGluc/mg protein; n=6). In HFD rat cardiomyocytes, treatment with 10 nM insulin and a combination of 10 uM aspalathin and 10 nM insulin for 1 and a half hours both significantly increased glucose uptake compared to basal (26.4± 5.3 pmol dGluc/mg protein; n=3; p<0.01 and 24.2±5.3 pmol dGluc/mg protein; n=4; p<0.05 vs 10.3±2.0 pmol dGluc/mg protein; n=4). No further increase in glucose uptake by aspalathin was observed for either older controls or HFD rats when the experiment was extended to 3 hours. Consistently, younger rats had the most robust glucose uptake response with or without treatments, whereas aged-rats had similar responses to each other, but weak in comparison with the young rats.

CHAPTER 6

RESULTS: ASPALATHIN AND DIFFERENTIATED H9C2 CELLS

1. CELL VIABILITY ASSAYS

1.1 METABOLIC ACTIVITY OF DIFFERENTIATED H9C2 CELLS AFTER TREATMENT

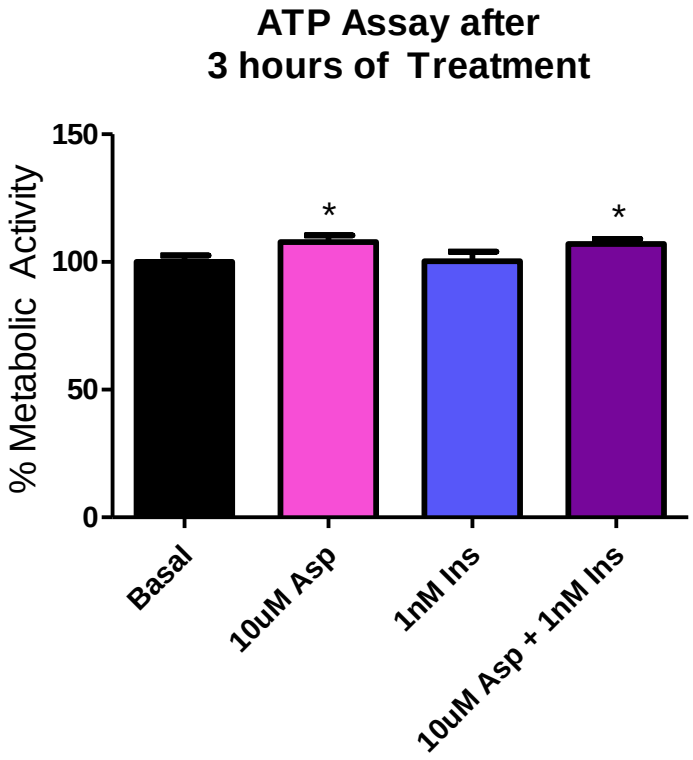

Figure 6.1 Metabolic Activity (ATP Assay) after 3h of treatment. Asp: Aspalathin, Ins: Insulin; n = 3 individual culture preparations; *p<0.05 (Basal vs. 10 uM Asp and 10 uM Asp + 1 nM Ins)

The metabolic activity of differentiated H9C2 cells were determined after being pretreated for 3 hours with 10 uM aspalathin, or 1 nM insulin for the last 15 mins or a combination of both (**Figure 6.1**). Treating differentiated H9C2 cells with 10 μM aspalathin for 3 hours, as well as 3 hour 10 μM aspalathin treatment with 15 mins 1 nM insulin co-treatment significanly increased metabolic activity (107.8±2.6%, p<0.05 and 107.0±2.0%, p<0.05), respectively by 7.8% and 7.0% compared to basal (100.1±2.5%). 1 nM insulin treatment for 15 mins did not significanly increase metabolic activity (100.4±3.7%) compared to basal.

1.2 MEMBRANE INTEGRITY OF DIFFERENTIATED H9C2 CELLS AFTER TREATMENT

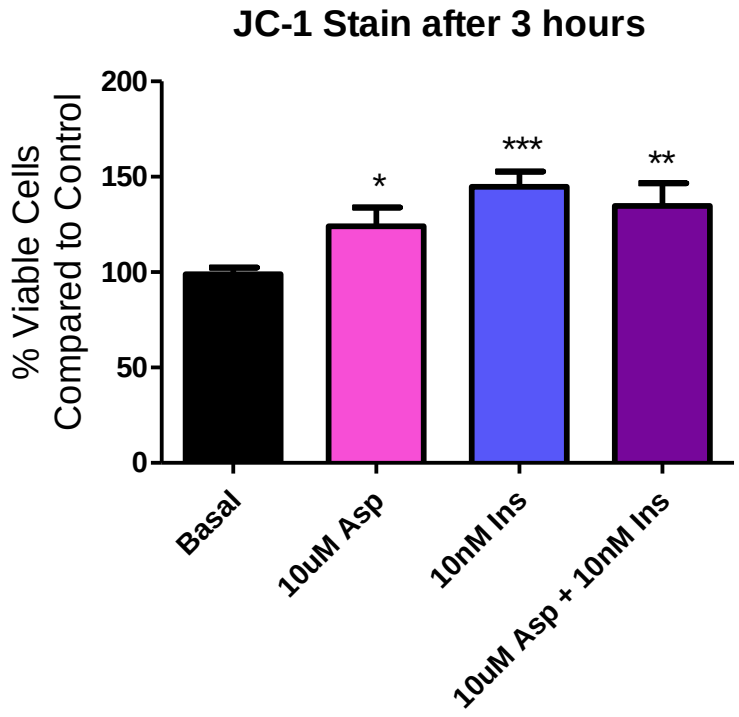

Figure 6.2 JC-1 Staining assay after 3h of treatment. Asp: Aspalathin, Ins: Insulin; n = 3 individual culture preparations; *p<0.05 (Basal vs. 10 uM Asp), **p<0.01 (Basal vs 10 uM Asp + 10 nM Insulin), ***p<0.001 (Basal vs 10 nM Ins)

In order to determine the cell viability of differentiated H9C2 cells, cells were treated for 3 hours with or without 10 uM aspalathin, 10 nM insulin or a combination of both, after which the membrane depolarization was determined using JC-1 staining. Unfortunately, fluorescence was only qauntified at 596 nm (**Figure 6.2**), an indication of the effective viable portion of cells, whereas it is orthodox to quantify the green fluorescence at 520 nm as well, indicative of the non-viable portion of cells. The ratio of viable to non-viable would then be calculated as an overall indication of viability for the treatment groups. **Figure 6.3** shows the JC-1 staining fluorescence of the respective treatment groups, and it is immediately evident that the viable portion of cells (yellow/red fluorescence) is significantly greater than the non-viable portion of cells (green fluorescence) for each of the treatment groups. We therefore concluded that the treatments were not toxic to the differentiated H9C2 cells.

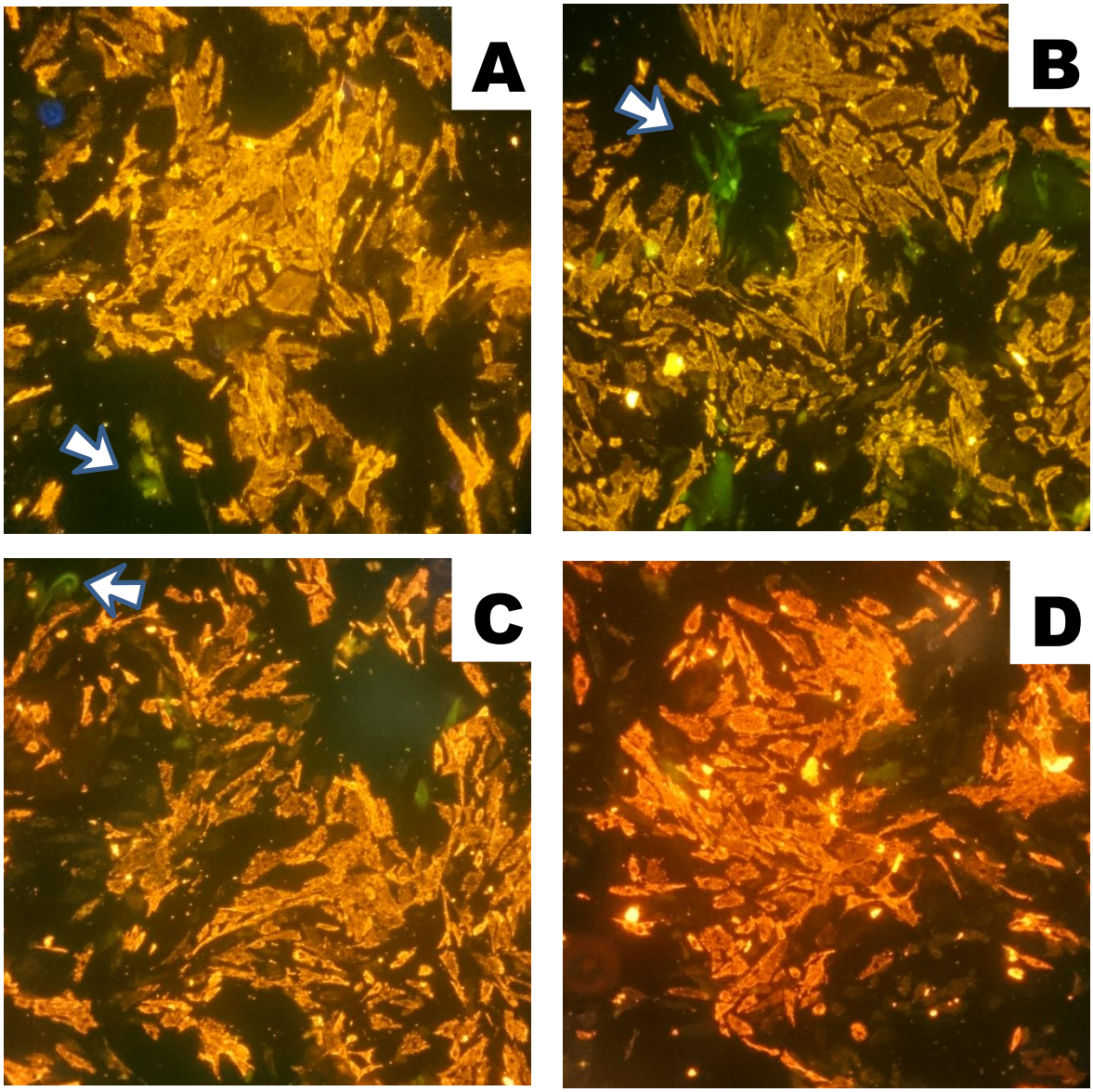

Figure 6.3 JC-1 Staining assay of Differentiated H9C2 cells after 3h of treatment. Image magnification at 40x. Panels (**A**) represent control cells without treatment, (**B**) 10 uM aspalathin treatment for 3 hours, (**C**) 1 0nM insulin treatment for the last 15 mins of 3h incubation, and (**D**) 10 uM aspalathin for 3 hours, together with 10 nM insulin for the last 15 mins of 3h incubation. The fluorescent yellow/red cells indicate the viable cells, while the green stains, indicated by the arrow in (**B**), is a measure of non-viable cells.

2. GLUCOSE UPTAKE ASSAY IN DIFFERENTIATED H9C2 CELLS

2.1 DELAYED ASPALATHIN AND INSULIN RESPONSE IN DIFFERENTIATED H9C2 CELLS

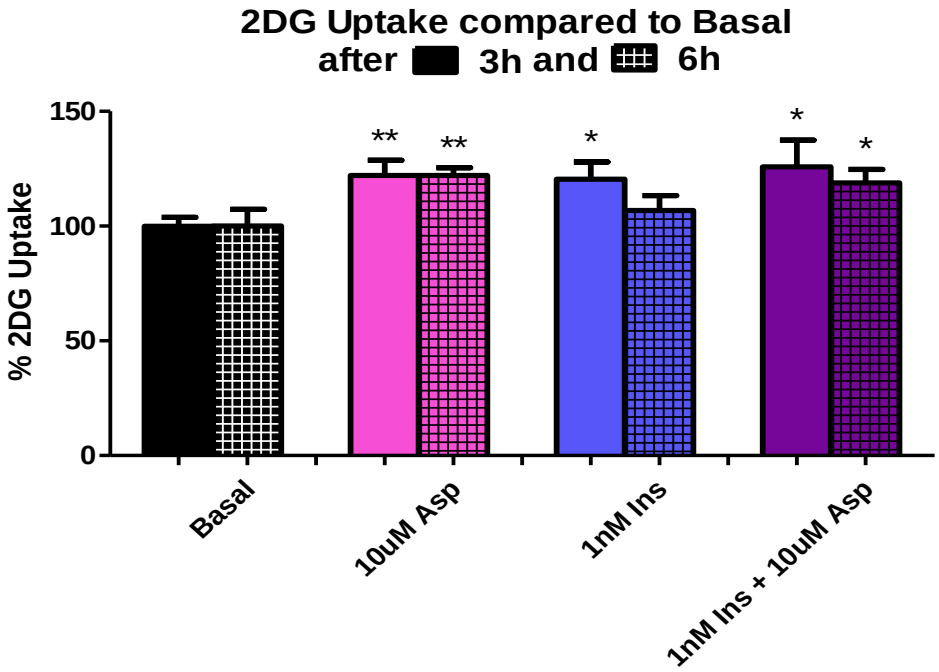

Figure 6.4 2DG uptake in differentiated H9C2 cells after 3h and 6h of treatment. 2DG: 2-deoxyglucose-D-[H^3]-glucose, Asp: Aspalathin, Ins: Insulin; n = 4 individual culture preparations; *p<0.05 (Basal vs. 1 nM Ins and 1 nM Ins + 10 uM Asp at 3h, and Basal vs. 1 nM Ins + 10 uM Asp at 6h), **p<0.01 (Basal vs. 10 uM Asp at 3h and 6h)

Differentiated H9C2 cells were assayed for glucose uptake in the presence of a 5.5 mM glucose solution (**Figure 6.4**). After 3 and 6 hours respectively of aspalathin treatment, with or without insulin for the last 15 mins of the protocol, glucose uptake was initiated by addition of 2DG for 15 mins. 10 μM aspalathin was able to significantly increase glucose uptake after both 3 and 6 hours of treatment (122.1±6.6%, p<0.01 and 122.0±3.3%, p<0.01) compared to basal (99.9±3.9% and 100.0±7.3% respectively), equating to an average of increase in glucose uptake of 22%. 1 nM insulin was also able to significantly increase glucose uptake when added 15 mins prior to the 3 hours timepoint (120.5±7.5%, p<0.05) compared to basal, however the same effect could not be confirmed when 1 nM insulin was added 15 mins before the 6 hour time point (109.9±6.2%, p=0.3120). 2 hours 45 mins of treatment with 10 uM aspalathin, followed by the addition of 1 nM insulin also prompted a significant increase in glucose uptake (125.8±11.7%, p<0.05), equating to a 25.8% increase. Likewise, after 5 hours 45 mins of treatment with 10 uM aspalathin, followed by the addition of 1 nM insulin, glucose uptake was significantly increased (122.9±4.9%, p<0.05) compared to basal, which was similar to 10 uM aspalathin independently.

CHAPTER 7

RESULTS: THE MECHANISM OF ACTION OF ASPALATHIN

1. INSULIN-DEPENDENT GLUCOSE UPTAKE INHIBITION

1.1 ACUTE ASPALATHIN WITH WORTMANNIN IN ISOLATED CARDIOMYOCYTES FROM YOUNG RATS

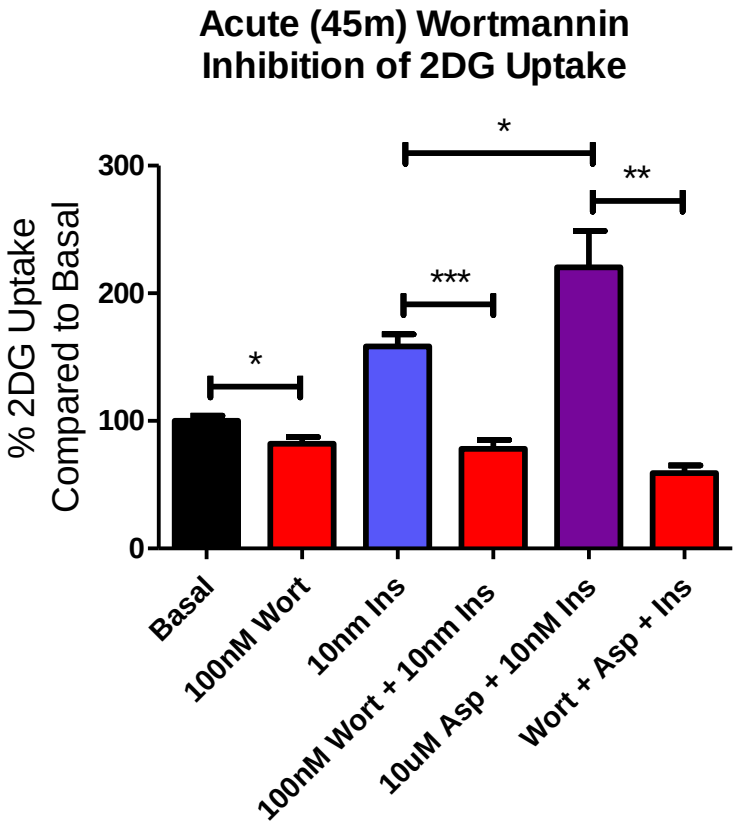

Figure 7.1 2DG uptake after inhibition of PI3K with wortmannin and stimulation with aspalathin and insulin in cardiomyocytes (from young rats)**.** 2DG: 2-deoxy-D-[H^3]-glucose, Wort: Wortmannin, Asp: Aspalathin, Ins: Insulin; n = 3 individual preparations; *p<0.05 (Basal vs. 100 nM Wort; 10 nM Ins vs 10 uM Asp + 10 nM Ins), **p<0.01 (10 uM Asp + 10 nM Ins vs 100 nM Wort + 10 uM Asp + 10 nM Ins), ***p<0.001 (10 nM Ins vs 100 nM Wort + 10 nM Ins)

To investigate the mechanism whereby aspalathin may induce glucose uptake, wortmannin was added to isolated cardiomyocytes from young rats as a selective inhibitor of PI3K, thus inhibiting the insulin-dependent pathway of glucose uptake (**Figure 7.1**). 100 nM wortmannin was able to significantly decrease basal glucose uptake (82.15±5.1% vs 100.0±4.1%, n=3; p<0.05). Co-treating 10 nM insulin with 100 nM wortmannin significantly decreased glucose uptake (78.1±7.0%; n=3; p<0.001) compared to 10 nM insulin alone (158.3±9.4%; n=3). Furthermore, co-stimulating 10 nM insulin with 10uM aspalathin again (Refer **Figure 5.6; Figure 5.8; Figure 5.9**) significantly

increased glucose uptake in isolated young rat heart cells (220.5±28.4%; n=3; p<0.05) compared to 10 nM insulin, while addition of 100 nM wortmannin completely inhibited all of the glucose uptake potential of the combination of aspalathin and insulin (59.0±6.2%; n=2; p<0.01).

1.2 Extended Aspalathin with Wortmannin In Isolated Cardiomyocytes from Control and HFD Rats

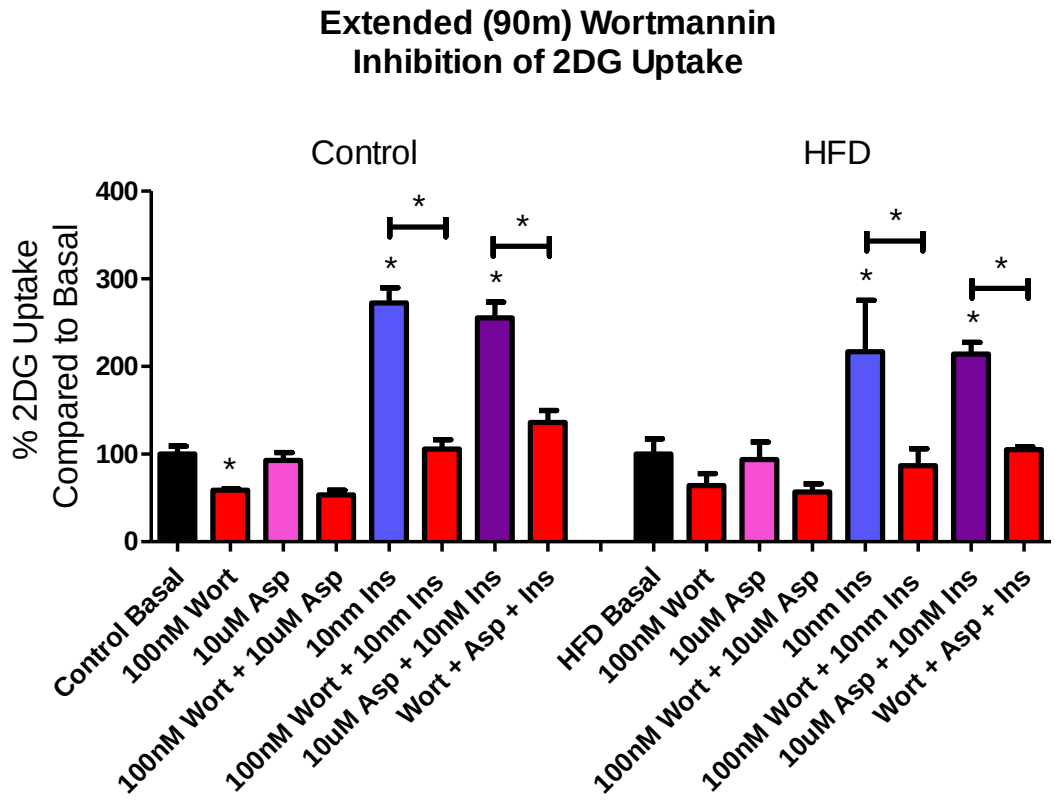

Figure 7.2 2DG uptake after inhibition of PI3K with wortmannin and stimulation with aspalathin and insulin in cardiomyocytes (from control and HFD rats)**.** HFD: High-fat, high-sucrose diet, 2DG: 2-deoxy-D-[H^3]-glucose, Wort: Wortmannin, Asp: Aspalathin, Ins: Insulin; n = 2 individual preparations; *p<0.05 (Control Basal vs. 100 nM Wort, 10 nM Ins and 10 uM Asp + 10 nM Ins; Control 10 nM Ins vs 100nM Wort + 10 nM Ins; Control 10 uM Asp + 10 nM Ins vs 100 nM Wort + 10 uM Asp + 10 nM Ins; HFD Basal vs. 10 nM Ins and 10 uM Asp + 10 nM Ins; HFD 10nM Ins vs 100nM Wort + 10nM Ins; HFD 10uM Asp + 10nM Ins vs 100nM Wort + 10 uM Asp + 10 nM Ins).

To investigate the mechanism whereby aspalathin may induce glucose uptake in aged rats, wortmannin was added to isolated cardiomyocytes from control and HFD rats as a selective inhibitor of PI3K, thus inhibiting the insulin-dependent pathway of glucose uptake (**Figure 7.2**). 100nM wortmannin was also able to significantly decrease basal glucose uptake in control rats (58.7±1.4% vs 100.0±9.1%; n=2; p<0.05). Co-treating 10 nM insulin with 100 nM wortmannin significantly decreased glucose uptake in both controls (106.0±10.6 vs 272.4±17.4; n=2; p<0.05)

and HFD rats (86.8±19.4 vs 216.8±58.6; n=2; p<0.05). Furthermore, inhibiting PI3K signaling with 100 nM wortmannin, completely inhibited the additive effects of 10 nM insulin and 10 uM aspalathin on glucose uptake for control rats (136.2±13.6 vs 255.6±18.0; n=2; p<0.05).

2. Protein Expression After Acute Aspalathin Treatment in Young Rats

2.1 Myocardial PKB Content and Activation

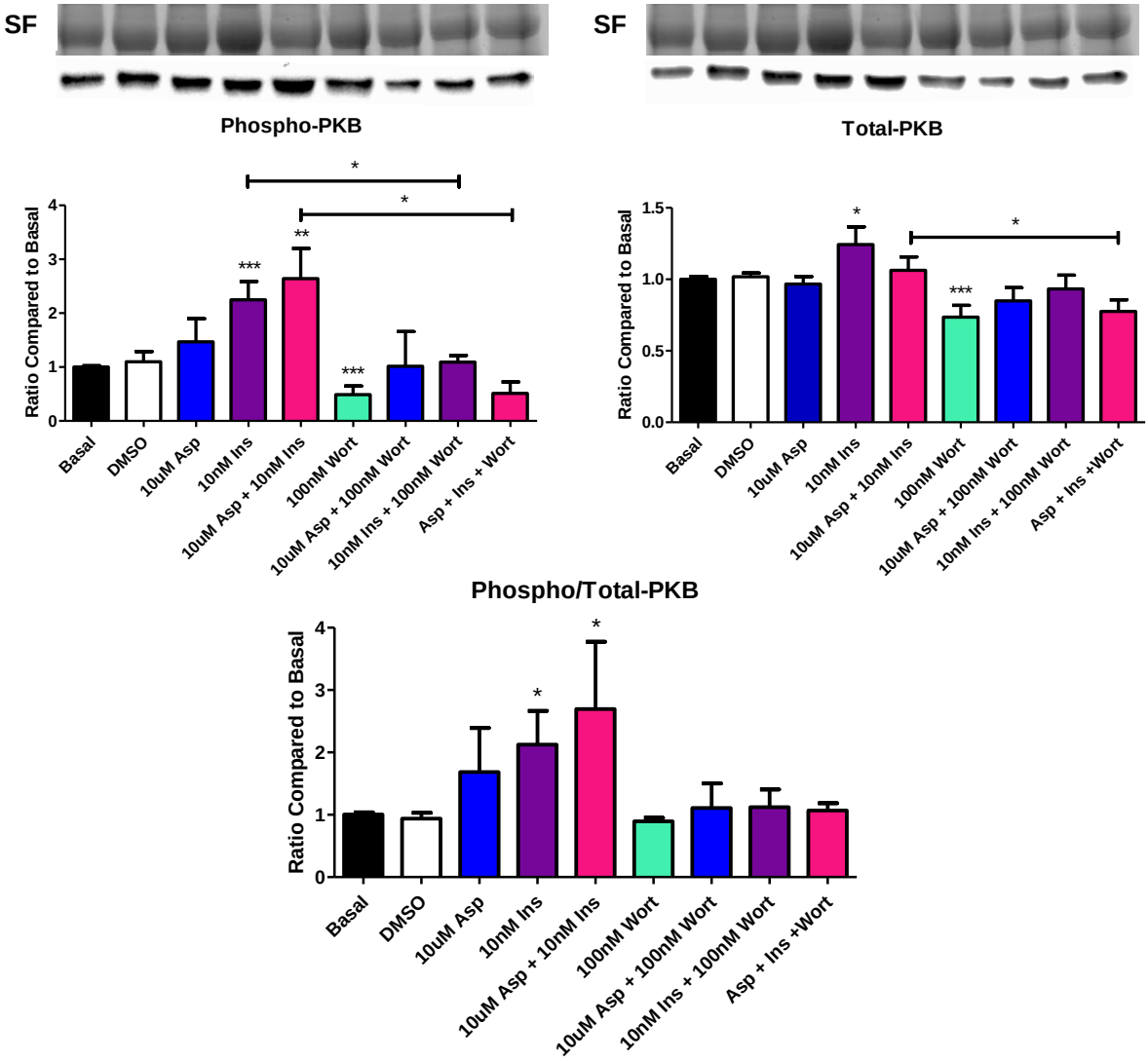

Figure 7.3 PKB expression and activation in isolated cardiomyocytes from young rats after 15 minutes in vitro stimulation. SF: Stain-free Technology for Normalization, Asp: Aspalathin, Ins: Insulin, Wort: Wortmannin. **A)** Phospho-PKB (Ser^{473}) content. n = 4 individual preparations; *p<0.05 (10 nM Ins vs 10 nM Ins + 100 nM Wort; 10 uM Asp + 10 nM Ins vs 10 uM Asp + 10 nM Ins + 100 nM Wort), **p<0.01 (Basal vs. 10 uM Asp + 10 nM Ins), ***p<0.001 (Basal vs. 10 nM Ins and 100 nM Wort). **B)** Total-PKB content.; n = 6 individual preparations; *p<0.05 (Basal vs. 10 nM Ins; 10 uM Asp + 10 nM Ins vs. 10 uM Asp + 10 nM Ins + 100 nM Wort), ***p<0.001 (Basal vs. 100 nM Wort). **C)** Phospho- to Total-PKB. n = 3 individual preparations; *p<0.05 (Basal vs. 10 nM Ins and 10 uM Asp + 10 nM Ins).

Lysates were prepared from cardiomyoyctes isolated from young rats acutely (15 mins) treated with 0.1% DMSO, 10 uM aspalathin, 10 nM insulin and 100 nM wortmannin, and assayed for the relative total PKB expressed and PKB activation as measured by Ser^{473} phosphorylation, as a measure of the insulin-dependent mechanism of signaling (**Figure 7.3**). Normalization was done for each sample by using the Stain-Free™ technology (Bio-Rad Laboratories Inc., USA) embedded in the composition of gels, allowing for visualization of the total protein for each lane. Phosphorylated (activated) PKB was increased in samples treated with insulin (2.25±0.3 fold increase; n=4; $p<0.001$), while insulin in combination with aspalathin had a similar increase (2.64±0.6 fold increase; n=3; $p<0.01$) compared to basal (1.00±0.02; n=4). Wortmannin completely inhibited the activation of basal PKB levels (0.49±0.19 fold decrease; n=4; $p<0.001$). Addition of wortmannin before insulin resulted in a 2-fold decrease (1.04±0.10 compared to 2.25±0.34; n=4; $p<0.05$), whereas addition of wortmannin before aspalathin and insulin also completely inhibited PKB activation resulting in a 5-fold decrease (0.51±0.21 compared to 2.64±0.6; n=3; $p<0.05$). Furthermore, total (expressed) PKB was only upregulated in insulin stimulated samples (1.19±0.12; n=4; $p<0.05$) compared to basal (1.00±0.02; n=4) and not in samples co-stimulated with aspalathin and insulin. Wortmannin decreased the expression of PKB (0.74±0.08; n=4; $p<0.001$) compared to basal, while pretreating insulin plus aspalathin with wortmannin also significantly decreased PKB expression compared to insulin plus aspalathin (0.78± 0.08 compared to 1.06±0.09; n=4; $p<0.05$). The phospho to total ratio of PKB, a determinant of how much of the total PKB is activated, showed significant increases on stimulation with insulin (2.12±0.54 fold increase; n=4; $p<0.05$) and a similar increase for insulin in combination with aspalathin (2.70±1.08; n=3; $p<0.05$) compared to basal (1.00±0.03; n=4). DMSO did not influence the total, phosphorylated or total-to-phosphorylated ratio of PKB compared to basal.

2.2 MYOCARDIAL AMPK CONTENT AND ACTIVITY

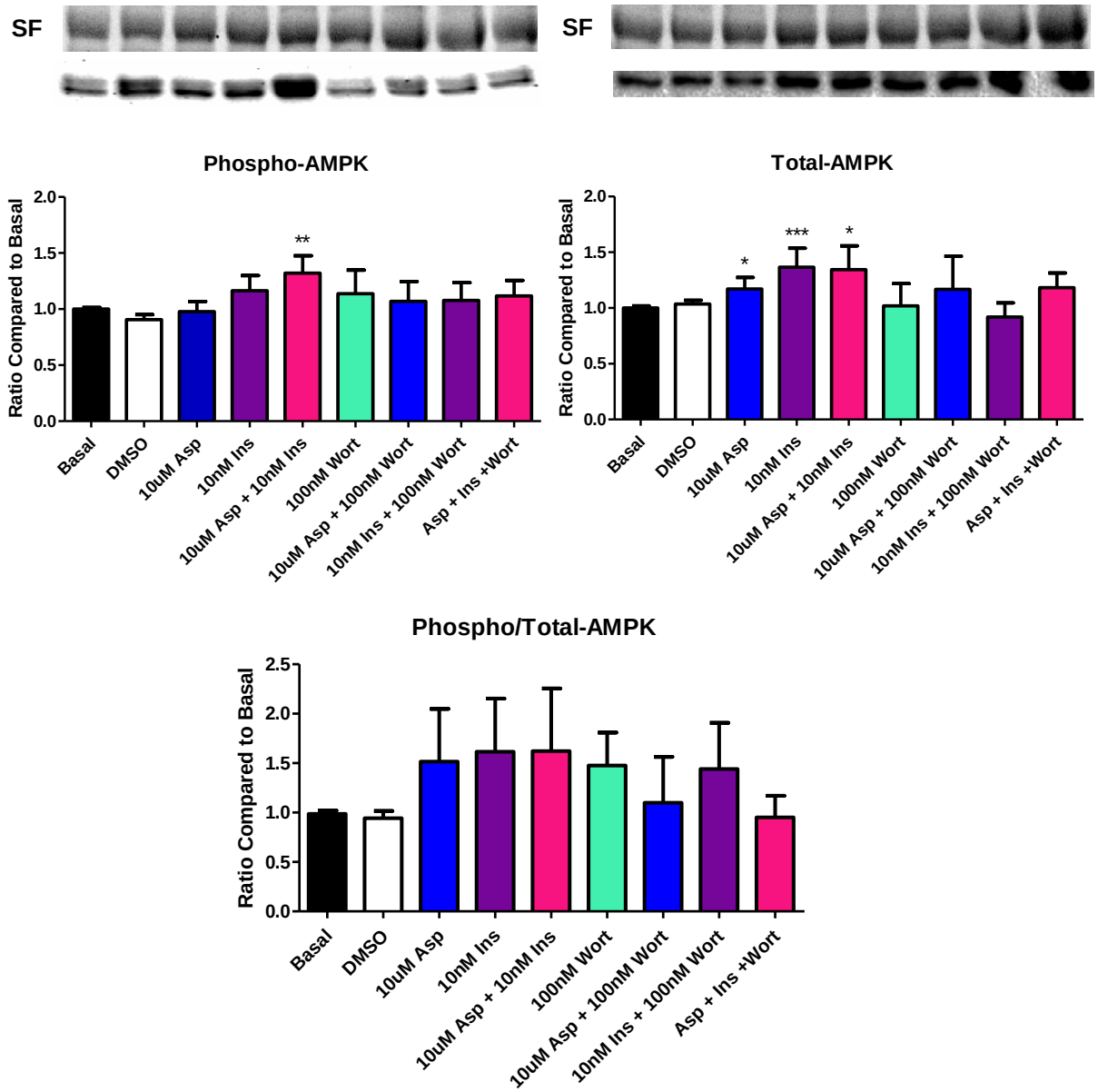

Figure 7.4 AMPK expression and activation in isolated cardiomyocytes from young rats after 15 minutes in vitro stimulation. SF: Stain-free Technology for Normalization, Asp: Aspalathin, Ins: Insulin, Wort: Wortmannin. **A)** Phospho-AMPK content. n = 6 individual preparations; **p<0.01 (Basal vs. 10 uM Asp + 10 nM Ins). **B)** Total-AMPK content; n = 5 individual preparations; *p<0.05 (Basal vs. 10 uM Asp and 10 uM Asp + 10nM Ins), ***p<0.001 (Basal vs. 10 nM Ins). **C)** Phospho- to Total-AMPK Ratio. n = 5 individual preparations

Lysates were prepared from cardiomyoyctes isolated from young rats acutely (15 mins) treated with 0.1% DMSO, 10 uM aspalathin, 10 nM insulin and 100 nM wortmannin, and assayed for the relative total AMPK expressed and AMPK activated, as a measure of the insulin-independent mechanism of aspalathin (**Figure 7.4**). Normalization was done for each sample by using the Stain-Free™ technology (Bio-Rad Laboratories Inc., USA) embedded in the composition of gels,

allowing for visualization of the total protein for each lane. Phosphorylated (activated) AMPK was significantly increased in samples treated with 10 nM insulin plus 10 uM aspalathin (1.32±0.15 fold increase; n=3; p<0.01) compared to basal (1.00±0.01; n=3), whereas neither insulin nor aspalathin had a significant effect on their own (0.98±0.09; n=3; p=0.7321 and 1.16±0.14; n=3; p=0.1040). Furthermore, the total (expressed) AMPK was upregulated in response to aspalathin (1.17±0.10 fold increase; n=4; p<0.05) and insulin (1.37±0.17 fold increase; n=3; p<0.001) while insulin and aspalathin co-treatment had a similiar response to insulin alone (1.34±0.21 fold increase; n=4; p<0.05) compared to basal. There were no significant differences in the phospho to total ratio of AMPK, a determinant of how much of the total AMPK is activated, between any of the treatment groups. Furthermore, as expected, wortmannin did not induce any significant differences in AMPK expression or activation, since wortmannin only selectively inhibits PI3K, a signaling pathway that is not essential for AMPK expression and activation.

3. Protein Expression after extended Aspalathin Treatment in Young, control and HFD Rats

3.1 Myocardial PKB Content and Activity

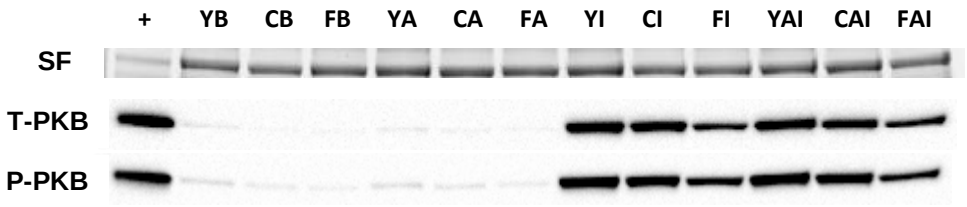

Figure 7.5 Treating cardiomyocytes with 10 nM insulin for 1 h 30 mins, leads to overexpression and activation of PKB compared to baseline. SF: Stain-free technology for normalization, + Positive Control, Y: Young, C: Control, F: High-fat, high-sucrose diet, B: Basal, A: 10uM Aspalathin, I: 10nM Insulin, AI: 10uM Aspalathin + 10nM Insulin.

The treatment time of samples was extended by an additional 1 h and 15 mins and lysates prepared for immunoblot analaysis. **Figure 7.5** shows that PKB expression and activation differered significantly between samples treated with or without insulin for 1 and a half hours. As a result, samples had to be run separately to investigate the mechanism of aspalathin. The membranes were overexposed and analysed separately in **Figure 7.6** and **Figure 7.7**.

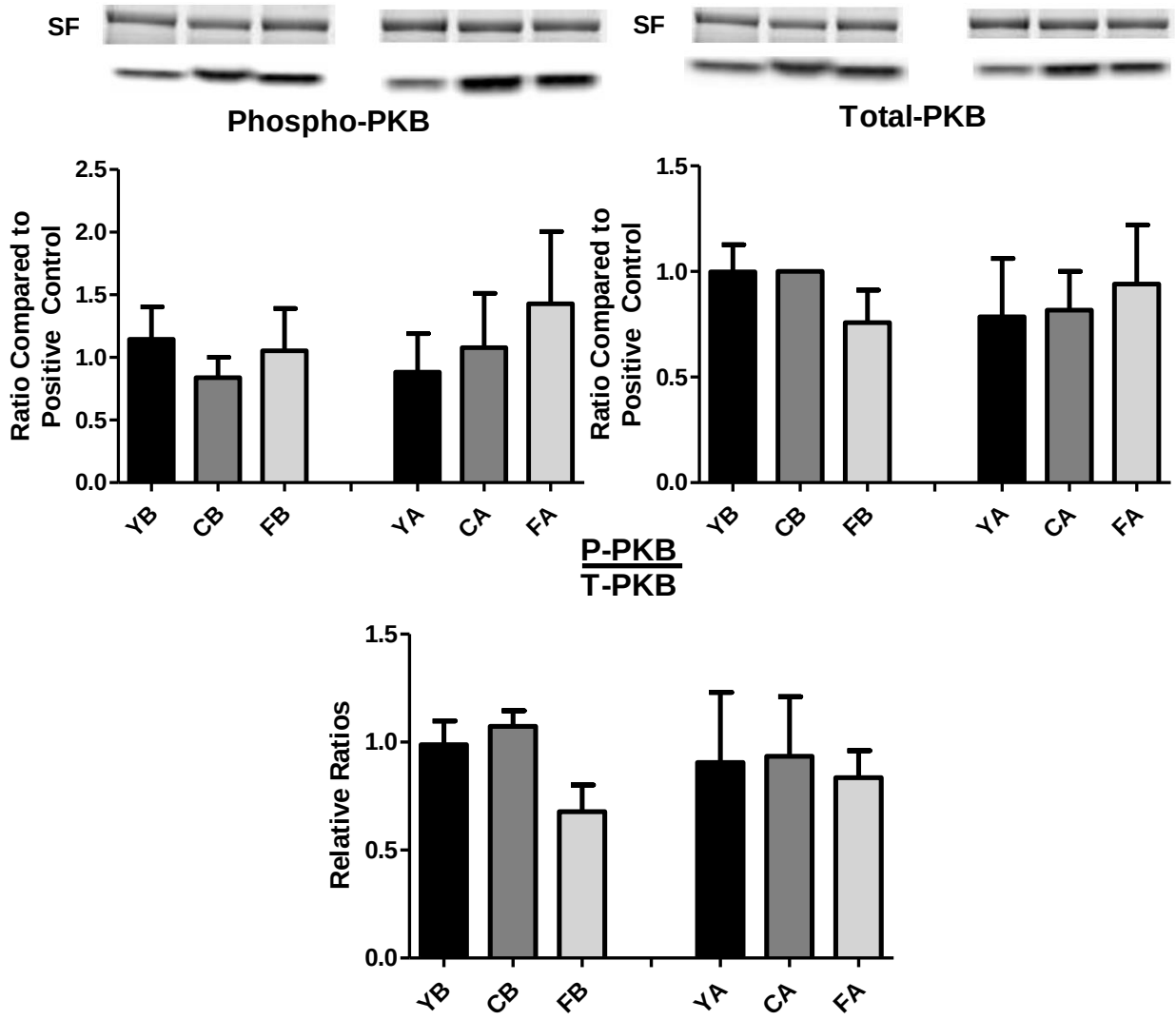

Figure 7.6 PKB expression and activation in isolated cardiomyocytes from young, control and HFD rats after 1h 30 mins in vitro stimulation with aspalathin. SF: Stain-free Technology for Normalization, Y: Young, C: Control, F: High-fat, high-sucrose diet, B: Basal, A: 10 uM Aspalathin. **A)** Phospho-PKB content. **B)** Total-PKB content. **C)** Phospho- to Total-PKB.

In the present experiment, untreated cardiomyocytes from a young control rat was used as positive control. Isolated cardiomyocytes from young, control and HFD rats treated with aspalathin for 1h 30 mins showed no significant differences between basal and aspalathin treated groups for either or between either of the 3 animal models (**Figure 7.6**)

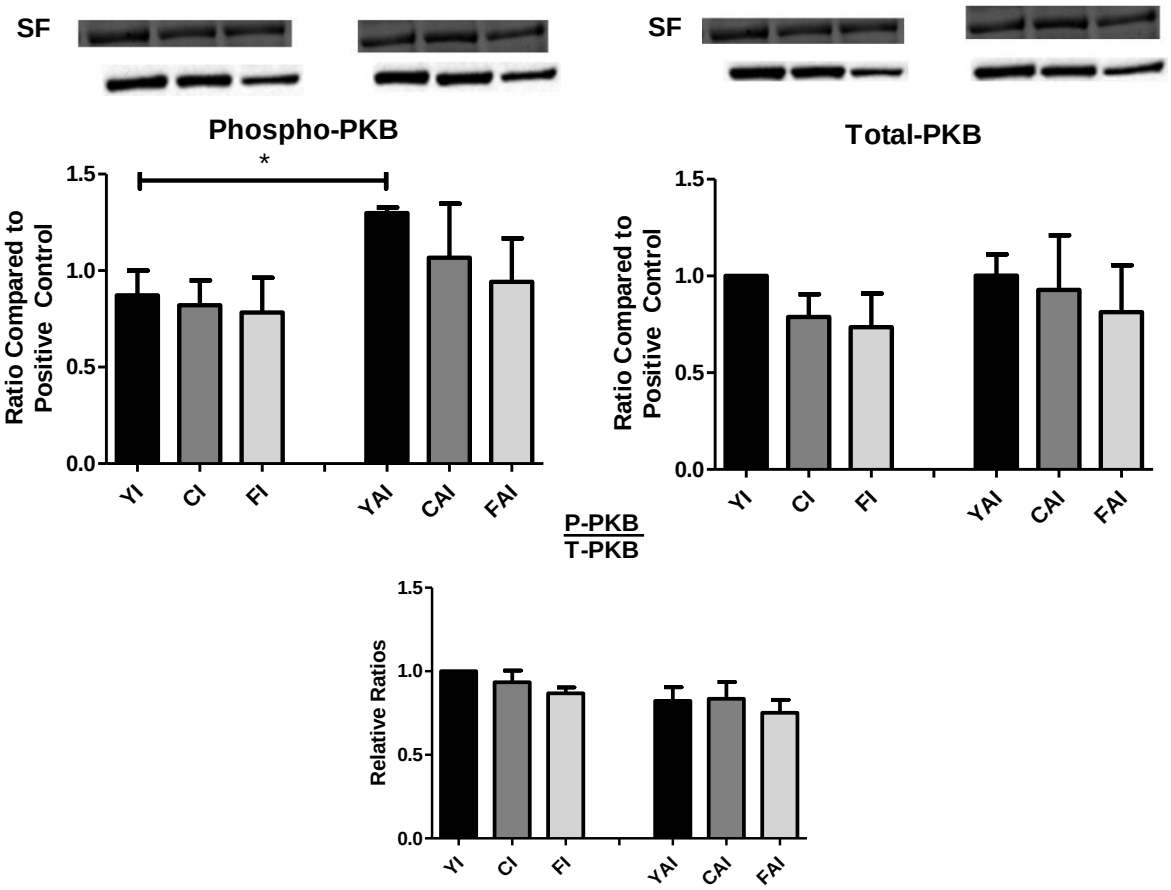

Figure 7.7 PKB expression and activation in isolated cardiomyocytes from young, control and HFD rats after 1h 30 mins in vitro stimulation with aspalathin plus insulin. SF: Stain-free Technology for Normalization, Y: Young, C: Control, F: High-fat, high-sucrose diet, I: 10 nM Insulin, AI: 10 uM Aspalathin + 10 nM Insulin. **A)** Phospho-PKB content; *p<0.05 (10 nM Ins vs. 10 uM Asp + 10 nM Ins for Young Rats). **B)** Total-PKB content. **C)** Phospho- to Total-PKB.

In the present experiment, untreated cardiomyocytes from a young control rat was used as positive control. Isolated cardiomyocytes from young, control and HFD rats were treated with insulin and/or aspalathin for 1 h 30 mins. In the young group, co-treating 10 nM insulin with 10 uM aspalathin led to significant increase in PKB activation (1.30±0.03 fold increase; n=3; p<0.05) compared to the 10 nM insulin treatment. No significant differences between insulin and aspalathin co-treatment was found for the age-matched control and HFD group (**Figure 7.7**).

3.2 MYOCARDIAL AMPK CONTENT AND ACTIVATION

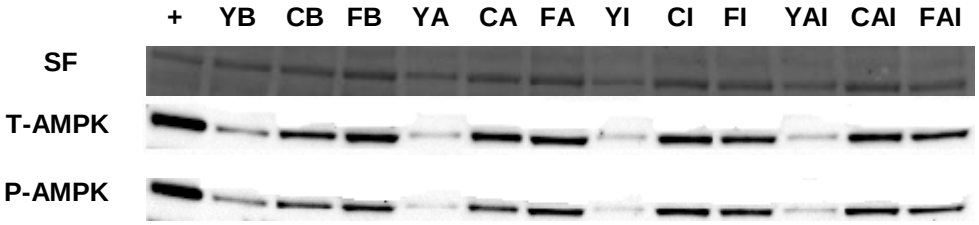

Figure 7.8 Representative blot of AMPK expression and activation in young, control and HFD rats. SF: Stain-free technology for normalization, + Positive Control, Y: Young, C: Control, HFD/F: High-fat, high-sucrose diet, B: Basal, A: 10 uM Aspalathin, I: 10 nM Insulin, AI: 10 uM Aspalathin + 10 nM Insulin.

AMPK expression and activation was observably higher in aged-rats compared to young rats. This might in part be due to a variation in whole lysate composition (SF in **Figure 7.8**), i.e. the specific protein profile present in cardiomyocytes from young and aged rats after a concentration of 50 ug 'protein' /ul was loaded onto the gels for separation with SDS-PAGE.

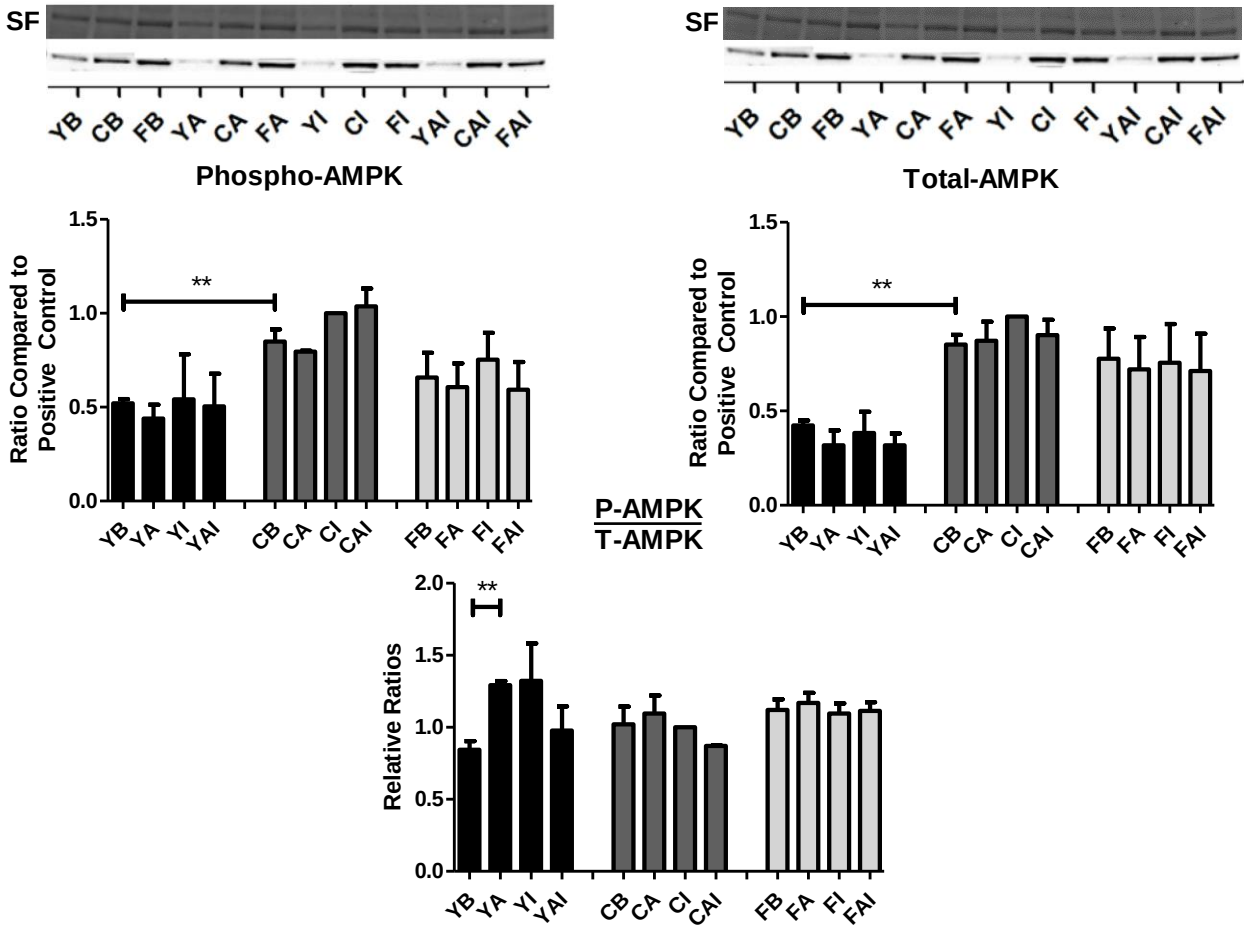

Figure 7.9 AMPK expression and activation in isolated cardiomyocytes from young, control and HFD rats after 1h 30 mins in vitro stimulation. SF: Stain-free Technology for Normalization, Y: Young, C: Control, F: High-fat, high-sucrose diet, B: Basal, A: 10 uM Aspalathin, I: 10 nM Insulin, AI: 10 uM Aspalathin + 10 nM Insulin. **A)** Phospho-AMPK content; *p<0.05 (Young Basal vs Control Basal). **B)** Total-PKB content; *p<0.05 (Young Basal vs Control Basal) **C)** Phospho- to Total-PKB; *p<0.05 (Young Basal vs 10 uM Aspalathin)

Isolated cardiomyocytes from young, control and HFD rats were treated with 10 uM aspalathin, 10 nM insulin or both for 1 h 30 mins (**Figure 7.9**). The phospho-to-total AMPK ratio, or the measure of the amount of total expressed AMPK activated, was significantly increased after treatment with aspalathin in young controls (1.29±0.03; p<0.01) compared to basal (0.84±0.06), resulting in a 54% increase. This might be indicative of the mechanism by which glucose uptake was induced in **Figure 5.8**. There were no significant differences between the treatment groups for the age-matched control and HFD group. However, comparison of the basal AMPK activation and expression levels, showed a significant increase in the older controls (0.52±0.03 vs 0.85±0.07 for AMPK activation, p<0.01; 0.42±0.03 vs 0.85±0.05 for AMPK expression, p<0.01).

3.3 MYOCARDIAL GLUT4 CONTENT AND ACTIVITY

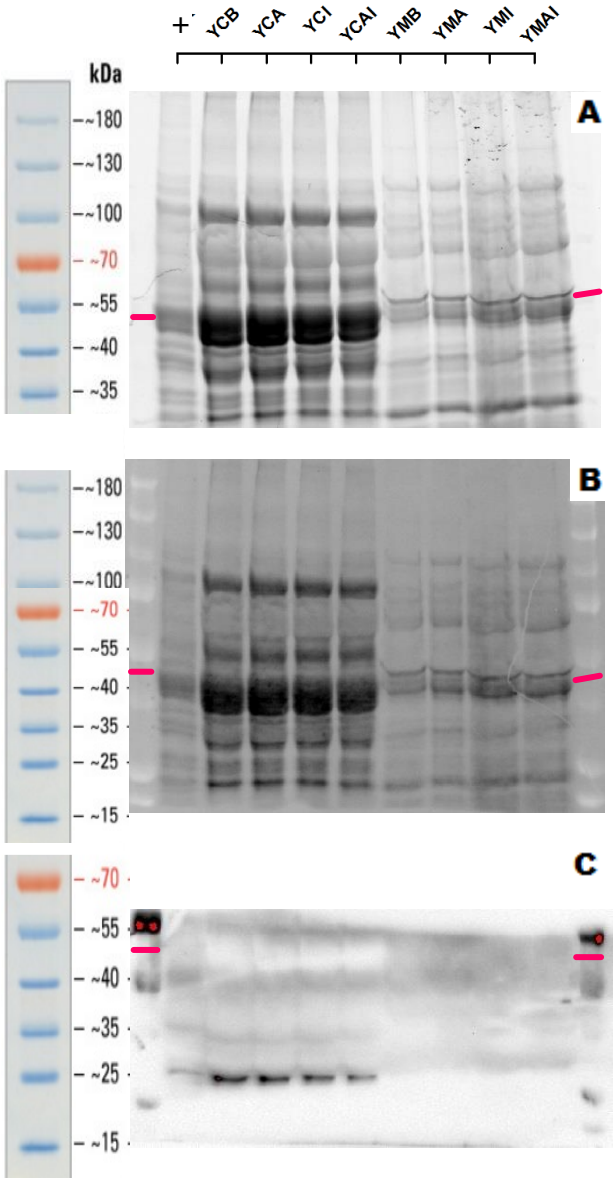

Figure 7.10 GLUT4 expression in cytosolic and membrane fractions obtained from young, rat cardiomyocytes (using Mini-PROTEAN® TGX Stain-Free™ Precast Gels). +, positive control; 1st letter abbreviations (Y: Young, C: Control, F: High-fat, high-sucrose diet); 2nd letter abbreviations (C: Cytosolic, M: Membrane); 3rd letter abbreviations (B: Basal, A: 10 uM Aspalathin: 10 nM Insulin, AI: 10 uM Aspalathin + 10 nM Insulin). **A)** Stain-Free™ technology gel after protein separation of 1st set of samples. **B)** PVDF membrane after transfer of gel proteins in A. **C)** GLUT4 expression of 1st set of samples, following addition of ECL Clarity.

Cardiomyocytes isolated from young control rats were treated with 10 uM aspalathin, 10 nM insulin or a combination of both, after which they were fractionated into membrane and cytosolic fractions for determination of GLUT4 translocation (**Figure 7.10)**. The GLUT4 primary antibody and the anti-

mouse IgG HRP-linked secondary antibody and were diluted in TBS-Tween Buffer. Initial determination with total GLUT4 antibodies, using Clarity ECL as a chemiluminescence agent, resulted in non-specific binding to the 25 kDa region of the cytosolic fractions. This is well below the expected locus of GLUT4, which is between 45 kDa, the established molecular weight of GLUT4, and 50 kDa, according to the manufacturer's data sheets (Cell Signaling Technology, USA). Initially, It was speculated that the primary antibody used in question, might have lost it's binding specificity.GLUT4 expression could not be determined from this experiment.

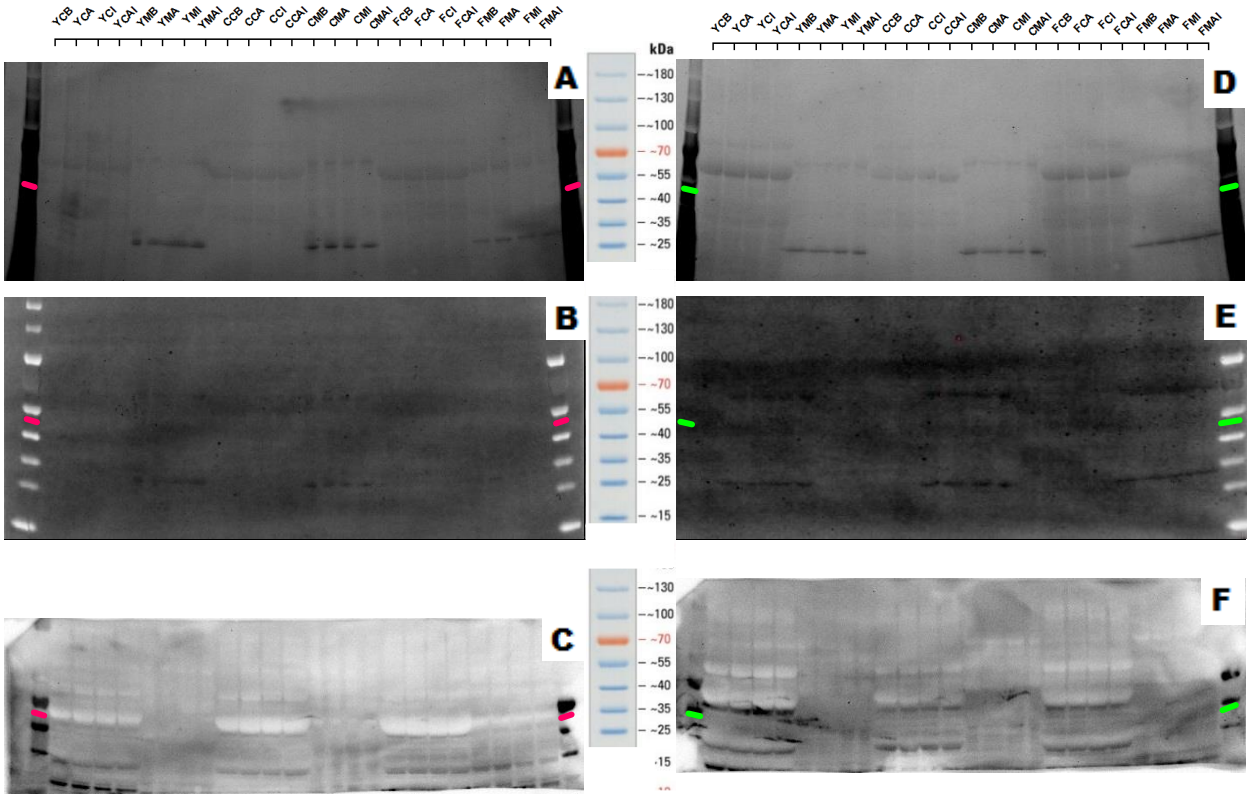

Figure 7.11 GLUT4 expression in cytosolic and membrane fractions obtained from young, age-matched control and HFD rat cardiomyocytes (using Mini-PROTEAN® Precast Gels). 1st letter abbreviations (Y: Young, C: Control, F: High-fat, high-sucrose diet); 2nd letter abbreviates (C: Cytosolic, M: Membrane); 3rd letter abbreviations (B: Basal, A: 10 uM Aspalathin: 10 nM Insulin, AI: 10 uM Aspalathin + 10 nM Insulin). **A)** Precast gel after protein separation of 1st set of samples. **B)** PVDF membrane after transfer of gel proteins in A. **C)** GLUT4 expression of 1st set of samples, following addition of Luminata Forte Western HRP substrate. **D)** Precast gel after protein separation of 2nd set of samples. **E)** PVDF membrane after transfer of gel proteins in D. **F)** GLUT4 expression of 2nd set of samples, following addition of Luminata Forte Western HRP substrate.

Cardiomyocytes isolated from young control, age-matched control and HFD rats were treated with 10 uM aspalathin, 10 nM insulin or a combination of both, after which they were fractionated into membrane and cytosolic fractions for determination of GLUT4 translocation (**Figure 7.11)**. After

being unable to find total GLUT4 expression with the previous protocol (**Figure 7.9**), a new total GLUT4 antibody was diluted in TBS-Tween Buffer. The chemiluminescent agent was also changed to Luminata Forte Western HRP substrate. Normally, the HRP of the secondary antibody catalyze the oxidation of luminol into photons (or chemiluminescence) which can be detected by charged coupled devices. Luminata Forte prevents spontaneous oxidation of luminol, which results in a stronger and more stable signal detectable. The addition of Luminata Forte resulted in various non-specific signals, and the same non-specific binding at 25 kDa was observed as in (**Figure 7.9**). Overexposed bands in line with GLUT4's size (45 - 50 kDa) were observed for all the cytosol fractions of young, control and HFD groups. However, determining the specific optical density between the treatment groups was not possible due to the overexposure.

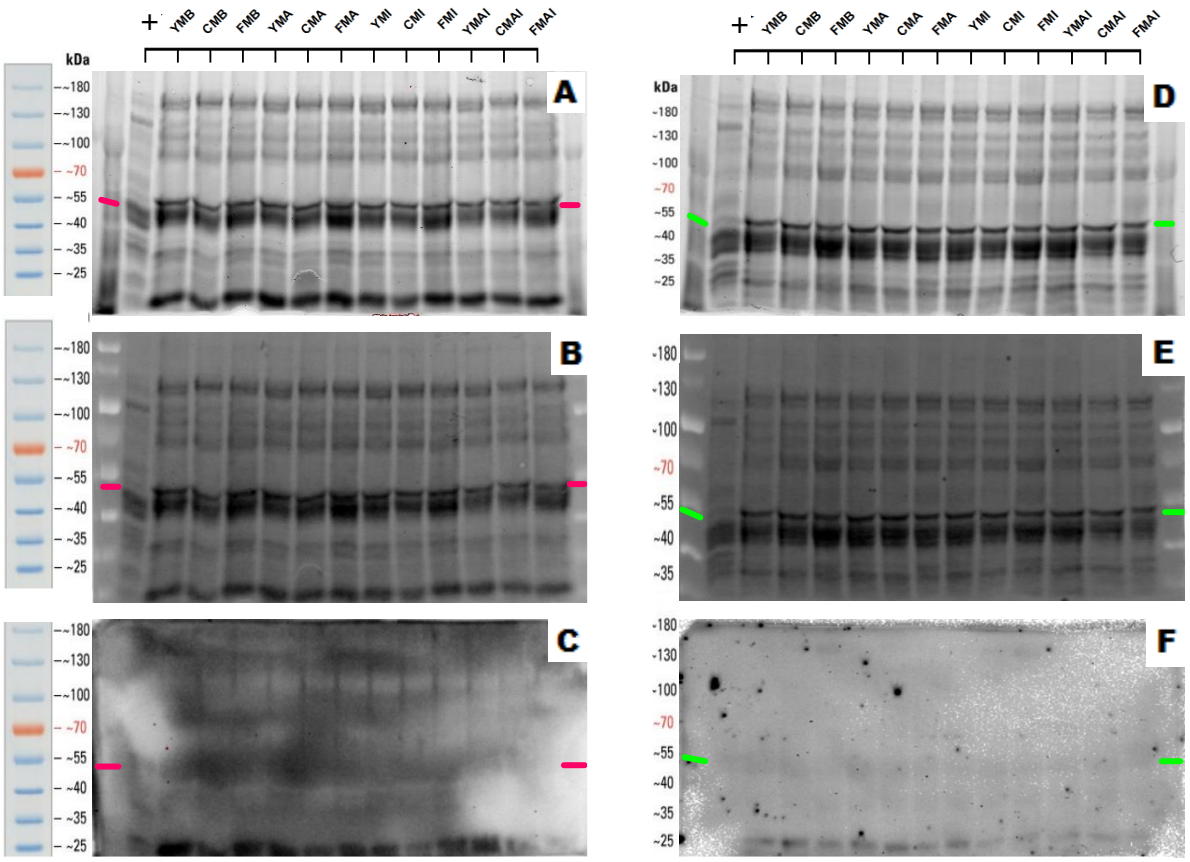

Figure 7.12 GLUT4 expression in membrane fractions obtained from young, age-matched control and HFD rat cardiomyocytes. +, positive control; 1st letter abbreviations (Y: Young, C: Control, F: High-fat, high-sucrose diet); 2nd letter abbreviations (M: Membrane); 3rd letter abbreviations (B: Basal, A: 10 uM Aspalathin: 10 nM Insulin, AI: 10 uM Aspalathin + 10 nM Insulin). **A)** Stain-free technology gel after protein separation of 1st set of samples. **B)** Stain-free technology membrane after transfer of gel proteins in A. **C)** GLUT4 expression of 1st set of samples, following addition of Luminata Forte Western HRP substrate. **D)** Stain-free technology gel after protein separation of 2nd set of samples. **E)** Stain-free technology membrane after transfer of gel proteins in D. **F)** GLUT4 expression of 2nd set of samples, following addition of Luminata Forte Western HRP substrate.

Cardiomyocytes isolated from young control, age-matched control and HFD rats were treated with 10uM aspalathin, 10nM insulin or a combination of both, after which they were fractionated into membrane fractions for determination of GLUT4 translocation (**Figure 7.12)**. The same protocol was followed as in **Figure 7.9**, except the primary and secondary antibody were diluted in TBS-Tween Buffer with 2.5% Milk in order to reduce non-specific binding of proteins that led to the overexposure of bands observed in the previous experiment. Non-specific binding was significantly less after addition of Luminata Forte in this experiment, but still presented with the same non-specific binding at 25 kDa as observed in (**Figure 7.9**). GLUT4 expression could not be determined from this experiment.

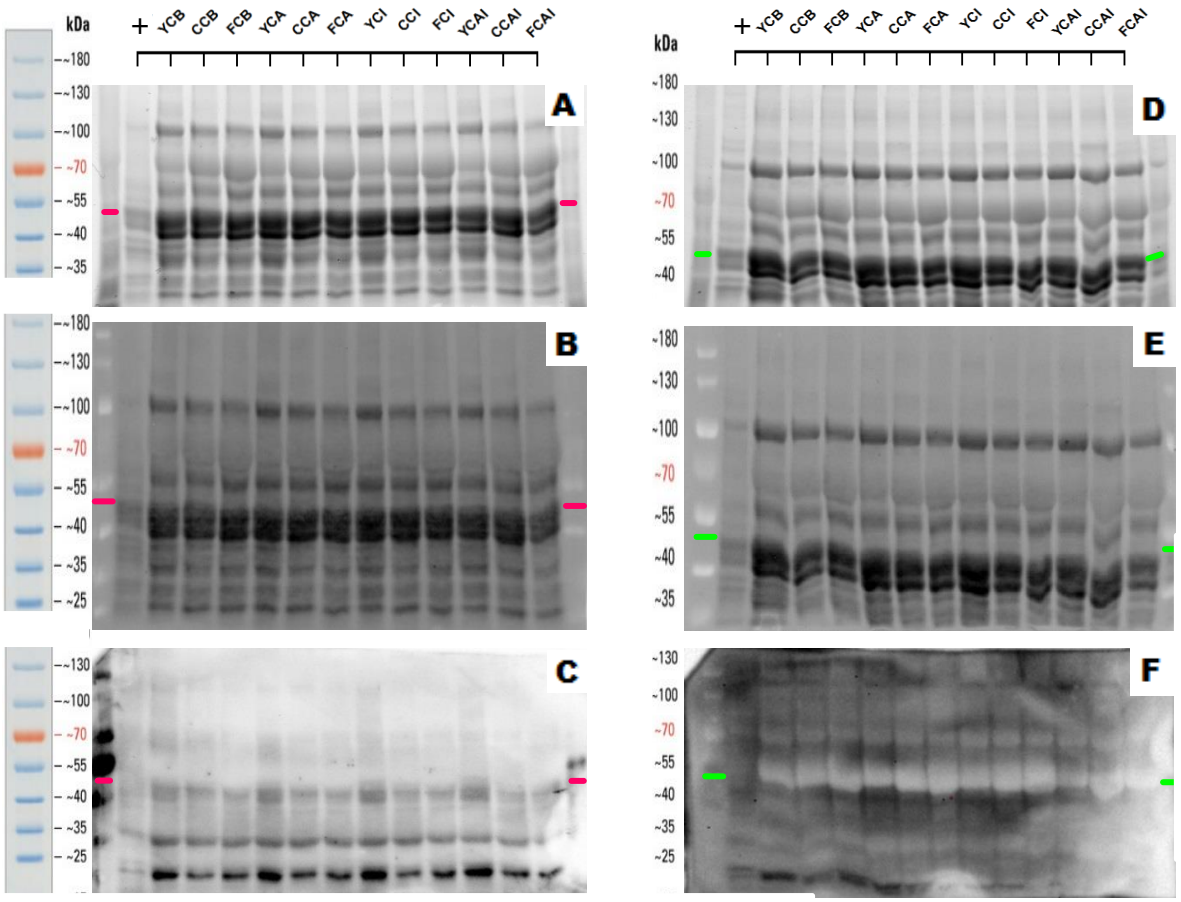

Figure 7.13 GLUT4 expression in cytosolic fractions obtained from young, age-matched control and HFD rat cardiomyocytes (using a TGX Stain-Free™ FastCast™ Acrylamide Kit). +, positive control, 1st letter abbreviations (Y: Young, C: Control, F: High-fat, high-sucrose diet); 2nd letter abbreviations (C: Cytosolic); 3rd letter abbreviations (B: Basal, A: 10 uM Aspalathin: 10 nM Insulin, AI: 10 uM Aspalathin + 10 nM Insulin). **A)** TGX Stain-Free™ FastCast™ gel after protein separation of 1st set of samples. **B)** PVDF membrane after transfer of gel proteins in A. **C)** GLUT4 expression of 1st set of samples, following addition of Luminata Forte. **D)** Stain-free technology gel after protein separation of 2nd set of samples. **E)** PVDF membrane after transfer of gel proteins in D. **F)** GLUT4 expression of 2nd set of samples, following addition of Luminata Forte.

Cardiomyocytes isolated from young control, age-matched control and HFD rats were treated with 10 uM aspalathin, 10 nM insulin or a combination of both, after which they were fractionated into cytosolic fractions for determination of GLUT4 translocation (**Figure 7.13)**. The blocking protocol was changed (3 washes with 5% BSA in TBS-Tween) and the total GLUT4 antibody was diluted in Calbiochem® Signalboost™ and the result was less non-specific binding resulting in a clearer image. The same non-specific binding at 25 kDa was observed as in **Figure 7.9**, and the bands present at the 45-50 kDa region were very diffused, making it questionable whether it can be assumed to represent GLUT4. GLUT4 expression could not be determined from this experiment.

CHAPTER 8
DISCUSSION

1. INTRODUCTION

Obesity is associated with increased risk for insulin resistance and defective glucose homeostasis (Boden et al., 2011). Furthermore, in the majority of type 2 diabetic patients, insulin resistance is the earliest detectable abnormality (DeFronzo & Tripathy, 2009). Even severe insulin resistance can however still be managed by normal β-cell function. In this case, sufficient insulin is still produced to balance out faulty insulin action. Thus, in order for the condition to progress to type 2 diabetes, both insulin action AND insulin secretion need to be defective. By the time type 2 diabetes is diagnosed, both of these conditions are well established and determining the primary defect or initial cause is impossible (DeFronzo, 2004). Nevertheless, it is known that no matter which defect (insulin resistance or impaired insulin secretion) first disturbed glucose homeostasis, with time both conditions will present in type 2 diabetic patients. Since various current medication available to treat T2D have problems with remaining effective after prolonged treatment (Misbin, 2005) or become toxic to liver and heart as the treatment progresses (Boussageon et al., 2011), a search for safer alternatives has been instigated in recent years. One of these promising nutraceuticals, aspalathin, has recently attracted many investigators for its potential in regulating glucose metabolism (Kawano et al., 2009; Muller et al., 2012; Mazibuko et al., 2013; Son et al., 2013). Aspalathin has been shown to induce glucose uptake directly in rat L6 skeletal muscle cells (Kawano et al., 2009, Son et al., 2013). Treating with ARF was also able to increase glucose uptake in mouse C2C12 skeletal muscle cells (Muller et al., 2012). Furthermore, treating palmitate-induced insulin-resistant C2C12 skeletal muscle cells with green rooibos extract (GRE) and fermented rooibos extract (FRE) induced elevated glucose uptake levels (Mazibuko et al., 2013). Also, aspalathin suppressed elevated fasting blood glucose and improved impaired glucose tolerance in *ob/ob* mice (Son et al., 2013) and *db/db* mice (Kawano et al., 2009). In view of these previous observations and to deepen our understanding of myocardial glucose metabolism in ageing, obesity and insulin-resistance, we investigated the potential of aspalathin to induce glucose uptake in isolated cardiomyocytes from young (8 weeks old), age-matched control (22 weeks old) and HFD (22 weeks old: 6 weeks + 16 weeks of a high fat, high sucrose diet) rats.

In the present study, we aimed to elucidate the effects and mechanism of aspalathin treatment on glucose homeostasis, focusing on glucose uptake by isolated adult ventricular cardiomyocytes from normal and obese, insulin resistant rats, as well as H9C2 cardiomyoblasts.

2. CHARACTERISTICS OF A HIGH-FAT, HIGH-CALORIC DIET

The prevalence of obesity and insulin-resistance increases the risk for cardiovascular diseases (Cardiovascular Disease, WHO, 2015). In order to investigate these conditions, we made use of a diet-induced obese and insulin resistant Wistar rat model. Obesity is the consequence of overconsumption coupled to a reduced energy expenditure (Hill et al., 2012). This mechanism was exploited in our present study by using a high-fat, high-sucrose diet (rat chow, supplemented with holsum fat, sucrose and condensed milk) for 16-30 weeks to induce obesity by hyperphagia and insulin-resistance in caged rats. They were compared to age-matched controls (normal rat chow). In the present study, the high-fat, high-sucrose diet rats had a significantly higher body weight (**Figure 4.1**) and visceral fat (excess fat) content (**Figure 4.2**) compared to the age-matched controls, similar to what was previously published (Huisamen et al., 2013). As indicated by the biometric parameters, they also became insulin resistant (**Table 4.1**). This included raised fasting insulin levels and a higher HOMA-IR index. In genetically and environmentally susceptible individuals, chronic overnutrition with an excessive energy intake and low energy expenditure causes the subcutaneous fat to saturate, consequently leading to enlarged adipocytes and visceral fat formation (Blüher, 2013). Furthermore, diet-induced visceral fat accumulation is an important factor in the development of insulin resistance and a risk factor for the metabolic syndrome (Grundy, 2012).

One of the first clinical consequences of insulin resistance is a dysregulation in glucose homeostasis, the maintenance of blood glucose concentration within very narrow physiological limits (Norris & Rich, 2012). This abnormality can be determined by measuring the fasting blood glucose concentration. Fasting blood glucose is closely regulated by endogenous glucose production (hepatic glycogenolysis, gluconeogenesis) and glucose utilization by insulin-senstive tissues. In the present study, an OGTT of the diet rats, showed the HFD group to have a significantly higher fasting blood glucose levels compared to the controls, and following administration of glucose, the HFD group's blood glucose remained significantly elevated for at least 45 minutes compared to the controls (**Figure 4.3**). It was also significantly higher at the clinically relevant 2-hour time point. In addition, concurringly, the non-fasting blood glucose levels (or random blood glucose test levels) taken just prior to sacrificing of rats, also showed a significant increase (**Figure 4.4**). The cardiovascular effects of a 16 week high-sucrose diet without high-fat has been well characterised by Huisamen et al. (2011). These rats presented with whole-body insulin resistance, as well as myocardial insulin resistance. In the present study, increasing concentrations (1-100nM) of insulin elicited a weak response in glucose uptake in cardiomyocytes isolated from HFD rats (**Figure 5.7**), corroborating previous studies using a similar model (Huisamen et al., 2011; Huisamen et al., 2013). In contrast, age-matched control diet rats had a dose-dependent increase in glucose uptake, and cardiomyocytes isolated from young control rats

had the most robust increases in glucose uptake response to increasing concentrations of insulin. We speculate that the mechanism for insulin resistance formation following a high-fat, high-caloric diet is due to an increase in adipose tissue which causes elevated circulating free fatty acids (FFA) levels, altering adipose tissue derived factors, such as increasing leptin (responsible for inhibiting appetite) and TNFα (known to induce peripheral insulin resistance) and decreasing adiponectin (sensitize insulin action) (Yadav et al., 2013), followed by the eventual viceral fat accumulation (Ding, 2015, Grundy, 2012). In this regard, an increase in plasma FFA may have contributed to the elevated glucose levels as follows: (i) induction of insulin resistance by altering glucose transport, phosphorylation or both (inhibition of insulin-mediated glucose uptake pathways) in cardiac muscle and possibly skeletal muscle and adipose tissue, (ii) increasing endogenous glucose production by increasing hepatic glucose output (Boden, 2011), (iii) and increased FFA-induced insulin secretion exacerbated by FFA-induced insulin resistance (Boden, 1999).

3. ACUTE (45 MINUTES) TREATMENT WITH ASPALATHIN

3.1 CELL VIABILITY OF CARDIOMYOCYTES FOLLOWING THE ISOLATION PROTOCOL

Our first experiment was the determination of cell viability following the isolation in cardiomyocytes from young rats. According to the International Organization for Standardization (ISO 10993, 2009), cell viability percentages above 80% are considered non-cytotoxic, 60-80% weak cytotoxic, 40-60% moderate cyotoxic and below 40% strong cytotoxic. In the present study, cell viability after the isolation protocol of cardiomyocytes from young rats was always maintained between 60-75% (**Figure 5.1 and Figure 5.2**), effectively being categorized as a 'weak' cytotoxic cell environment. Fortunately, the cardiomyocytes were robust enough to still allow further investigation. Likewise, aspalathin as a strong anti-oxidant (Van der Merwe, 2010), and possible metabolic regulator, also overcame this obstacle, which led to the obtainment of significant results.

3.2 EFFECTS OF ACUTE ASPALATHIN TREATMENT ON GLUCOSE UPTAKE IN CARDIOMYOCYTES ISOLATED FROM YOUNG RATS

We first tested the hypothesis that aspalathin treatment has the ability to stimulate glucose uptake by using cardiomyocytes. In order to achieve this, we tried to establish an aspalathin dose response (1-100μM) in cardiomyocytes of young control rats (**Figure 5.5**). 10 μM aspalathin was able to significantly increase glucose uptake above DMSO while 100μM seemed to attenuate this effect. The vehicle, DMSO, also attenuated basal glucose uptake by the cardiomyocytes. To test for the possible cytotoxic effects of aspalathin and DMSO, we performed a cell viability assay using propidium iodide (**Described under Section 2.2.2 in the Materials and Methods Chapter)**. There was no significant difference in cell viability between the treatment groups (**Figure 5.2**), therefore the observed suppression in glucose uptake was not due to DMSO toxicity, but possibly through some other responsive mechanism. In a study done by Berenquer et al. (2011) on 3T3-L1

adipocytes and L6 myotubes, they found that low concentrations of DMSO was able to induce GLUT1 and GLUT4 recruitment to the cell surface, but simultaneously also inhibit the activity of the glucose transporters. The half-life for reversing the effects was t1/2 ~ 12 mins in 3T3-L1 adipocytes, and could possibly be longer in cardiomyocytes. No similar studies had been done to test for the possible glucose transport inhibiting effects of DMSO in cardiomyocytes. We thus speculate that aspalathin, solubilized in DMSO, would need an extended time to elicit a response on glucose uptake in cardiomyocytes. We also propose that, since 0.1% DMSO was not toxic to the cells, the reduction in glucose uptake observed could be due to DMSO inhibiting GLUT4 activity, and this effect is exacerbated by an increasing DMSO concentration. This would explain why 10μM aspalathin, containing a lower concentration of 0.01% DMSO, showed a significant increase in glucose uptake, compared to the 0.1% DMSO in 100μM aspalathin. Also, the marked increase in glucose uptake in 10μM aspalathin compared to 1μM aspalathin would have to be solely due to the glucose uptake potential of aspalathin in cardiomyocytes.

3.3 Effects of acute aspalathin co-treated with insulin on glucose uptake in cardiomyocytes isolated from young and aged obese-insulin resistant rats

We explored the possibility that aspalathin might have an indirect effect on glucose uptake in cardiomyocytes through a synergistic effect with insulin's action in young control rats (**Figure 5.6; Figure 5.8 and Figure 5.9**). When 10nM insulin was co-treated with 10μM aspalathin for 45 mins, glucose uptake significantly increased compared to 10nM insulin. The fact that aspalathin could not acutely induce glucose uptake independent of insulin, infer that insulin plays an important role in eliciting aspalathin's response through increasing co-activation or co-expression of the insulin-dependent signaling pathway proteins. This mechanism has been noted by Mazibuko et al. (2013), who showed palmitate-induced insulin resistant C2C12 muscle cells had a low glucose uptake response to treatment with insulin, but once co-treated with GRE (high aspalathin content) there was a markable increase in glucose uptake. However, in the present study cardiomyocytes isolated from obese, insulin-resistant and age-matched control rats, showed no significant differences in glucose uptake when treated with aspalathin, or aspalathin in conjuction with insulin (**Figure 5.8 and Figure 5.9**). The decline in insulin sensitivity, observed when determining the effect of increasing insulin concentrations on glucose uptake between cardiomyocytes isolated from from young rats, aged control rats and obese-insulin resistant rats (**Figure 5.7**), implicates the importance of insulin sensitivity in facillitating aspalathin's response. The fact that aspalathin in conjunction with insulin was able to induce glucose uptake in cardiomyocytes from young control rats, indicate that the mechanisms of ageing, which independently reduce the sensitivity of the insulin signaling pathways, is an important factor diminishing aspalathin's glucose uptake potential.

4. EXTENDED (1H - 6H) TREATMENT WITH ASPALATHIN

4.1 EFFECTS OF CHRONIC ASPALATHIN CO-TREATED WITH INSULIN IN DIFFERENTIATED H9C2 CELLS

In order to confirm that aspalathin can in fact induce glucose uptake independent of insulin, cultured rat-heart derived embryonic H9C2 cell line, were used as an analog for the isolated cardiomyocytes from rats, to test the efficacy of aspalathin as treatment. First, the immortal H9C2 cells were differentiated using the protocol established by Ménard et al. (1999). Chronic treatment of the H9C2 cells with 10nM retinoic acid (RA) enhances Ca^{2+}-channel expression, which is a defining feature of the cardiac phenotype. Simultaneously, by virtue of cardiac differentiation, myogenic transdifferentiation is also inhibited, preventing the cells from differentiating into skeletal myocytes. Full differentiaton was established 6 days after initiation of a reduced serum concentration of 1% HS and addition of 10nM RA, after which the experiment was performed on homogeneous cell populations. The cells were cultured in the presence of 5.5 mM glucose as opposed to being completely glucose starved. It was argued this would give a more natural insight into the effect of aspalathin, which would clinically be used to lower blood glucose in hyperglycemic patients. ATP levels were determined as a measure of the metabolic activity and therefore the overall health of the cell population (**Described under Section 3.4 in the Materials and Methods Chapter**). Our first observation was that aspalathin treatment, as well as co-treating cells with 1nM insulin for the last 15 mins, significantly increased metabolic activity of differentiated H9C2 cells after 3 hours of incubation (**Figure 6.1**). The same effect was not seen when insulin was treated independently for the last 15 minutes. In addition, staining the cells with JC-1 to show mitochondrial integrity, also demonstrated that aspalathin improved the percentage of live cells at this time point (**Figure 6.2 and Figure 6.3**). This observation was underscored by measuring 2DG accumulation after 3 and 6 hours respectively. Aspalathin significantly enhanced 2DG uptake in the absence or presence of insulin (**Figure 6.4**). Balderas-Villalobos et al. (2013) showed that oxidative stress in cardiomyocytes resulted in impaired sarco(endo)plasmic reticulum Ca^{2+} ATPase activity. This correlates with cardiac contractile dysfunction which impairs overall cell health, however, these effects could be reversed by treatment with strong anti-oxidants (Balderas-Villalobos et al., 2013). In this regard, aspalathin, a known strong anti-oxidant (Joubert, 2006) may have been able to improve cell health by reversing the basal oxidative stress of the cell population induced by the cell culture environment, such as fluctuations in temperature, oxygen, carbon dioxide and nitrogen. H9C2 cells, similar to fetal and early postnatal cardiomyocytes, primarily contain GLUT1 as opposed to GLUT4 (Montessuit & Lerch, 2013), and will therefore rely more heavily on inducing GLUT1 to the cell membrane. In this regard, the inherent characteristics of H9C2 cells are significantly different from isolated cardiomyocytes, and determining the mechanism of aspalathin's glucose transport potential in cell culture, would not be a true indicator of what occurs in cardiomyocytes. However, it has been shown by Yu et al. (1999) in H9C2

myotubes that insulin and K+ depolarization can increase glucose uptake through recruitment of GLUT4 from the intracellular vesicles to the cell membrane. It is possible that aspalathin also made use of these signaling mechanisms to induce glucose uptake in differentiated H9C2 cardiomyocytes although this was not determined in the current study.

4.2 Effects of extended aspalathin/insulin co-treatment on glucose uptake in young, control and HFD rats

After demonstrating that aspalathin was able to induce 2DG uptake in H9C2 cells with longer incubation times, we extended our experiments on adult ventricular cardiomyocytes to 3 hours (**Figure 5.10 and Figure 5.11**). Surprisingly, incubating aspalathin for 1 and a half hours (a mere 45 mins longer than in the acute model) (**Figure 5.8 and Figure 5.9**) resulted in a significant increase in glucose uptake in cardiomyocytes from young controls, which persisted for 3 hours of treatment. Surprisingly, the effect in conjunction with insulin in young control cardiodiomyocytes was only pronounced in the acute model, but not after 1 and a half hours of treatment. This is contrary to the older controls with aspalathin inducing a significant increase in insulin-mediated glucose uptake after 1 and a half hours of treatment. The high fat diet group showed no significant increases when treated with aspalathin with or without insulin, but insulin treatment for 1 and a half hours did stimulate glucose uptake significantly. Aspalathin's surpressed effect in aged, obese, insulin resistant rats strengthens the argument that aspalathin's actions are in part dependent on the insulin-signaling pathway of glucose uptake. In a study done by Purintrapiban & Ratanachaiyavong (2003), L8 myotubes were co-treated with insulin and metformin (a known hypoglycemic agent and anti-diabetic treatment) for 5 hours in culture, after which they determined glucose uptake and found that 2mM metformin was able to induce glucose uptake independent of insulin, but co-treatment resulted in a further activation of glucose uptake. Similarly, we also propose aspalathin is able to induce glucose uptake independent of insulin, but downregulation of the insulin signaling pathway in older animals, and even more so in obese animals, result in a desensitization of the entire insulin-signaling pathway and subsequently surpress glucose uptake induced by aspalathin.

5. Aspalathin's mechanism of action

We investigated the mechanism by which aspalathin induced this slight increase in myocardial glucose uptake by western blot analysis. In particular, the markers of interest was: PKB, an insulin-dependent, pro-'life', growth marker; and AMPK – the body's key metabolic regulator, which is an insulin-independent marker of glucose uptake quite central to all metabolic cell signaling. Furthermore, we made use of wortmannin pretreatment, a selective inhibitor of PI3K, to inhibit the insulin-dependent mechanism of glucose uptake and thus elucidate the degree of dependance aspalathin has on the same signaling pathway.

5.1 PI3K-DEPENDENCE

Insulin is dependent on PI3K to elicit it's cellular responses after binding of the insulin receptor. Inhibiting PI3K through selective pretreatment with wortmannin, can result in total inhibition of insulin's beneficial effects. This was the case when wortmannin was administered before insulin and aspalathin samples, which resulted in a complete loss of glucose uptake potential in cardiomyocytes isolated from young rats (**Figure 7.1**), as well as aged, obese, insulin-resistant rats and age-matched controls (**Figure 7.2**). This also indicates the importance of PI3K's activity, and arguably the entire PI3K pathway's downstream effectors, in eliciting glucose uptake after aspalathin treatment. Pretreatment with wortmannin also resulted in inhibition of PKB activation and expression to levels below baseline (**Figure 7.3**).

5.1.1 PKB-MEDIATED EFFECTS

The role of PKB in eliciting the responses of aspalathin is still controversial. In rats supplemented for 7 weeks with GRE and FRE, Pantsi et al. (2011) found low to no effect by rooibos flavonoids (including aspalathin) on total PKB levels in the hearts. To the contrary, Mazibuko et al. (2013) found that rooibos did in fact increase phospho-PKB levels in C2C12 mouse skeletal myotubes. In another study done by Son et al. (2013), rooibos also did not activate PKB in normal L6 myocytes, whereas Mazibuko et al. (2013) was able to show the mechanism in insulin resistant C2C12 myocytes. Mazibuko et al. observed that phospho-PKB levels of the palmitate treated cells resembled that of normal PKB levels when stimulated by insulin, suggesting that rooibos can resensitise downstream insulin signaling. In agreement with Mazibuko et al. (2013), in our present study, PKB activation was significantly increased in young rats treated for 15 minutes with both insulin and aspalathin (**Figure 7.3**). This effect was also observed when comparing the ratio of activated PKB to the total amount of PKB expressed, and could explain the potential glucose uptake observed after 45 mins of aspalathin co-treatment with insulin (**Figure 5.6, Figure 5.8 and Figure 5.9**). After 1 and a half hours of treatment, PKB activation was also significantly increased in cardiomyocytes from young rats when insulin was co-treated with aspalathin. However, there were no significant differences found in the older diet rats, possibly indicating that the PKB pathway becomes less sensitive as ageing progress. In a study done by Frøsig et al. (2013), aged mice fed a high-fat diet had reduced signaling of PKB, coinciding with insulin resistance and impaired glucose homeostasis. Even though in our present study we could not find a marked decrease in PKB expression or activation between young and older rats, the observed decrease in glucose uptake potential in aged rats when treated with insulin, a known PKB activator, and aspalathin, a possible PKB activator, could be a direct consequence of a reduced PKB sensitivity.

5.2 PI3K-INDEPENDENCE

One of the earliest detectable signs of insulin resistance, is an impairment of insulin-stimulated glucose transport (Wilcox, 2005). The impairment also correlates with a reduction in GLUT4 protein expression, as well as impaired GLUT4 translocation (Wilcox, 2005). However, GLUT4 translocation can still be induced through an insulin-independent pathway of glucose uptake, such as AMPK, which phosphorylates AS160, a gate-keeper protein also independently stimulated by insulin, which induce glucose uptake by promoting the translocation of GLUT4 to the plasma membrane.

5.2.1 AMPK-MEDIATED EFFECTS

Mazibuko et al. (2013) found that insulin resistant mouse C2C12 skeletal muscle cells treated with rooibos, resulted in the activation of the insulin-independent AMPK pathway which culminated in increased levels of GLUT4. Similiarly, Son et al. (2013) found that aspalathin activated AMPK signaling and promoted endogenous GLUT4 translocation to the plasma membrane in L6 myocytes and in skeletal muscle of ob/ob mice. In C2C12 mouse skeletal muscle cells, Muller et al. (2012) also showed aspalathin is able to improve glucose uptake, while this same effect could not be mimicked in Chang liver cells, which does not contain GLUT4. This strongly implicates GLUT4 and AMPK as essential role players in eliciting aspalathin's response. In our present study, aspalathin significantly increased the expression of AMPK independent of insulin in young rats after 15 minutes of stimulation (**Figure 7.3**). This, however, did not correlate with an increase in glucose uptake (**Figure 5.6; Figure 5.8 and Figure 5.9**). It could be that an increase in AMPK expression is the first step towards recruiting the necessary downstream signaling proteins, such as AS160, to induce glucose uptake and a longer incubation time would give a more pronounced response in glucose uptake. Furthermore, after 15 minutes of incubation in cardiomyocytes isolated from young rats, aspalathin increased AMPK activation in the presence of insulin (**Figure 7.4**), which strongly implicates AMPK's role in eliciting aspalathin's acute effects on glucose uptake when co-treated with insulin (**Figure 5.6; Figure 5.8 and Figure 5.9**). After one and a half hours of stimulation, aspalathin signficantly increased the phospho-to-total ratio of AMPK in young rats, correlating with the glucose uptake induced at the hour and a half time point (**Figure 5.10 and Figure 5.11**). Taken together, we propose that initially aspalathin induces an increase in AMPK expression, followed by a time-dependent AMPK activation the longer aspalathin is incubated in isolated young rat cardiomyocytes. This process potentiates glucose uptake, which can have a hypoglycemic effect.

5.2.2 AMPK AND AGEING

The effect of AMPK on ageing is still controversial. Ageing is often associated with poor stress tolerance and decreased insulin sensitivity, which has been linked to a decline in AMPK activity (Mulligan et al., 2005). Poor stress tolerance could indicate a decline in basal AMPK levels, while an acute onset of stress could be met with a diminished AMPK activity (Mulligan et al., 2005). Conversely, Jin et al. (2004), found that ageing increased AMPK activation in rat kidneys, while Frøsig et al. (2013) found increased AMPK activation in mice livers. In our present study, we also found that both expression and basal activation of AMPK was increased in aged controls compared to young rats (**Figure 7.9**). The fact that aspalathin was not able to induce glucose uptake independent of insulin in aged rats (**Figure 5.10 and Figure 5.11**), suggest that upregulation of AMPK expression alone is not sufficient to induce aspalathin-stimulated glucose uptake, but relative activation of AMPK need to exceed AMPK expression in order to elicit the same response observed in younger rats. In this regard, ageing attenuates AMPK's sensitivity through an unexplored mechanism. This further implicates the role of AMPK as a prominent metabolic regulator as ageing progresses.

5.3 GLUT4-MEDIATED EFFECTS

The first step of glucose metabolism is the transport of glucose across the plasma membrane. Within the heart, glucose enters through either facillitated diffusion or active diffusion accompanied by the glucose transporters, GLUT1 and GLUT4. Blood glucose is always higher within the blood, than intracellularly, causing a glucose gradient which drives the influx of glucose. The gradient is maintained by abundant hexokinase enzymes, which phosphorylate glucose as it enters the cardiomyocytes, leaving the transport into cells as the rate-limiting step (Montessuit & Lerch, 2013). GLUT4 is primarily located in intracellular membrane compartments and translocated to the cell membrane in response to known stimuli, including increased workload, adrenaline and insulin (Wheeler et al., 1994). Both GLUT1 and GLUT4 have similiar structures and enzymatic turnover, but GLUT4 has a higher affinity for glucose. The higher expression and higher affinity for glucose, makes GLUT4 the primary determinant of glucose uptake within cardiomyocytes with an average 4-7mM concentration or number of GLUT4 transporters present at the cell surface (Montessuit & Lerch, 2013). In our present study we proposed to determine GLUT4 translocation by fractionating aspalathin and insulin treated isolated cardiomyocytes into plasma membrane and cytosolic fractions, followed by immunoblotting for the total GLUT4 content. We were, however, unsuccessful in detecting GLUT4 in either of our positive control, young rat, aged obese and insulin resistant, or age-matched control group samples (**Figure 7.10, Figure 7.11, Figure 7.12 and Figure 7.13**). Regardless, Purintrapiban & Ratanachaiyavong (2003), discussed above, showed that insulin stimulated glucose uptake resulted in increased membrane translocation of GLUT4 from the intracellular compartment. Wang et al. (1999) demonstrated that constitutively activated PKB (through transfection of a viral Gag protein) resulted in upregulated GLUT4

translocation in L6 myoblasts. Furthermore, Yamaguchi et al. (2005) showed in 3T3-L1 adipocytes, activation of AMPK, by the known AMPK activators, 5-aminoimidazole-4-carboxamide-1-beta-D-ribofuranoside (AICAR) and 2,4-dinitrophenol (DNP), also resulted in acceleration of GLUT4 translocation. Combining both our findings that aspalathin induced AMPK and PKB activation, we propose that aspalathin's mechanism of glucose uptake, in the absence or presence of insulin, would similarly result in GLUT4 translocation to the plasma membrane (**Figure 8.1**).

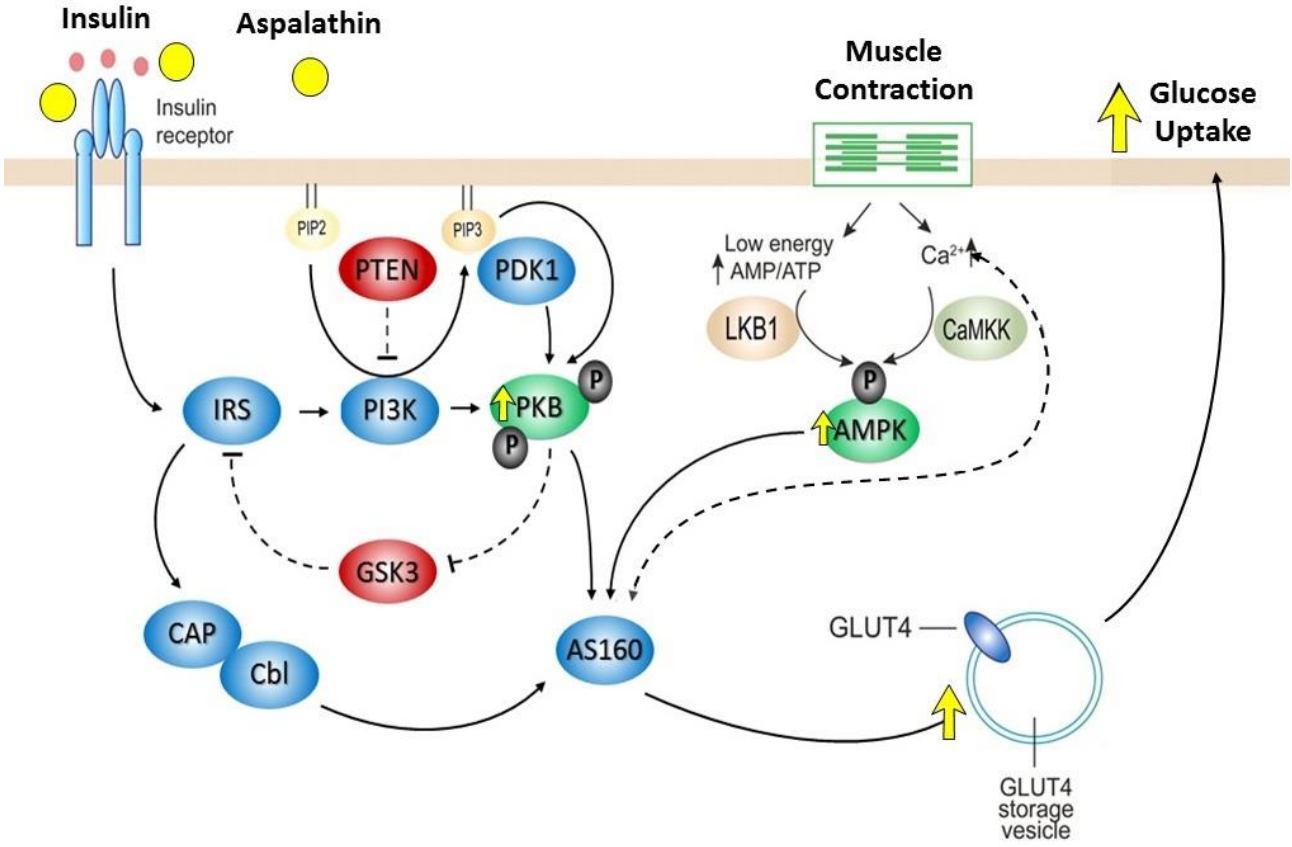

Figure 8.1 Aspalathin's proposed mechanism of action to induce glucose uptake in cardiomyocytes

5.4 ANTIOXIDANT-MEDIATED EFFECTS

The balance between reactive oxygen species, antioxidants and their related co-factors are critical when managing health, ageing and age-related disorders (Rahman, 2007). Oxidative stress is constantly in balance between the body's endogenous antioxidant systems, regulated by co-factors, and exogenous antioxidants ingested as part of a diet. If the protection provided by the body's inherent antioxidants and certain co-factors are surpassed by an abundance of free radicals, oxidative damage start to accumulate, and as aging progress can result in various complications, including CVD and diabetes (Rahman, 2007). Elevated blood glucose levels have been shown to increase oxidative stress (Midaoui & Champlain, 2005). In a study done by Yasunari et al. (1999), the antioxidants, probucol and α-tocopherol, increased glucose uptake in

coronary vascular smooth muscle cells (VSMC) in a high glucose medium (22.2mM) by reducing protein kinase C (activated PKC generates reactive oxygen species) and glycoxidation (results in oxidative stress following the oxidation of proteins in the presence of glucose), effectively supressing intracellular oxidative stress. In contrast, in another study done by Kim et al. (2013), 50-100μM capsaicin was able to induce glucose uptake in C2C12 muscle cells via ROS generation and activation of the ROS/AMPK/p38/MAPK pathway (**refer to Section 1.4.6 in the Literature Review Chapter**). Co-treatment with the non-specific antioxidant, N-acetyl-cysteine (NAC), resulted in attenuation of the increases in both capsaicin-induced AMPK phosphorylation and capsaicin-induced glucose uptake. It has been shown that aspalathin can exhibit both pro- and antioxidant properties depending on the concentration administered (Mennen et al., 2005; Dludla et al., 2014). In the present study we did not measure the anti-oxidant activity of aspalathin, but aspalathin could induce glucose uptake through either of these two independent mechanisms: (i) by acting as a pro-oxidant, inducing glucose uptake via ROS generation, which is a known activator of AMPK, or (ii) by acting as an antioxidant, attenuating the oxidative stress induced by hyperglycemia.

6. SUMMARY OF FINDINGS

The individual findings are as follows:

- a high-fat, high-sucrose diet of at least 16 weeks is an effective model to induce insulin-resistant, obese rats
    - (i) a high-fat, high-sucrose diet of at least 16 weeks raise body weight and induce obesity (**Figure 4.1**);
    - (ii) a high-fat, high-sucrose diet of at least 16 weeks raise visceral fat accumulation (**Figure 4.2**);
    - (iii) a high-fat, high-sucrose diet of at least 16 weeks induce fasting hyperglycemia (**Figure 4.3**);
    - (iv) a high-fat, high-sucrose diet of at least 16 weeks induce non -fasting hyperglycemia (**Figure 4.4**);
    - (v) a high-fat, high-sucrose diet of at least 16 weeks raise fasting blood insulin levels (**Figure 4.5**);
    - (vi) a high-fat, high-sucrose diet of at least 16 weeks raise the HOMA-IR index (**Table 4.1**);
    - (vii) insulin treatment for 45 mins dose-dependently increase glucose uptake more significantly in cardiomyocytes isolated from young rats, followed by older control rats, and had a weak response HFD rats (**Figure 5.7**);

- aspalathin and insulin co-treatment for 45 mins induce glucose uptake in cardiomycoytes isolated from young rats
    - (viii) the isolation protocol persistently yielded a cell viability between 65 – 70% in cardiomyocytes isolated from young rats (**Figure 5.1**);
    - (ix) aspalathin treatment for 1 to 3 h did not affect cell viability in cardiomyocytes isolated from young rats (**Figure 5.2**);
    - (x) aspalathin treatment for 45 mins did not induce glucose uptake in cardiomyocytes isolated from young rats (**Figure 5.5**);
    - (xi) aspalathin co-treatment with insulin for 45 mins increase glucose uptake compared to insulin in cardiomyocytes isolated from young rats (**Figure 5.6; Figure 5.8**), while this effect is not observed in aged rats (**Figure 5.8; Figure 5.9**);

- aspalathin treatment for 3 and 6 hours induce glucose uptake in differentiated H9C2 cells
    - (xii) aspalathin treatment for 3 h, as well as co-treating with 1nM insulin for the last 15 mins increased metabolic activity in differentiated H9C2 cardiomyocytes (**Figure 6.1**);
    - (xiii) aspalathin treatment for 3 h increased cell integrity in differentiated H9C2 cardiomyocytes (**Figure 6.2, Figure 6.3**);
    - (xiv) aspalathin treatment for 3 and 6 h increased glucose uptake in differentiated H9C2 cardiomyocytes (**Figure 6.4**);

- aspalathin treatment for 1 hour 30 minutes to 3 hours induce glucose uptake in cardiomyocytes isolated from young rats, whilst stimulating insulin-mediated glucose uptake in aged controls after 1 hour 30 minutes
    - (xv) aspalathin treatment for 1 h 30 mins, 2 h and 3 h increased glucose uptake in cardiomyocytes isolated from young control rats (**Figure 5.10, Figure 5.11**);
    - (xvi) aspalathin treatment for 1 h 30 mins increased, in a concentration-dependent manner, the insulin-stimulated glucose uptake in cardiomyocytes isolated from aged control rats (**Figure 5.10**);
    - (xvii) aspalathin treatment (0 – 3 h) did not affect insulin-stimulated glucose uptake by cardiomyocytes isolated from obese, insulin resistant animals (**Figure 5.10, Figure 5.11**) ;

- aspalathin treatment for 15 minutes induce AMPK expression, while co-treatment with insulin increase AMPK activation, PKB activation and PKB activation/expression ratio in cardiomyocytes isolated from young rats.
    (xviii) aspalathin and insulin pretreatment with wortmannin for 45 mins results in complete inhibition of glucose uptake in cardiomyocytes isolated from young rats (**Figure 7.1**), aged control and HFD rats (**Figure 7.2**);
    (xix) aspalathin and insulin pretreatment with wortmannin for 15 mins results in a complete loss of PKB activation and expression in cardiomyocytes isolated from young rats (**Figure 7.3**);
    (xx) aspalathin and insulin co-treatment for 15 mins resulted in increased PKB activation and PKB activation/expression ratio in cardiomyocytes isolated from young rats (**Figure 7.3**);
    (xxi) aspalathin treatment for 15 mins resulted in increased AMPK expression in cardiomyocytes isolated from young rats, while co-treatment with insulin increased AMPK activation (**Figure 7.4**);

- aspalathin treatment for 1 hour 30 mins increase the AMPK activation/expression ratio, while co-treatment with insulin increase PKB activation in cardiomyocytes isolated from young rats. AMPK expression and activation increases with age in wistar rats.
    (xxii) aspalathin treatment for 1 h 30 mins did not result in increased PKB activation or expression in cardiomyocytes isolated from either young, aged obese and insulin resistant, or age-matched control rats (**Figure 7.6**);
    (xxiii) aspalathin and insulin co-treatment for 1 h 30 mins resulted in increased PKB activation in cardiomyocytes isolated from young control rats (**Figure 7.7**);
    (xxiv) aspalathin treatment for 1 h 30 mins resulted in increased AMPK activation/expression ratio in cardiomyocytes isolated from young rats (**Figure 7.9**);
    (xxv) aged control rats have significantly higher AMPK expression and activation compared to young rats (**Figure 7.9**);

Controversially, in the present study, aspalathin had no significant effect on glucose uptake, or mechanistically, in isolated cardiomyocytes from obese, insulin-resistant rats.

7. STUDY LIMITATIONS

The rats used in the study were housed in a controlled environment without exposure to toxins, environmental hazards, and related factors that would further exacerbate obesity and insulin resistance in humans (Murea et al., 2012). Furthermore, caging of the animals force them to become sedentary, accelerating obesity, glucose intolerance and effectively increase their

susceptibility for premature death (Martin et al., 2010) which might not serve as accurate controls for the disease conditions in humans. Furthermore, the diet program (weeks of feeding) was not kept constant throughout the study, necessitating the use of diet rats differing up to 14 weeks in age. Experiments were always performed in same-aged animals after which the results were normalized to the baseline treatment group. These factors can potentially skew interspecie extrapolation with regards to obesity, metabolism and T2D.

In the present study we only investigated the effect of aspalathin in the ventricular cardiac tissue. Given that the heart comprises various different cell types in which aspalathin could induce an effect, further investigation using isolated perfused hearts would be needed to explore aspalathin's role on functional parameters of the whole heart. Furthermore, we were unable to find GLUT4 translocation in membrane and cytosol fractions of ventricular cardiomyocytes isolated from rat hearts. We have tried various different methods to visualize the total GLUT4 antibody in our tissue lysates, but was unsuccessful at the culmination of this thesis.

CHAPTER 9

CONCLUSION AND FUTURE RESEARCH

1. CONCLUSION

Aspalathin has been shown to have certain effects on skeletal muscle glucose transport in lean and diabetic animals, but it's myocardial effects, as well as it's role in obesity and insulin resistance are not well established. We considered aspalathin's potential as a hypoglycemic agent in treatment of hyperglycemia in obesity and insulin resistance.

The present thesis demonstrated the glucose uptake effects of relatively short-term *in vivo* treatment with aspalathin on cardiomyocytes isolated from the hearts of healthy, young and aged rats, as well as aged obese and insulin resistant rats. To determine the safety and efficacy of using aspalathin, we also demonstrated the glucose uptake ability of aspalathin in cultured differentiated H9C2 cardiomyocytes.

The main findings of this thesis are the following:

- the high-fat, high-sugar diet is an effective model to induce insulin resistance in rats
- aspalathin enhances metabolic activity and retain membrane integrity in cultured H9C2 cells
- aspalathin induces myocardial glucose uptake directly and potentiated the effects of insulin in cardiomyocytes isolated from young rats
- in older animals, aspalathin had a more indirect effect on glucose uptake through mediating insulin's action
- the possible mechanism of aspalathin is through:
    - activation of PKB
    - increasing the expression and activation to expression ratio of AMPK
- aspalathin had no significant effect when used as treatment in heart cells from obese, insulin-resistant rats.

Finally, this thesis demonstrated that aspalathin, as a pleiotropic compound, has a very specific dosage duration and elicits its effects in a dose dependent manner.

2. PERSPECTIVES FOR THE FUTURE

Rooibos' success in reducing cardiovascular risk factors when consumed daily is evident (Marnewick et al., 2012). Dietary intake has especially been met with favorable outcomes, and could reinforce existing treatments (Coman et al., 2012). The next step is consumption of the main

compounds within rooibos, such as aspalathin as part of a dietary regime in order to clinically investigate the effects of aspalathin. For future studies, aspalathin, as a phytomedicine, needs to be used as part of a feeding regimen, therefore *in vivo*, to investigate its effects on insulin resistance (induced by a high-fat diet), obesity, heart function and protection, metabolism, long-term oxidative status and anti-inflammatory properties. It is not possible to culture adult cardiomyocytes indefinitely as they are terminally differentiated cells, and therefore it is questionable whether the pathology induced by metabolic changes in cell culture is retained. Therefore, we need to study the effects of aspalathin on the hearts of control and obese, insulin-resistant animals as commercial cell lines only partially represent true heart cells. Furthermore, aspalathin (acute- and long-term) still needs to be investigated as treatment for ischeamia/reperfusion injury and its role in mitochondrial autophagy (mitophagy) and dysfunction determined.

Aspalathin's mechanism has only been partially elucidated in vitro with specific regards to two proteins (AMPK and PKB). Future studies need to elaborate on the signaling molecules involved in other pathways, including the map kinases, ERK42/44, the glycogen synthase regulator, GSK-3β and auto-immune regulators, such as STAT-3. Of special importance, the role of aspalathin on GLUT4 expression and translocation to the cell membrane still needs to be elucidated.

CHAPTER 10
APPENDIX A

1. SECONDARY FACTORS CONTRIBUTING TO OBESITY

1.1 INACTIVITY

Physical inactivity, especially during adolescence, is an genetically independent indicator of total and abdominal obesity in young adulthood (Pietiläinen. 2008). In short, a physically inactive lifestyle triggers weight gain by altering our energy balance. Conversely, leading an active lifestyle triggers weight loss by discarding more energy than is consumed.

1.2 UNHEALTHY DIET

A diet is fine-tuned for personal needs based on health goals, taste, satiety, cost and experience. However, certain food is classified as unhealthy based on the long-term health implications. These include a high caloric diet (not dispensed by activity), inadequate consumption of fruits and vegetables high in anti-oxidants, high consumption of salted products and processed sugars, as well as high consumption of saturated- and trans-fatty acids (Obesity, WHO, 2015).

1.3 PREGNANCY

The childbearing years can be an essential period for most women, but possibly also result in substantial increase in weight during pregnancy. In a study done by the Center for Disease Control and Prevention (CDC) in 2009, an estimated 43% of pregnant women gain more weight than is recommended. High gestational gain also increases the risk of becoming overweight post-pregnancy, possibly due to altered lifestyle habits in the postpartum period (Gunderson, 2009).

Obese or overweight women undergoing their first pregnancy tend to also retain and gain more weight postpartum compared to women of average weight (Gunderson & Abrams, 1999). Maternal overweight and obesity increases the risk for gestational diabetes mellitus, hypertensive disorders, and newborn macrosomia (Catalano, 2007).

1.4 LACK OF SLEEP

Sleep is an essential regulator of neuroendocrine function and glucose metabolism and 8 hours is recommended (Beccuti & Pannain, 2011). However, a lack of sleep (below 7 hours) alters metabolism by reducing glucose tolerance and disrupts endocrine function through the appetite regulating hormones leptin (decreasing satiety) and ghrelin (stimulating hunger). Multiple laboratory and epidemiological studies link short sleep duration and poor sleep quality (overall sleep loss) to obesity risk (Beccuti & Pannain, 2011).

1.5 MEDICATION

Various psychiatric medications, including certain anti-depressants, antipsychotics, anti-seizure medication and moodstabilizers, have shown to increase weight gain and ultimately lead to obesity in certain patients (Griggs, 1991; Schwartz et al., 2004). It is still speculated as to the extent of weight gain caused by short term versus long term treatments with these medications.
Corticosteroids, effective in treatment of acute inflammatory conditions such as ashtma, inflammatory bowel disease and rheumatoid arthritis, is also well documented to cause weight gain (Manson et al., 2009).

Sulfonylureas, used in the treatment of type 1 and type 2 diabetes to lower blood glucose, have been shown to increase appetite and weight gain (Nathan et al., 2009). Similarly, Insulin was also shown to increase weight gain, but the exact mechanism remains unknown (Russell-Jones & Khan, 2007). It is speculated that, by reducing blood glucose without reducing caloric intake, insulin may trigger the excess calories to be stored as added weight.

β-blockers, used in the treatment of hypertension to reduce elevated cardiac output, increases the patients propensity for weight gain (Sharma et al., 2001). This is primarily due to changes in the metabolic profile of patients taking these drugs.

Hormonal contraceptives have long been speculated to increase weight gain (Gallo et al., 2011). However, it is still unclear to date whether weight fluctuations noticed in women on birth control are due to increases in fat explicitly or due to temporary fluid retention and muscle composition changes.

1.6 MEDICAL PROBLEMS

Obesity can also be induced by medical conditions, including Prader-Willi syndrome and Cushing's syndrome (Heart Disease, Mayo Clinic, 2015). Certain conditions, such as arthritis, can indirectly cause obesity by decreasing a person's physicality as a consequence of pain or discomfort. To date, it is still unclear whether a decrease in thyroid function, a condition often synonymous with having a "slow metabolism", influences the development of obesity (Longhi & Radetti, 2013).

2. HEART DISORDERS

The World Health Organization defines cardiovascular diseases as “a group of disorders of the heart and blood vessels,” including:

- coronary heart disease (compromised blood supply to the heart muscle)
- cerebrovascular disease (compromised blood supply to the brain)
- peripheral arterial disease (compromised blood supply to arms and legs)
- rheumatic heart disease (weakening of the heart due to rheumatic fever)
- congenital heart disease (heart defects since birth)
- deep vein thrombosis (bloot clots in periphery of body)
- pulmonary embolism (dislodged blood clots travelling to the heart and lungs)

Heart attacks refer to a blockage that prevents blood from flowing to the heart and brain. This event is most commonly caused by deposits of adipose tissue that clog the inner linings of blood vessels supplying the heart and brain.

2.1 CAUSES

Behavioural risk factors, such as an unbalanced diet, inactive lifestyle, smoking and alcohol abuse give way to heart disease and strokes. Clinically, these risks manifest as hyperglycemia, hypertension, hyperlipidemia and obesity. These preliminary symptoms can be detected at primary care facillities and aid in assessing the risk for cardiovascular diseases. Also, the forces driving social, economic and cultural change, such as globalization, urbanization, population ageing, poverty, stress and hereditary factors can be added determinants of cardiovascular disease.

2.2 EPIDEMIOLOGY

Cardiovascular diseases (CVD) are the leading cause of death in the world (Cardiovascular Disease, WHO, 2015). An estimated 17.5 million people died from CVD in 2012 alone, representing 31% of all global deaths. Of these 7.4 million were due to coronary heart disease and 6.7 million were due to strokes. Low- and middle-income countries account for 75% of CVD deaths. People in these countries are often not exposed to early detection and subsequent treatments, leading to younger deaths. Furthermore, the poorest people are affected most. This seems to create a vicious circle in which increasing health expenses contribute to poverty, placing a heavy burden on the economy of these countries.

2.3 TREATMENTS FOR CARDIOVASCULAR DISEASES

The fact is, CVD can be prevented by addressing behavioural risk factors such as smoking, physical inactivity, alcohol abuse, consuming unbalanced diets and being obese. These risk factors, left unaddressed, cause hypertension, diabetes and hyperlipidemia, culminating in

cardiovascular diseases. When early detection of these risk factors fails, the disease needs to be controlled through counselling and medication.

2.3.1 Lifestyle Changes

Reducing salt and alcohol intake, avoiding smoking, increasing consumption of fruits and vegetables and regular physical exercise have been shown to reduce CVD complications. Health policies essentially serve to enforce these habits by creating an environment tolerant of healthy behaviours. Unfortunately, complications arise when risk factors are not addressed, necessitating drug treatment to prevent further progression of CVD's.

2.3.2 Interventions

Currently there are two approaches to alleviate the CVD burden: population-wide interventions and individual interventions. Population-wide interventions include amongst others, tobacco control policies, taxation to reduce the intake of foods high in fat, sugar and salt, building manual infrastructure such as walking and cycling paths, strategies to prevent alcohol abuse and enforcing good meal plans for youth programs. Individual level interventions are primarily targeted to people with a high total cardiovascular risk or having extreme single risk factor levels such as hypertension and hypercholesterolaemia.

2.3.3 Medication

Secondary prevention in patients who already have cardiovascular diseases, include medicinal treatment with aspirin (anti-prostaglandin action – reduces inflammation, fever and pain; and anti-platelet action – blood thinner), beta-blockers (blocks the action of adrenaline, reducing heart rate and effectively lowering blood pressure), angiotensin-converting enzyme inhibitors (inhibits constriction of blood vessels, reducing blood pressure) and statins (block formation of cholesterol in the liver, reducing LDL-cholesterol in the blood) (Mayo Clinic Staff, 2014). Furthermore, if the disease evolves, surgical interventions are needed. These operations include coronary artery bypass, balloon angioplasty, valve repair and replacement, heart transplantation and artificial heart operations. Medical devices can also be inserted to treat CVDs. These specialized equipments include pacemakers, prosthetic valves and patches to cover heart damage.

3. INVESTIGATING HEART FUNCTION

Various disease states negatively targets heart function and as a consequence, the whole organism becomes susceptible to the disease. In order to investigate the effect of treatments and disease states on heart function, models are used to test the efficacy of intervention protocols (Lumkwana, 2014). These models can be broadly categorized into:

- *in vivo* models (using the whole organism/animal)
- *ex vivo* models (isolating the organs of an animal), and
- *in vitro* models (culturing isolated organ cells).

These models will be discussed with specific reference to the heart.

3.1 IN VIVO MODEL (WHOLE BODY ORGANISM)

In vivo models utilize the entire animal, in either a conscious or subconscious (induced by anaesthesia) state. This approach shares a close resemblance to human clinical studies, and can therefore serve as a strong indicator of possible effective therapies (Ytrehus, 2006). Animals most commonly used include rats, mice, rabbits and dogs. However, the cause and effect observed in animals are often difficult to establish, given uncontrollable factors, unrelated to the heart. These include the techniques and instruments used to isolate hearts during surgery, and the unpredictability of inducing anaesthesia on the central nervous system of the animals. Drawbacks for these models include time-consuming maintenance when treating the animals (Ytrehus, 2006).

3.2 EX VIVO MODEL (ISOLATED HEARTS)

Isolated heart models have been employed with varying success to explore the principles of cardio-protection, cell signaling and investigating metabolic changes in the myocardium (Ytrehus, 2006). Two prominent models exist, including the Langendorff perfusion model and the Morgan working heart model. Isolated heart models enable researchers to study contractile function, as well as biochemical and metabolic changes (Mirica, 2009). However, these models remain very expensive and time-consuming, and in addition needs to be operated by a perfusion specialist.

3.2.1 RAT AND MICE HEART MODELS

A popular animal model used to mimic the human pathophysiology in obese patients, is the diet-induced obesity model, whereby an elevated caloric intake via fat in the diet results in increased fat and insulin resistance (Sumiyoshi et al., 2006). Studies using isolated working heart models from obese and insulin resistant *ob/ob* and *db/db* mice noted elevated fatty acid oxidation compared to normal control mice (Mazumber, 2004; Belke et al., 2000). The elevated fatty acid oxidation was paralleled by a suppression of glucose oxidation and glycolysis and a suppression in cardiac efficiency. Mitochondrial respiration, when using palmitate as fuel source, was also kept constant,

even in obese mice, but pyruvate oxidation and pyruvate dehydrogenase activity was reduced. This indicated that obesity did not impair fatty acid oxidation, but rather negatively affected carbohydrate metabolism in a manner consistent to diabetes (Boudina et al., 2005). Also, in isolated rat hearts with diet-induced obesity and insulin resistance, as the fatty acids' contribution to total energy production increased, the rats were prone to become more glucose intolerant and insulin resistant. Other mechanisms, however, such as LPL (lipoprotein lipase) activity can also increase β-oxidation, as was observed in an obese mouse model prior to substrate changes (Burkhoff et al., 1991).

3.3 In vitro model (Heart Cells)

Cellular models enable investigators to study the heart at cell function level. These models can also be employed in analyzing biochemical pathways, observe changes in morphology and investigate the effects of genetic manipulation. In general, there are three different types of heart cell models, including cardiac cell lines, neonatal cardiomyocytes and adult cardiomyocytes. The major advantage of using cell models is that there is no need for animals, saving cost on handling and feeding of animals, and saving time by not having to complete the feeding regimes or gain ethical clearance.

3.3.1 Cardiac Cell Lines

Cardiac cell lines are isolated from embryonic hearts and are available commercially as immortalised cell lines. The most popular cell lines include HL-1 (Claycomb et al., 1998) and H9C2 (Hescheler et al., 1991). The primary advantage of cell lines is their ability to remain viable in culture for extended periods of time, not necessitating constant re-isolations. However, this is also their drawback, since constant division of cells is not a function of terminally differentiated cardiomyocytes of in vivo adult hearts (Watkins et al., 2010). Furthermore, both HL-1 and H9C2 differ from adult cardiomyocytes in morphology and metabolism. HL-1 cells are round-shaped and H9C2 spindle-shaped, and both rely on glucose as their primary energy substrate, whereas adult cardiomyocytes are rod-shaped and utilize both glucose and fatty acids for energy metabolism (Eimre, 2008).

3.3.2 Neonatal Cardiomyocytes

Neonatal cardiomyocytes are obtained from newborn rats or mice, usally 1-5 days in age (Chlopčíková et al., 2001). The isolation process is considered to be simpler than isolating adult heart cells since the young rat heart are calcium tolerant and maintains viability, whereas adult hearts are calcium sensitive, making it difficult to completely arrest the heart and reduce infarct size (Louch et al., 2011). However, neonatal cardiomyocytes do not represent fully differentiated rod-shaped adult cardiomyocytes, utilize only glucose as energy substrate and contains a

pseudopodia shape (“false feet” visible as extended branches protruding from the cell membrane) (Lumkwana, 2014).

3.3.3 Adult Cardiomyocytes

Adult cardiomyocytes are most similar to in vivo hearts when comparing development, morphology and metabolism (White et al., 2004). Compared to the other two cell models, adult cardiomyocytes give the best representation of the human adult when investigating diseases more prevalent in the adult population, such as myocardial infarction and diabetes type 2.

Adult ventricular cardiomyocytes was first isolated by Powell & Twist in 1976, and the protocol has been modified several times since (Lumkwana, 2014). However, no single isolation procedure produces high quality, viable cells without modifications. This drawback makes isolating and culturing of adult cardiomyocytes the least common model used and is therefore only performed by perfusion specialists (Döring, 1990). Various factors can influence the viability of cells acquired during isolating, including:

- **Anaesthesia**

Administration of an anaestethic, by either injection of barbiturates (pentobarbital) or inhalation of ether, halothane or isoflurane, can influence heart performance (Biebuyck et al., 1987). In a study done by Segal et al., (1990), the effects of anaesthesia on rat heart function in response to calcium-influx-mediated activity was compared to that of non-anaesthetized animals using the Langendorff system. Both hearts experienced an increase in inotropic activity (the force of muscle contraction) in response to gradual increases in calcium concentration of the perfused medium. However, anaesthesia inhibited thyroid hormonal function, dissipating the added inotropic activity of thyroid hormones. Also, hearts subjected to anaesthesia was more prone to arrhythmias in response to gradual increases of calcium (Segal et al., 1990). Although administering anaesthesia has its disadvantages, intraperitoneal injection of barbiturates is most widely used given that no complicated equipment is necessary and the depressive effect on heart function is entirely eliminated after 10 minutes of ceasing anaesthesia (Döring & Dehnert, 1988).

- **Animal Handling**

Regardless of the procedure to follow, conscious effort needs to be taken to reduce exposing the animal to a stressful environment prior to its sacrifice. This also includes minimizing its handling altogether. Before surgery can commence, the animal needs to present with a total lack of pain response, determined by initiating a pain stimulus, such as pinching its paws (the pedal withdrawal reflex) (Skrzypiec-Spring et al., 2007).

- **EXCISION OF THE HEART**

The time between excision of the heart, the subsequent transferring into ice cold saline (Krebs-Henseleit) solution with low calcium (to stop the heart from beating and prevent ischemic injury prior to perfusion), followed by mounting of the heart on the perfusion system is the most crucial aspect in acquiring healthy, viable cells. It is recommended that this entire step be performed in less than 30 seconds and kept constant between experiments, since prolonged exposure to this ischemic period establishes ischemic preconditioning of the heart (Sutherland & Hearse, 2000).

- **CANNULATION OF THE HEART**

Before the heart is cannulated onto the perfusion apparatus, the cannula and tubes of the system need to be inspected for leakages and air bubbles. It is advised to let the perfusate drip freely before mounting the heart (Doring & Dehnert, 1988). Upon mounting of the heart, stretching or ripping of the aorta need to be avoided and the cannula should not penetrate the aortic heart valve, giving inadequate perfusion of the coronary arteries (**Figure. 10.1**)(Xu & Colecraft, 2009). Once the aorta is secured in place using sutures, the appropriate flow rate or flow pressure of the perfusate is established. The heart will turn pink as residual blood from the capillaries are removed. Within 10 minutes, normal contractile function and regular heart rhythm are reinstilled (Doring & Dehnert, 1988).

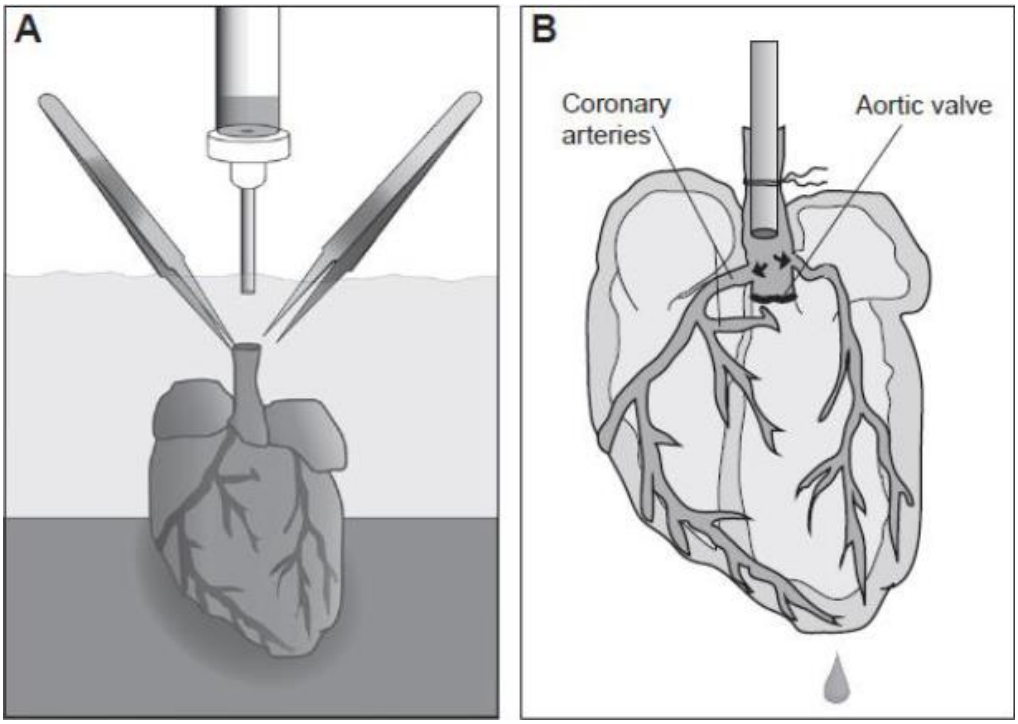

Figure 10.1 Cannulation of the rat heart. (A) After excision from the rat, the heart is kept in ice cold Krebs-Henseleit buffer and mounted onto a cannula. **(B)** The cannula is inserted into the aorta and fastened in position with adequate space to allow proper flow through the coronary arteries (Louch et al., 2011)

- **PERFUSION SOLUTIONS**

Most perfusion studies make use of a bicarbonate-based physiological salt solution, developed by Krebs and Henseleit. The solution mimics the contents of blood plasma, has a pH of 7.4 at 37°C and is continuously gassed with 95% O_2 and 5% CO_2. The most common perfusion solution constitutes 118.5mM NaCl, 25.0mM $NaHCO_3$, 4.7mM KCl, 1.2mM $MgSO_4$, 11mM Glucose and 2.5mM $CaCl_2$ (Sutherland & Hearse, 2000). Popular modifications to the solution include lowering calcium and potassium concentrations (these bind to proteins present blood plasma, but no proteins are present in perfusates), lowering glucose concentration (5.5mM), adding insulin (2-10 IU/L), pyruvate (2-10mM) or fatty acids (0.3-0.9mM) (Skrzypiec-Spring et al., 2007). The drawbacks of using buffer preparations include elevated coronary flow rates, the lack of hemoglobin makes oxygen transport problematic, as well as the absence of proteins, hormones and cellular components present in and when compared to blood (Skrzypiec-Spring et al., 2007).

- **TEMPERATURE OF PERFUSION**

Cardiac contractile function, especially heart rate, is strongly influenced by temperature. Therefore, perfusion need to be performed at body temperature of the specie (37°C for Rats and Humans) used in the experiment (Sutherland & Hearse, 2000). In order to negate the effects of the room temperature air surrounding the heart and perfusates, a glass reservoir with recirculating water (thermostatically controlled), encapsulates the heart and perfusion solutions.

- **OXYGEN DURING PERFUSION**

In the Langendorff perfusion system, oxygen availability results from the product of coronary flow and the oxygen content of the medium (Kammermeier, 1994). A mixture of 95% oxygen and 5% carbon dioxide (maintain the correct pH of the Krebs-Henseleit buffer at 37°C) is added to the perfusion solutions through gassing. However, crystalloid buffers have very low oxygen carrying capacity, resulting in elevated coronary perfusion rates. Some researchers supplement the perfusion solutions with red blood cells, known for their ability to carry oxygen, which results in normalization of coronary flow rates (Bergmann et al., 1979).

- **CALCIUM PARADOX**

When normal calcium-levels are reintroduced in cardiac muscles, after perfusion with calcium-free buffers, calcium overload of the cells can occur, whereby they remain in a sustained contracted state and die. This phenomenon is known as the calcium paradox (Piper, 2000). In order to prevent this and produce calcium-tolerant cardiomyocytes, calcium needs to be systematically reintroduced to the cells, starting at concentrations far below physiological calcium concentrations. During perfusion the first stepwise increase of calcium is started, as well as during further enzymatic digestion of the hearts after removing the hearts from the Langendorff perfusion system.

- **ENZYMATIC DIGESTION**

Using a Langendorff Apparatus, hearts are retrogradely perfused with a calcium free solution to rinse out all the blood from the coronary arteries (Mitcheson et al., 1998). The perfusion solution is then switched to contain enzymes, such as Colleganse Type II, to digest the extracellular matrix. Due to the high cost of enzymatic solutions, the perfused medium is recycled till the heart reaches "streaming" – the point where solution freely runs through the heart by gravitational pull, denoting that the bulk of the heart's inner matrix is fully digested (Louch et al., 2011).

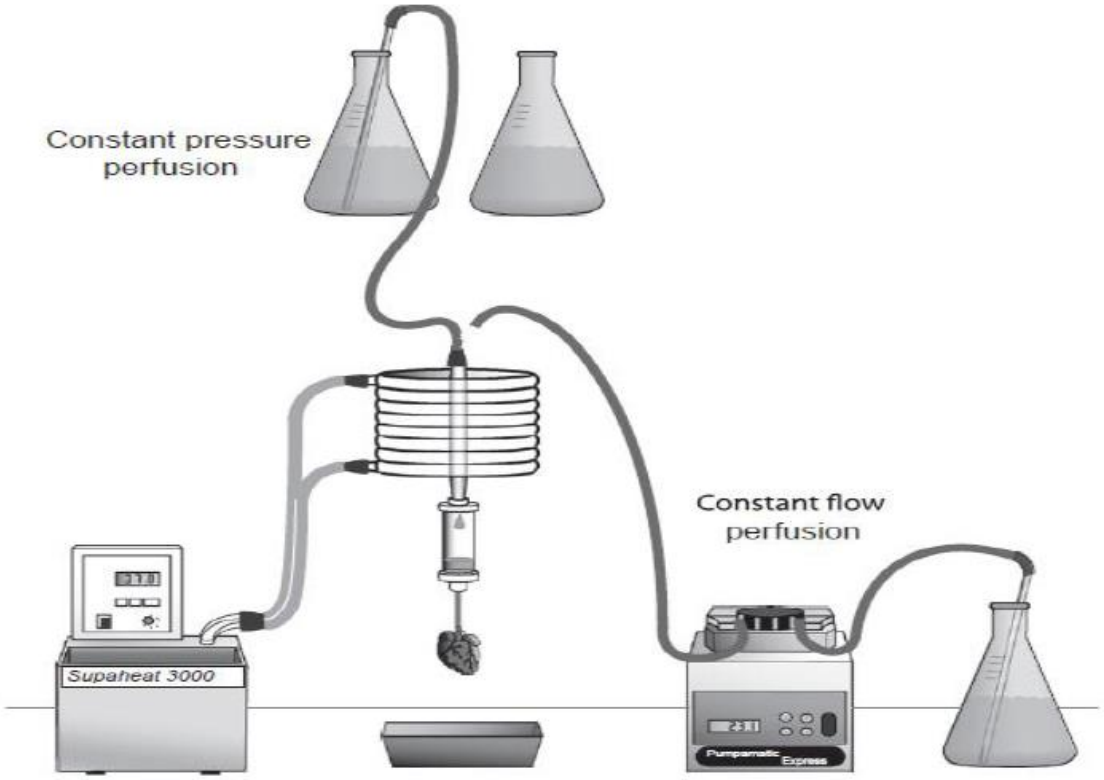

Figure 10.2 Langendorff apparatus. The heart can be perfused by either constant pressure perfusion, under gravitational pull **(LEFT)** or constant flow perfusion, using a mechanised flow regulator **(RIGHT)** (Louch et al., 2011)

The choice of enzymes used, is also a significant indicator of the overall health of cardiomyocytes. The most widely used enzyme for cardiomyocyte isolation is Collagenase Type II (Worthington), containing the highest clostripain activity of any enzyme (Louch et al., 2011). Other suitable enzymes include proteases and pancreatin, as well as collagenase B & D (Roche). Significant variation can be observed between batches, and it is therefore recommended that newly purchased batches be tested for their enzyme activity. A simple technique to calculate enzyme activity is to perform a cell count after isolation, by comparing the amount of rod-shaped and round-shaped cells (Mitcheson et al, 1998).

4. ALTERNATIVE PATHWAYS OF INSULIN-DEPENDENT GLUCOSE UPTAKE

4.1. ERK PATHWAY

ERK (extracellular-signal-regulated kinases) or mammalian MAPK (mitogen-activated protein kinases) are intracellular protein kinases which plays a diverse role in cell differentiation and cell division. The ERK pathway is activated in response to a multitude of extracellular effectors, including growth factors, cytokines, viral infections, transforming agents, GPCR (G-protein coupled receptor) ligands and carcinogens.

The best understood MAPK is ERK1 (p44 MAPK) and ERK2 (p42 MAPK) which are distributed in all tissue types. ERK p42/p44 are MAPK subtypes that mediate the mitogenic and the pro-inflammatory effects of insulin (Sasaoka et al., 1994). In resting cells, ERK1/2 immediately accumulates in the nucleus upon stimulation. The activation of the ERK cascade is mediated by upstream mitogen-activated protein kinase kinase 1/2 (MEK1/2). Once activated, ERK1/2 phosphorylate a variety of substrates, such as the membrane proteins, CD120a, Syk and calnexin, the nuclear substrates, SRC-1, Pax-6, Elk-1, MEF2, c-Fos, c-Myc and STAT3, several MAPK-activating protein kinases (MK's), MAPK-interacting (MNK's) and cytoskeletal proteins. Due to the magnitude of influence of the ERK pathway, is has been seen to play conflicting roles in cellular processing, including proliferation, differentiation, metabolism, morphology, survival and programmed cell death (Deng et al., 2012). The ERK cascade consists of Ras, Rafs, MEK1/2, ERK1/2 and the MAPKAPK's (MAPK-activating protein kinases), Elk-1, Sap1a and c-Fos.

4.2. P38 PATHWAY

p38's, also called CSBP (cytokinin specific binding proteins), are a class of MAPK's sensitive to cytokines and stress signals. They play a role in cell differentiation, apoptosis and autophagy. The p38 family has 4 different isoforms, p38α, p38, p38γ and p38δ and similar to the other MAPK's are expressed throughout all tissue types (Deng et al., 2012). The p38 consists of the upstream molecules MEKK3, MKK3/4/6, which activates p38 and in turn activates the MK's, MK2/3/5. Elk-1, CHOP, ATF2 and MEF2A. The p38 MAPK cascade is stimulated by promigratory factors, such as platelet-derived growth factor (PDGF), Ang II, S1P and thrombin, environmental stresses, including ultraviolet radiation, heat shock and osmotic shock, and inflammatory cytokines (Deng et al., 2012).

4.3. JNK PATHWAY

JNK (c-Jun N-terminal kinases) or SAPK (Stress-activated protein kinases) are kinases that form part of the MAPK family and is activated in response to cytokines and cellular stress. The JNK family comprises 3 different isoforms, JNK1, JNK2 and JNK3, also known as SAPKγ, SAPKα and SAPKβ resprectively. Generally, JNK1/2 are localised throughout every tissue type, whereas JNK3 is primarily found in the brain (Bode & Dong, 2007). The MAPK's, MKK4 and MKK7, activate JNK,

which then binds and phosphorylates the Ser-63 and Ser-73 subunits of c-Jun, leading to inflammation. JNK can also be inactivated by Ser/Thr and Tyr protein phosphatases (Ip & Davis, 1998).

JNK is more sensitive to upstream activators compared to the other MAPK's and in turn lends to the complexity and role of JNK. The JNK pathway can be stimulated in response to UV-radiation, protein synthesis inhibitors (anisomycin), osmotic shock, heat shock, toxins, anticancer drugs, ceramide, peroxide, anti-inflammatory cytokines and ischemia/reperfusion injury during heart attacks (Deng et al., 2012). Upon activation, JNK translocates to the nucleus where subsequent phosphorylation of effector molecules occur. These include ATF2, NF-ATc1, HSF-1, c-Myc, p53, STAT3 and DPC4/SMAD4/MADH4. JNK can also regulate non-transcription factors, including Bcl-2, Bcl-xL and paxillin. The cascade is involved in various cellular processes, including neuronal degeneration and development, as well as cell development, differentiation and death. It also regulates inflammation and cytokine production.

CHAPTER 11
REFERENCES

Abdel-Aleem, S. & Lowe, J.E. 1998. *Cardiac metabolism in health and disease*. Springer US

Abdul-Ghani, M.A. & DeFronzo, R.A. 2010. Pathogenesis of Insulin Resistance in Skeletal Muscle. *Journal of Biomedicine and Biotechnology*, 2010:1-19.

Abel, E.D. 2007. Glucose for the Aging Heart? *Circulation*, 116(8):884-887.

Aguirre, V., Uchida, T., Yenush, L., Davis, R. & White, M.F. 2000. The c-Jun NH2-Terminal Kinase Promotes Insulin Resistance during Association with Insulin Receptor Substrate-1 and Phosphorylation of Ser307. *Journal of Biological Chemistry*, 275(12):9047-9054.

Ahrén, B. & Taborsky, G.J. 1986. The Mechanism of Vagal Nerve Stimulation of Glucagon and Insulin Secretion in the Dog*. *Endocrinology*, 118(4):1551-1557.

Alberti, K.G.M.M. 2009. Harmonizing the Metabolic Syndrome: A Joint Interim Statement of the International Diabetes Federation Task Force on Epidemiology and Prevention; National Heart, Lung, and Blood Institute; American Heart Association; World Heart Federation; International Atherosclerosis Society; and International Association for the Study of Obesity. *Circulation*, 120(16):1640-1645.

Alessi, D.R. 1996. Mechanism of Activation of Protein Kinase B by Insulin and IGF-1. *The EMBO Journal*, 15(23):6541-6551.

Ali, A., Hoeflich, K.P. & Woodgett, J.R. 2001. Glycogen Synthase Kinase-3: Properties, Functions, and Regulation. *Chemical reviews*, 101(8):2527-2540.

Altomare, D.A., Guo, K., Cheng, J.Q., Sonoda, G., Walsh, K. & Testa, J.R. 1995. Cloning, Chromosomal Localization and Expression Analysis of the Mouse Akt2 Oncogene. *Oncogene*, 11(6):1055-1060.

American Diabetes Association. 2003. Gestational Diabetes Mellitus. *Diabetes Care*, 26(SUPPL. 1):S103-S105.

An, D. & Rodrigues, B. 2006. Role of Changes in Cardiac Metabolism in Development of Diabetic Cardiomyopathy. *AmericanJournal of Physiology:Cell Physiology.*, 60(4):H1489.

Arora, K. & Pedersen, D. 1988. Functional Significance of Mitochondrial Bound Hexokinase in Tumor Cell Metabolism: Evidence for Preferential Phosphorylation of Glucose by Intramitochondrially Generated ATP. *J Biol Chem*, 263:17422–17428.

Arts, I.C. & Hollman, P.C. 2005. Polyphenols and Disease Risk in Epidemiologic Studies. *The American Journal of Clinical Nutrition*, 81(1 Suppl):317S-325S.

Augustin, R. 2010. The Protein Family of Glucose Transport Facilitators: It's Not Only about Glucose After all. *IUBMB life*, 62(5):315-333.

Baba, H., Ohtsuka, Y., Haruna, H., Lee, T., Nagata, S., Maeda, M., Yamashiro, Y. & Shimizu, T. 2009. Studies of anti-inflammatory effects of Rooibos tea in rats. *Pediatrics International*, 51(5):700-704.

Baggio, L.L. & Drucker, D.J. 2007. Biology of Incretins: GLP-1 and GIP. *Gastroenterology*, 132(6):2131-2157.

Baggish, A.L. & Wood, M.J. 2011. Athlete's Heart and Cardiovascular Care of the Athlete: Scientific and Clinical Update. *Circulation*, 123(23):2723-2735.

BaHammam, A. & Al Dabal, L. 2009. Obesity Hypoventilation Syndrome. *Ann Thorac Med*, 4(2):41.

Balderas-Villalobos, J., Molina-Munoz, T., Mailloux-Salinas, P., Bravo, G., Carvajal, K. & Gomez-Viquez, N.L. 2013. Oxidative Stress in Cardiomyocytes Contributes to Decreased SERCA2a Activity in Rats with Metabolic Syndrome. *AJP: Heart and Circulatory Physiology*, 305(9):H1344-H1353.

Banting, F., Best, C., Collip, J., Campbell, W. & Fletcher, A. 1956. Pancreatic Extracts in The Treatment of Diabetes Mellitus. Diabetes, 5(1):69-71.

Barnett, S., Bilodeau, M. & Lindsley, C. 2005. The Akt/PKB Family of Protein Kinases: A Review of Small Molecule Inhibitors and Progress Towards Target Validation. *CTMC*, 5(2):109-125.

Bayascas, J.R. & Alessi, D.R. 2005. Regulation of Akt/PKB Ser473 Phosphorylation. *Molecular cell*, 18(2):143-145.

Bayascas, J.R. & Alessi, D.R. 2005. Regulation of Akt/PKB Ser473 Phosphorylation. *Molecular Cell*, 18(2):143-145.

Beale, E.G. 2013. Insulin Signaling and Insulin Resistance. *Journal of Investigative Medicine*, 61(1):11-14.

Beaser, R.S., Hollander, P.A. & Silvestri, R. 2015. Inhaled Insulin: Pulmonary Considerations. *Medscape*. Available at: http://www.medscape.org/viewarticle/556041

Beauloye, C. 2001. Insulin Antagonizes AMP-Activated Protein Kinase Activation by Ischemia Or Anoxia in Rat Hearts, without Affecting Total Adenine Nucleotides. *FEBS Letters*, 505(3):348-352.

Beccuti, G. & Pannain, S. 2011. Sleep and Obesity. *Current Opinion in Clinical Nutrition and Metabolic Care*, 14(4):402-412.

Belke, D.D., Larsen, T.S., Gibbs, E.M. & Severson, D.L. 2000. Altered Metabolism Causes Cardiac Dysfunction in Perfused Hearts from Diabetic (*db/db*) Mice. *American Journal of Physiology - Endocrinology and Metabolism*, 279(5 42-5):E1104-E1113.

Benito, M. 2011. Tissue Specificity on Insulin Action and Resistance: Past to Recent Mechanisms. *Acta Physiologica*, 201(3):297-312.

Berenguer, M., Zhang, J., Bruce, M.C., Martinez, L., Gonzalez, T., Gurtovenko, A.A., Xu, T., Le Marchand-Brustel, Y. & Govers, R. 2011. Dimethyl Sulfoxide Enhances GLUT4 Translocation through a Reduction in GLUT4 Endocytosis in Insulin-Stimulated 3T3-L1 Adipocytes. *Biochimie*, 93(4):697-709.

Bergmann, O. 2009. Evidence for Cardiomyocyte Renewal in Humans. *Science*, 324(5923):98-102.

Bergmann, S.R., Clark, R.E. & Sobel, B.E. 1979. An Improved Isolated Heart Preparation for External Assessment of Myocardial Metabolism. *American Journal of Physiology - Heart and Circulatory Physiology*, 5(4):H644-H651.

Bertrand, L., Horman, S., Beauloye, C. & Vanoverschelde, J. 2008. Insulin Signaling in the Heart. *Cardiovascular Research*, 79(2):238-248.

Besson, A., Robbins, S.M. & Yong, V.W. 1999. PTEN/MMAC1/TEP1 in Signal Transduction and Tumorigenesis. *European Journal of Biochemistry*, 263(3):605-611.

Bhattacharya, S., Dey, D. & Roy, S.S. 2007. Molecular Mechanism of Insulin Resistance. *J Biosci*, 32(2):405-413.

Biebuyck, J.F., Rusy, B.F. & Komai, H. 1987. Anesthetic Depression of Myocardial Contractility. *Anesthesiology*, 67(5):745-766.

Bing, R.J., Siegel, A., Ungar, I. & Gilbert, M. 1954. Metabolism of the Human Heart. II. Studies on Fat, Ketone and Amino Acid Metabolism. *The American Journal of Medicine*, 16(4):504-515.

Blüher, M. 2013. Adipose Tissue Dysfunction Contributes to Obesity Related Metabolic Diseases. *Best Practice & Research Clinical Endocrinology & Metabolism*, 27(2):163-177.

Bode, A.M. & Dong, Z. 2007. The Functional Contrariety of JNK. *Molecular carcinogenesis*, 46(8):591-598.

Boden, G. 1999. Free Fatty Acids, Insulin Resistance, and Type 2 Diabetes Mellitus. *Proceedings of The Association of American Physicians*, 111(3):241-248.

Boden, G. 2008. Obesity and Free Fatty Acids. *Endocrinology and metabolism clinics of North America*, 37(3):635-646.

Boden, G. 2011. Obesity, Insulin Resistance and Free Fatty Acids. *Current Opinion in Endocrinology, Diabetes and Obesity*, 18(2):139-143.

Bøhn, S.K., Ward, N.C., Hodgson, J.M. & Croft, K.D. 2012. Effects of Tea and Coffee on Cardiovascular Disease Risk. *Food & Function*, 3(6):575.

Bonadonna, R.C. 1993. Transmembrane Glucose Transport in Skeletal Muscle of Patients with Non-Insulin-Dependent Diabetes. *Journal of Clinical Investigation*, 92(1):486-494.

Borges, F., Fernandes, E. & Roleira, F. 2002. Progress Towards the Discovery of Xanthine Oxidase Inhibitors. *CMC*, 9(2):195-217.

Boudina, S., Sena, S., O'Neill, B.T., Tathireddy, P., Young, M.E. & Abel, E.D. 2005. Reduced Mitochondrial Oxidative Capacity and Increased Mitochondrial Uncoupling Impair Myocardial Energetics in Obesity. *Circulation*, 112(17):2686-2695.

Boussageon, R., Bejan-Angoulvant, T., Saadatian-Elahi, M., Lafont, S, Bergeonneau, C., Kassaï, B., Erpeldinger, S., Wright, J.M., Gueyffier, F. & Cornu, C. 2011. Effect of Intensive Glucose Lowering Treatment on all Cause Mortality, Cardiovascular Death, and Microvascular Events in Type 2 Diabetes: Meta-Analysis of Randomised Controlled Trials. *BMJ*, 343(July 26):d4169-d4169.

Bradford, M. 1976. A Rapid and Sensitive Method for the Quantitation of Microgram Quantities of Protein Utilizing the Principle of Protein-Dye Binding. *Analytical Biochemistry*, 72(1-2):248-254.

Bray, G.A. & Hamman, R.F. 2014. Insulin Resistance and Prediabetes. *National Institutes of Health*, 14(4893).

Breet, P., Kruger, H.S., Jerling, J.C. & Oosthuizen, W. 2005. Actions of Black Tea and Rooibos on Iron Status of Primary School Children. *Nutrition Research*, 25(11):983-994.

Breiter, T., Laue, C., Kressel, G., Gröll, S., Engelhardt, U. & Hahn, A. 2011. Bioavailability and antioxidant potential of rooibos flavonoids in humans following the consumption of different rooibos formulations. *Food Chemistry*, 128(2):338-347.

Burgering, B.M.T. & Coffer, P.J. 1995. Protein Kinase B (c-Akt) in Phosphatidylinositol-3-OH Kinase Signal Transduction. *Nature*, 376(6541):599-602.

Burkhoff, D., Weiss, R., Schulman, S., Kalil-Filho, R., Wannenburg, T. & Gerstenblith, G. 1991. Influence of metabolic substrate on rat heart function and metabolism at different coronary flows. *Am J Physiol*, 261(3 Pt 2):H741-50.

Carnero, A., Blanco-Aparicio, C., Renner, O., Link, W. & Leal, J. 2008. The PTEN/PI3K/AKT Signaling Pathway in Cancer, Therapeutic Implications. *Current Cancer Drug Targets*, 8(3):187-198.

Catalano, P.M. 2007. Increasing Maternal Obesity and Weight Gain during Pregnancy. *Obstetrics & Gynecology*, 110(4):743-744.

Cavaghan, M.K., Ehrmann, D.A. & Polonsky, K.S. 2000. Interactions between Insulin Resistance and Insulin Secretion in the Development of Glucose Intolerance. *Journal of Clinical Investigation*, 106(3):329-333.

Center for Disease Control & Prevention. 2009. Pediatric and Pregnancy: Health Indicators. Available at: http://www.cdc.gov/pednss/pnss_tables/tables_health_indicators.htm

Centers for Disease Control & Prevention. 2013. Defining Adult Overweight and Obesity. Available at: http://www.cdc.gov/obesity/adult/defining.html

Chhabra, N. 2015. Insulin Biosynthesis, secretion and action. *Biochemistry for medics*. Available at: http://www.namrata.co/insulin-biosynthesis-secretion-and-action/

Chamie, K., Oberfoell, S., Kwan, L., Labo, J., Wei, J.T. & Litwin, M.S. 2013. Body Mass Index and Prostate Cancer Severity: Do Obese Men Harbor More Aggressive Disease on Prostate Biopsy? *Urology*, 81(5):949-955.

Chandrasekera, P.C. & Pippin, J.J. 2014. Of Rodents and Men: Species-Specific Glucose Regulation and Type 2 Diabetes Research. *ALTEX*, 31(2):157-176.

Chen, W., Sudji, I.R., Wang, E., Joubert, E., Van Wyk, B. & Wink, M. 2013. Ameliorative Effect of Aspalathin from Rooibos (Aspalathus Linearis) on Acute Oxidative Stress in Caenorhabditis Elegans. *Phytomedicine*, 20(3-4):380-386.

Chlopcikova, S., Psotova, J. & Miketova, P. 2001. Neonatal Rat Cardiomyocytes - a Model for the Study of Morphological, Biochemical and Electrophysiological Characteristics of the Heart. *Biomed Pap Med Fac Univ Palacky Olomouc Czech Repub.*, 145(2):49-55.

Chrousos, G.P. 2009. Stress and Disorders of the Stress System. *Nat Rev Endocrinol*, 5(7):374-381.

Chu, E.C. & Tarnawski, A.S. 2004. PTEN Regulatory Functions in Tumor Suppression and Cell Biology. *Medical Science Monitor*, 10(10).:RA235-RA241.

Claycomb, W.C., Lanson, N.A. Jr., Stallworth, B.S., Egeland, D.B., Delcarpio, J.B., Bahinski, A. & Izzo, N.J. Jr. 1998. HL-1 Cells: A Cardiac Muscle Cell Line that Contracts and Retains Phenotypic

Characteristics of the Adult Cardiomyocyte. *Proceedings of the National Academy of Sciences*, 95(6):2979-2984.

Cohen, P., Alessi, D.R. & Cross, D.A.E. 1997. PDK1, One of the Missing Links in Insulin Signal Transduction? *FEBS Letters*, 410(1):3-10.

Coimbra, S., Castro, E., Rocha-Pereira, P., Rebelo, I., Rocha, S. & Santos-Silva, A. 2006. The Effect of Green Tea in Oxidative Stress. *Clinical Nutrition*, 25(5):790-796.

Coimbra, S., Santos-Silva, A., Rocha-Pereira, P., Rocha, S. & Castro, E. 2006. Green Tea Consumption Improves Plasma Lipid Profiles in Adults. *Nutrition Research*, 26(11):604-607.

Coman, C., Rugin, O.D. & Socaciu, C. 2012. Plants and Natural Compounds with Antidiabetic Action. *Notulae Botanicae Horti Agrobotanici Cluj-Napoca*, 40(1):314-325.

Cooper, C. 1998. Individual Risk Factors for Hip Osteoarthritis: Obesity, Hip Injury and Physical Activity. *American Journal of Epidemiology*, 147(6):516-522.

Cornier, M., Dabelea, D., Hernandez, T., Lindstrom, R., Steig, A., Stob, N., Van Pelt, R., Wang, H. and Eckel, R. 2008. The Metabolic Syndrome. *Endocrine Reviews*, 29(7):777-822.

Cossarizza, A., Baccaranicontri, M., Kalashnikova, G. & Franceschi, C. 1993. A New Method for the Cytofluorometric Analysis of Mitochondrial Membrane Potential using the J-Aggregate Forming Lipophilic Cation 5,5',6,6'-Tetrachloro-1,1',3,3'-Tetraethylbenzimidazolcarbocyanine Iodide (JC-1). *Biochemical and Biophysical Research Communications*, 197(1):40-45.

Courts, F.L. & Williamson, G. 2009. The C -Glycosyl Flavonoid, Aspalathin, is Absorbed, Methylated and Glucuronidated Intact in Humans. *Molecular Nutrition & Food Research*, 53(9):1104-1111.

Craig, F.E. 2007. *Flow cytometry*. Saunders

Dawson, J., Quinn, T. & Walters, M. 2007. Uric Acid Reduction: A New Paradigm in the Management of Cardiovascular Risk? *CMC*, 14(17):1879-1886.

Day, A.J., Bao, Y., Morgan, M.R.A. & Williamson, G. 2000. Conjugation Position of Quercetin Glucuronides and Effect on Biological Activity. *Free Radical Biology and Medicine*, 29(12):1234-1243.

De Beer, D., Joubert, E., Viljoen, M. & Manley, M. 2011. Enhancing aspalathin stability in rooibos (Aspalathus linearis) ready-to-drink iced teas during storage: the role of nano-emulsification and beverage ingredients, citric and ascorbic acids. *Journal of the Science of Food and Agriculture*, 92(2):274-282.

DeFronzo, R.A. & Tripathy, D. 2009. Skeletal Muscle Insulin Resistance is the Primary Defect in Type 2 Diabetes. *Diabetes care*, 32(Supplement 2):S157-S163.

DeFronzo, R.A. 1999. Pathogenesis of Type 2 Diabetes. *Drugs*, 58(Supplement 1):29-30.

DeFronzo, R.A. 2004. Pathogenesis of Type 2 Diabetes Mellitus. *Medical Clinics of North America*, 88(4):787-835.

Deng, M., Deng, L. & Xue, Y. 2012. MAP Kinase-Mediated and MLCK-Independent Phosphorylation of MLC20 in Smooth Muscle Cells. *Current Basic and Pathological Approaches to the Function of Muscle Cells and Tissues - From Molecules to Humans*,

Deng, M., Ding, W., Min, X. & Xia, Y. 2011. MLCK-Independent Phosphorylation of MLC20 and its Regulation by MAP Kinase Pathway in Human Bladder Smooth Muscle Cells. *Cytoskeleton,* 68(3):139-149.

Depré, C., Rider, M.H. & Hue, L. 1998. Mechanisms of Control of Heart Glycolysis. *Eur J Biochem,* 258(2):277-290.

Derakhshan, F. & Toth, C. 2013. Insulin and the Brain. *Current Diabetes Reviews,* 9(2):102-116.

Dicker, D. 2011. DPP-4 Inhibitors: Impact on Glycemic Control and Cardiovascular Risk Factors. *Diabetes care,* 34(SUPPL. 2):S276-S278.

Ding, L. 2015. Serum Lipoprotein (a) Concentrations are Inversely Associated with T2D, Prediabetes, and Insulin Resistance in a Middle-Aged and Elderly Chinese Population. *J.Lipid Res.,* 56(4):920-926.

Dludla, P.V. 2014. The Cardioprotective Effect of an Aqueous Extract of Fermented Rooibos (Aspalathus Linearis) on Cultured Cardiomyocytes Derived from Diabetic Rats. *Phytomedicine,* 21(5). :595-601.

Döring H.J. & Dehnert, H. 1988. *The Isolated Perfused Heart According to Langendorff*, English edition, Biomesstechnick-Verlag, West Germany.

Döring, H.J. 1990. The Isolated Perfused Heart According to Langendorff Technique--Function--Application. *Physiologia Bohemoslovaca,* 39(6):481-504.

Dummler, B. & Hemmings, B.A. 2007. Physiological Roles of PKB/Akt Isoforms in Development and Disease. *Biochemical Society transactions,* 35(2):231-235.

Duthie, S.J. 2005. The Effects of Cranberry Juice Consumption on Antioxidant Status and Biomarkers Relating to Heart Disease and Cancer in Healthy Human Volunteers. *European Journal of Nutrition,* 45(2):113-122.

Dzeja, P. & Terzic, A. 2009. Adenylate Kinase and AMP Signaling Networks: Metabolic Monitoring, Signal Communication and Body Energy Sensing. *International Journal of Molecular Sciences,* 10(4). :1729-1772.

Eckel, R.H. 1997. Obesity and Heart Disease: A Statement for Healthcare Professionals from the Nutrition Committee, American Heart Association. *Circulation,* 96(9):3248-3250.

Eimre, M. 2008. Distinct Organization of Energy Metabolism in HL-1 Cardiac Cell Line and Cardiomyocytes. *Biochimica et Biophysica Acta (BBA) - Bioenergetics,* 1777(6):514-524.

Eiselein, L., Schwartz, H.J. & Rutledge, J.C. 2004. The Challenge of Type 1 Diabetes Mellitus. *ILAR Journal,* 45(3):231-236.

Eldar-Finkelman, H. & Krebs, E.G. 1997. Phosphorylation of Insulin Receptor Substrate 1 by Glycogen Synthase Kinuse 3 Impairs Insulin Action. *Proceedings of the National Academy of Sciences of the United States of America,* 94(18):9660-9664.

Emmerson, B. 1997. The Management of Gout. *Clinical biochemistry,* 30(3):253.

Erlinger, S. 2000. Gallstones in Obesity and Weight Loss. *European Journal of Gastroenterology & Hepatology,* 12(12):1347-1352.

Fajans, S.S., Bell, G.I. & Polonsky, K.S. 2001. Molecular Mechanisms and Clinical Pathophysiology of Maturity-Onset Diabetes of the Young. *New England Journal of Medicine,* 345(13):971-980.

Fam, B., Rose, L., Sgambellone, R., Ruan, Z., Proietto, J. & Andrikopoulos, S. 2012. Normal muscle glucose uptake in mice deficient in muscle GLUT4. *Journal of Endocrinology*, 214(3):313-327.

Farese, R.V. 2002. Function and Dysfunction of α-PKC Isoforms for Glucose Transport in Insulin-Sensitive and Insulin-Resistant States. *American Journal of Physiology - Endocrinology and Metabolism*, 283(1 46-1):E1-E11.

Finkel, T. & Holbrook, N.J. 2000. Oxidants, Oxidative Stress and the Biology of Ageing. *Nature*, 408:239–247.

Fischer, Y., Rose, H. & Kammermeier, H. 1991. Highly Insulin-Responsive Isolated Rat Heart Muscle Cells Yielded by a Modified Isolation Method. *Life Sciences*, 49(23):1679-1688.

Fisher, J.S., Gao, J., Han, D.H., Holloszy, J.O. & Nolte, L.E. 2002. Activation of AMP Kinase Enhances Sensitivity of Muscle Glucose Transport to Insulin. *Am J Physiol Endocrinol Metab*, 282:E18–E23.

Flepisi, T.B., Lochner, A. & Huisamen, B. 2013. The Consequences of Long-Term Glycogen Synthase Kinase-3 Inhibition on Normal and Insulin Resistant Rat Hearts. *Cardiovasc Drugs Ther*, 27(5):381-392.

Folmes, C.D.L., Clanachan, A.S. & Lopaschuk, G.D. 2006. Fatty Acids Attenuate Insulin Regulation of 5'-AMP-Activated Protein Kinase and Insulin Cardioprotection After Ischemia. *Circulation research*, 99(1):61-68.

Frederich, M. & Balschi, J.A. 2002. The Relationship between AMP-Activated Protein Kinase Activity and AMP Concentration in the Isolated Perfused Rat Heart. *Journal of Biological Chemistry*, 277(3):1928-1932.

Frøsig, C., Jensen, T.E., Jeppesen, J., Pehmøller, C., Treebak, J.T., Maarbjerg, S.J., Kristensen, J.M., Sylow, L., Alsted, T.J., Schjerling, P., Kiens, B., Wojtaszewski, J.F. & Richter, E.A. 2013. AMPK and Insulin Action - Responses to Ageing and High Fat Diet. *PLoS ONE*, 8(5):e62338.

Fu, Z., R. Gilbert, E. & Liu, D. 2013. Regulation of Insulin Synthesis and Secretion and Pancreatic Beta-Cell Dysfunction in Diabetes. *Current Diabetes Reviews*, 9(1):25-53.

Fujio, Y., Nguyen, T., Wencker, D., Kitsis, R.N. & Walsh, K. 2000. Akt Promotes Survival of Cardiomyocytes in Vitro and Protects Against Lschemia-Reperfusion Injury in Mouse Heart. *Circulation*, 101(6):660-667.

Gallo, M.F., Lopez, L.M., Grimes, D.A., Schulz, K.F. & Helmerhorst, F.M. 2011. Combination Contraceptives: Effects on Weight. *Cochrane Database of Syst Rev*, 9:D003987.

Garvey, W.T., Maianu, L., Zhu, J.H., Brechtel-Hook, G., Wallace, P. & Baron, A.D. 1998. Evidence for Defects in the Trafficking and Translocation of GLUT4 Glucose Transporters in Skeletal Muscle as a Cause of Human Insulin Resistance. *Journal of Clinical Investigation*, 101(11):2377-2386.

Girolamo, M., Rodman, D., Malkin, M. & Garcia, L. (1965). Inactivation of Insulin by Adipose Tissue. *Diabetes*, 14(2):87-92.

Global Diabetes Community. 2015. Body mass index. Available at: http://www.diabetes.co.uk/bmi.html

Gouws, P., Hartel, T. & van Wyk, R. 2014. The Influence of Processing on the Microbial Risk Associated with Rooibos (Aspalathus Linearis) Tea. Journal of the science of food and agriculture, 94(15):3069-3078.

Gray, D.S. 1990. Skinfold Thickness Measurements in Obese Subjects. *American Journal of Clinical Nutrition*, 51(4):571-577.

Griggs, R.C. 1991. Prednisone in Duchenne Dystrophy. *Arch Neurol*, 48(4):383.

Grundy, S. 2012. Pre-Diabetes, Metabolic Syndrome, and Cardiovascular Risk. *Journal of the American College of Cardiology*, 59(7):635-643.

Grundy, S.M. 2004. Definition of Metabolic Syndrome: Report of the National Heart, Lung, and Blood Institute/American Heart Association Conference on Scientific Issues Related to Definition. *Circulation*, 109(3). :433-438.

Gunderson, E.P. & Abrams, B. 1999. Epidemiology of Gestational Weight Gain and Body Weight Changes After Pregnancy. *Epidemiologic Reviews*, 21(2):261-275.

Gunderson, E.P. 2009. Childbearing and Obesity in Women: Weight before, during, and After Pregnancy. *Obstetrics and Gynecology Clinics of North America*, 36(2):317-332.

Gupta, A. & Dey, C. 2012. PTEN, a widely known negative regulator of insulin/PI3K signaling, positively regulates neuronal insulin resistance. *Molecular Biology of the Cell*, 23(19):3882-3898.

Hale, L.J. & Coward, R.J.M. 2013. Insulin Signaling to the Kidney in Health and Disease. *Clinical Science*, 124(6):351-370.

Hansen, P., Wang, W., Marshall, B., Holloszy, J. & Mueckler, M. 1998. Dissociation of GLUT4 Translocation and Insulin-stimulated Glucose Transport in Transgenic Mice Overexpressing GLUT1 in Skeletal Muscle. *Journal of Biological Chemistry*, 273(29):18173-18179.

Haq, S. 2000. Glycogen Synthase Kinase-3β is a Negative Regulator of Cardiomyocyte Hypertrophy. *Journal of Cell Biology*, 151(1):117-129.

Hardie, D. & Carling, D. 1997. The AMP-Activated Protein Kinase. Fuel Gauge of the Mammalian Cell? *Eur J Biochem*, 246(2):259-273.

Hardie, D.G., Hawley, S.A. & Scott, J.W. 2006. AMP-Activated Protein Kinase - Development of the Energy Sensor Concept. *Journal of Physiology*, 574(1):7-15.

Heinrich, T., Willenberg, I. & Glomb, M. 2012. Chemistry of Color Formation during Rooibos Fermentation. *J. Agric. Food Chem.*, 60(20):5221-5228.

Heiss, M.L. & Heiss, R.J. 2007. *The story of tea.* Ten Speed Press

Hemmings, B. & Restuccia, D. 2012. PI3K-PKB/Akt Pathway. *Cold Spring Harbor Perspectives in Biology*, 4(9):a011189-a011189.

Hescheler, J., Meyer, R., Plant, S., Krautwurst, D., Rosenthal, W. & Schultz, G. 1991. Morphological, Biochemical, and Electrophysiological Characterization of a Clonal Cell (H9C2) Line from Rat Heart. *Circulation Research*, 69(6):1476-1486.

Hesseling, P.B., Klopper, J.F. & Van Heerden, P.D.R. 1979. Die Effek Van Rooibostee Op Ysterabsorpsie. *South African Medical Journal*, 55:631–632.

Hill, J.O., Wyatt, H.R. & Peters, J.C. 2012. Energy Balance and Obesity. *Circulation*, 126(1):126-132.

Himsworth, H.P. 1936. Diabetes Mellitus. its Differentiation into Insulin-Sensitive and Insulin-Insensitive Types. *The Lancet*, 227(5864):127-130.

How, O., Aasum, E., Severson, D.L., Chan, W.Y.A., Essop, M.F. & Larsen, T.S. 2006. Increased Myocardial Oxygen Consumption Reduces Cardiac Efficiency in Diabetic Mice. *Diabetes*, 55(2):466-473.

Hu, F.B. 2003. Plant-Based Foods and Prevention of Cardiovascular Disease: An Overview. *Am.J.Clin.Nutr*, 78:544S–551S.

Hu, F.B. 2008. *Obesity epidemiology.* Oxford University Press

Huang, E., Basu, A., O'Grady, M. & Capretta, J. 2009. Projecting the Future Diabetes Population Size and Related Costs for the U.S. *Diabetes Care*, 32(12):2225-2229.

Huang, M., du Plessis, J., du Preez, J., Hamman, J. & Viljoen, A. 2008. Transport of aspalathin, a Rooibos tea flavonoid, across the skin and intestinal epithelium. Phytother. Res., 22(5):699-704.

Huisamen, B. & Flepisi, B. 2014. P757 * Chronic GSK-3 Inhibition may be Good for Diabetes, but is Bad for the Heart. *Cardiovascular research*, 103(suppl 1):S138-S139.

Huisamen, B. & Lochner, A. 2010. GSK-3 Protein and the Heart: Friend Or Foe? *SAHeart*, 7:48-57.

Huisamen, B., Dietrich, D., Bezuidenhout, N., Lopes, J., Flepisi, B., Blackhurst, D. & Lochner, A. 2012. Early Cardiovascular Changes Occurring in Diet-Induced, Obese Insulin-Resistant Rats. *Molecular and Cellular Biochemistry*, 368(1-2):37-45.

Huisamen, B., Genis, A., Marais, E. & Lochner, A. 2011. Pre-treatment with a DPP-4 Inhibitor is Infarct Sparing in Hearts from Obese, Pre-diabetic Rats. *Cardiovasc Drugs Ther*, 25(1):13-20.

Huisamen, B., George, C., Dietrich, D. & Genade, S. 2013. Cardioprotective and Anti-Hypertensive Effects of Prosopis Glandulosa in Rat Models of Pre-Diabetes : Cardiovascular Topics. *Cardiovascular Journal Of Africa*, 24(2):10-16.

Iliadis, F., Kadoglou, N. & Didangelos, T. 2011. Insulin and the Heart. *Diabetes Research and Clinical Practice*, 93(Supplement 1):S86-S91.

Ip, Y.T. & Davis, R.J. 1998. Signal Transduction by the c-Jun N-Terminal Kinase (JNK) - from Inflammation to Development. *Current opinion in cell biology*, 10(2):205-219.

ISO 10993. 2009. Biological Evaluation of Medical Devices. Part 5: Tests for in Vitro Cytotoxicity. *International Organization for Standardization*, (Geneva, Switzerland):5:2009.

Jennings, J.H. & Lesser, M. 2012. Weight Loss and Calorie Restriction at 50% Fasting Rate. *Pakistan J.of Nutrition*, 11(3):282-287.

Jensen, T. & Richter, E. 2012. Regulation of glucose and glycogen metabolism during and after exercise. *The Journal of Physiology*, 590(5):1069-1076.

Jin, Q., Jhun, B.S., Lee, S.H., Lee, J., Pi, Y., Cho, Y.H., Baik, H.H. & Kang, I. 2004. Differential Regulation of Phosphatidylinositol 3-kinase/Akt, Mitogen-Activated Protein Kinase, and AMP-Activated Protein Kinase Pathways during Menadione-Induced Oxidative Stress in the Kidney of Young and Old Rats. *Biochemical and Biophysical Research Communications*, 315(3):555-561.

Johnson, R., Dludla, P.V., Muller, C.J.F., February, F. & Louw, J. 2014. Recommendations for Short Term Culturing of Viable Rod Shaped Rat Cardiomyocytes. *Bioenergetics*, 03(02).

Joost, H. & Thorens, B. 2001. The Extended GLUT-Family of sugar/polyol Transport Facilitators: Nomenclature, Sequence Characteristics, and Potential Function of its Novel Members. *Molecular membrane biology*, 18(4):247-256.

Jose, A.D. & Collison, D. 1970. The Normal Range and Determinants of the Intrinsic Heart Rate in Man. *Cardiovascular research*, 4(2):160-167.

Joubert, E. & De Beer, D. 2012. Phenolic content and antioxidant activity of rooibos food ingredient extracts. *Journal of Food Composition and Analysis*, 27(1):45-51.

Joubert, E. & Schulz, H., 2006. Production and quality aspects of rooibos tea and related products. A review. *Journal of Applied Botany and Food Quality* 80:138–144.

Joubert, E. 1994. Processing of rooibos tea (*Aspalathus linearis*) under controlled conditions. Ph.D. thesis. *University of Stellenbosch*, South Africa

Joubert, E. 1996. HPLC quantification of the dihydrochalcones, aspalathin and nothofagin in rooibos tea (Aspalathus linearis) as affected by processing. *Food Chem* 55: 403–411.

Joubert, E., Gelderblom, W.C.A. & De Beer, D. 2009. Phenolic Contribution of South African Herbal Teas to a Healthy Diet. *Nat.Prod.Commun*, 4:701–718.

Joubert, E., Viljoen, M., De Beer, D., Malherbe, C., Brand, D. & Manley, M. 2010. Use of Green Rooibos (Aspalathus linearis) Extract and Water-Soluble Nanomicelles of Green Rooibos Extract Encapsulated with Ascorbic Acid for Enhanced Aspalathin Content in Ready-to-Drink Iced Teas. *J. Agric. Food Chem.*, 58(20):10965-10971.

Kahn, C.R., Chen, L. & Cohen, S.E. 2000. Unraveling the Mechanism of Action of Thiazolidinediones. *Journal of Clinical Investigation*, 106(11):1305-1307.

Kammermeier, H. 1994. Isolated, (Langendorff) Hearts Perfused with an Aqueous Buffer (should) have Excess Oxygen Availability. *Basic Res Cardiol*, 89(6):545-548.

Kannel, W.B. & McGee, D.L. 1979. Diabetes and Glucose Tolerance as Risk Factors for Cardiovascular Disease: The Framingham Study. *Diabetes Care*, 2(2):120-126.

Kawano, A., Nakamura, H., Hata, S., Minakawa, M., Miura, Y. and Yagasaki, K. (2009). Hypoglycemic effect of aspalathin, a rooibos tea component from Aspalathus linearis, in type 2 diabetic model *db/db* mice. *Phytomedicine*, 16(5):437-443.

Kennedy, J.W. 1999. Acute Exercise Induces GLUT4 Translocation in Skeletal Muscle of Normal Human Subjects and Subjects with Type 2 Diabetes. *Diabetes*, 48(5):1192-1197.

Kershaw, E.E. & Flier, J.S. 2004. Adipose Tissue as an Endocrine Organ. *Journal of Clinical Endocrinology and Metabolism*, 89(6):2548-2556.

Kiffmeyer, W.R. & Farrar, W.W. 1991. Purification and Properties of Pig Heart Pyruvate Kinase. *Journal of protein chemistry*, 10(6):585-591.

Kim, S., Hwang, J., Park, H., Kwon, D. & Kim, M. 2013. Capsaicin stimulates glucose uptake in C2C12 muscle cells via the reactive oxygen species (ROS)/AMPK/p38 MAPK pathway. *Biochemical and Biophysical Research Communications*, 439(1):66-70.

Kjems, L.L., Holst, J.J., Volund, A. & Madsbad, S. 2003. The Influence of GLP-1 on Glucose-Stimulated Insulin Secretion: Effects on -Cell Sensitivity in Type 2 and Nondiabetic Subjects. *Diabetes*, 52(2):380-386.

Knekt, P., Kumpulainen, J., Järvinen, R., Rissanen, H., Heliövaara, M., Reunanen, A., Hakulinen, T. & Aromaa, A. 2002. Flavonoid Intake and Risk of Chronic Diseases. *American Journal of Clinical Nutrition*, 76(3):560-568.

Koch, I.S., Muller, N., de Beer, D., Næs, T. & Joubert, E. 2013. Impact of Steam Pasteurization on the Sensory Profile and Phenolic Composition of Rooibos (Aspalathus Linearis) Herbal Tea Infusions. *Food Research International*, 53(2):704-712.

Koeppen, B. & Roux, D. 1966. C -Glycosylflavonoids. the Chemistry of Aspalathin. *Biochem.J.*, 99(3):604-609.

Kondo, M., Hirano, Y., Nishio, M., Furuya, Y., Nakamura, H. & Watanabe, T. 2013. Xanthine Oxidase Inhibitory Activity and Hypouricemic Effect of Aspalathin from Unfermented Rooibos. *Journal of Food Science*, 78(12):H1935-H1939.

Konhilas, J.P., Widegren, U., Allen, D.L., Paul, A.C., Cleary, A. & Leinwand, L.A. 2005. Loaded Wheel Running and Muscle Adaptation in the Mouse. *American Journal of Physiology - Heart and Circulatory Physiology*, 289(1 58-1):H455-H465.

Koster, H., Halsema, I., Scholtens, E., Knippers, M. & Mulder, G.J. 1981. Dose-Dependent Shifts in the Sulfation and Glucuronidation of Phenolic Compounds in the Rat in Vivo and in Isolated Hepatocytes. *Biochemical pharmacology*, 30(18):2569-2575.

Kotecki, J.E. 2011. Physical activity & health: An interactive approach. 3rd Edition. *Jones & Bartlett Publishers.*

Koutsari, C. & Jensen, M.D. 2006. Free Fatty Acid Metabolism in Human Obesity. *Journal of Lipid Research*, 47(8):1643-1650.

Krafczyk, N. & Glomb, M. 2008. Characterization of Phenolic Compounds in Rooibos Tea. *J. Agric. Food Chem.*, 56(9):3368-3376.

Kreuz, S., Joubert, E., Waldmann, K. & Ternes, W. 2008. Aspalathin, a Flavonoid in Aspalathus Linearis (Rooibos), is Absorbed by Pig Intestine as a C-Glycoside. *Nutrition Research*, 28(10):690-701.

Kuo, C., Browning, K. & Ivy, J. 1999. Regulation of GLUT4 protein expression and glycogen storage after prolonged exercise. *Acta Physiol Scand*, 165(2):193-201.

Kurien, V.A. & Oliver, M.F. 1971. Free Fatty Acids during Acute Myocardial Infarction. *Progress in cardiovascular diseases*, 13(4):361-373.

Kwan, A.C. 2014. Coronary Artery Plaque Volume and Obesity in Patients with Diabetes: The Factor-64 Study. *Radiology*, 272(3). :690-699.

Lahlou, M. 2013. The Success of Natural Products in Drug Discovery. Pharmacology & Pharmacy, 04(03). :17-31.

Laue, E., Gröll, S., Breiter, T. & Engelhardt, U.H. 2009. Bioverfügbarkeit Von Flavonoiden Aus Grünem Rooibos. *Lebensmittelchemi*, 64:259.

Laughlin, M. & Taylor, J. 1994. Non-Glucose Substrates Increase Glycogen Synthesis in Vivo in Dog Heart. *Am J Physiol*, 267:H219–H223.

Lee, S., Murphy, C.T. & Kenyon, C. 2009. Glucose Shortens the Life Span of C. Elegans by Downregulating DAF-16/FOXO Activity and Aquaporin Gene Expression. *Cell Metabolism*, 10(5). :379-391.

Leibiger, I.B., Leibiger, B. & Berggren, P. 2008. Insulin Signaling in the Pancreatic ß-Cell. *Paper presented at Annual Review of Nutrition*.

Leichman, J.G., Aguilar, D., King, T.M., Vlada, A., Reyes, M. & Taegtmeyer, H. 2006. Association of Plasma Free Fatty Acids and Left Ventricular Diastolic Function in Patients with Clinically Severe Obesity. *American Journal of Clinical Nutrition*, 84(2):336-341.

Levy, J.C., Matthews, D.R. & Hermans, M.P. 1998. Correct Homeostasis Model Assessment (HOMA) Evaluation Uses the Computer Program. *Diabetes Care*, 21(12):2191-2192.

Liberman, Z. & Eldar-Finkelman, H. 2005. Serine 332 Phosphorylation of Insulin Receptor Substrate-1 by Glycogen Synthase Kinase-3 Attenuates Insulin Signaling. *Journal of Biological Chemistry*, 280(6):4422-4428.

Lodish, H.F. 2000. *Molecular cell biology*. W.H. Freeman

Longhi, S. & Radetti, G. 2013. Thyroid Function and Obesity. *JCRPE Journal of Clinical Research in Pediatric Endocrinology*, 5(SUPPL.1):40-44.

Lopaschuk G.D., Ussher J.R., Folmes C.D., Jaswal J.S. & Stanley W.C. 2010. Myocardial Fatty Acid Metabolism in Health and Disease. *Physiological Reviews*, 90(1):207-58.

Lopaschuk, G., Belke, D., Gamble, J., Toshiyuki, I. & Schönekess, B. 1994. Regulation of fatty acid oxidation in the mammalian heart in health and disease. *Biochimica et Biophysica Acta - Lipids and Lipid Metabolism*, 1213(3):263-276.

Lopaschuk, G.D. & Russell, J.C. 1991. Myocardial Function and Energy Substrate Metabolism in the Insulin-Resistant JCR:LA Corpulent Rat. *Journal of Applied Physiology*, 71(4):1302-1308.

Lotito, S. & Frei, B. 2006. Consumption of Flavonoid-Rich Foods and Increased Plasma Antioxidant Capacity in Humans: Cause, Consequence, Or Epiphenomenon? *Free Radical Biology and Medicine*, 41(12):1727-1746.

Louch, W.E., Sheehan, K.A. & Wolska, B.M. 2011. Methods in Cardiomyocyte Isolation, Culture, and Gene Transfer. *Journal of Molecular and Cellular Cardiology*, 51(3):288-298.

Lowry, O., Rosebrough, N., Farr, A. & Randall, R. 1951. Protein Measurement with the Folin Phenol Reagent. *The Journal of Biological Chemistry*, 193:265-275.

Lumkwana, D. 2015. Identifying Appropriate Attachment Factors for Isolated Adult Rat Cardiomyocyte Culture and Experimentation. *Stellenbosch University Archive*, 128(Suppl. 2):45-49.

Macfarlane, A. & Macfarlane, I. 2004. *The empire of tea*. Overlook Press

MacFarlane, A. & MacFarlane, I. 2004. *The empire of tea*. New York: Overlook Press.

Manach, C., Morand, C., Demigné, C., Texier, O., Régérat, F. & Rémésy, C. 1997. Bioavailability of Rutin and Quercetin in Rats. *FEBS letters,* 409(1):12-16.

Manchester, J., Kong, X., Nerbonne, J., Lowry, O.H. & Lawrence, J.C.J. 1994. Glucose Transport and Phosphorylation in Single Cardiac Myocytes: Rate-Limiting Steps in Glucose Metabolism. *Am.J.Physiol,* 266:E326-E333.

Manning, B.D. & Cantley, L.C. 2007. AKT/PKB Signaling: Navigating Downstream. *Cell*, 129(7):1261-1274.

Manson, S.C., Brown, R.E., Cerulli, A. & Vidaurre, C.F. 2009. The Cumulative Burden of Oral Corticosteroid Side Effects and the Economic Implications of Steroid use. *Respiratory medicine,* 103(7):975-994.

Marais, C., Van Rensburg, W.J., Ferreira, D. & Steenkamp, J.A. 2000. (S)- and (R)-Eriodictyol-6-C-ß-D-Glucopyranoside, Novel Keys to the Fermentation of Rooibos (Aspalathus Linearis). Phytochemistry, 55(1):43-49.

Marnewick, J., Joubert, E., Swart, P., van der Westhuizen, F. and Gelderblom, W. 2003. Modulation of Hepatic Drug Metabolizing Enzymes and Oxidative Status by Rooibos (Aspalathus linearis) and Honeybush (Cyclopia intermedia), Green and Black (Camellia sinensis) Teas in Rats. *J. Agric. Food Chem*., 51(27):8113-8119.

Marnewick, J., Rautenbach, F., Venter, I., Neethling, H., Blackhurst, D., Wolmarans, P. and Macharia, M. 2011. Effects of rooibos (Aspalathus linearis) on oxidative stress and biochemical parameters in adults at risk for cardiovascular disease. *Journal of Ethnopharmacology*, 133(1):46-52.

Martin, B., Ji, S., Maudsley, S. & Mattson, M.P. 2010. Control Laboratory Rodents are Metabolically Morbid: Why it Matters. Proceedings of the National Academy of Sciences, 107(14):6127-6133.

Mayo Clinic. 2015. Heart Disease. Available at: http://from www.mayoclinic.org/diseases-conditions/heart-disease/basics/definition/con-20034056

Mazibuko, S.E. 2013. Amelioration of Palmitate-Induced Insulin Resistance in C2C12 Muscle Cells by Rooibos (Aspalathus Linearis). *Phytomedicine,* 20(10):813-819.

Mazumder, P.K. 2004. Impaired Cardiac Efficiency and Increased Fatty Acid Oxidation in Insulin-Resistant *ob/ob* Mouse Hearts. *Diabetes,* 53(9):2366-2374.

McCormack, J.G. & Denton, R.M. 1990. Intracellular Calcium Ions and Intramitochondrial Ca in the Regulation of Energy Metabolism in Mammalian Tissues. *Proceedings of the Nutrition Society,* 49(01):57-75.

McGurk, K.A., Brierley, C.H. & Burchell, B. 1998. Drug Glucuronidation by Human Renal UDP-Glucuronosyltransferases. *Biochemical pharmacology,* 55(7):1005-1012.

McLaughlin, T., Allison, G., Abbasi, F., Lamendola, C. & Reaven, G. 2004. Prevalence of insulin resistance and associated cardiovascular disease risk factors among normal weight, overweight, and obese individuals. *Metabolism,* 53(4):495-499.

Ménard, C., Pupier, S., Mornet, D., Kitzmann, M., Nargeot, J. & Lory, P. 1999. Modulation of L-Type Calcium Channel Expression during Retinoic Acid-Induced Differentiation of H9C2 Cardiac Cells. *J Biol Chem.*, 274(41):29063-29070.

Mennen, L.I., Walker, R., Bennetau-Pelissero, C. & Scalbert, A. 2005. Risks and Safety of Polyphenol Consumption. *American Journal of Clinical Nutrition*, 81(Suppl.1):326S–329S.

Metzger, B.E. & Coustan, D.R. 1998. Proceedings of the Fourth International Work-Shop-Conference on Gestational Diabetes Mellitus. *Diabetes care*, 21(Suppl. 2) :B1–B167.

Midaoui, A. and Champlain, J. 2005. Effects of glucose and insulin on the development of oxidative stress and hypertension in animal models of type 1 and type 2 diabetes. *Journal of Hypertension*, 23(3):581-588.

Mîinea, C. 2005. AS160, the Akt Substrate Regulating GLUT4 Translocation, has a Functional Rab GTPase-Activating Protein Domain. *Biochem.J.*, 391(1):87-93.

Mirica, S.N. 2009. Langendorff Perfused Heart - the 110 Years Old Experimental Model that Gets Better with Age. *Studia Universitatis Vasile Goldis Arad, Seria Stiintele Vietii*, 19(1):81-86.

Misbin, R.I. 2005. Evaluating the Safety of Diabetes Drugs: Perspective of a Food and Drug Administration Insider. *Diabetes Care*, 28(10):2573-2576.

Mitcheson, J. 1998. Cultured Adult Cardiac Myocytes Future Applications, Culture Methods, Morphological and Electrophysiological Properties. *Cardiovascular Research*, 39(2):280-300.

Mochizuki, S. 1979. Control of Glyceraldehyde-3-Phosphate Dehydrogenase in Cardiac Muscle. *Journal of Molecular and Cellular Cardiology*, 11(3):221-236.

Montessuit, C. & Lerch, R. 2013. Regulation and Dysregulation of Glucose Transport in Cardiomyocytes. *Biochimica et Biophysica Acta (BBA) - Molecular Cell Research*, 1833(4):848-856.

Mora, A. 2003. Deficiency of PDK1 in Cardiac Muscle Results in Heart Failure and Increased Sensitivity to Hypoxia. *EMBO Journal*, 22(18):4666-4676.

Mora, A., Sakamoto, K., McManus, E.J. & Alessi, D.R. 2005. Role of the PDK1-PKB-GSK3 Pathway in Regulating Glycogen Synthase and Glucose Uptake in the Heart. *FEBS letters*, 579(17):3632-3638.

Morgan, H.E. & Parmeggiani, A. 1964. Regulation of Glycogenolysis in Muscle. II. Control of Glycogen Phosphorylase Reaction in Isolated Perfused Heart. *J.Biol.Chem*, 239:2435-2439.

Moule, S.K. & Denton, R.M. 1997. Multiple Signaling Pathways Involved in the Metabolic Effects of Insulin. *The American Journal of Cardiology*, 80(3):41A-49A.

Muller, C., Joubert, E., de Beer, D., Sanderson, M., Malherbe, C., Fey, S. & Louw, J. 2012. Acute assessment of an aspalathin-enriched green rooibos (Aspalathus linearis) extract with hypoglycemic potential. *Phytomedicine*, 20(1):32-39.

Mulligan, J.D., Gonzalez, A.A., Kumar, R., Davis, A.J. & Saupe, K.W. 2005. Aging Elevates Basal Adenosine Monophosphate-Activated Protein Kinase (AMPK) Activity and Eliminates Hypoxic Activation of AMPK in Mouse Liver. *The Journals of Gerontology Series A: Biological Sciences and Medical Sciences*, 60(1):21-27.

Mungai, P.T. 2011. Hypoxia Triggers AMPK Activation through Reactive Oxygen Species-Mediated Activation of Calcium Release-Activated Calcium Channels. *Mol Cell Biol.*, 31(17):3531-3545.

Muniyappa, R. & Quon, M.J. 2007. Insulin Action and Insulin Resistance in Vascular Endothelium. *Current Opinion in Clinical Nutrition and Metabolic Care*, 10(4):523-530.

Murea, M., Ma, L. & Freedman, B.I. 2012. Genetic and Environmental Factors Associated with Type 2 Diabetes and Diabetic Vascular Complications. *The Review of Diabetic Studies*, 9(1):6-22.

Nagao, A., Seki, M. & Kobayashi, H. 1999. Inhibition of Xanthine Oxidase by Flavonoids. *Bioscience, Biotechnology, and Biochemistry*, 63(10):1787-1790.

Nakae, J., Kido, Y. & Accili, D. 2001. Distinct and Overlapping Functions of Insulin and IGF-I Receptors. *Endocrine reviews*, 22(6).:818-835.

Nakagawa, T. 2005. A Causal Role for Uric Acid in Fructose-Induced Metabolic Syndrome. *AJP: Renal Physiology*, 290(3):F625-F631.

Nathan, D.M. Buse. J.B., Davidson, M.B., Ferrannini, E., Holman, R.R., Sherwin, R. & Zinman, B. 2009. Medical Management of Hyperglycemia in Type 2 Diabetes: A Consensus Algorithm for the Initiation and Adjustment of Therapy: A Consensus Statement of the American Diabetes Association and the European Association for the Study of Diabetes. *Clinical Diabetes*, 27(1):4-16.

National Institutes of Health. 2015. Insulin Resistance and Prediabetes. Available at: http://www.niddk.nih.gov/health-information/health-topics/Diabetes/insulin-resistance-prediabetes/.

Nelson, D.L., Nelson, D.L., Lehninger, A.L. & Cox, M.M. 2008. *Lehninger principles of biochemistry*. W.H. Freeman

Neubauer, S. 2007. The Failing Heart — an Engine Out of Fuel. *New England Journal of Medicine*, 356(11):1140-1151.

Newsholme, P. 2003. Glutamine and Glutamate as Vital Metabolites. *Braz J Med Biol Res*, 36(2):153-163.

Nicholson, K.M. & Anderson, N.G. 2002. The Protein Kinase B/Akt Signaling Pathway in Human Malignancy. *Cellular Signaling*, 14(5):381-395.

Noble, R.E. 2001. Waist-to-Hip Ratio Versus BMI as Predictors of Cardiac Risk in Obese Adult Women. *Western Journal of Medicine*, 174(4):240-241.

Norris, J.M. & Rich, S.S. 2012. Genetics of Glucose Homeostasis: Implications for Insulin Resistance and Metabolic Syndrome. *Arteriosclerosis, Thrombosis, and Vascular Biology*, 32(9):2091-2096.

O'Leary, K.A., Day, A.J., Needs, P.W., Mellon, F.A., O'Brien, N.M. & Williamson, G. 2003. Metabolism of Quercetin-7- and Quercetin-3-Glucuronides by an in Vitro Hepatic Model: The Role of Human ß-Glucuronidase, Sulfotransferase, Catechol-O-Methyltransferase and Multi-Resistant Protein 2 (MRP2) in Flavonoid Metabolism. *Biochemical pharmacology*, 65(3):479-491.

Ogden, C.L., Carroll, M.D., Kit, B.K. & Flegal, K.M. 2014. Prevalence of Childhood and Adult Obesity in the United States, 2011–2012. *Survey of Anesthesiology*, 58(4):206.

Ogihara, T. 2002. Angiotensin II-Induced Insulin Resistance is Associated with Enhanced Insulin Signaling. *Hypertension*, 40(6):872-879.

Olson, A.L. & Pessin, J.E. 1996. Structure, Function, and Regulation of the Mammalian Facilitative Glucose Transporter Gene Family. *Annu.Rev.Nutr.*, 16(1):235-256.

Opie, L.H. 1968. Metabolism of the Heart in Health and Disease. Part I. *American Heart Journal*, 76(5):685-698.

Opie, L.H. 1969. Metabolism of the Heart in Health and Disease. Part II. *American Heart Journal*, 77(1):100-122.

Opie, L.H. 1969. Metabolism of the Heart in Health and Disease. Part III. *American Heart Journal*, 77(3):383-410.

Ottensmeyer, F.P., Beniac, D.R., Luo, R.Z.-. & Yip, C.C. 2000. Mechanism of Transmembrane Signaling: Insulin Binding and the Insulin Receptor. *Biochemistry*, 39(40):12103-12112.

Pampel, F.C., Denney, J.T. & Krueger, P.M. 2012. Obesity, SES, and Economic Development: A Test of the Reversal Hypothesis. *Social science & medicine*, 74(7):1073-1081.

Pantsi, W.G., Marnewick, J.L., Esterhuyse, A.J., Rautenbach, F. & Van Rooyen, J. 2011. Rooibos (Aspalathus Linearis) Offers Cardiac Protection Against ischaemia/reperfusion in the Isolated Perfused Rat Heart. *Phytomedicine*, 18(14):1220-1228.

Pasquali, R., Patton, L. & Gambineri, A. 2007. Obesity and Infertility. *Current Opinion in Endocrinology, Diabetes and Obesity*, 14(6):482-487.

Patel, D., Prasad, S., Kumar, R. & Hemalatha, S. 2012. An overview on antidiabetic medicinal plants having insulin mimetic property. *Asian Pacific Journal of Tropical Biomedicine*, 2(4):320-330.

Petersen, K. & Shulman, G. 2002. Pathogenesis of skeletal muscle insulin resistance in type 2 diabetes mellitus. *The American Journal of Cardiology*, 90(5):11-18.

Peuhkurinen, K.J., Nuutinen, E.M., Pietiläinen, E.P., Hiltunen, J.K. & Hassinen, I.E. 1982. Role of Pyruvate Carboxylation in the Energy-Linked Regulation of Pool Sizes of Tricarboxylic Acid-Cycle Intermediates in the Myocardium. *Biochem. J.*, 208(3):577-581.

Pietiläinen, K.H. 2008. Physical Inactivity and Obesity: A Vicious Circle. *Obesity*, 16(2):409-414.

Piper, H. 2000. The Calcium Paradox Revisited an Artefact of Great Heuristic Value. *Cardiovascular research*, 45(1):123-127.

Polonsky, K.S. 2012. The Past 200 Years in Diabetes. *New England Journal of Medicine*, 367(14):1332-1340.

Poole, R. & Halestrap, A. 1993. Transport of Lactate and Other Monocarboxylates Across Mammalian Plasma Membranes. *Am J Physiol*, 264:761–782.

Popkin, B.M. 2009. The World is Fat: The Fads, Trends, Policies, and Products that are Fattening the Human Race. *New York: Avery*.

Prasad, K.N., Cole, W.C., Kumar, B. & Che Prasad, K. 2002. Pros and Cons of Antioxidant use during Radiation Therapy. *Cancer treatment reviews*, 28(2):79-91.

Printz, R.L., Ardehali, H., Koch, S. & Granner, D.K. 1995. Human Hexokinase II mRNA and Gene Structure. *Diabetes*, 44(3):290-294.

Prior, R.L., Gu, L., Wu, X., Jacob, R.A., Sotoudeh, G., Kader, A.A. & Cook, R.A. 2007. Plasma Antioxidant Capacity Changes Following a Meal as a Measure of the Ability of a Food to Alter in Vivo Antioxidant Status. *Journal of the American College of Nutrition*, 26(2):170-181.

Quattrocchi, U. 2012. *CRC world dictionary of medicinal and poisonous plants.* CRC

Raff, H. 2003. *Physiology secrets.* Hanley & Belfus

Rahman, K. 2007. Studies on free radicals, antioxidants, and co-factors. *Clin Interv Aging*, 2(2):219-236.

Raptis, S.A. & Dimitriadis, G.D. 2001. Oral Hypoglycemic Agents: Insulin Secretagogues, a-Glucosidase Inhibitors and Insulin Sensitizers. *Experimental and Clinical Endocrinology & Diabetes*, 109(Suppl 2):S265-S287.

Rayasam, G.V., Tulasi, V.K., Sodhi, R., Davis, J.A. & Ray, A. 2009. Glycogen Synthase Kinase 3: More than a Namesake. *British Journal of Pharmacology*, 156(6):885-898.

Re, R.N. 2015. Obesity-Related Hypertension. *Ochsner J*, 9(3):133–136.

Reaven, G. 1988. Banting lecture 1988. Role of insulin resistance in human disease. *Diabetes*, 37(12):1595-1607.

Roche, T.E. & Hiromasa, Y. 2007. Pyruvate Dehydrogenase Kinase Regulatory Mechanisms and Inhibition in Treating Diabetes, Heart Ischemia, and Cancer. Cell.Mol.Life Sci., 64(7-8):830-849.

Russell, R.R., Mrus, J.M., Mommessin, J.I. & Taegtmeyer, H. 1992. Compartmentation of Hexokinase in Rat Heart. A Critical Factor for Tracer Kinetic Analysis of Myocardial Glucose Metabolism. *Journal of Clinical Investigation*, 90(5):1972-1977.

Russell-Jones, D. & Khan, R. 2007. Insulin-Associated Weight Gain in Diabetes – Causes, Effects and Coping Strategies. *Diabetes Obes Metab*, 9(6):799-812.

Saboor Aftab, S., Reddy, N., Smith, E. & Barber, T. 2014. Obesity and Type 2 Diabetes Mellitus. *Journal of Internal Medicine*, S6(002).

Saddik, M. & Lopaschuk, G.D. 1991. Myocardial Triglyceride Turnover and Contribution to Energy Substrate Utilization in Isolated Working Rat Hearts. *Journal of Biological Chemistry*, 266(13):8162-8170.

Saltiel, A.R. & Kahn, C.R. 2001. Insulin Signaling and the Regulation of Glucose and Lipid Metabolism. *Nature*, 414(6865):799-806.

Sano, H. 2003. Insulin-Stimulated Phosphorylation of a Rab GTPase-Activating Protein Regulates GLUT4 Translocation. *Journal of Biological Chemistry*, 278(17):14599-14602.

Sasaoka, T., Wada, T. & Tsuneki, H. 2006. Lipid Phosphatases as a Possible Therapeutic Target in Cases of Type 2 Diabetes and Obesity. *Pharmacology and Therapeutics*, 112(3):799-809.

Scalbert, A., Morand, C., Manach, C. & Rémésy, C. 2002. Absorption and Metabolism of Polyphenols in the Gut and Impact on Health. *Biomedicine & Pharmacotherapy*, 56(6):276-282.

Schloms, L. & Swart, A.C. 2014. Rooibos Flavonoids Inhibit the Activity of Key Adrenal Steroidogenic Enzymes, Modulating Steroid Hormone Levels in H295R Cells. *Molecules*, 19(3):3681-3695.

Schlotterer, A., Kukudov, G., Bozorgmehr, F., Hutter, H., Du, X., Oikonomou, D., Ibrahim, Y., Pfisterer, F., Rabbani, N., Thornalley, P., Sayed, A., Fleming, T., Humpert, P., Schwenger, V., Zeier, M., Hamann,

A., Stern, D., Brownlee, M., Bierhaus, A., Nawroth, P. & Morcos, M. 2009. *C. elegans* as Model for the Study of High Glucose- Mediated Life Span Reduction. Diabetes, 58(11):2450-2456.

Schneider, C., Nguyêñ, V. & Taegtmeyer, H. 1991. Feeding and Fasting Determine Postischemic Glucose Utilization in Isolated Working Rat Hearts. *Am J Physiol*, 260:H542–H548.

Schulz H., Joubert E. & Schutze W. 2003. Quantification of quality parameters for reliable evaluation of green rooibos (Aspalathus linearis). *Eur Food Res Technol* 216: 539–543

Schwartz, T.L., Nihalani, N., Jindal, S., Virk, S. & Jones, N. 2004. Psychiatric Medication-Induced Obesity: A Review. *Obesity Reviews,* 5(2):115-121.

Segal, J., Schwalb, H., Shmorak, V. & Uretzky, G. 1990. Effect of Anesthesia on Cardiac Function and Response in the Perfused Rat Heart. *Journal of Molecular and Cellular Cardiology,* 22(11):1317-1324.

Sengupta, S. & Chattopadhyay, M.K. 1993. Lowry's method of protein estimation: some more insights. *J Pharm Pharmacol,* 45(1):80.

Sesti, G. 2006. Pathophysiology of Insulin Resistance. *Best Practice and Research: Clinical Endocrinology and Metabolism,* 20(4):665-679.

Sesti, G., Federici, M., Hribal, M.L., Lauro, D., Sbraccia, P. & Lauro, R. 2001. Defects of the Insulin Receptor Substrate System in Human Metabolic Disorders. *FASEB Journal,* 15(12):2099-2111.

Shah, A. & Shannon, R.P. 2003. Insulin Resistance in Dilated Cardiomyopathy. *Reviews in Cardiovascular Medicine,* 4(Suppl 6):S50-7.

Shanik, M.H., Xu, Y., Skrha, J., Dankner, R., Zick, Y. & Roth, J. 2008. Insulin Resistance and Hyperinsulinemia: Is Hyperinsulinemia the Cart Or the Horse? *Diabetes Care*, 31(Supplement 2):S262-S268.

Sharma, A.M., Pischon, T., Hardt, S., Kunz, I. & Luft, F.C. 2001. Hypothesis: Beta-Adrenergic Receptor Blockers and Weight Gain : A Systematic Analysis. *Hypertension,* 37(2):250-254.

Sharma, S. 2004. Intramyocardial Lipid Accumulation in the Failing Human Heart Resembles the Lipotoxic Rat Heart. *FASEB Journal,* 18(14):1692-1700.

Shelley, H. 1961. Cardiac Glycogen in Different Species before and After Birth. *Br Med Bull,* 17:137-156.

Shibata, R. 2005. Adiponectin Protects Against Myocardial Ischemia-Reperfusion Injury through AMPK- and COX-2-Dependent Mechanisms. *Nature medicine,* 11(10):1096-1103.

Shimokawa, T. 2000. Glucose Uptake Stimulator YM-138552 Activates Gene Expression and Translocation of Glucose Transporter Isotype 4. *Drug Dev.Res.,* 51(1):43-48.

Shioi, T. 2002. Akt/protein Kinase B Promotes Organ Growth in Transgenic Mice. *Molecular and Cellular Biology*, 22(8):2799-2809.

Shiojima, I. 2002. Akt Signaling Mediates Postnatal Heart Growth in Response to Insulin and Nutritional Status. *Journal of Biological Chemistry,* 277(40):37670-37677.

Simpson, M.J. 2013. Anti-Peroxyl Radical Quality and Antibacterial Properties of Rooibos Infusions and their Pure Glycosylated Polyphenolic Constituents. *Molecules,* 18(9):11264-11280.

Sinisalo, M., Enkovaara, A. & Kivistö, K. 2010. Possible hepatotoxic effect of rooibos tea: a case report. *European Journal of Clinical Pharmacology*, 66(4):427-428.

Sissing, L., Marnewick, J., De Kock, M., Swanevelder, S., Joubert, E. & Gelderblom, W. 2011. Modulating Effects of Rooibos and Honeybush Herbal Teas on the Development of Esophageal Papillomas in Rats. *Nutrition and Cancer*, 63(4):600-610.

Skrzypiec-Spring, M., Grotthus, B., Szelag, A. & Schulz, R. 2007. Isolated Heart Perfusion According to Langendorff-Still Viable in the New Millennium. *Journal of Pharmacological and Toxicological Methods*, 55(2):113-126.

Skurk, C. 2005. The FOXO3a Transcription Factor Regulates Cardiac Myocyte Size Downstream of AKT Signaling. *Journal of Biological Chemistry*, 280(21):20814-20823.

Smeekens, S.P. 1992. Proinsulin Processing by the Subtilisin-Related Proprotein Convertases Furin, PC2, and PC3. Proceedings of the National Academy of Sciences, 89(18):8822-8826.

Snijman, P.W., Swanevelder, S., Joubert, E., Green, I.R. & Gelderblom, W.C.A. 2007. The Antimutagenic Activity of the Major Flavonoids of Rooibos (Aspalathus Linearis): Some Dose-Response Effects on Mutagen Activation-Flavonoid Interactions. *Mutation Research - Genetic Toxicology and Environmental Mutagenesis*, 631(2):111-123.

Soltani, Z., Rasheed, K., Kapusta, D. & Reisin, E. (2013). Potential Role of Uric Acid in Metabolic Syndrome, Hypertension, Kidney Injury, and Cardiovascular Diseases: Is It Time for Reappraisal? *Curr Hypertens Rep*, 15(3):175-181.

Son, M.J., Minakawa, M., Miura, Y. & Yagasaki, K. 2013. Aspalathin Improves Hyperglycemia and Glucose Intolerance in Obese Diabetic *ob/ob* Mice. *European Journal of Nutrition*, 52(6):1607-1619.

Stalmach, A., Mullen, W., Pecorari, M., Serafini, M. & Crozier, A. 2009. Bioavailability of C -Linked Dihydrochalcone and Flavanone Glucosides in Humans Following Ingestion of Unfermented and Fermented Rooibos Teas. *J.Agric.Food Chem.*, 57(15) :7104-7111.

Stanford, K.I. 2012. Brown Adipose Tissue Regulates Glucose Homeostasis and Insulin Sensitivity. *Journal of Clinical Investigation*, 123(1):215-223.

Stanley, W. 1997. Regulation of energy substrate metabolism in the diabetic heart. *Cardiovascular Research*, 34(1):25-33.

Statistics South Africa. 2011. Mortality and causes of death in South Africa, 2010: Findings from death notification. Available at: http://www.statssa.gov.za/publications/P03093/P030932010.pdf

Stener-Victorin, E., Benrick, A., Kokosar, M., Maliqueo, M., Behre, C., Højlund, K. & Sazonova, A. 2014. Acupuncture increases whole body glucose uptake during and after stimulation in women with polycystic ovary syndrome. *Fertility and Sterility*, 102(3):e29.

Støy, J., Steiner, D.F., Park, S., Ye, H., Philipson, L.H. & Bell, G.I. 2010. Clinical and Molecular Genetics of Neonatal Diabetes due to Mutations in the Insulin Gene. *Reviews in Endocrine and Metabolic Disorders*, 11(3):205-215.

Street, R. & Prinsloo, G. 2013. Commercially Important Medicinal Plants of South Africa: A Review. *Journal of Chemistry*, 2013:1-16.

Sumiyoshi, M., Sakanaka, M. & Kimura, Y. 2006. Chronic Intake of High-Fat and High-Sucrose Diets Differentially Affects Glucose Intolerance in Mice. *Journal of Nutrition*, 136(3):582-587.

Sutherland, F.J. & Hearse, D.J. 2000. The Isolated Blood and Perfusion Fluid Perfused Heart. *Pharmacological Research*, 41(6):613-627.

Szczepaniak, L.S. 2003. Myocardial Triglycerides and Systolic Function in Humans: In Vivo Evaluation by Localized Proton Spectroscopy and Cardiac Imaging. *Magnetic Resonance in Medicine*, 49(3):417-423.

Taniyama, Y. 2005. Akt3 Overexpression in the Heart Results in Progression from Adaptive to Maladaptive Hypertrophy. *Journal of Molecular and Cellular Cardiology*, 38(2):375-385.

The Normal Size of the Heart Muscle. 1951. *Acta Medica Scandinavica*, 139(S257):15-19.

Thiebaud, D., Jacot, E., Defronzo, R.A., Maeder, E., Jequier, E. & Felber, J.. 1982. The Effect of Graded Doses of Insulin on Total Glucose Uptake, Glucose Oxidation, and Glucose Storage in Man. *Diabetes*, 31(11):957-963.

Towler, M.C. & Hardie, D.G. 2007. AMP-Activated Protein Kinase in Metabolic Control and Insulin Signaling. *Circulation Research*, 100(3):328-341.

Treebak, J.T. 2006. AMPK-Mediated AS160 Phosphorylation in Skeletal Muscle is Dependent on AMPK Catalytic and Regulatory Subunits. *Diabetes*, 55(7):2051-2058.

Tsatsoulis, A., Mantzaris, M., Bellou, S. & Andrikoula, M. 2013. Insulin resistance: An adaptive mechanism becomes maladaptive in the current environment — An evolutionary perspective. *Metabolism*, 62(5):622-633.

Turcotte, L.P., Swenberger, J.R., Tucker, M.Z. & Yee, A.J. 2001. Increased Fatty Acid Uptake and Altered Fatty Acid Metabolism in Insulin-Resistant Muscle of Obese Zucker Rats. *Diabetes*, 50(6):1389-1396.

Uusitalo, A., Uusitalo, A. & Rusko, H. 1998. Exhaustive Endurance Training for 6-9 Weeks did Not Induce Changes in Intrinsic Heart Rate and Cardiac Autonomic Modulation in Female Athletes. *International Journal of Sports Medicine*, 19(08):532-540.

Uyeda, K. 1979. Phosphofructokinase. *Adv Enzymol Relat Areas Mol Biol*, 48:193–244.

Van Der Merwe, J.D., Joubert, E., Manley, M., De Beer, D., Malherbe, C.J. & Gelderblom, W.C.A. 2010. In Vitro Hepatic Biotransformation of Aspalathin and Nothofagin, Dihydrochalcones of Rooibos (Aspalathus Linearis), and Assessment of Metabolite Antioxidant Activity. *Journal of Agricultural and Food Chemistry*, 58(4):2214-2220.

Van der Merwe, J.D., Joubert, E., Richards, E.S., Manley, M., Snijman, P.W., Marnewick, J.L. & Gelderblom, W.C.A. 2006. A Comparative Study on the Antimutagenic Properties of Aqueous Extracts of Aspalathus Linearis (Rooibos), Different Cyclopia Spp. (Honeybush) and Camellia Sinensis Teas. *Mutation Research - Genetic Toxicology and Environmental Mutagenesis*, 611(1-2):42-53.

Van Der Vusse, G.J., Van Bilsen, M. & Glatz, J.F.C. 2000. Cardiac Fatty Acid Uptake and Transport in Health and Disease. *Cardiovascular research*, 45(2):279-293.

Verstraeten, S.V., Keen, C.L., Schmitz, H.H., Fraga, C.G. & Oteiza, P.I. 2003. Flavan-3-Ols and Procyanidins Protect Liposomes Against Lipid Oxidation and Disruption of the Bilayer Structure. *Free Radical Biology and Medicine*, 34(1):84-92.

Vgontzas, A.N. 2000. Sleep Apnea and Daytime Sleepiness and Fatigue: Relation to Visceral Obesity, Insulin Resistance, and Hypercytokinemia. *Journal of Clinical Endocrinology & Metabolism,* 85(3):1151-1158.

Viglietto, G., Motti, M., Bruni, P., Melillo, R., D'Alessio, A., Califano, D., Vinci, F., Chiappetta, G., Tsichlis, P., Bellacosa, A., Fusco, A. and Santoro, M. 2002. Cytoplasmic relocalization and inhibition of the cyclin-dependent kinase inhibitor p27(Kip1) by PKB/Akt-mediated phosphorylation in breast cancer. *Nature Medicine,* 8(10):1136-1144.

Villaño, D., Pecorari, M., Testa, M.F., Raguzzini, A., Stalmach, A., Crozier, A., Tubili, C. & Serafini, M. 2010. Unfermented and Fermented Rooibos Teas (Aspalathus Linearis) Increase Plasma Total Antioxidant Capacity in Healthy Humans. *Food Chemistry,* 123(3):679-683.

Viollet, B., Guigas, B., Sanz Garcia, N., Leclerc, J., Foretz, M. & Andreelli, F. 2012. Cellular and Molecular Mechanisms of Metformin: An Overview. *Clinical science,* 122(6):253-270.

Volchuk, A. 1998. Intracellular Traffic of the Insulin Responsive Glucose Transporter GLUT4. *DAI,* 01B:31.

Vucenik, I. & Stains, J.P. 2012. Obesity and Cancer Risk: Evidence, Mechanisms, and Recommendations. *Annals of the New York Academy of Sciences,* 1271(1):37-43.

Walle, T. 2004. Absorption and Metabolism of Flavonoids. *Free Radical Biology and Medicine,* 36:829–837.

Walsh, K. 2006. Akt Signaling and Growth of the Heart. *Circulation,* 113(17):2032-2034.

Wang, Q., Somwar, R., Bilan, P., Liu, Z., Jin, J., Woodgett, J. & Klip, A. 1999. Protein Kinase B/Akt Participates in GLUT4 Translocation by Insulin in L6 Myoblasts. *Molecular and Cellular Biology*, 19(6):4008-4018.

Watkins, S.J., Borthwick, G.M. & Arthur, H.M. 2010. The H9C2 Cell Line and Primary Neonatal Cardiomyocyte Cells show Similar Hypertrophic Responses in Vitro. *In Vitro Cellular & Developmental Biology - Animal,* 47(2):125-131.

Watson, S. 2009. Amazing Facts about Heart Health and Heart Disease. *WEBMD.* Available at: http://www.webmd.com/heart/features/amazing-facts-about-heart-health-and-heart-disease_

Webster, I., Friedrich, S.O., Lochner, A. & Huisamen, B. 2010. AMP Kinase Activation and glut4 Translocation in Isolated Cardiomyocytes. *Cardiovasc J Afr,* 21(2):72–78.

Wheeler, T.J., Fell, R.D. & Hauck, M.A. 1994. Translocation of Two Glucose Transporters in Heart: Effects of Rotenone, Uncouplers, Workload, Palmitate, Insulin and Anoxia. *Biochimica et Biophysica Acta (BBA) - Biomembranes,* 1196(2):191-200.

White, S.M., Constantin, P.E. & Claycomb, W.C. 2004. Cardiac Physiology at the Cellular Level: Use of Cultured HL-1 Cardiomyocytes for Studies of Cardiac Muscle Cell Structure and Function. *AJP: Heart and Circulatory Physiology,* 286(3):823H-829.

Widlansky, M.E., Duffy, S.J., Hamburg, N.M., Gokce, N., Warden, B.A., Wiseman, S., Keaney, J.F. Jr., Frei, B. & Vita, J.A. 2005. Effects of Black Tea Consumption on Plasma Catechins and Markers of Oxidative Stress and Inflammation in Patients with Coronary Artery Disease. *Free Radical Biology and Medicine,* 38(4):499-506.

Wieser, V., Moschen, A.R. & Tilg, H. 2013. Inflammation, Cytokines and Insulin Resistance: A Clinical Perspective. *Arch .Immunol. Ther. Exp.,* 61(2):119-125.

Wijesekara, N. 2005. Muscle-Specific Pten Deletion Protects Against Insulin Resistance and Diabetes. *Molecular and Cellular Biology,* 25(3):1135-1145.

Wilcox, G. 2005. Insulin and Insulin Resistance. *Clin Biochem Rev.,* 26(2):19-39.

Wild, S., Roglic, G., Green, A., Sicree, R. & King, H. 2004. Global Prevalence of Diabetes: Estimates for the Year 2000 and Projections for 2030. Diabetes care, 27(5):1047-1053.

Williams, A.H. 1964. Dihydrochalcones; their Occurrence and use as Indicators in Chemical Plant Taxonomy. *Nature,* 202(4934):824-825.

Willms, B., Lubke, D., Ahrens, K. & Arends, J. 1991. Delayed Resorption of Carbohydrates in Type 2 Diabetes: Dietetic Measure (Musli) Compared with α-Glucosidase Inhibition. *Schweizerische medizinische Wochenschrift,* 121(38):1379-1382.

Woodgett, J.R. 1990. Molecular Cloning and Expression of Glycogen Synthase Kinase-3/factor A. *EMBO J,* 9(8):2431–2438.

Woods, A. 2003. LKB1 is the Upstream Kinase in the AMP-Activated Protein Kinase Cascade. *Current Biology,* 13(22):2004-2008.

World Health Organisation. 2014. Global Status Report on Noncommunicable Diseases. Available at: http://apps.who.int/iris/bitstream/10665/148114/1/9789241564854_eng.pdf

World Health Organisation. 2015. Cardiovascular Diseases. Available at: http://www.who.int/mediacentre/factsheets/fs317/en/

World Health Organisation. 2015. Obesity. Available at: http://www.who.int/topics/obesity/en/

Xu, X. & Colecraft, H.M. 2009. Primary Culture of Adult Rat Heart Myocytes. *Journal of Visualized Experiments,* (28).

Yadav, A., Kataria, M., Saini, V. & Yadav, A. 2013. Role of leptin and adiponectin in insulin resistance. *Clinica Chimica Acta,* 417:80-84.

Yamaguchi, S., Katahira, H., Ozawa, S., Nakamichi, Y., Tanaka, T., Shimoyama, T., Takahashi, K., Yoshimoto, K., Imaizumi, M., Nagamatsu, S. & Ishida, H. 2005. Activators of AMP-activated protein kinase enhance GLUT4 translocation and its glucose transport activity in 3T3-L1 adipocytes. *AJP: Endocrinology and Metabolism*, 289(4):E643-E649.

Yang, J. 2002. Molecular Mechanism for the Regulation of Protein Kinase B/Akt by Hydrophobic Motif Phosphorylation. *Molecular cell*, 9(6):1227-1240.

Yasunari, K., Kohno, M., Kano, H., Yokokawa, K., Minami, M. & Yoshikawa, J. 1999. Antioxidants Improve Impaired Insulin-Mediated Glucose Uptake and Prevent Migration and Proliferation of Cultured Rabbit Coronary Smooth Muscle Cells Induced by High Glucose. *Circulation,* 99(10):1370-1378.

Yepremyan, A., Salehani, B. & Minehan, T. 2010. Concise Total Syntheses of Aspalathin and Nothofagin. *Org. Lett.,* 12(7):1580-1583.

Yoshida, T., Wei-Sheng, F. & Okuda, T. 1993. Two Polyphenol Glycosides and Tannins from Rosa Cymosa. *Phytochemistry*, 32(4):1033-1036.

Ytrehus, K. 2006. Models of Myocardial Ischemia. *Drug Discovery Today: Disease Models*, 3(3):263-271.

Yu, B., Poirier, L.A. & Nagy, L.E. 1999. Mobilization of GLUT-4 from Intracellular Vesicles by Insulin and K+ Depolarization in Cultured H9C2 Myotubes. *American Physiological Society*, 277(2):E259-E267.

Zaha, V.G. & Young, L.H. 2012. AMP-Activated Protein Kinase Regulation and Biological Actions in the Heart. *Circulation Research*, 111(6):800-814.

Zang, M., Xu, S., Maitland-Toolan, K.A., Zuccollo, A., Hou, X., Jiang, B., Wierzbicki, M., Verbeuren, T.J. & Cohen, R.A. 2006. Polyphenols Stimulate AMP-Activated Protein Kinase, Lower Lipids, and Inhibit Accelerated Atherosclerosis in Diabetic LDL Receptor-Deficient Mice. *Diabetes*, 55(8):2180-2191.

Zhang, L., Zuo, Z. & Lin, G. 2007. Intestinal and Hepatic Glucuronidation of Flavonoids. *Mol.Pharmaceutics*, 4(6):833-845.

Zhang, X. 2002. WHO Traditional Medicine Strategy 2002–2005. *World Health Organization*: Geneva

Zhao, W. & Alkon, D.L. 2001. Role of Insulin and Insulin Receptor in Learning and Memory. *Molecular and cellular endocrinology*, 177(1-2):125-134.